AD NUMBER: AD0900244

LIMITATION CHANGES

TO:

Approved for public release; distribution is unlimited.

FROM:

Distribution authorized to U.S. Gov't. agencies only;
Test and Evaluation Use; 01 JAN 1972. Other requests shall be
referred to Air Force Avionics Laboratory, Wright-Patterson, OH 45433.

AUTHORITY

AFAL ltr dtd 4 Jun 1975

AFAL-TR-72-5

LIGHTNING EFFECTS RELATING TO AIRCRAFT PART I - LIGHTNING EFFECTS ON AND ELECTROMAGNETIC SHIELDING PROPERTIES OF BORON AND GRAPHITE REINFORCED COMPOSITE MATERIALS

F.A. Fisher
High Voltage Laboratory
General Electric Company

and

W.M. Fassell
Materials and Processes Laboratory
Aeronutronic Division
Philco-Ford Corporation

Technical Report AFAL-TR-72-5

January 1972

Air Force Avionics Laboratory
Air Force Systems Command
Wright-Patterson Air Force Base, Ohio

NOTICE

When Government drawings, specifications, or other data are used for any purpose other than in connection with a definitely related Government procurement operation, the United States Government thereby incurs no responsibility nor any obligation whatsoever; and the fact that the government may have formulated, furnished, or in any way supplied the said drawings, specifications, or other data, is not to be regarded by implication or otherwise as in any manner licensing the holder or any other person or corporation, or conveying any rights or permission to manufacture, use, or sell any patented invention that may in any way be related thereto.

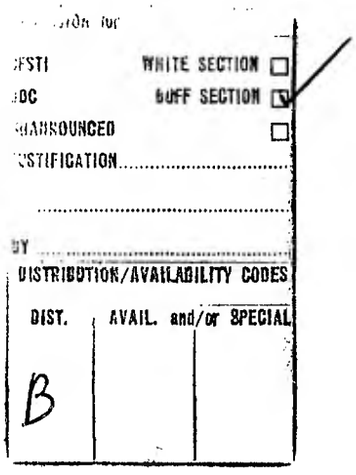

Copies of this report should not be returned unless return is required by security considerations, contractual obligations, or notice on a specific document.

AFAL-TR-72-5

LIGHTNING EFFECTS RELATING TO AIRCRAFT PART I - LIGHTNING EFFECTS ON AND ELECTROMAGNETIC SHIELDING PROPERTIES OF BORON AND GRAPHITE REINFORCED COMPOSITE MATERIALS

F.A. Fisher
High Voltage Laboratory
General Electric Company

and

W.M. Fassell
Materials and processes Laboratory
Aeronutronic Division
Philco-Ford Corporation

Technical Report AFAL-TR-72-5
January 1972

Air Force Avionics Laboratory
Air Force Systems Command
Wright-Patterson Air Force Base, Ohio

FOREWORD

This document is Technical Report AFAL-TR-72-5, Part I and covers Lightning Effects on Composite Materials and Electromagnetic Shielding Properties of Composite Materials. Part II covers the Effects of Simulated Lightning Strokes on Lightning Arresters and Avionic Equipment and the Electrical Characteristics of Simulated Lightning Flashes. Part III covers simulated lightning tests on the F-4 aircraft avionics systems.

This Final Technical Report was prepared by General Electric Co. High Voltage Laboratory, Pittsfield MA in response to USAF contract F33615-70-C-1144. The contract was initiated under AFAL exploratory development project 4357 task 12 under the direction of Mr. H.M. Bartman, Project Engineer, AFAL/AAA and supported by Mr. Herbert Schwartz of the Air Force Materials Laboratory (AFML/LN).

The contractor's activity was under the direction of Mr. F.A. Fisher, Project Manager, assisted by L.C. Walko, B. Macchiaroli, D.B. McElhinny and G.W. Maihl of General Electric and supported by W.M. Fassell, Project Manager, and J.W. McCamont of Philco Ford.

This report covers the period of 15 November 1969 through 15 October 1971 and was submitted by the authors in January 1972.

This Technical Report AFAL-TR-72-5, Part I has been reviewed and is approved.

W. A. Studabaker

WILLIAM A. STUDABAKER
Lt Colonel, USAF
Chief, System Avionics Div
AF Avionics Laboratory

ABSTRACT

An investigation employing both destructive and nondestructive testing techniques affirms that lightning-produced currents adversely affect boron- and graphite-reinforced composites for aircraft. While such composite materials offer significant structural advantages over conventional metals, they are much more easily damaged by the high currents associated with lightning. A majority of the coatings tested to determine their ability to protect composites in a lightning environment actually aggravated composite deterioration. To mitigate lightning damage, composite coatings must be either highly conductive or highly insulating. Limitations are identified that must be overcome before coatings of either type can be deemed acceptable.

Several nondestructive testing evaluation techniques are compared. Acoustic impedance measurement holds the greatest promise, because it requires access to only one side of the material and it correlates well with physical inspections. This technique is potentially effective in locating cracks and delaminations. Resistance measurements are shown to be more meaningful for boron-based than for graphite-based materials. Other nondestructive material techniques such as ultrasonic "C"-Scans, X-ray extractions, sonic-vibrations are found to be no better for lightning damage appraisal than ordinary visual inspections.

Parametric studies verify that damage severity increases as higher lightning currents are applied. It was also established that current division in multi-ply composites is not determined by ply layup, but by the external electromagnetic field orientation associated with a lightning stroke. Electrically, the panels seem to behave as homogeneous bodies.

Studies were made of the electromagnetic shielding properties of composite materials. It is shown that they have much poorer shielding properties than conventional metal structures. The implications as regards the electrical design of future aircraft are discussed.

It is shown that since shielding effectiveness of structural materials depends largely on the field impedance, attention must be concentrated on the lower impedance fields associated with lightning current flow on an aircraft skin or at the stroke attachment point. The use of high level pulse fields to evaluate shielding effectiveness is conducive to problems, largely because of the limited spectral range of the available pulses. The most meaningful, consistent test results were obtained by continuous wave or discrete frequency measurement. Shielding effectiveness comparisons are made for various panels at frequencies selected after judicious determination of the spectral characteristics of a long electrical arc.

TABLE OF CONTENTS

ILLUSTRATIONS

TABLES

SECTION 1

1.0 Introduction

This report covers work done in three broad areas under Contract F33615-70-C-1144/Project 4357, all of the areas dealing with the subject of lightning flashes to aircraft. These three broad areas were:

A) To investigate the direct burning and blasting effects of lightning, particularly as to how they relate to the newer composite panels and structural elements.

B) To investigate the indirect effects of lightning on aircraft, particularly the electromagnetic effects, but also including the physical shock wave from a lightning discharge.

C) To provide investigator services for such special problems as might arise during the course of the contract.

The impetus for this work comes largely from the increasing use of composite materials as replacements for aluminum in aircraft. The composite materials, notably boron-epoxy and graphite-epoxy, have many virtues but resistance to the effects of lightning is not one of them. In contrast to aluminum which, by virtue of its good conductivity, has good resistance to the direct burning and blasting effects of lightning and provides excellent electromagnetic shielding, the composite materials are neither good conductors nor good insulators nor very good in providing shielding against electromagnetic radiation. If these composite materials are used in aircraft in locations where they might be struck by lightning, they will require some form of protection. Questions immediately arise as to how vulnerable are the composite materials to lightning and how best may protection be provided.

A substantial part of the test effort during this program was directed at determining these direct effects of lightning on composite materials. The work involved tests on a variety of boron-epoxy and graphite-epoxy test panels. In this test effort the High Voltage Laboratory of the General Electric Company was ably assisted by the Aeroneutronic Division of the Philco-Ford Corporation. They performed all of the extensive mechanical analysis of the test specimens, both before and after the high voltage tests in the High Voltage Laboratory.

Test samples were supplied by the Air Force Materials Laboratory and the Air Force Flight Dynamics Laboratory. Delays in procurement of the test specimen had an impact on the test program and as a result some of the desired continuity of the test effort was lost. The loss of continuity of test effort was not too serious, but the delays did seriously delay the completion of the

test effort.

The total work effort is covered in three volumes of which this is the first. It deals with the direct effects of lightning on composite materials in Section 2 and with the electromagnetic shielding properties, or lack thereof, in Section 3.

The indirect effects of lightning are also important particularly as regards the electromagnetic fields associated with the lightning flash. These electromagnetic fields can lead to surge voltages on aircraft electrical systems, either by direct contact with an electrical circuit, as for instance a lightning flash to an antenna, or by induction through the fuselage of the aircraft. These are dealt with in Part II of this total report effort.

Section 2 of Part II deals with a series of tests made on aircraft lightning arresters to show what voltages might appear on avionic equipment in the event of a lightning flash to an antenna.

SECTION 2

2.0 Lightning Effects on Composite Materials

A major effort during this contract was directed at determining the effects on composite materials of high intensity electrical discharges representative of natural lightning. The tests were divided into several phases, each directed at a slightly different end. These were:

1. A screening test of different coating materials to see which, if any, offered any merit as protective coatings for composite materials.
2. A series of tests on 6" x 12" rectangular panels, both boron and graphite, to determine their intrinsic resistance to lightning effects and to evaluate the effectiveness of several protective coatings.
3. A series of tests on graphite panels to determine the effects of simulated lightning current level, panel thickness and panel coating.
4. A series of tests to determine how lightning current divided within a composite material.
5. A series of tests on structural samples composed of two composite panels over an aluminum honeycomb center.

These tests were made to determine if the coatings applied could withstand a 200 kA lightning dicharge.

The simulated lightning tests to be described were performed in the High Voltage Laboratory. The tests of material properties before and after the tests were made by the Aeroneutronic Division of the Philco-Ford Company.

2.1 Screening Tests of Different Coatings

2.1.1 Sample Description

This phase of the test was a screening test of a number of different types of coatings to see if any of them offered any merit as protective coatings for composite materials. To this end there were supplied a total of 28 samples with dimensions of 3" x 12" x 1/16" thick. Most of these were graphite material, but a few were nonconductive fiberglass. The graphite panels had 4 plies, the outer plies running parallel to the long direction of the strip and the two inner plies running perpendicular to the long direction of the strip. The coatings were described in detail in Table I. Most of the materials were carbon black or carbon black plus a conductive salt loaded urethane coating. Two samples were

TABLE I

Description of Coatings on 3 inch by 12 inch Test Panels

Sample No.	Material	Coating
1	Graphite-Epoxy	1.5 mils grey epoxy, 2.5 mils NH_4BF_4 loaded urethane
2	Graphite-Epoxy	4 mils clear urethane, 5 mils LiCl loaded urethane
3	Graphite-Epoxy	3 mils clear urethane, 4 mils LiCl loaded urethane
4	Graphite-Epoxy	3 mils clear urethane, 6 mils NH_4BF_4 loaded urethane
4A	Fiberglass-Epoxy	4 mils NH_4BF_4 loaded urethane
5	Graphite-Epoxy	3 mils clear urethane, 4 mils ferrocene loaded urethane
5A	Fiberglass-Epoxy	3 - 5 mils ferrocene loaded urethane
6	Graphite-Epoxy	4 mils clear urethane,
7	Graphite-Epoxy	8 mils NH_4BF_4 loaded urethane
8	Graphite-Epoxy	6 mils NH_4BF_4 loaded urethane
9	Graphite-Epoxy	Electroplated 1 mil nickel
10	Graphite-Epoxy	Electroplated 1 mil nickel
11	Graphite-Epoxy	5 mils urethane, 8 mils spray Kel-F, 12 mils salt loaded urethane
12	Graphite-Epoxy	5 mils urethane, 7 mils strip coat, 12 mils salt loaded urethane
13	Fiberglass-Epoxy	3 mils urethane, 4 mils strip coat, 7 mils salt loaded urethane
13A	Graphite-Epoxy	None
13B	Graphite-Epoxy	None
13D	Graphite-Epoxy	None
14	Fiberglass-Epoxy	3 mils clear urethane, 11 mils salt loaded urethane
15	Fiberglass-Epoxy	5 mils clear urethane
15A, 15B, 15C, 15D	Not returned after General Electric Lightning Tests	
16	Graphite-Epoxy	10 mils spray Kel-F, 10 mils salt loaded urethane
17	Graphite-Epoxy	5 mils clear urethane, 15 mils salt loaded urethane
18	Graphite-Epoxy	3 mil layer of epoxy bonded Al foil

nickel plated and one was coated with aluminum foil.

2.1.2 Test Methods

The samples were clamped at one end in a grounded test jig and subjected to electrical arcs from the high current generator. The test jig is shown on Figure 1. Current flowed from the surge generator into the test panel through a 3/4" arc. It then flowed down the sample (or ideally down the conductive coating) to the ground clamp at the base of the sample, through a resistive current shunt and back to the surge generator. Lightning current levels of between 30 kA and 80 kA were used. The surge generator was damped by Thyrite to give a unidirectional current wave. The waveshape of a typical discharge is shown in Figure 2. The current amplitude and waveshape, as measured by the resistive shunt, were recorded on a Tektronix Model 507 oscilloscope in an adjacent shielded measurement enclosure. The test sample was backed by a non-conductive polyester glass backing plate in order to add rigidity to the test sample and to prevent added destruction of the test sample by the physical blast of the high current arc.

Tests were first run on four uncoated samples to determine a critical damage threshold. The definition of critical threshold was highly subjective, but it seemed to be about 60 kA. Currents of 30 and 40 kA produced only localized damage while currents of 76 kA produced extensive damage over most of the sample. All of the coated samples were tested at current levels of nominally 60 kA. In some cases the generator malfunctioned, discharging before the storage capacitors had reached their full voltage. In these cases the discharge current was lower.

2.1.3 Test Results

In general none of the carbon loaded paints or carbon plus salt loaded paints showed any particular merit as protective coatings. Damage to the test samples was just as extensive, and often more extensive, on the coated samples as it was on the uncoated control samples. The metallic coatings, nickel plating or aluminum showed generally good protective properties. Detailed test results were as follows:

Sample L-13C (30.6 kA Test Current Level)

A photograph of the damage to this panel is shown on Figure 3. On this uncoated sample the damage was confined mostly to the arc attachment point. At this point there was a diamond-shaped burn approximately 1.2" wide along the long axis of the sample and about 2.7" wide transverse to the sample axis. Fibers were lifted on both the top ply and the ply

FIGURE 1

Jig for Test Samples

Lightning Effects Tests on Composite Materials

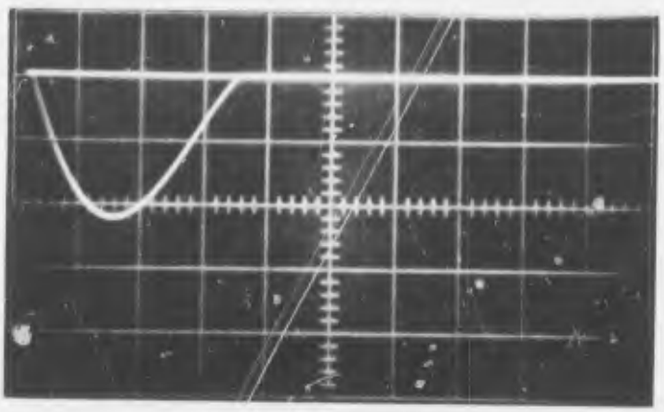

25.5 kA/Div. 5 μsec/Div.

FIGURE 2

Applied Current Waveshapes

Lightning Effects Tests on Composite Materials

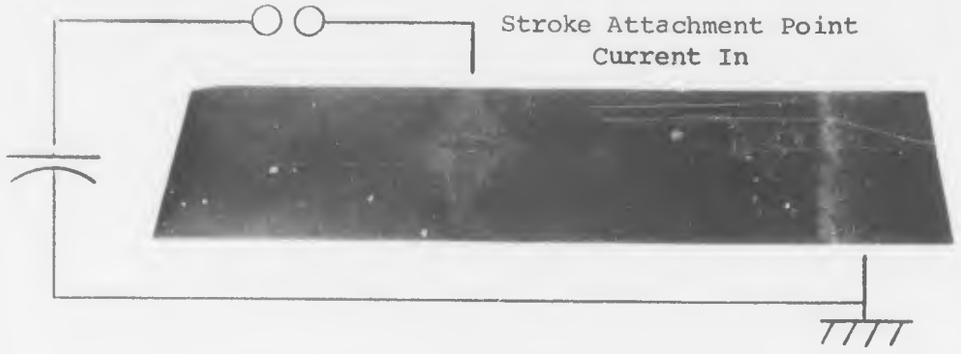

Specimen

L-13C
30.6 kA
Positive Polarity

L-13B
40.9 kA
Positive Polarity

L-13C
56 kA
Positive Polarity

L-13D
76.6 kA
Positive Polarity

L-15A
56.1 kA
Negative Polarity

FIGURE 3 - Damage to Uncoated Samples

underneath it. The back of the panel was not damaged. Apparently current flowed from the top ply into the ply underneath and was then carried out toward the edges of the panel, thus causing pyrolysis of the underlying plies as well as pyrolysis to the top ply. The current then apparently flowed through the graphite material to the grounded end and then flowed back up through the plies to the ground structure at the end of the panel. Near the grounded end of the panel there was again pyrolysis of the fibers, apparently only on the top ply. There was no damage at the back of the panel at the ground end. Between the arc and attachment point and the grounded end of the sample there was apparently no further damage, at least to the surface ply.

In later sections of this report it will be developed that the various nondestructive test techniques do not usually show any evidence of damage beyond that visible to the naked eye. Accordingly, we could conclude that a current density of 163 kA per square inch of cross-sectional area did not cause damage except at the points of current entry and current exit.

Sample L-13B (40.9 kA)

This sample suffered the same general kind of damage as the previous sample except slightly more severe. The triangular area of damage was about 2 inches along the length of the panel and extended the full width of the panel at the current entry point. At the current exit point the damage again was similar to the previous panel, but somewhat more extensive. On the top ply, pyrolized fibers extended about 0.4 inches up the panel from the arc attachment point. Between the current entry and current exit points there were individual fibers on the outer ply that seemed to be broken or pyrolized. The current density in the undamaged section of the panel would be 216 kA per square inch.

Sample L-13A (56 kA)

This current level was considered a critical damage threshold. Individual fibers were violently lifted at the point of impact. Damage extended through to the back surface at which point the back surface plies were cracked, but not violently lifted.

Pyrolized fibers extended the full length of the panel from the arc attachment point to the ground point and at the ground point burning was sufficient to begin to lift the individual fibers on the top ply. The corresponding current density along the center portion of the panel was 298 kA per square inch.

Sample L-13D (76.6 kA)

There was extensive damage at the point of current entry with individual fibers being lifted on both the top ply and underlying plies. Pyrolized fibers extended the full length of the panel from the arc attachment point to the grounded point on both the front surface and the back surface. The panel was not cracked through the back surface at the point of current attachment. The resultant current density was 406 kA per square inch.

Sample L-15A (56.1 kA)

The previous samples were tested with a positive polarity discharge, one involving electron flow from the arc attachment point into the high voltage electrode and into the generator. Sample L-15A was tested with a negative polarity discharge, one with electron flow from the electrode into the arc attachment point in order to see if polarity effects made any difference. They did not. Damage was virtually identical to that observed on Sample L-13A at the same current level. A photograph of this panel is also shown on Figure 3.

Sample No. 1 (56.2 kA)

This sample is protected by about 4 mils of grey epoxy and NH_4BF_4 coatings. The coating did not provide any protection. The coating itself was blown clear of the panel over about a 5" length along the long axis of the sample and was about 1" width. The sample was delaminated at its edge at the stroke attachment point and at the ground return point, damage that was not noted on the unprotected panel at the same current level. The back face of the panel was not really punctured at the stroke attachment point but there was pyrolysis of the sample on the back surface. This pyrolysis was, if anything, more pronounced at this 56 kA level than it was on the unprotected Sample L-13D at the 76.6 kA level. No quantitative tests were made, but the sample seems to have lost all its strength at the stroke attachment point.

Sample No. 2 (less than 60 kA)

This sample was given a coating of 4 mils of clear urethane followed by 5 mils of LiCl loaded urethane. This coating seemed to provide better protection than the coating on Sample No. 1, but damage still seemed to be as pronounced on the unprotected sample. The damage cannot be directly related to current level since the surge generator fired prematurely and an oscillogram of the true current level was not recorded. The coating was

lifted for about 3.3 inches along the axis of the panel and about 1 inch across the panel. As the coating was blown upward from the attachment point it exposed the second and third layers of fibers underneath. These two were broken loose and the damage extended through the back face of the panel. The back face was only slightly damaged. There was no pyrolysis of the back surface and no apparent discoloration of the protective coating except at the stroke attachment point. The panel was not delaminated at any place.

Sample No. 3 (less than 60 kA)

This sample was given a 3 mil coating of clear urethane followed by 4 mils of LiCl loaded urethane. Damage was more intense than on Sample No. 2 but less than on Sample No. 3. Again the surge generator misfired and the true current level was not recorded. The coating was blown clear for about 4.4 inches along the length of the panel and about 0.7 inches in width across the panel. There was a burned spot at the ground attachment point where the coating bubbled up from the panel, but not sufficiently to blow the coating free of the panel. Again the damage seemed to involve all the plies at the stroke attachment point. On the back of the panel there was some pyrolysis, but only around the stroke attachment point.

Sample No. 4 (35.8 kA)

On this sample the generator misfired again, but the actual current amplitude was measured at the above value. This sample received an initial 3 mil coating of clear urethane followed by 6 mil coating of NH_4BF_4 loaded urethane. The coating was blown clear of the panel for about 3 inches along the length of the panel and 6.6 inches across the panel. The panel did not appear to be split nor was there any real damage on the back surface of the panel.

Sample No. 4A (61.3 kA)

This was a control sample of nonconducting fiberglass material with a 4 mil coating of NH_4BF_4 loaded urethane. The electrical arc apparently caused no damage to this sample. The arc crept across the top surface of the coating and did not penetrate to the nonconductive fiberglass material. Apparently there was no current flowing between the coating and the panel itself. The coating did not appear to be damaged in any way except possibly for a bit of discoloration along the arc path. There is no way

to tell how much of the total current flowed in the surface arc and how much flowed through the coating itself. Presumably most of it went to the surface arc.

This kind of behavior is what one would expect. Since the test sample was not backed by any sort of a conductive plate, there was no particular electric field pointing normal to the face of the panel, hence no reason for the arc to puncture into the sample. Loosely speaking, if an electrical arc impinges on a nonconductive surface, it splashes around, with conductive filaments of the arc spreading out in random directions and seeking the nearest grounded point or the nearest point at which the current can return to its source. In this case the grounded strap along the bottom edge of the panel was the nearest path. Accordingly the electric field strength is highest in a direction along the axis of the panel and toward the ground return point and the electric arc is concentrated in that direction.

The situation is different with the graphite composite panels in that the graphite tends to remain an equipotential plane running from the ground attachment point up underneath of the stroke attachment point. Accordingly there is then a high electric field strength from the impinging arc in through the sample. The electrical arc then penetrates the sample and the bulk of the current flows through the conductive graphite in the test sample. The field conditions are not such as to promote a surface flashover. This is unfortunate because the surface flashover would remove most of the lightning current from the material.

If the fiberglass sheet had been backed up by a metal backing, one of two things might have occurred. The arc might have punctured the fiberglass material and gone to the conductive back plate or it might have crept around the edge of the fiberglass material on its way to the back plate. With only a 3" total width of the panel, it is most probable that the arc would have crept around the surface of the panel and gone to the conductive plate around in back rather than puncturing the fiberglass sheet. If the fiberglass sheet were of sufficient width, however, it would be punctured before the voltage gradient along the surface got high enough to promote a surface flashover. No tests were made with a conductive back plate to determine what would actually have happened.

Accordingly, one cannot truly decide whether the 4 mil NH_4BF_4 coating would have carried the lightning current by itself without damage or not. On the fiberglass sample 4A the electrical arc most probably crept along the

surface of the material with only a small amount of current flowing through the material. On Sample No. 3 with the same nominal coating the electrical arc punctured the coating into the graphite and the graphite material probably carried all of the lightning current. At the arc impingement point the coating would be blown clear by the explosive energy release when the current flows through the arc.

Sample No. 5 (56.3 kA)

This sample was coated with 3 mils of clear urethane and 4 mils of ferrocene loaded urethane. Damage looked about the same as on Sample No. 2. The coating was blown off over an area of about 3.2 inches in length along the panel and 1 inch in width across the panel. All of the plies were exposed through to the back ply. The back ply was slightly cracked, but there was no pyrolysis of the individual filaments on the back ply other than right around the stroke attachment point. There was a point near the ground point at which the fibers were blown out from the panel along the edge of the panel. Apparently in this case the electrical arc crept along the inside surface of the coating and emerged at or near the grounded end.

Sample No. 5A (61.3 kA)

This was a fiberglass sample like Sample 4A, and again coated with 3 - 5 mils of ferrocene loaded urethane. Again it seemed that there was a surface flashover along the panel. The fiberglass material itself was not damaged, but there was discoloration of the coating. The coating was not physically lifted from the fiberglass however. Again there is no real way of telling how much of the total discharge current flowed through the coating and how much through the surface flashover.

Sample No. 6 (56.2 kA)

This specimen was coated with 4 mils of clear urethane and 5 mils of ferrocene loaded urethane. Damage was more intense to this sample than it was to Sample No. 5. The coating was punctured and torn off for about the same area as on Sample No. 5. There was more pyrolysis of the back ply than on Sample No. 5, however. The edge of the panel was not split. Overall, the damage appears to be intermediate between that experienced on the protected Sample L-13C at 56 kA and the unprotected Sample L-13D at 76.6 kA.

Sample No. 7 (53.6 kA)

This sample was given an 8 mil coating of NH_4BF_4 loaded urethane. Damage was greater than to Samples No. 5 or No. 6. The panel was split at the edges and the back ply was cracked all the way across the panel. The coating was split over an area of 3.7 inches along the length of the panel and 1.2 inches across the width of the panel, but in this case the coating material was not blown completely clear of the panel. It was raised up and carried the top ply up with it. The back ply was pyrolized to about the same extent as on Sample No. 6 or perhaps slightly more pyrolized. The crack across the back face of Sample No. 7 did not appear to be in a pyrolized region. It would seem that this crack occurred as a result of a mechanical force at the arc attachment point.

Sample No. 8 (48.5 kA)

This sample was given a 6 mil coating of NH_4BF_4 loaded urethane. The impulse generator misfired on this sample, hence the lower current amplitude. Again the coating was blown upwards at the stroke contact point over a length of 3.3 inches in length and 0.6 inches in width. The panel was punctured through to the back surface and there was a bit of delamination at the stroke attachment point. There was no pyrolysis to speak of on the back surface. Overall, the damage is less than on panel No. 7 and probably is about what one would expect at the lower current level.

Sample No. 11 (46.0 kA)

This sample was covered with 5 mils of clear urethane, 8 mils of sprayed KEL-F followed by a 12 mil coating of salt-laden urethane. The coating thus becomes quite thick. The major effect of the coating seemed to be to confine the damage even more to the stroke attachment point. The current level was lower than the desired critical damage threshold level due to a prefiring of a surge generator. The lower current level did not lead to pyrolysis of the back surface, but did apparently lead to pyrolysis of the front surface underneath of the coatings. Damage at the stroke attachment point was quite extensive since the coating acted to confine the explosive buildup of pressure and did not allow it to be dissipated to the atmosphere in front of the panel. The panel was punctured through to the back and the back face was fractured.

Sample No. 12 (46.7 kA)

This coating was much the same as the previous sample except that it

had a 7 mil strip coat in place of the 8 mil spray KEL-F. Again the generator misfired giving a lower current level and again the damage was fairly extensive. The panel was cracked completely through on the back face. There was some pyrolysis of the individual fibers of the back face but not very much. Again the effects of the coating seemed primarily to confine the arc to the attachment point and hence cause it to release more energy immediately adjacent to the panel.

Sample No. 13 (35.8 kA)

This was a control sample of nonconductive fiberglass, with a coating about the same as that on Sample 12. The coating consisted of 3 mils of clear urethane, 4 mils of a strip coat and 7 mils of a salt loaded urethane. As on all the other panels the arc damage was very minor, and consisted only of a surface discoloration of the coating. There does not appear to be any damage to the fiberglass panel itself. The coating was peeled back at the stroke attachment point during the examination after the high current test and it was found that there was no damage to the back surface of the coatings. Apparently the arc was purely a surface creepage, though it is possible that some current was carried by conduction along the coating. Again there is no way of telling how much, if any current, was carried by conduction.

Sample No. 14 (61.2 kA)

This was again a control sample of fiberglass with a coating of 3 mils clear urethane followed by 11 mils of salt loaded urethane. As in other cases there was apparently only surface discoloration of the coating and no damage to the fiberglass material.

Sample No. 15 (58.7 kA)

This again was a control specimen of fiberglass with a 5 mil clear urethane coating. As on all other fiberglass panels the damage was confined only to surface discoloration of the coating. There was no damage to the fiberglass.

Sample No. 16 (58.6 kA)

This was a graphite panel with a 10 mil coating of sprayed KEL-F followed by a 10 mil coating of salt loaded urethane. As on most other coatings, the coating was blown away at the arc attachment point. In this case an elliptical piece of coating was blown away of dimensions 1.7 inches

by 1.8 inches. The coating was also punctured and blown loose from the panel adjacent to the grounded end of the conductor. The panel was punctured through the back surface and there was a minor amount of pyrolysis on the back surface.

Sample No. 17 (56.1 kA)

This coating consisted of 5 mils of clear urethane followed by 15 mils of salt loaded urethane. The panel was completely split through to the back side and the panel cracked in half with the two halves held together only by the coating. This coating seemed to have forced the current into the top ply of the material since there was a faint indication of discoloration inside the top ply. The coating was not blown clear of the panel, but was blown up from the panel. As it was blown up it carried most of the top ply of graphite away from the panel, exposing, partially at least, the center plies at right angles to the length of the panel. The damaged section of coating was about 4 inches in length and about 1.6 inch in width.

In summary, one can say that all of the paint coatings were ineffective in providing any protection to the panel. They all seemed to increase the damage and the thicker the coating, the greater the damage. In all cases the coatings were punctured, presumably because the conductivity of the coatings was much less than the conductivity of the graphite panels. When the coating was punctured, more of the energy of the arc was trapped underneath the coating and coupled more effectively through the composite panel. The greater the mass of the coating above the arc, the more effectively the explosive buildup of pressure from the arc is transmitted to the panel.

A similar effect can be noted with other kinds of explosions. If one lays a stick of dynamite on top of a rock and detonates it, there is a good chance the rock will not be damaged at all. All of the shock wave is reflected from the rigid surface of the rock into the surrounding air. If one covers the stick of dynamite with a layer of sand or a layer of mud, the explosive pressures are more confined and are reflected from the sand or mud layer onto the rock and hence the rock is more apt to be shattered.

It would seem that an effective coating for protection of composite materials must work in one of two ways. It must be either a dielectric coating of sufficient insulating properties to force a surface flashover from the arc attachment point to some adjacent metal structure or it must be so highly conducting that it carries the total stroke current and does not allow sufficient voltage drop along the current conducting path to cause a secondary flashover

into the material to be protected. None of the materials tested in this series seem to fall into either category. They are not sufficiently conductive to carry the current, nor sufficiently insulating to promote a surface flashover. Perhaps part of the reason for poor performance of the salt loaded coatings is that salts generally are a poor conductor in themselves. They provide conductively only in the presence of water or some other solvent. Possibly their protective abilities would be greater if they were wet from rain, though in any case they do not look like good candidates for protection.

Examples of typical damage to these panels protected by carbon or salt loaded paints are shown on Figure 4.

Sample No. 9 (63.8 kA)

This sample was covered with a 1 mil coating of electroplated nickel. The only damage visually evident was a discolored spot on the nickel of approximately 0.8 inches in diameter. When the coating was peeled back at the arc attachment point there was found a circular discolored mark on the graphite panel. Apparently all that happened was that the burned or hot metal caused a small amount of pyrolysis of the resin immediately under the metal coating. There did not appear to be any other damage to the graphite panel.

Sample No. 10 (61.2 kA)

This sample was again coated with a 1 mil coating of electroplated nickel. Damage, if such it can be called, was virtually identical to that observed on specimen 9.

Sample No. 18 (63.8 kA)

The protective surface here was a 3 mil coating of aluminum foil cemented with an epoxy adhesive to the panel. There did not appear to be any damage except for a slight pitting and burning of the aluminum foil burned through to the panel underneath, the burned spot being no more than .03 inches diameter.

Figure 5 shows photographs of the damage to the metal coated panels while Figure 6 shows enlargements of the arc attachment point on Sample No. 9.

2.2 Performance of 6" x 12" Boron and Graphite Test Panels

A total of 32 panels were supplied to evaluate the effectivenss of different types of coatings. Half of these were boron and half graphite. Details of

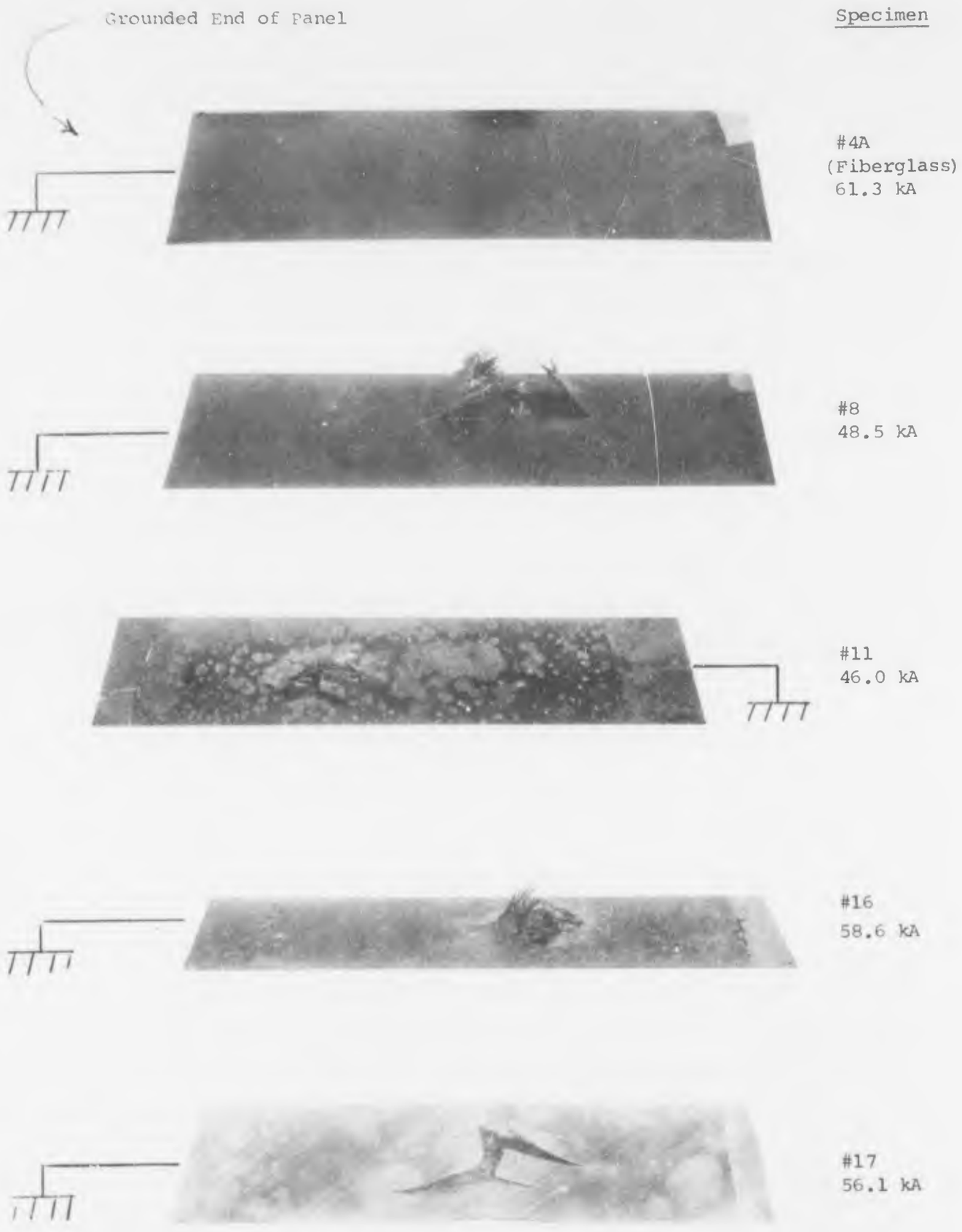

FIGURE 4 - Typical Damage to Carbon or Salt-Loaded Coatings

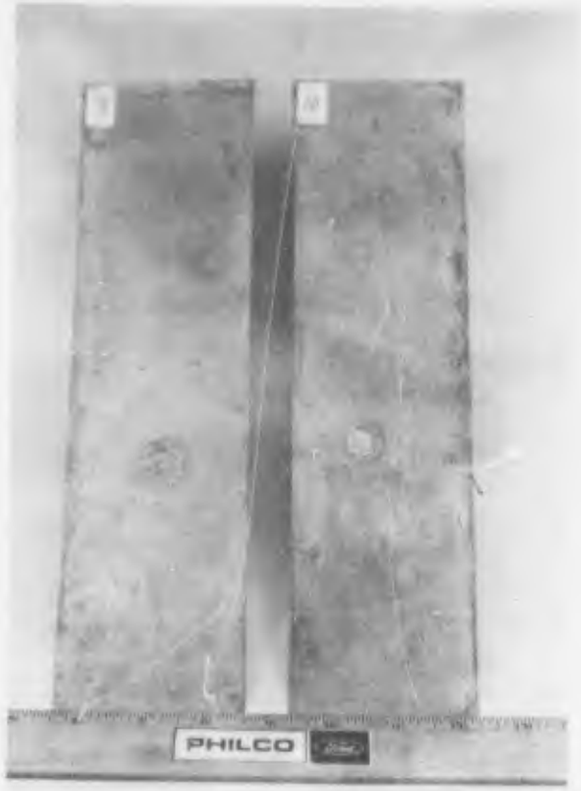

Samples 9 and 10 - Front

Samples 9 and 10 - Back

Sample 18 - Front

Sample 18 - Back

FIGURE 5 - Damage to Surfaces of Metal Coated Panels

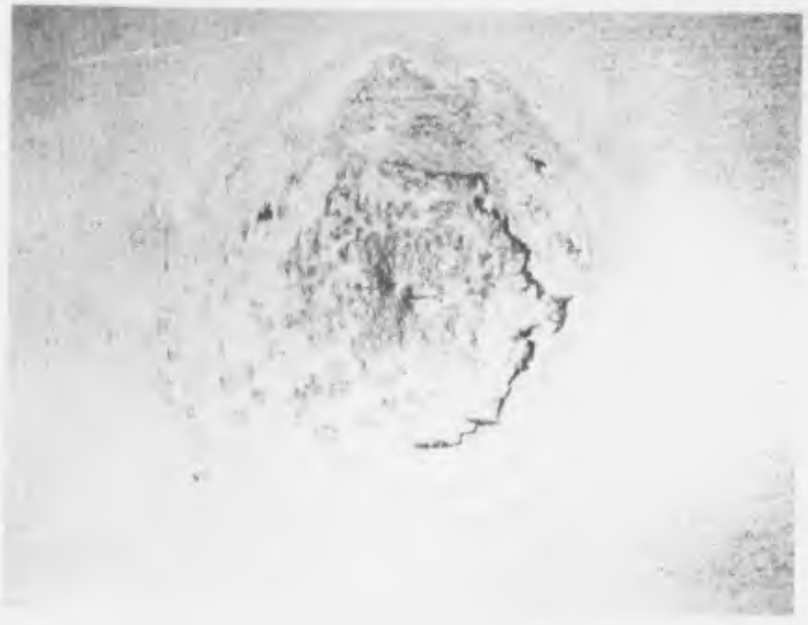

3X Enlargement of Burn at Arc Attachment Point

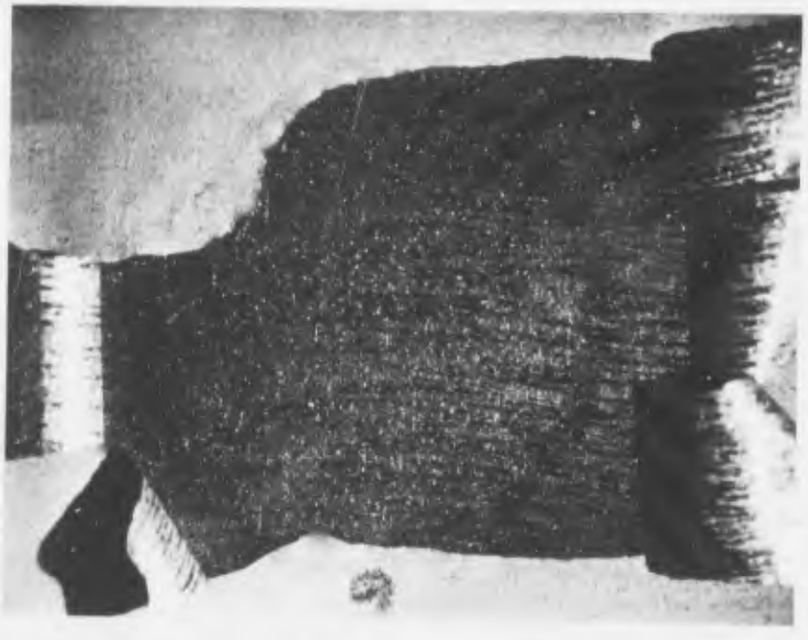

3X Enlargement of Peeled Nickel Coating

FIGURE 6 - Enlarged Views of Arc Attachment Point on Sample 9 After "Lightning" Exposure

the panels and the type of protective coatings will be found in Table II . The types of panels to be tested were a control group that was unprotected, a group with flame-sprayed aluminum coating, a group with a carbon black coating, a group with aluminum foil coatings and a group with aluminum strips as protection. All panels were of 0.083 inch nominal thickness.

Panels were assigned numbers of the form GD-LS-70-1B. The significance of the terminology is:

GD = General Dynamics

LS-70 = Lightning Sample, 1970

1 = Sample Number B - Boron (G for Graphite)

B (or G) = Type of material, Boron or Graphite

Flame-sprayed aluminum samples were given a number of the form GD-FSAL-1B where FSAL stands for flame-sprayed aluminum.

The other panels were given a number of the form GD-LS-70-1B-BC (or -AlF). BC stands for black carbon and AlF stands for aluminum foil. Typical photographs of the panels prior to a lightning test are shown on Figures 2.7 through 2.10. There was no particular difference between the front and back faces of panels, thus Figure 7 is representative of the appearance of the front face of the unprotected samples. No anomalies were noted on any of the panels.

2.2.1 Pretest Analyses

In addition to the photographs the panels were given an ultrasonic "C" scan and radiographed. The X-ray radiographs were extracted and the intermediate extractions printed to show the general quality of the test panels. The boron panels all showed a very good uniform X-ray density with only slight decrease in boron fiber density near the edges of the boron tape used to lay-up the panels. The graphite panels showed large variations of fiber-to-resin ratios in local regions together with the presence of large diameter graphite fiber bundles. These photos are not included since they are very similar to those that were observed on the 13" x 13" panels to be described in the next section of this report. In that section typical extraction X-ray photos are presented.

In general the ultrasonic "C"-scans showed the panels to be quite uniform, a finding consistent with the X-ray extraction radiographs. Typical "C"-scans will be shown in Section 2.2.3 to give a before and after test comparison of the panels.

TABLE II

Details on 6" x 12" Panels and Their Protective Coatings

1) Panels fabricated by General Dynamics

2) Panel size 6" x 12" x 0.083"

3) Boron Panels

   United Aircraft boron fiber

   Narmco 5505 resin

   16 plies

4) Graphite Panels

   Morganite II meter length graphite fiber

   Union Carbide ERCA 4617 resin system

   Impregnated by Fothergill and Harvey

   12 Plies

5) Fiber layup - 50% 0° and 50% 90°

6) Protective coatings

   a) no coating

   b) epoxy paint with carbon black additives

   c) aluminum foil

   d) aluminum foil strips

   e) flame-sprayed aluminum

FIGURE 7 - Front Surface of Sample Panel With Carbon-Black Coating

FIGURE 8 - Back Surface of Sample Panel with Carbon-Black Coating

FIGURE 9 - Front Surface of Sample Panel With Aluminum Foil Coating

FIGURE 10 - Front Surface of Sample Panel with Aluminum Foil Strips

It might be noted at this point that the "C"-scan method of analysis did not generally reveal any damage that was not equally well detected by a simple visual observation.

2.2.2 Test Methods

The method of test for these panels was very similar to that used for the panels described in Section 2.1. One end of the panel was clamped in a grounded structure and an electrical arc struck to the face of the panel. Differences were that the grounded end of the panel had a grounded piece of metal on both sides of the panel, that the panel was not backed by any sort of plate, conducting or nonconducting, an oscillatory discharge was used in contrast to the unidirectional current discharge used for the previous tests, and in some cases, Thermo tapes were used to get an indication of the temperature of the panel during the discharge. The high voltage electrode was positioned 1.5 inches away from the edge of the panel.

A sketch of the test setup along with typical current waveforms is shown on Figure 11. An oscillatory waveform is used to maximize the energy transfer from the surge generator into the test piece.

2.2.3 Test Results - Graphite-Epoxy Panels

Sample GD-LS-70-1G (64 kA)

This sample was tested at approximately the 60 kA critical threshold level observed on the 3" x 12" sample discussed in the previous section. A photograph of the damaged panel is shown on Figure 12. In a manner somewhat similar to that observed on the three-inch panels there is a region at the arc attachment point at which the arc completely destroyed fibers and lifted fibers from the board. Around this there is a region where the resin has apparently been heated sufficiently to cause a change in its appearance. At the grounded end of the sample there is a region in which additional damage was caused by current flowing out of the panel into the ground return circuit. Between the two there is a region that does not appear to be visually damaged. The area in which fibers were completely destroyed is an oval of about 1 inch length and 0.6 inch width. The region over which the resin was discolored was about a 3 inch diameter circle. On the three-inch samples one noted a significant effect caused by the ply orientation in that current apparently flowed from the top ply into the one underneath it and then out at right angles to the length of the sample. This caused the damaged region to be wider than it was long in the direction

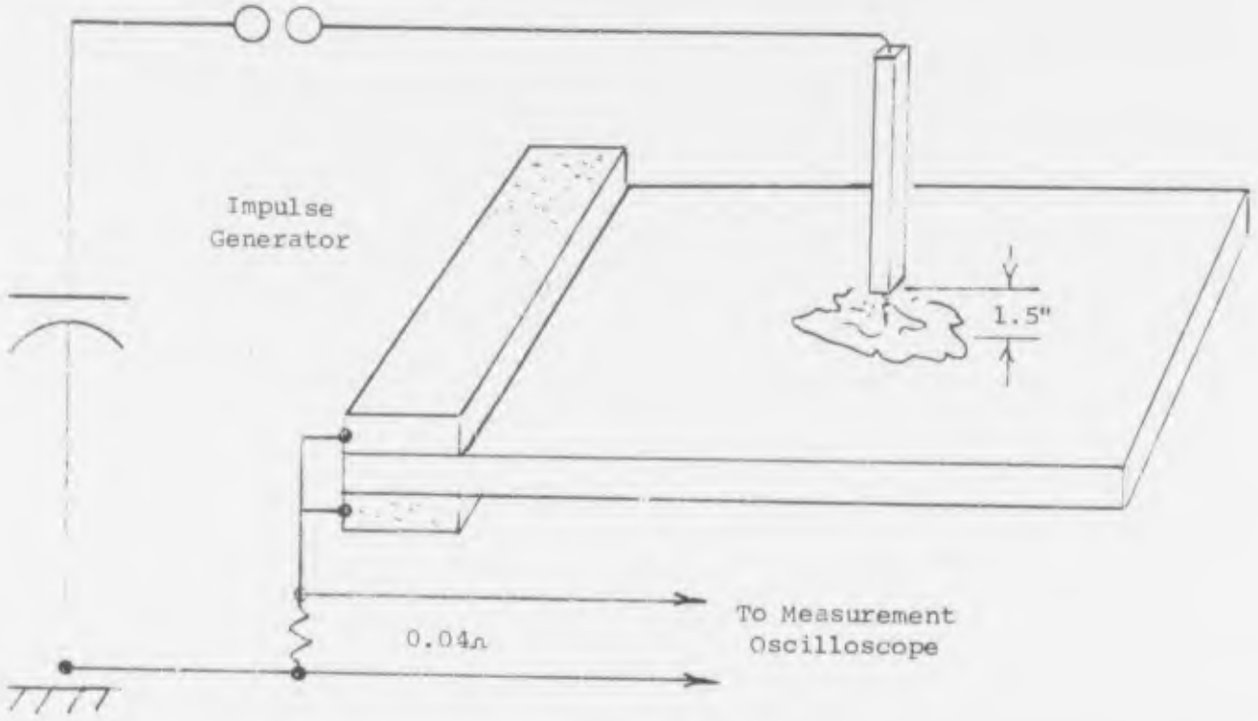

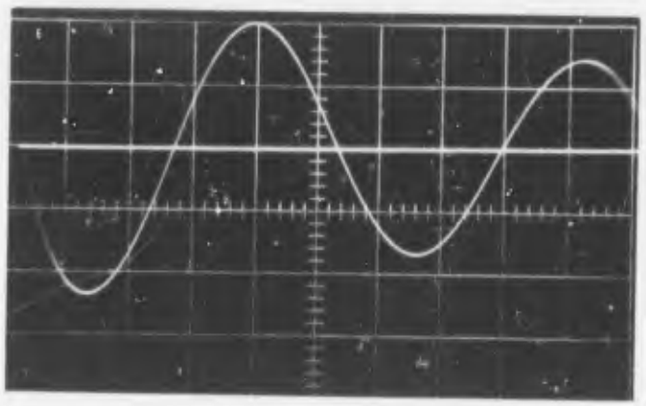

59 kA Peak 5 μs/cm

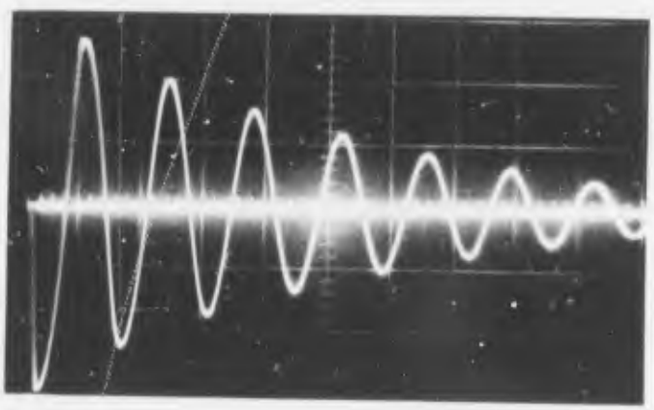

72 kA Peak 20 μs/cm

FIGURE 11

Setup For Tests on 6" by 12" High Modulus Samples

GD-LS-70-1C
(64 kA)

GD-LS-70-2G
(98 kA)

FIGURE 12 - Appearance of Uncoated Graphite Composite Panels After Simulated Lightning Tests

of the panel. On Sample GD-LS-70-1G one does not note as much of this ply effect. These samples have 16 plies as contrasted to the 4 plies of the samples previously discussed. There was no damage to the back of the panel.

Sample GD-LS-70-2G (98 kA)

A photograph of this panel after test is also shown on Figure 12. Differences are that the area of total destruction of fibers is a bit larger, an oval of about 1.6" x 0.8" and that the pyrolized region of resin surrounding the stroke attachment point extends almost down to the grounded end of the sample. The panel was not punctured by the arc.

Sample GD-LS-70-3G (142 kA)

A photograph of this panel is shown on Figure 13. The area of fiber damage is again an oval of 2 inches x 1.4 inches. The pyrolized region again extends almost all the way down to the grounded end of the panel. The panel was not punctured.

No measurements were taken of surface temperatures during the test on these uncoated samples.

2.2.3.1 **X-Ray Radiographs**

An extraction X-ray photograph of the damaged regions of Sample GD-LS-70-3G is shown on Figure 14. This photograph clearly shows the damage to the panel, but does not really show any damage not visible to the naked eye on the exterior of the panel. This is encouraging in that there does not appear to be internal damage that is not readily seen, but discouraging in that the extraction radiographs do not seem to be any more sensitive in detecting damage than a visual observation at the surface. For comparison Figure 2.15 shows an extraction X-ray photograph of panel GD-LS-70-4G which was not exposed to any test.

2.2.3.2 Resistivity Measurements

In previous work[1] it was found that the resistivity of boron composites increased by about one order of magnitude when exposed to damaging simulated lightning current flows. This effect is due to the axial and radial cracks observed in the boron filaments due to coefficient of expansion mismatch between the tungsten core (W_2B_5) and the amorphous boron. If similar changes were to

1 - W.M. Fassell, A.P. Penton, Aeronutronic Division of Philco-Ford Corporation and J.A. Plumer, General Electric Company, High Voltage Laboratory, Technical Note: "The Effects of High Intensity Electrical Currents on Advanced Composite Materials", Aeronutronic Publication No. U-4587, January 30, 1969.

GD-LS-70-3G
(142 kA)

FIGURE 13 - Appearance of Uncoated Graphite Composite Panel After Simulated Lightning Test

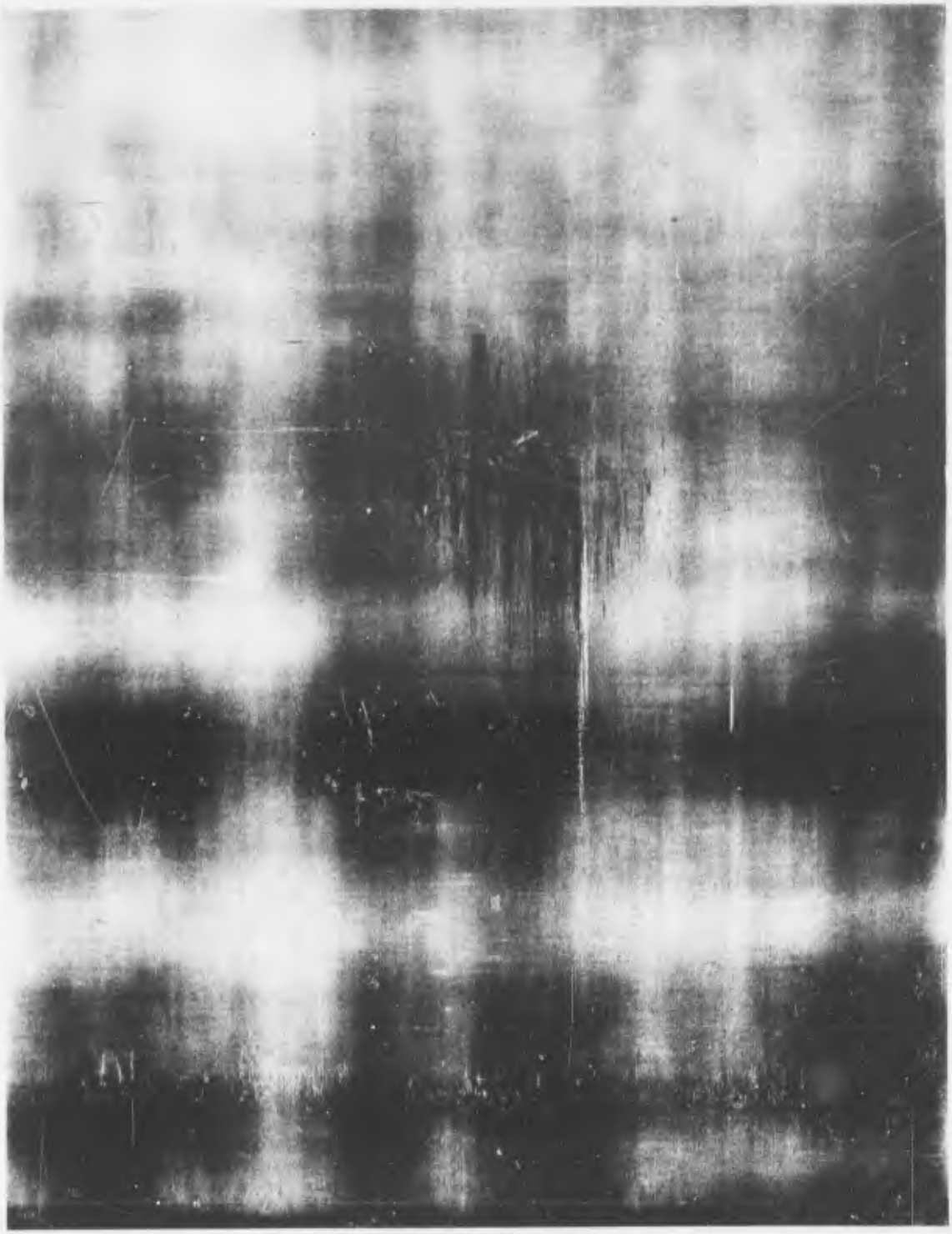

GD-LS-70-3G
(142 kA)

FIGURE 14 - Typical X-ray Radiograph of Uncoated Graphite Composite Panel After Simulated Lightning Test

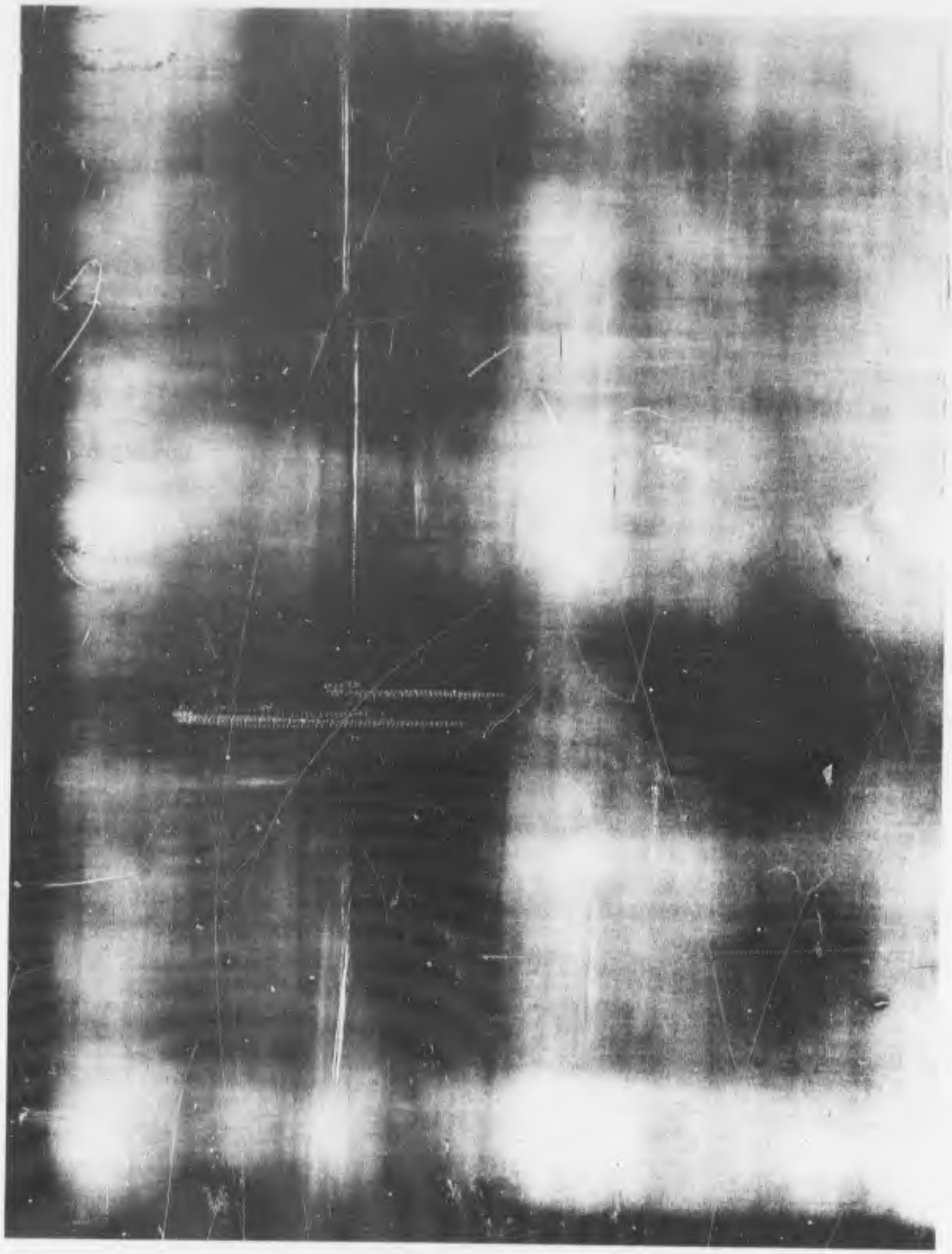

GD-LS-70-4G

FIGURE 15 - X-ray Radiograph of Unexposed Graphite-Epoxy Panel; 2X Photo-Extraction

occur in multidirectional panels, a measurement of electrical resistivity could be a simple method of damage assessment. Such a method might even be useful for in-flight inspections. Resistance measurements were made on the panels to see what the effect of the damaged areas might be.

To make the resistance measurements, silver tabs (conductive silver/epoxy paint) approximately 1/4-inch wide were applied to the edges of the panels. A pair of tabs were placed on opposite sides of the area of maximum damage and others were spaced at 1-1/2 inch intervals from this reference. A sketch showing the orientation and numbering of the tabs and drawing to the same scale as the photograph of the exposed panel GD-LS-70-2G (Figure 11) is shown on Figure 16. A similar sketch for panel GD-LS-70-3G is shown on Figure 17. Each of these figures shows the resistances measured between points of the panel. Measurements were made in the vicinity of the damaged area and near the top of the panel away from the panel. There does not appear to be any pronounced difference between the resistances measured in the vicinity of the damaged area and those measured in supposedly undamaged areas.

In order to make the measurements, a test fixture was built to provide a constant contact area and pressure on the sample. The resistance across the graphite panels was of the order of 0.5 ohms. This was measured with M-H Kelvin bridge and a 1.5 volt lantern battery. Large variations in reproducibility were noted. Also, in spite of the low voltage used and minimum dwell time on the battery button, a thermal (or capacitive) effect made the null point very elusive. Each of the graphite panels was measured three times, as shown in Tables III through VI. Some panels, due to the location of the damaged areas, had additional tab numbers 15 and 16.

The raw data in the tables likewise does not show any significant information in the region of the damaged area. There appears to be a definite difference in the individual panels, but this does not seem to correlate with the amount of damage to panels. Panels GD-LS-70-3G and -4G are most nearly alike on the basis of average resistances even though one panel did not get exposed to a simulated lightning test and one was exposed to a maximum of lightning current. The other panels are different from each of these.

Accordingly, while resistance measurements may be valuable for detecting damage in individual graphite fibers, they do not appear a promising method of evaluating damage on a laid-up graphite composite panel.

The effectiveness of resistance measurements in detecting damage is much better on boron panels, however. This data on the boron panels will be described

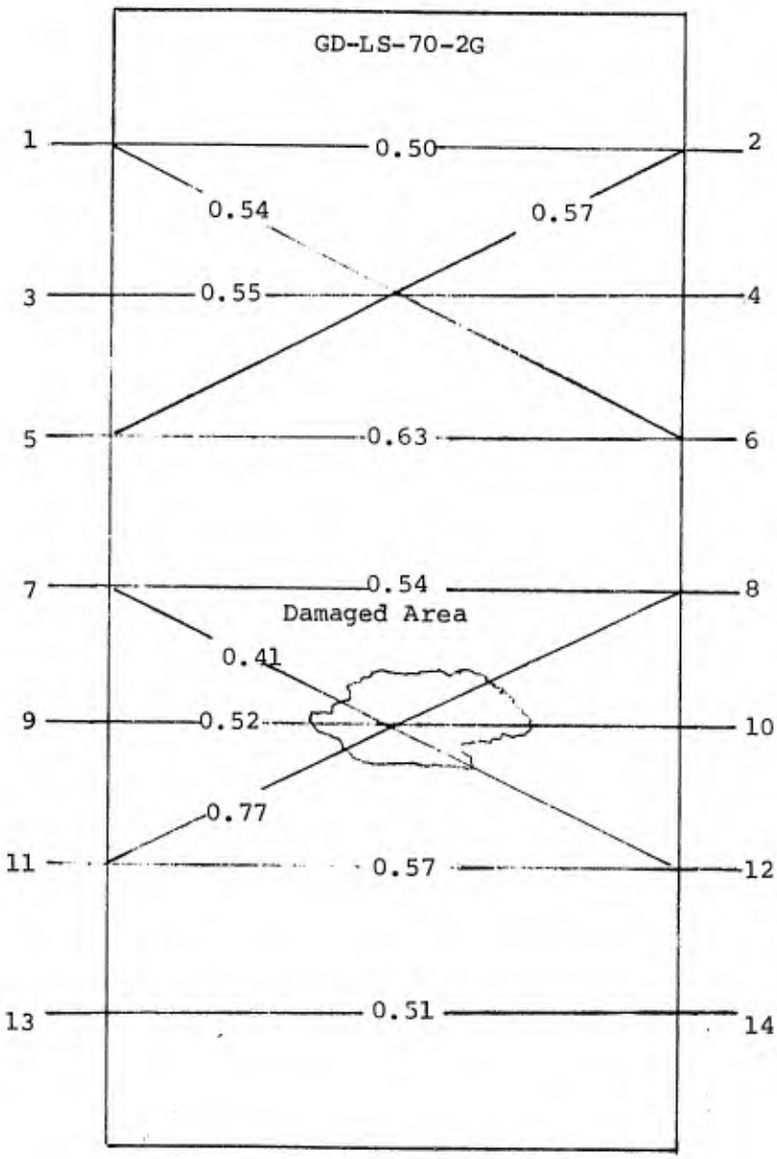

FIGURE 16 - Resistance Measurements on Graphite Composite Panel GD-LS-70-2G (Resistance Values in Ohms)

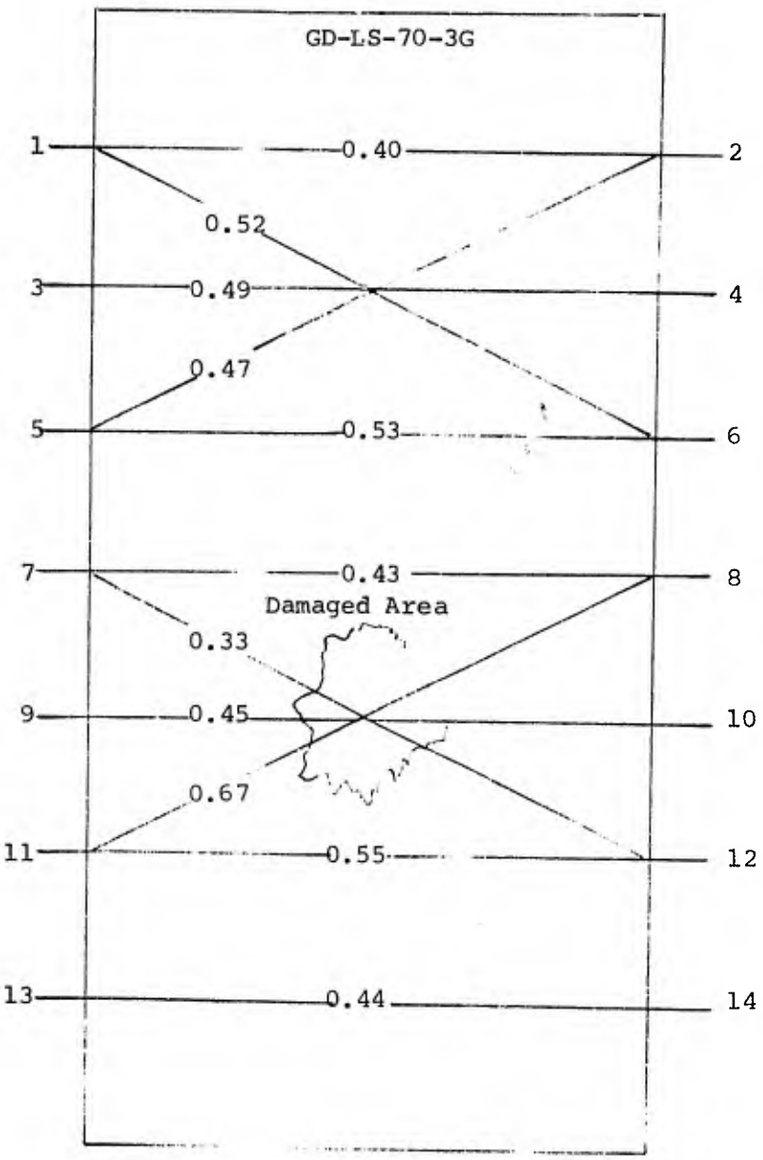

FIGURE 17 - Resistance Measurements on Graphite Composite Panel GD-LS-70-3G (Resistance Values in Ohms

TABLE III

HIGH MODULUS GRAPHITE AFTER EXPOSURE

Panel GD-LS-70-1G

Tabs	I	II	III
1 - 2	0.8438Ω	.5171Ω	.5102Ω
3 - 4	.6190	.6180	.5009
5 - 6	.9141	.6272	.6172
7 - 8	.9768	1.097	.6940
9 - 10	.9111	.7258	.7791
11-12	.8203	.4793	.7313
13-14	1.045	.9535	.7592
15-16	.5438	.4418	.4866
1 - 6	.6529	.7627	.4660
5 - 2	.7427	.9058	1.075
7 - 12	.8398	.7343	.6855
11 - 8	1.335	.7067	.8567

(Tab 8 was not silvered.)

TABLE IV

HIGH MODULUS GRAPHITE AFTER EXPOSURE

Panel GD-LS-70-2G

Tabs	I	II	III
1 - 2	0.5781Ω	.4473Ω	.4930Ω
3 - 4	.6670	.5180	.4781
5 - 6	.6825	.5841	.6425
7 - 8	.6503	.5181	.4454
9-10	.5900	.4906	.4768
11-12	.7034	.5579	.4433
13-14	.5288	.5186	.4740
1 - 6	.4835	.6635	.4442
5 - 2	.5677	.5703	.5760
7 - 12	.4333	.4115	.3796
11 - 8	.8846	.8319	.5882

TABLE V

HIGH MODULUS GRAPHITE AFTER EXPOSURE

Panel GD-LS-70-3G

Tabs	I	II	III
1 - 2	0.4310 Ω	.3561 Ω	.4203 Ω
3 - 4	.4906	.4389	.5350
5 - 6	.5509	.4898	.5600
7 - 8	.4700	.3690	.4550
9 - 10	.4615	.4554	.4446
11-12	.6855	.3984	.5750
13-14	.5225	.4222	.3560
1 - 6	.4249	.7621	.3795
5 - 2	.5615	.4728	.3650
7 - 12	.3562	.3136	.2822
11 - 8	.7188	.6342	.6727

TABLE VI

HIGH MODULUS GRAPHITE (NO EXPOSURE)

Panel GD-LS-70-4G

Tabs	I	II	III
1 - 2	0.5265 Ω	.4769 Ω	.4350 Ω
3 - 4	.4790	.6691	.4589
5 - 6	.3792	.4931	.3890
7 - 8	.3590	.3595	.3863
9 - 10	.4392	.5059	.4485
11-12	.4293	.4162	.3750
13-14	.4280	.4676	.3840
1 - 6	.6145	.4864	.4195
5 - 2	.5537	.5410	.3355
7 - 12	.4953	.4475	.4886
11 - 8	.3652	.5030	.2985

later.

2.2.3.3 Ultrasonic C-Scan Tests

Typical ultrasonic "C"-scan records for the three uncoated graphite panels are shown on Figures 18 through 20. The light coated areas show regions of poor or no ultrasonic transmission. While the damaged areas do show up there are other regions on the panel that seem to show no transmission. A good example is the long white streak to the left of the damaged area on Figure 18. Figure 11, a photograph of the damaged face of the panel, shows a streak on the surface that might be the cause of the poor ultrasonic transmission, but there are other streaks that do not seem to result in regions of poor transmission. Likewise, the damaged area as traced out on the "C"-scan does not tell any more than does visual observation of the damaged area. This same pattern seems to hold throughout the tests. None of the "C"-scans indicated damage that was not readily visible. The area of the white patch on the "C"-scans is more clearly defined than is the damaged area on the surface of the panels themselves and perhaps the area of this region of poor transmission would be a measure of the integrated damage to panels. On the other hand, the "C"-scan technique does not appear to be a really promising tool for investigation for damage in the field.

2.2.3.4 Short Beam Shear Tests

Following the nondestructive tests described, a number of short rectangular test tabs were cut from the exposed test panels. The exact locations of these tabs are shown on Figure 21 through Figure 23 and vary slightly from panel to panel. The general position and orientation of the test tabs is shown on Figure 24. This figure also shows the expected distribution of lightning current. Further discussion on the significance of the damage to individual tabs will be deferred until after we have discussed the boron panels. In general, however, the high modulus graphite composite panels had a remarkedly uniform modulus. The greatest variations observed occurred in samples 1G and 3G on the short beam shear specimens immediately adjacent to the arc attachment point (Samples 13 and 14).

Short beam shear specimens Nos. 4 and 14 were analyzed for resin content and compared with samples cut from undamaged areas. The resin analysis results are listed in Table VII. The resin analysis showed no loss of resin near the damaged area.

2.2.3.5 Photomicroscopic Analyses

As indicated in Figures 21 through 23, samples of each panel were

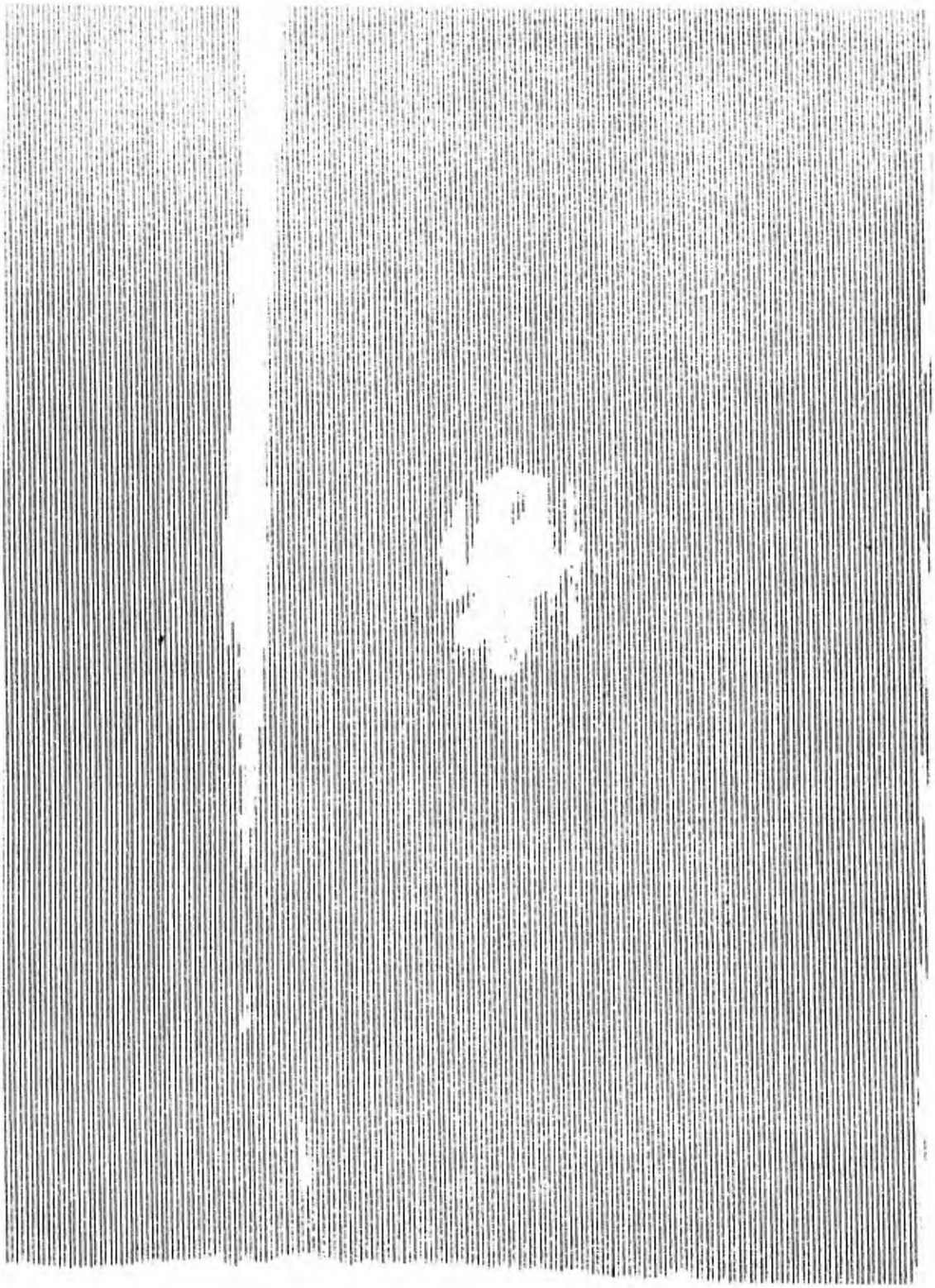

FIGURE 18

Ultrasonic "C"-Scan Uncoated Graphite/Epoxy Panel GD-LS-70-1G

FIGURE 19 - Ultrasonic "C"-Scan Uncoated Graphite/Epoxy Panel GD-LS-70-2G

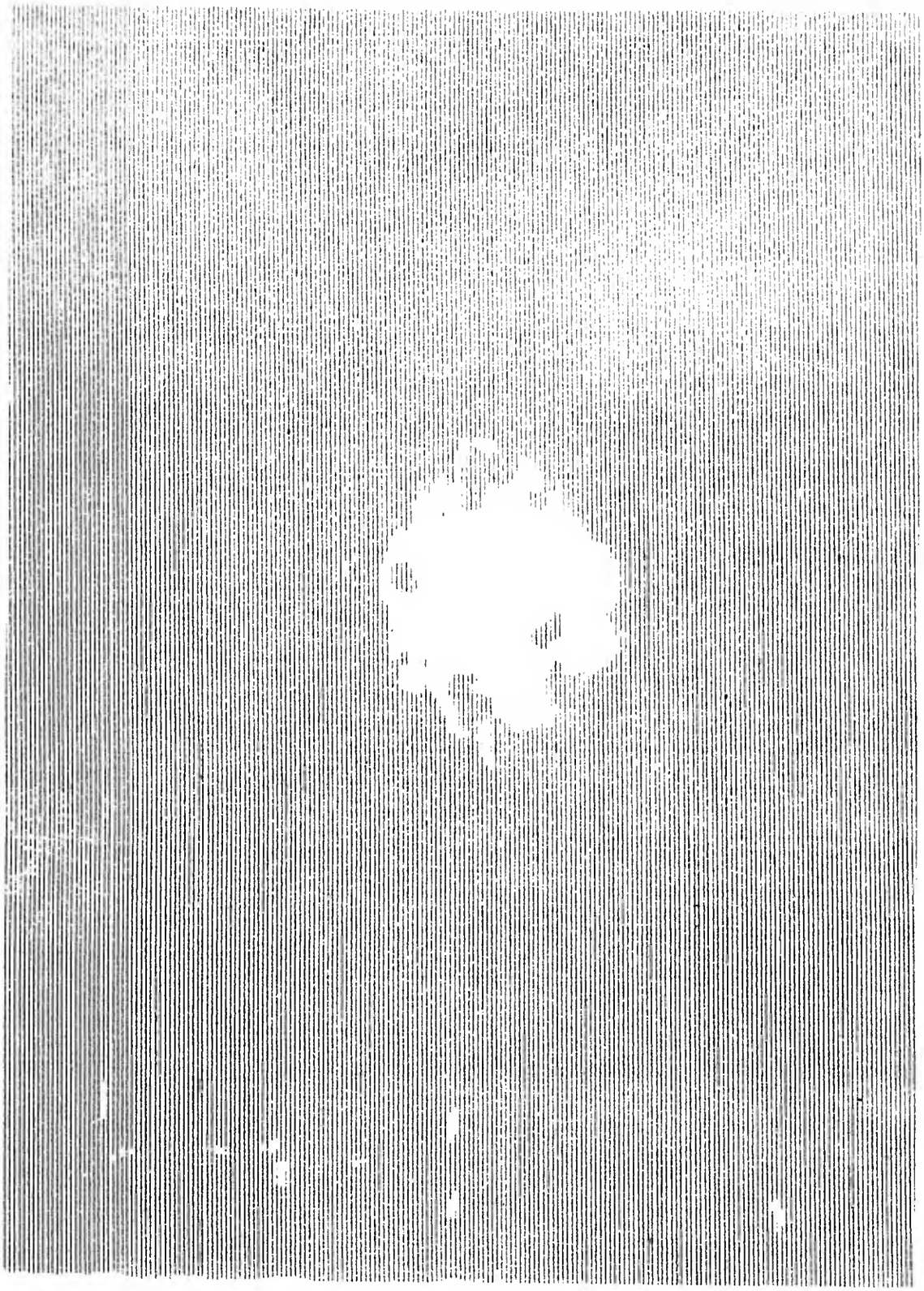

FIGURE 20 - Ultrasonic "C"-Scan of Uncoated Graphite Epoxy Panel GS-LS-70-3G

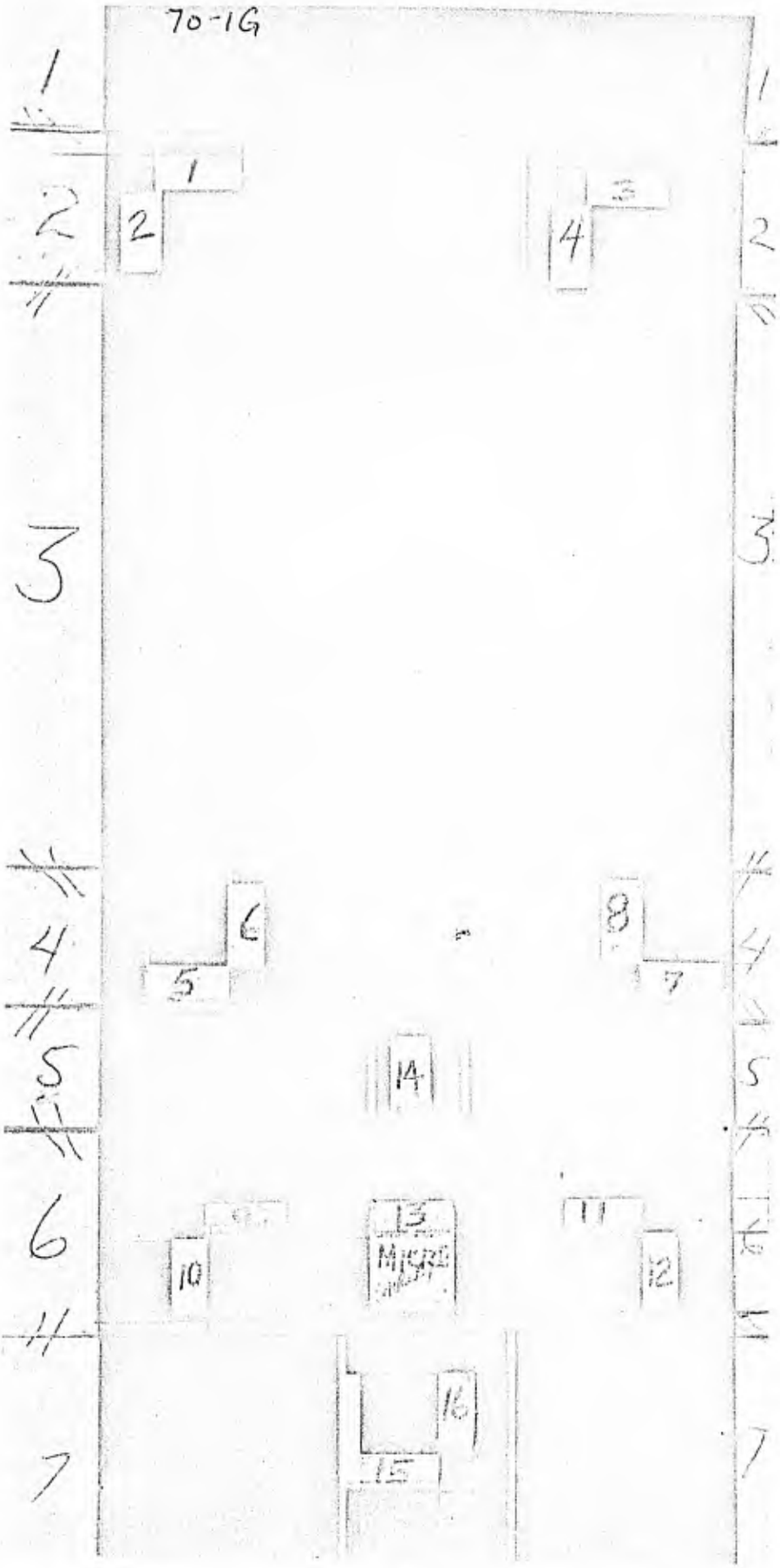

FIGURE 21 - Photo-copy Reduction of Sample Panel GD-LS-70-1G, Showing Sections for Shear Tabs

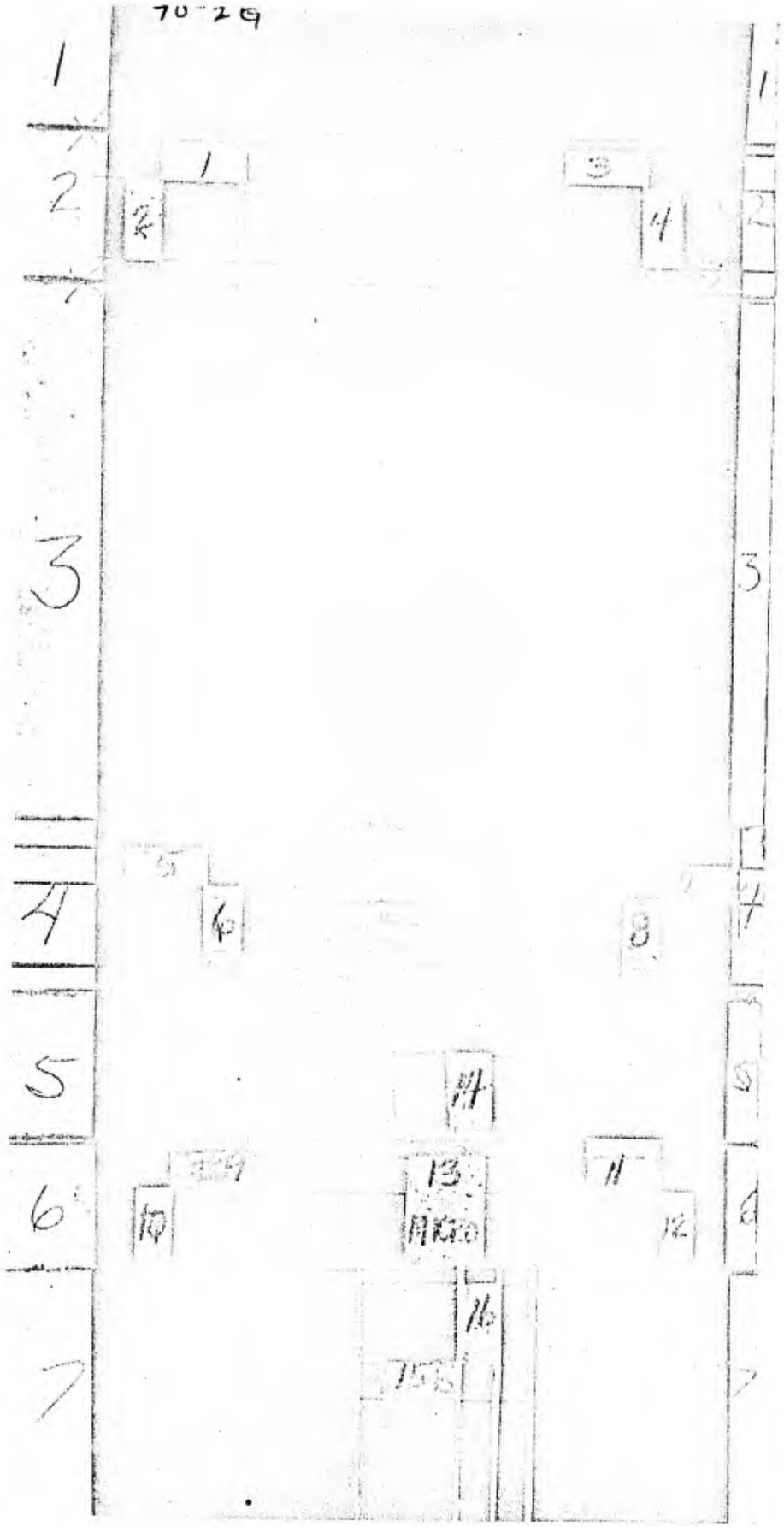

FIGURE 22 - Photo-copy Reduction of Sample Panel GD-LS-70-2G, Showing Sections for Shear Tabs

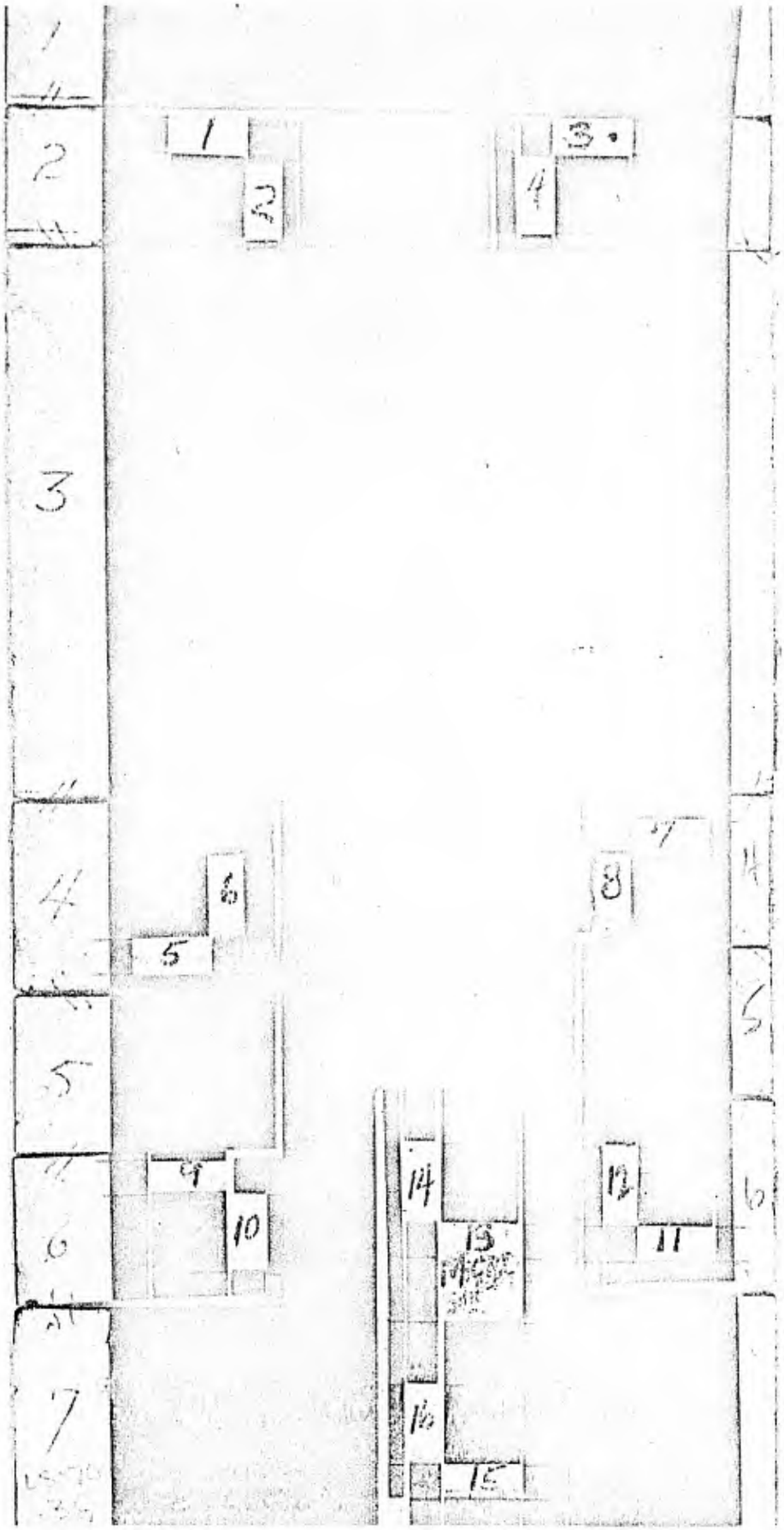

FIGURE 23 - Photo-copy Reduction of Sample Panel GD-LS-70-3G, Showing Sections for Shear Tabs

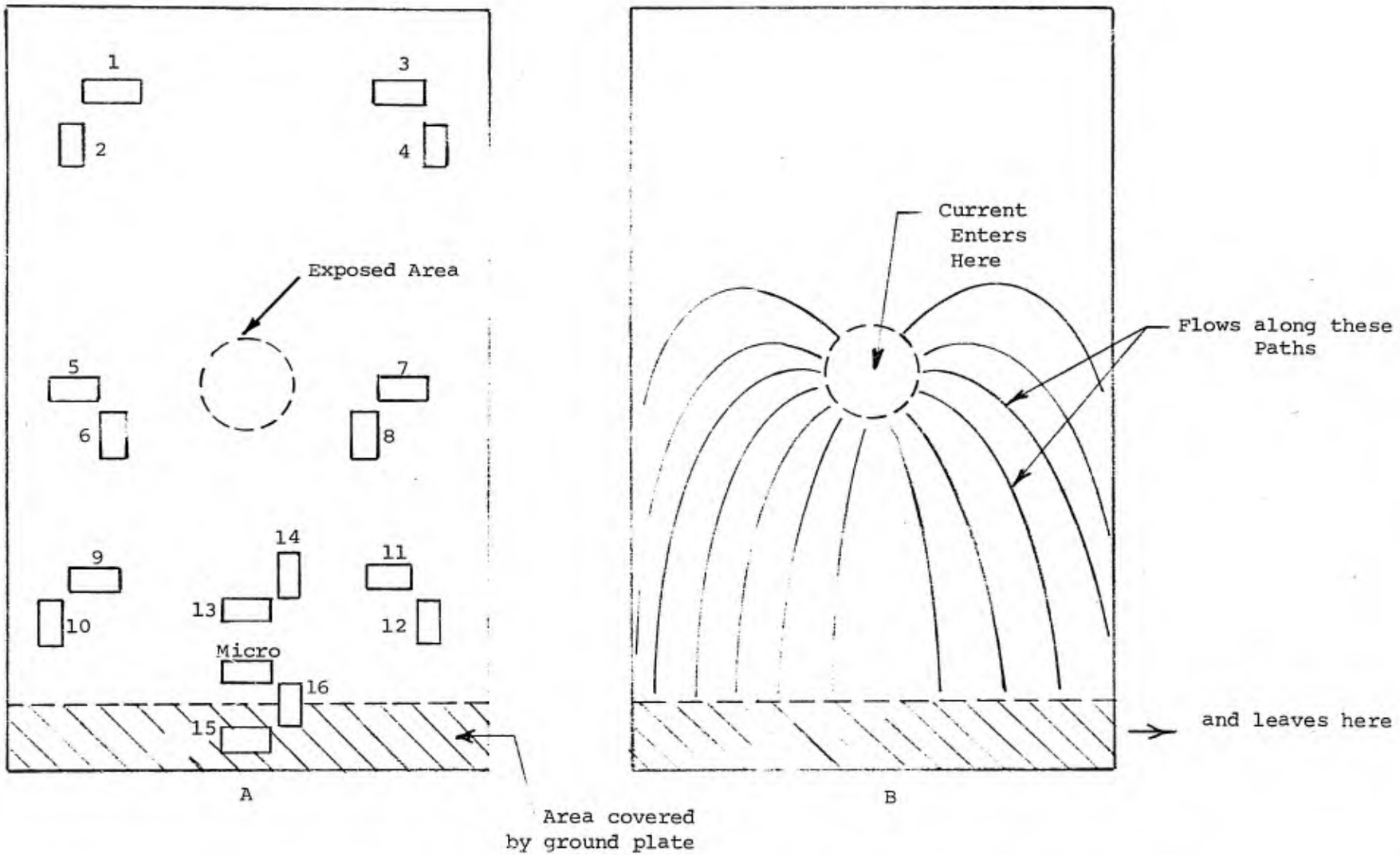

FIGURE 24 - Location of Test Tabs and Their Orientation With Respect to the Current Paths

TABLE VII

RESIN CONTENT ANALYSIS
GRAPHITE/EPOXY COMPOSITES

Panel Number	Short Beam Shear Sample Number	Resin Content Weight %
GD-LS-70-1G	4	35.6
	14	35.8
GD-LS-70-2G	4	36.0
	14	35.6
GD-LS-70-3G	4	35.8
	14	38.9

prepared for photomicroscopy. The 80X photomicrographs for the graphite/epoxy panels are shown on Figures 25 through 27. Figure 28 shows better the orientation of the photomicrograph prints. The top panel surface appears at the bottom of the photomicrographs. The photomicrographs do not seem to show any evidence of degradation on the panel even though the test samples came from points directly in line with the highest expected lightning current flow. They show the outer layer to be very similar in appearance to the inner layers, possibly with the exception that the fibers are packed a little tighter on the outer ply. They thus support the extraction X-ray pictures and the "C"-scan pictures in their story that there is no real damage except near the point of current entry or current exit from the panel.

In contrast to the thin graphite panels described in Section 2.1, it thus appears that peak currents which caused considerable damage to the thin panels did not cause nearly as extensive damage to these thicker panels, in spite of the fact that an oscillatory discharge, one capable of delivering more energy to the test panel, was used for this series of tests. But in the case of the boron panels the situation was somewhat different.

2.2.4 Test Results - Boron Epoxy Panels

GD-LS-70-1B (56 kA)

Figure 29A shows the condition of the uncoated boron panel after a current discharge comparable to that which produced damage to the graphite panel shown on Figure 11. Whereas the graphite panel had one big hole in it, a hole that did not extend through to the back plies of the panel, the boron panel had a number of smaller holes blown in it. How much of this is due to the behavior of the panels and how much to the behavior of the resulting high voltage, high current arc, is difficult to say. Possibly a sufficiently high voltage drop was introduced by the panel into the current discharge path that instead of the arc developing into one thin highly conductive path it developed into several branched paths. It is possible for an actual lightning arc to do this. High speed motion pictures taken of natural lightning arcs show the lightning plasma extending over a pretty broad area, perhaps of the order of a square meter or more for an actual lightning flash. The central regions, the ones that carry the current, are much more restricted, but there is no reason to believe that an actual lightning stroke truly is a pencil-thin column of plasma confining all its energy to one particular little spot. The simulated lightning discharge punctured through to the back of the panel,

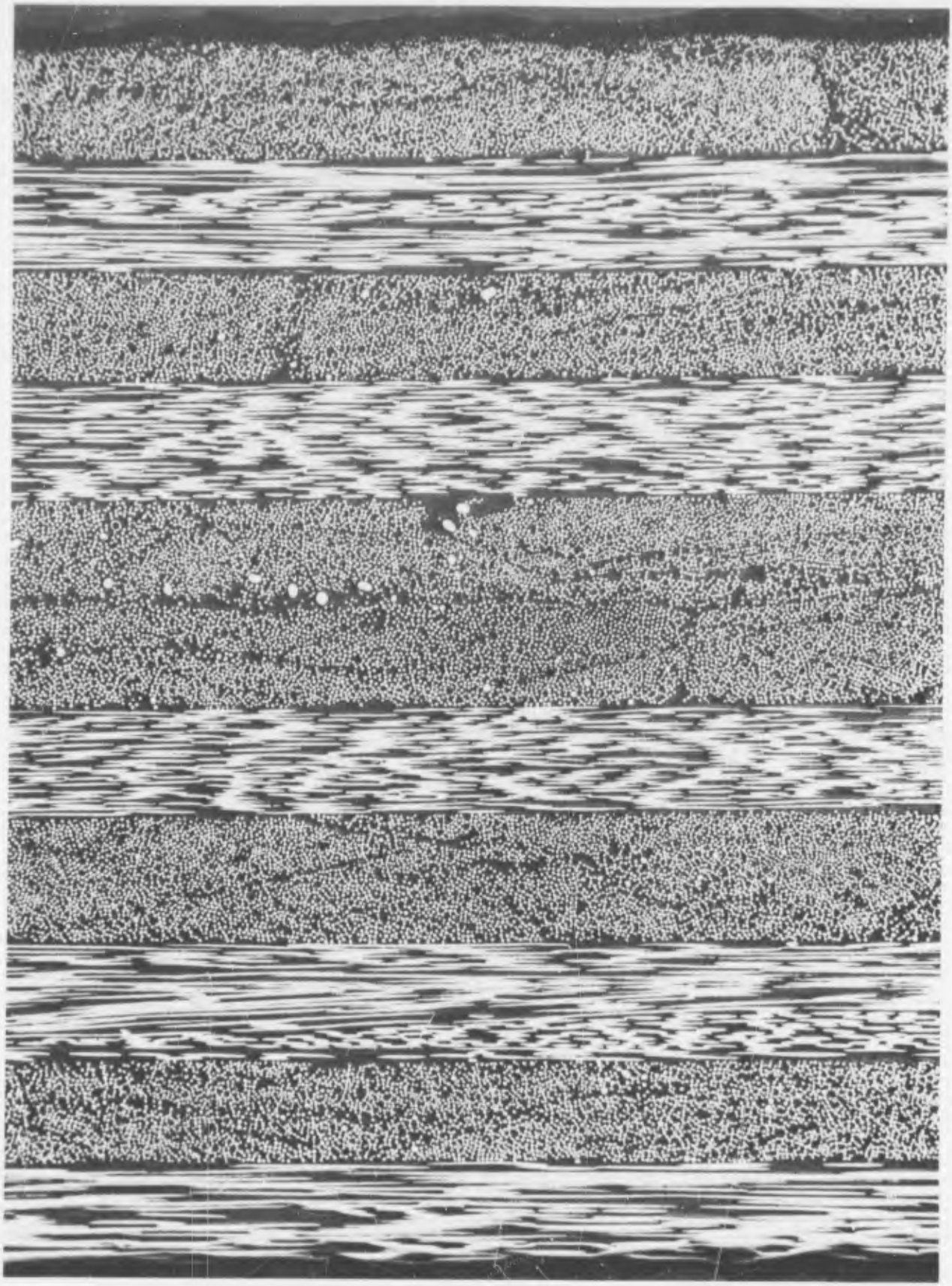

FIGURE 25 - 80X Photomicrograph of Panel GD-LS-70-1G. No Delamination Cracks (Panel Front is at Bottom)

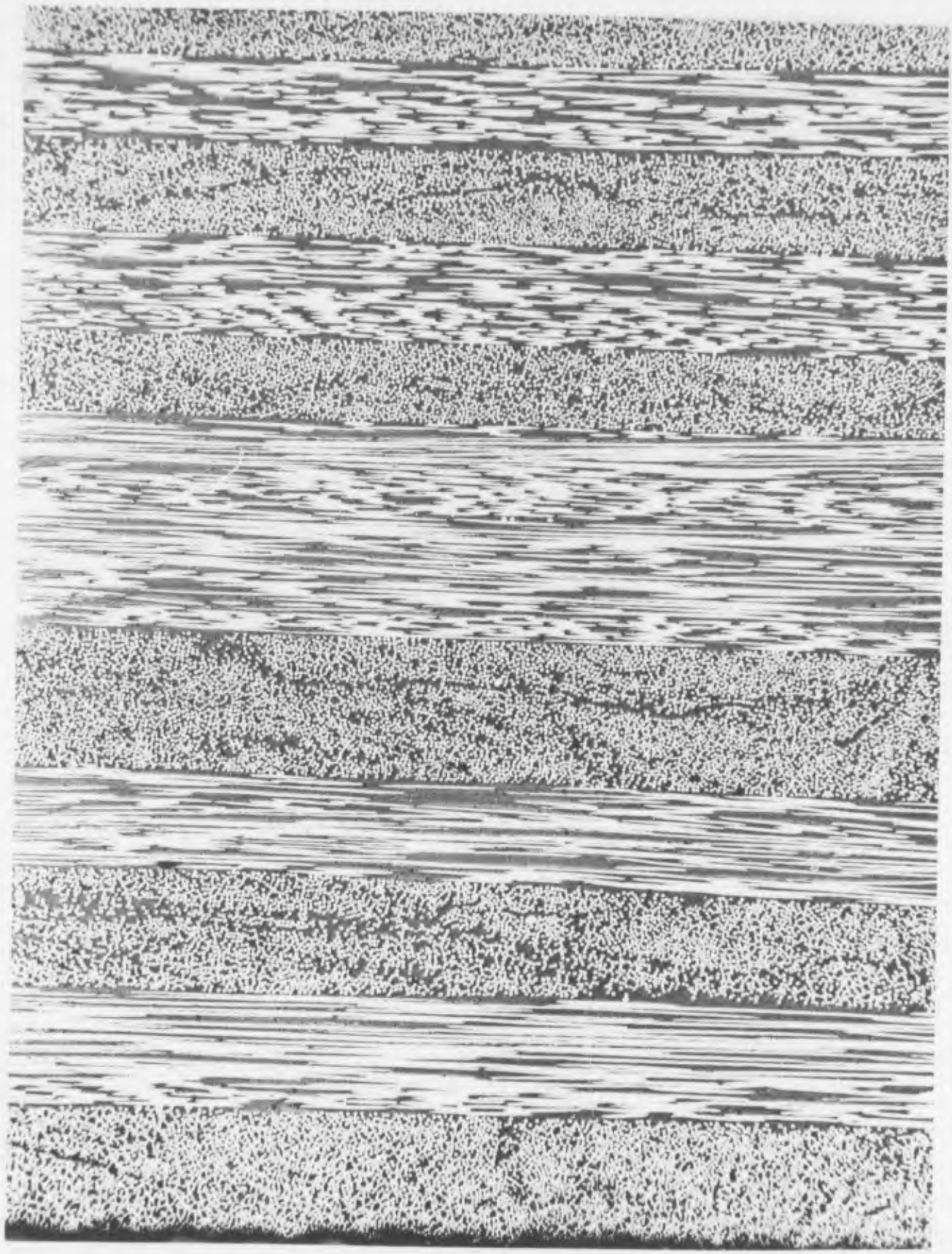

FIGURE 26 - 80X Photomicrograph of Panel GD-LS-70-2G. No Delamination Cracks (Panel Front is at Bottom)

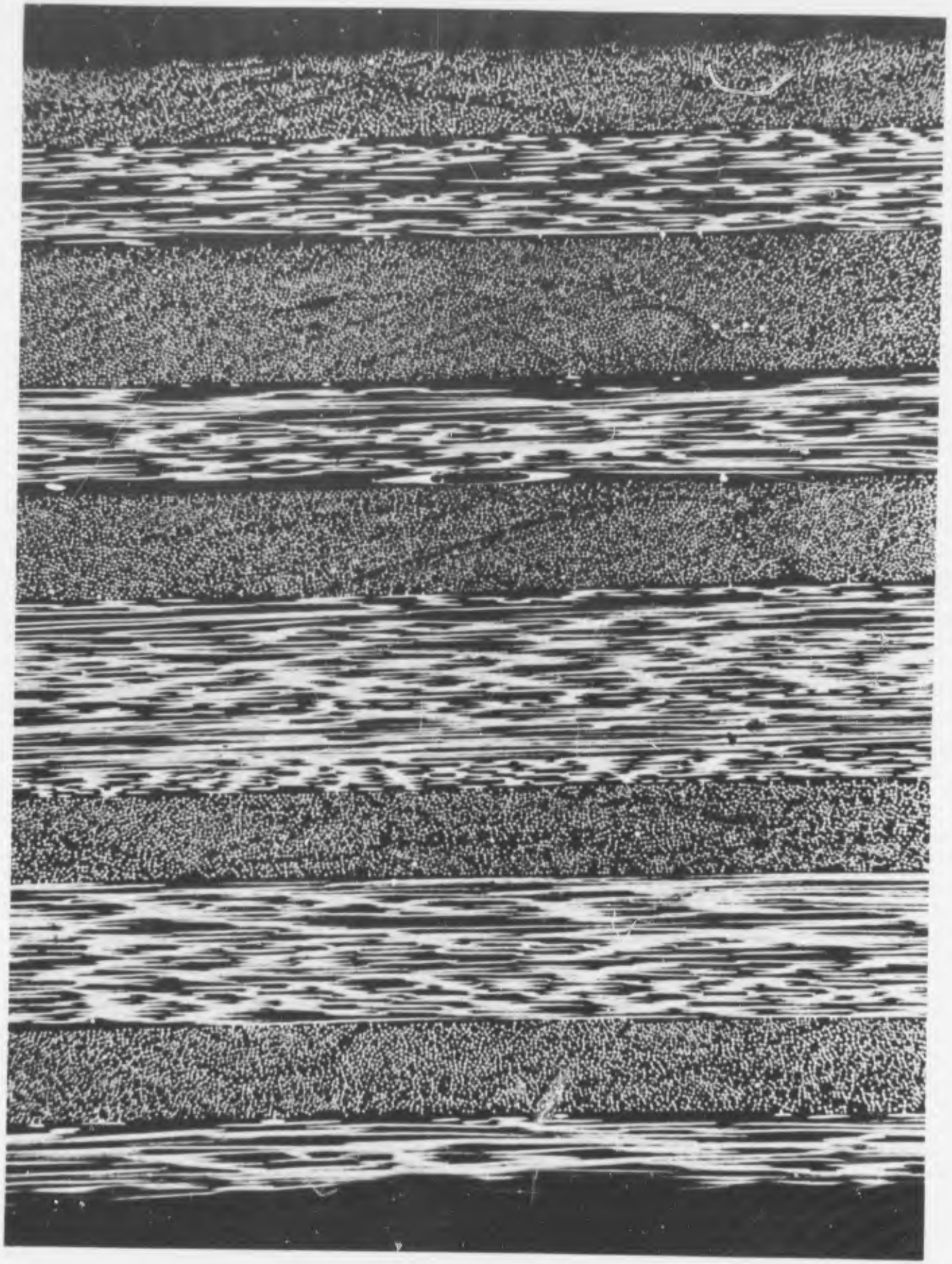

FIGURE 27 - 80X Photomicrograph of Panel GD-LS-70-3G. No Delamination Cracks (Panel Front is at Bottom)

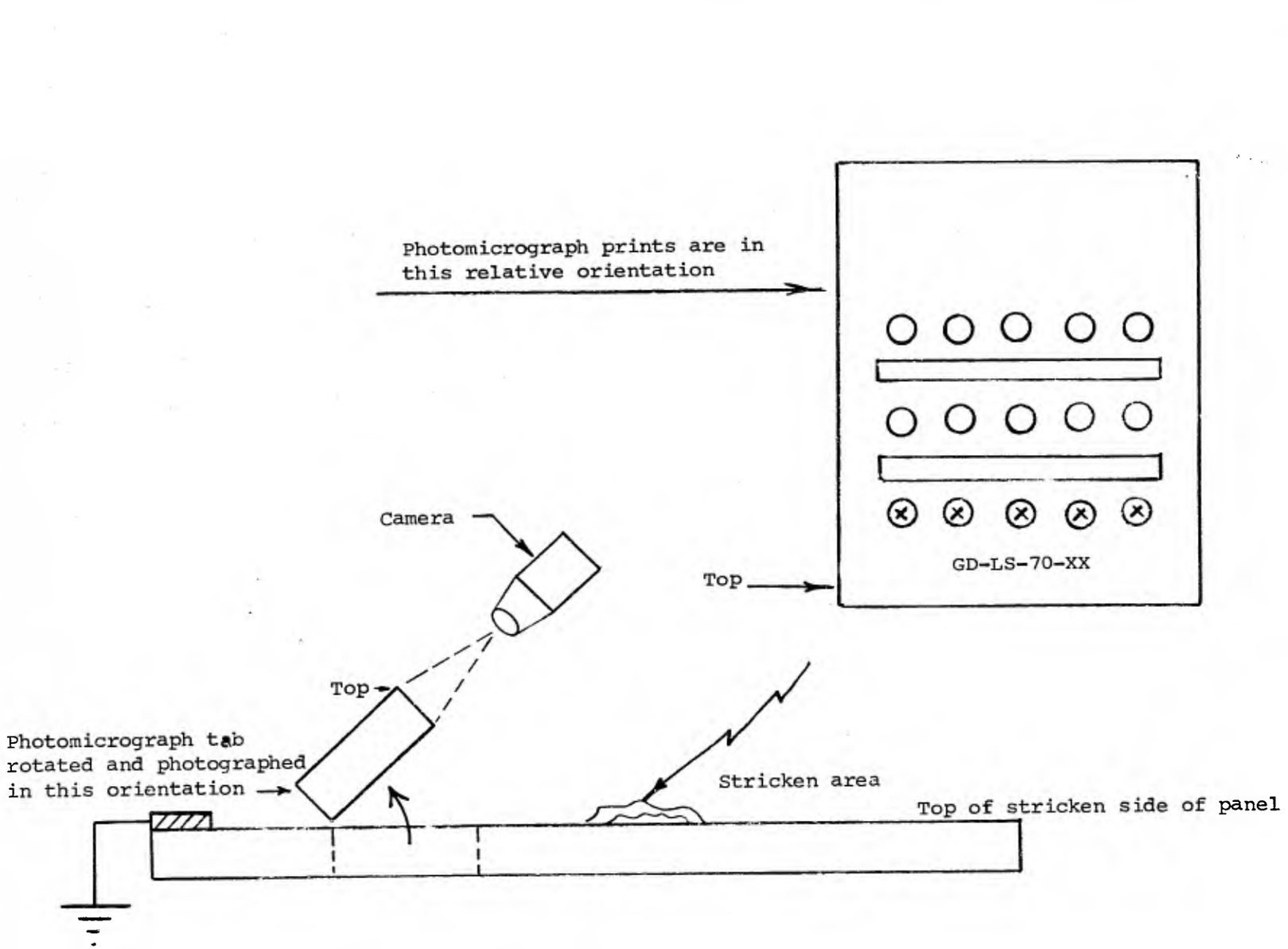

FIGURE 28 - Orientation of Photomicrograph Prints

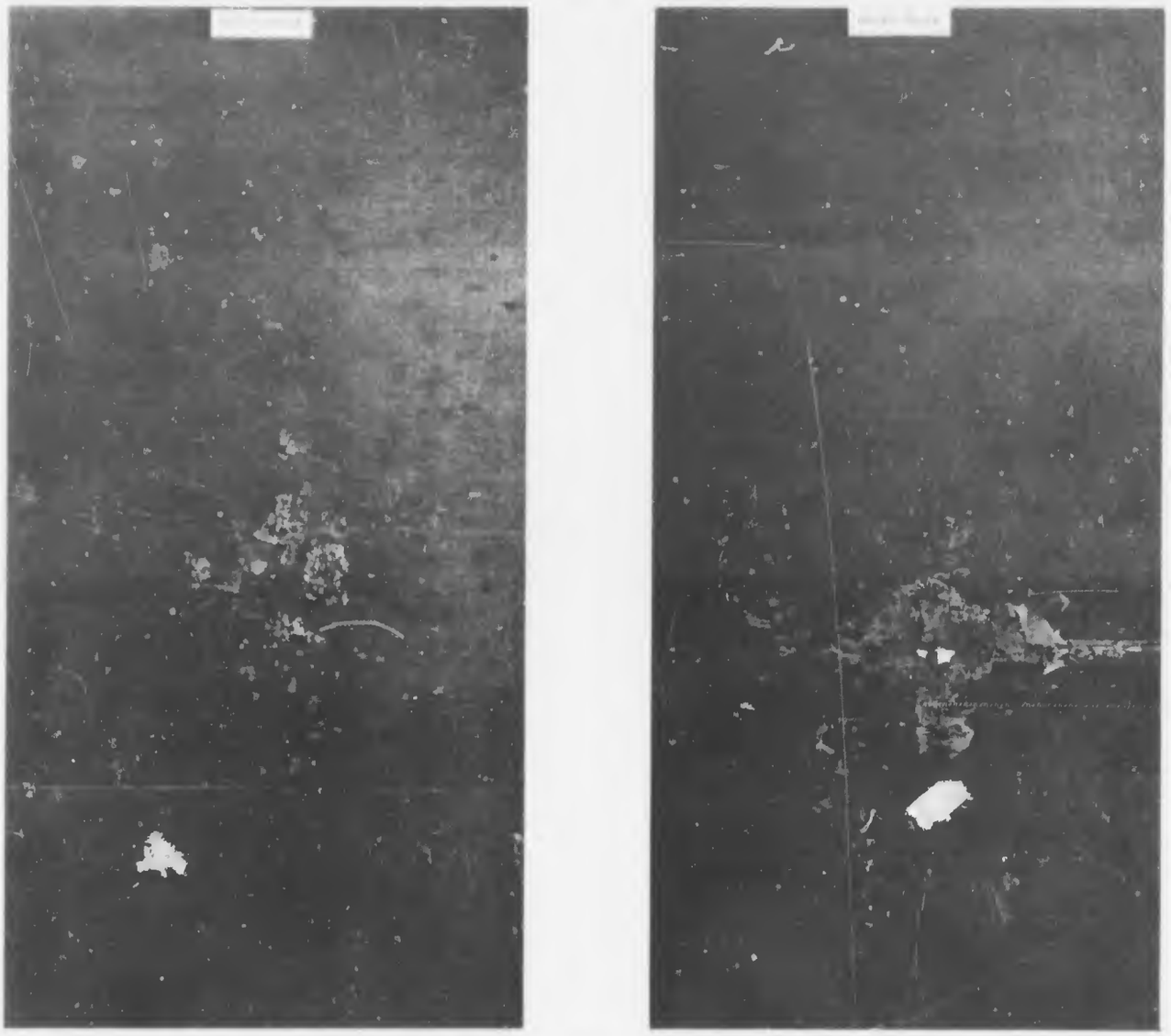

A GD-LS-70-1B (56 kA)

B GD-LS-70-2B (73 kA)

FIGURE 29 - Uncoated Boron Panels After Testing (Front Sides Shown)

causing one small broken spot on the back of the panel.

Sample GD-LS-70-2B (73 kA)

The damage to this panel is shown on Figure 29B. As indicated, the damage consists of a spalled region in which the boron composite material was blown away from the panel. In this way it is very similar to the kind of damage one observes if a high voltage simulated lightning arc strikes a piece of concrete and punctures the concrete to a conductive reinforcing bar inside the concrete. The concrete blown away leaves a shallow conical depression of width several times its depth.

Sample GD-LS-70-3B (88 kA)

This specimen is shown on Figures 30 and 31. This higher current causes progressively more damage. The damaged area is elliptical, of about 3 inches length and 1.5 inches width. The damage shows a definite ply effect. The fibers at right angles underneath the surface seem to conduct current out to the sides away from the arc-impingement point. There begins to appear damage also at the grounded current exit point where the current must flow across the surface of the panel out to the ground electrodes. As on all of the panels, the current blew a hole completely through the panel.

Sample GD-LS-70-4B (168 kA)

As was the pattern previously, the damage to the boron panel was much more severe than to the most nearly comparable graphite sample (Figure 12). There is a definite effect of the plies in spreading the damage at the arc impingement point out toward the edges of the panel. Damage was also observed all the way down the panel from the arc impingement point to the ground electrode.

2.2.4.1 X-Ray Radiographs

Extraction X-ray radiographs of the damaged areas of these four boron panels are shown on Figures 32 through 35. The atomic cross sections of boron are such that much more interesting radiographs can be taken of boron than can be taken of graphite. As on the graphite samples they show the outline of the damaged area, but not generally any better than does the panel itself. At the higher current levels they do begin to show a pattern of some nature surrounding the obviously damaged areas. On the high quality photographic prints they show speckled regions that are lighter than the surrounding dark

A GD-LS-70-3B
(88 kA)

B GD-LS-70-4B
(168 kA)

FIGURE 30 - Uncoated Boron Panels After Testing (Front Sides Shown)

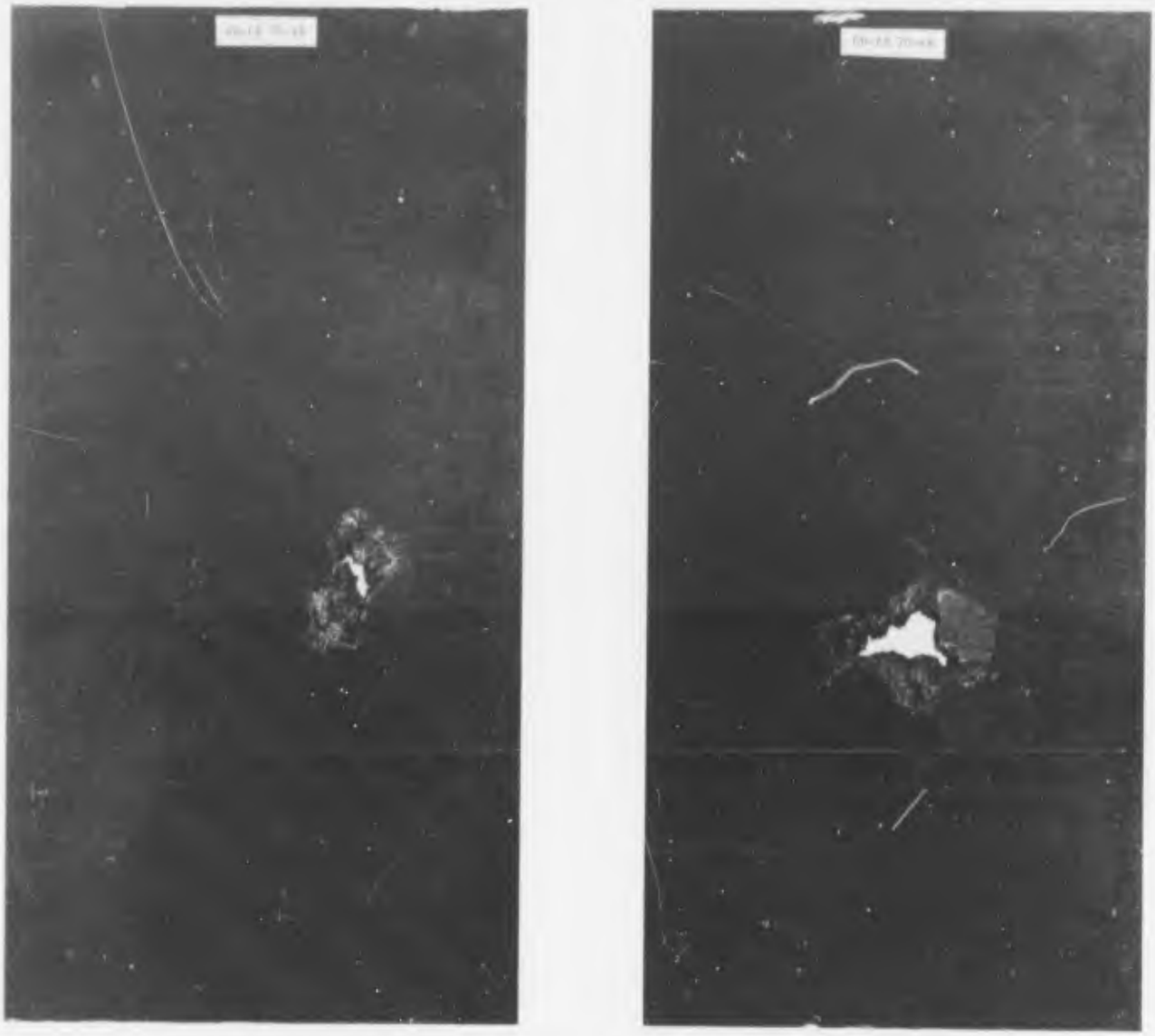

A GD-LS-70-3B (88 kA)

B GD-LS-70-4B (168 kA)

FIGURE 31 - Uncoated Boron Panels After Testing (Back Sides Shown)

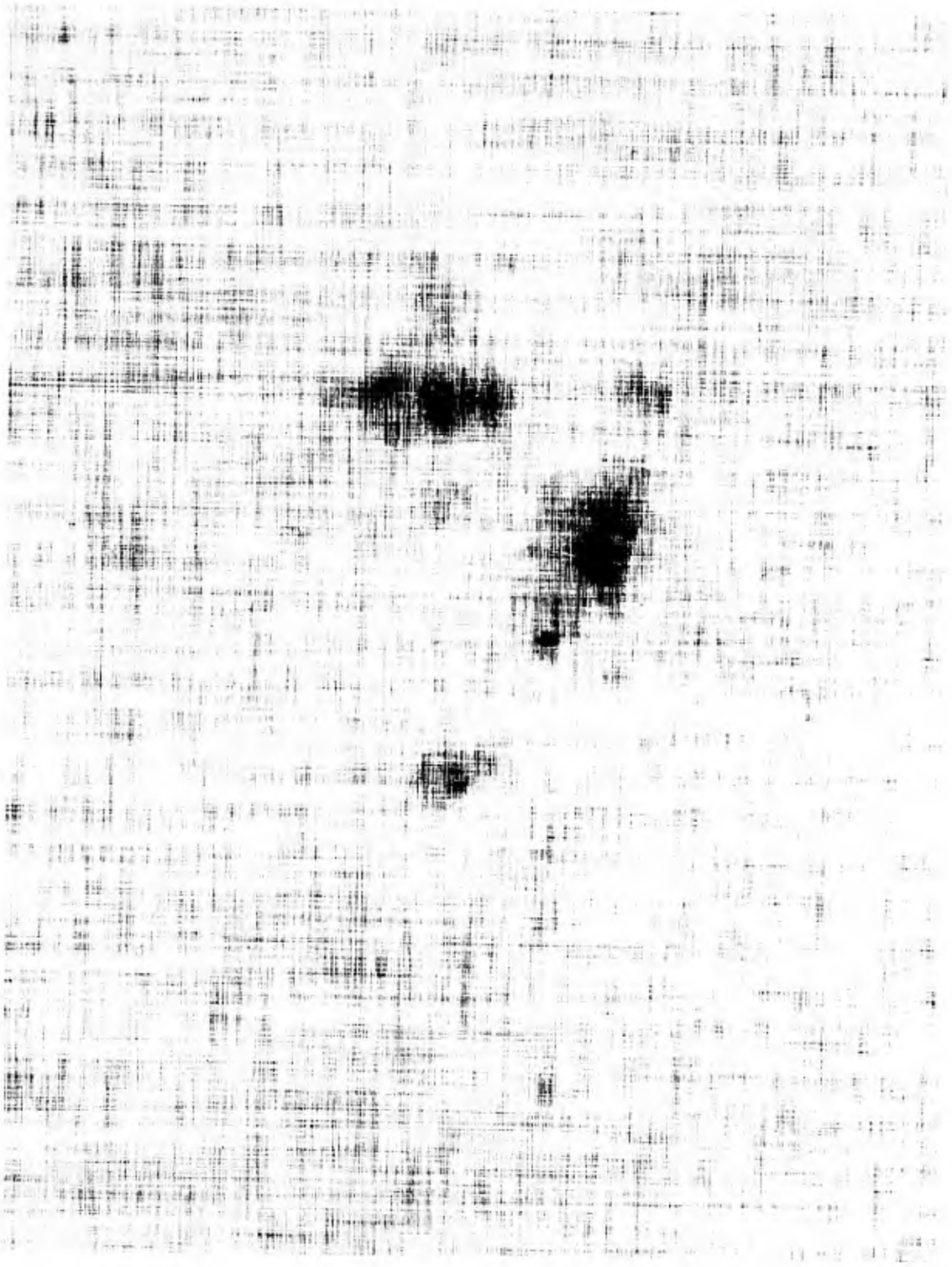

GD-LS-70-1B
(56 kA)

FIGURE 32 - 2X Extraction Enlargement of Radiograph of Boron-Epoxy Panel After Testing

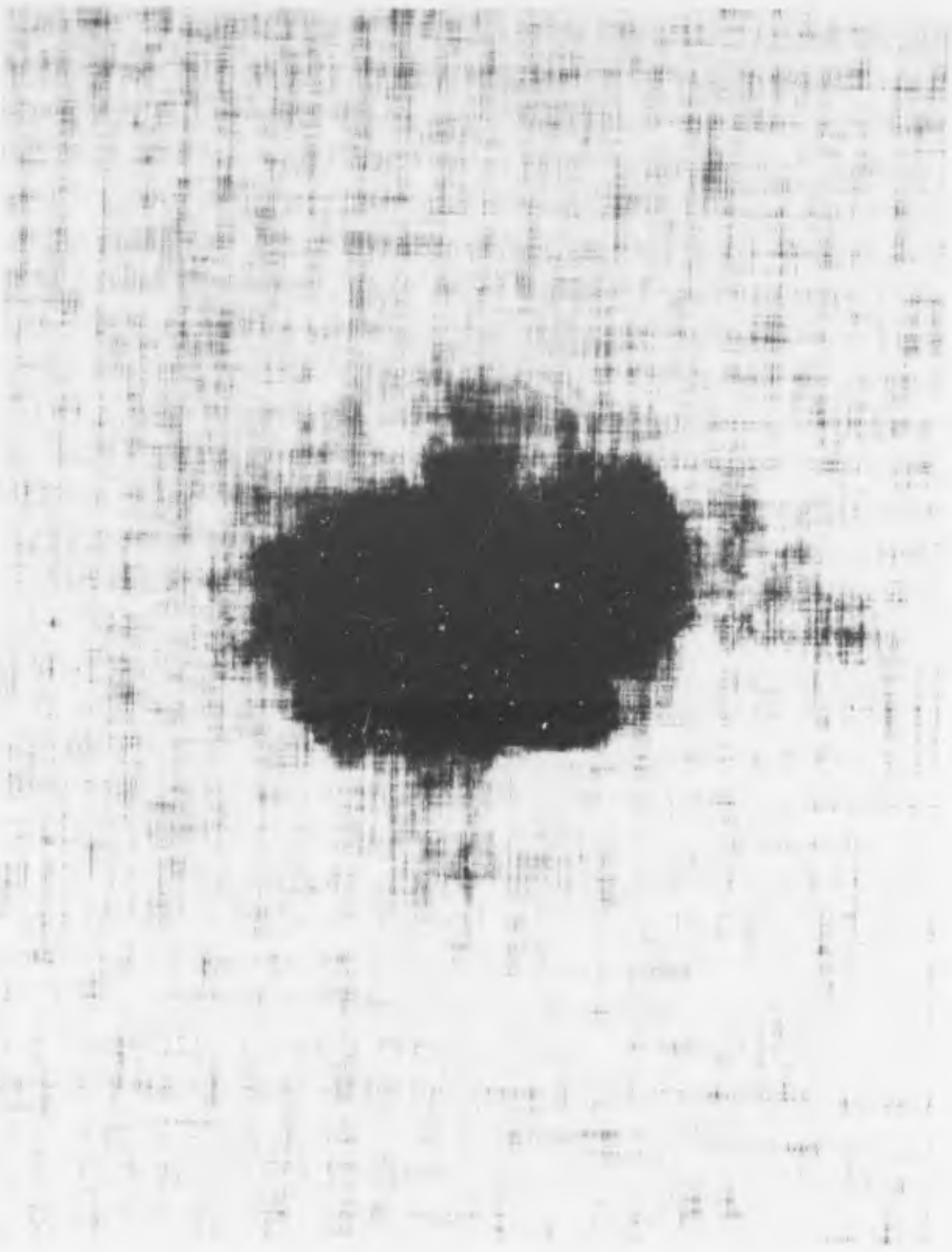

GD-LS-70-2B
(73 kA)

FIGURE 33 - 2X Extraction Enlargement of Radiograph of Boron-Epoxy Panel After Testing

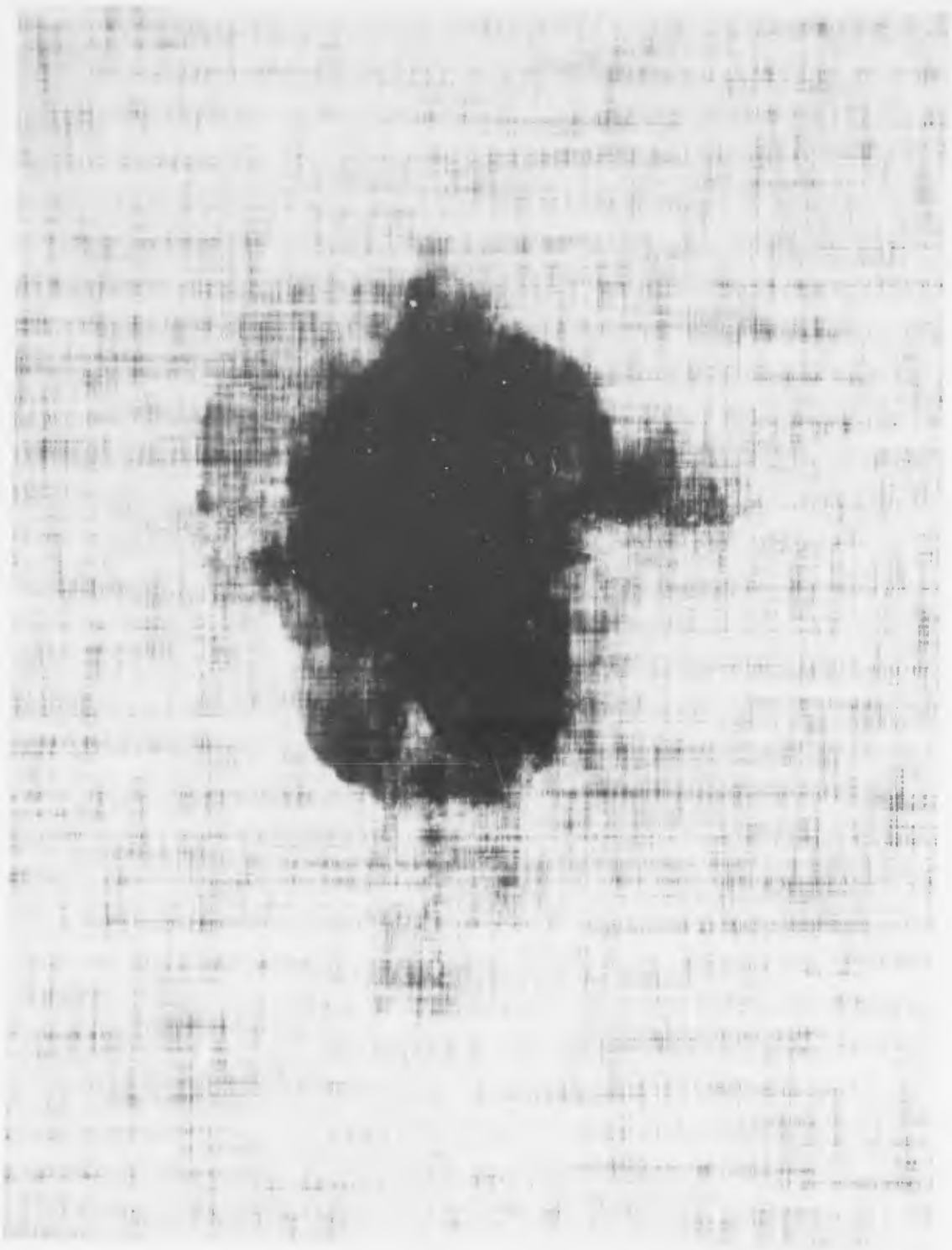

GD-LS-70-3B
(88 kA)

FIGURE 34 - 2X Extraction Enlargement of Radiograph of Boron-Epoxy Panel After Testing

GD-LS-70-4B
(168 kA)

FIGURE 35 - 2X Extraction Enlargement of Radiograph of Boron-Epoxy Panel After Testing

regions in which the boron fiber material was blown free of the panel. Possibly these are points where the individual strands of boron have intersected and were more badly burned at the point of intersection.

2.2.4.2 Ultrasonic "C"-scan Results

The ultrasonic "C"-scan displays of the damaged regions of the above four panels are shown on Figures 36 through 39. The damaged regions again show as a white area on the pictures, and again do not seem to show damaged regions that were not visually evident from the panels themselves. The area of the display on the "C"-scan pictures can serve as a rough measure of the damaged areas of the panels if one wishes to correlate damaged area to lightning current amplitude.

2.2.4.3 Resistivity Measurements

For resistance measurements on the boron fiber panels the same fixture was used for the graphite panels. These boron panels had resistance of 150 to 150,000 ohms. It was necessary to use the Leeds and Northrup Wheatstone bridge with two 1.5 ohm batteries in series. Contact resistance was negligible in this case, although the resistance did change with time if the panel was left energized. One panel was measured twice, showing reasonable duplication; the rest of the panels were measured only once.

The resistance measurements of each boron panel are shown on Figures 40 and 41. The tab measurements, 1-2, 3-4, 5-6, provide a base line for the undamaged panel in the short direction. Tabs 7-8, 9-10, and 11-21 represent the average resistance through the damaged area. In all boron panels the resistance changed by at least one order of magnitude through the damaged area, a behavior which was not noticed on the graphite panels. Sample 3B shows a much smaller change in resistance than the other three. Mechanical damage is estimated to be substantially less in this panel.

Initially, it was assumed that tabs 1-6 and 2-5 should represent a base line measurement of the resistance for the undamaged composite. It was assumed also that the values across tabs 7-12 and 8-11 would provide an "Integrated" index of the damage in the stroke attachment area for the 0 degrees and 90 degrees ply orientations. Examination of the data on boron composites in these two figures suggests that the current paths may not necessarily follow the anticipated course. First of all, the resistance values across tabs 1-6/5-2 and 7-12/8-11 are not self-consistent. In the case of panels 1B and 3B the

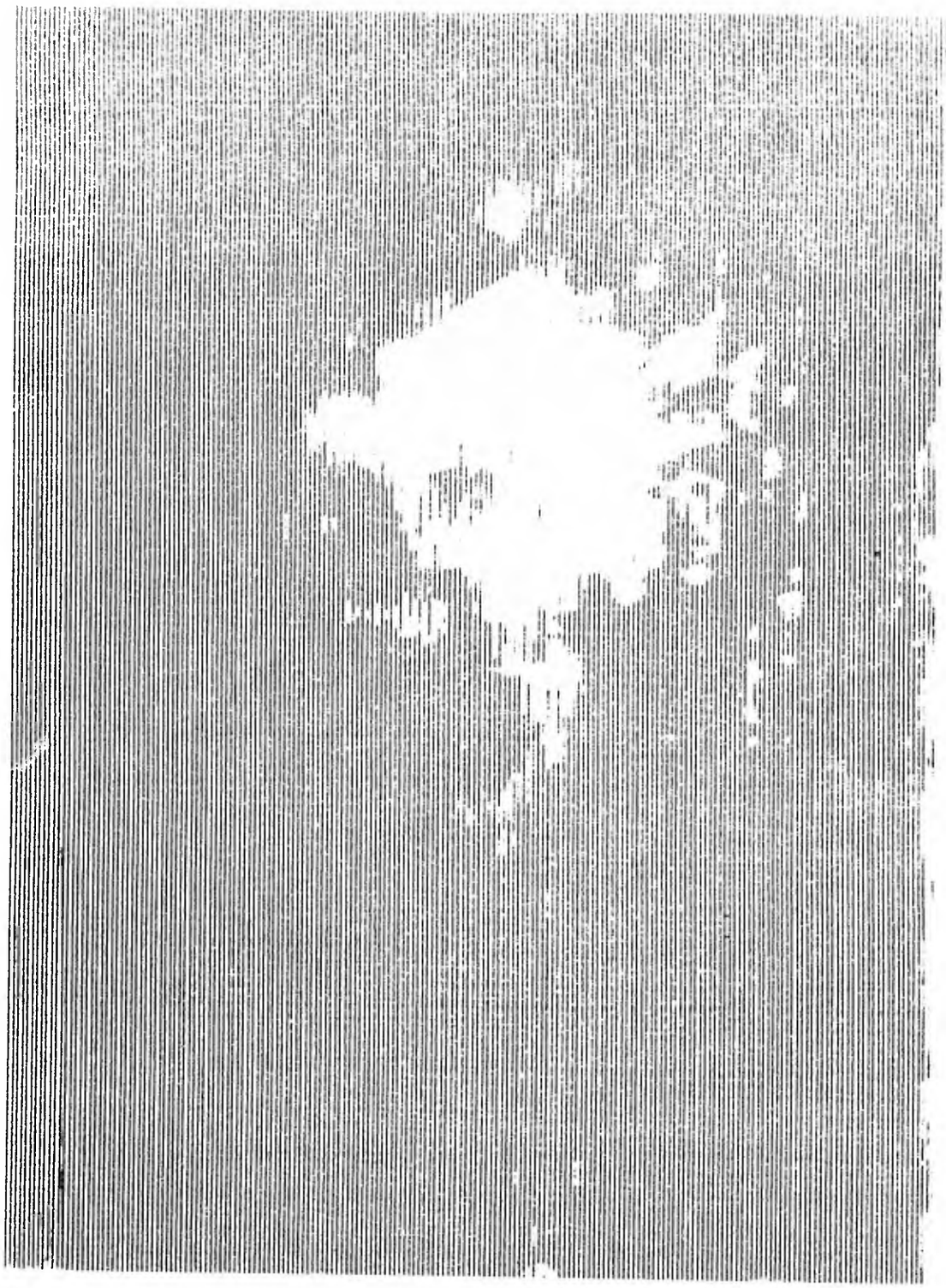

GD-LS-70-1B
(56 kA)

FIGURE 36 - Ultrasonic "C" Scan of Boron Epoxy Panel After Simulated Lightning Test

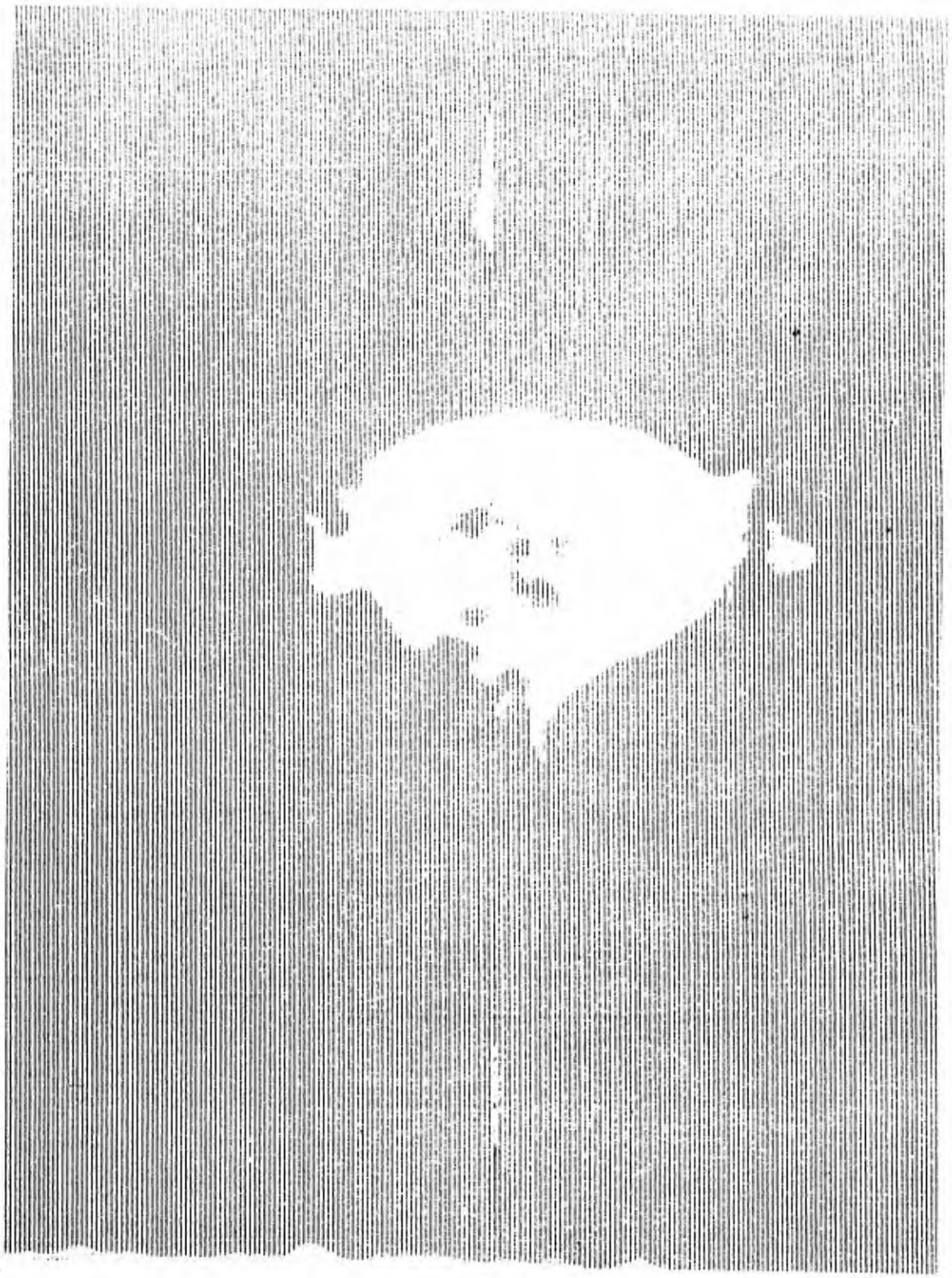

GD-LS-70-2B
(73 kA)

FIGURE 37 - Ultrasonic "C" Scan of Boron Epoxy Panel After Simulated Lightning Test

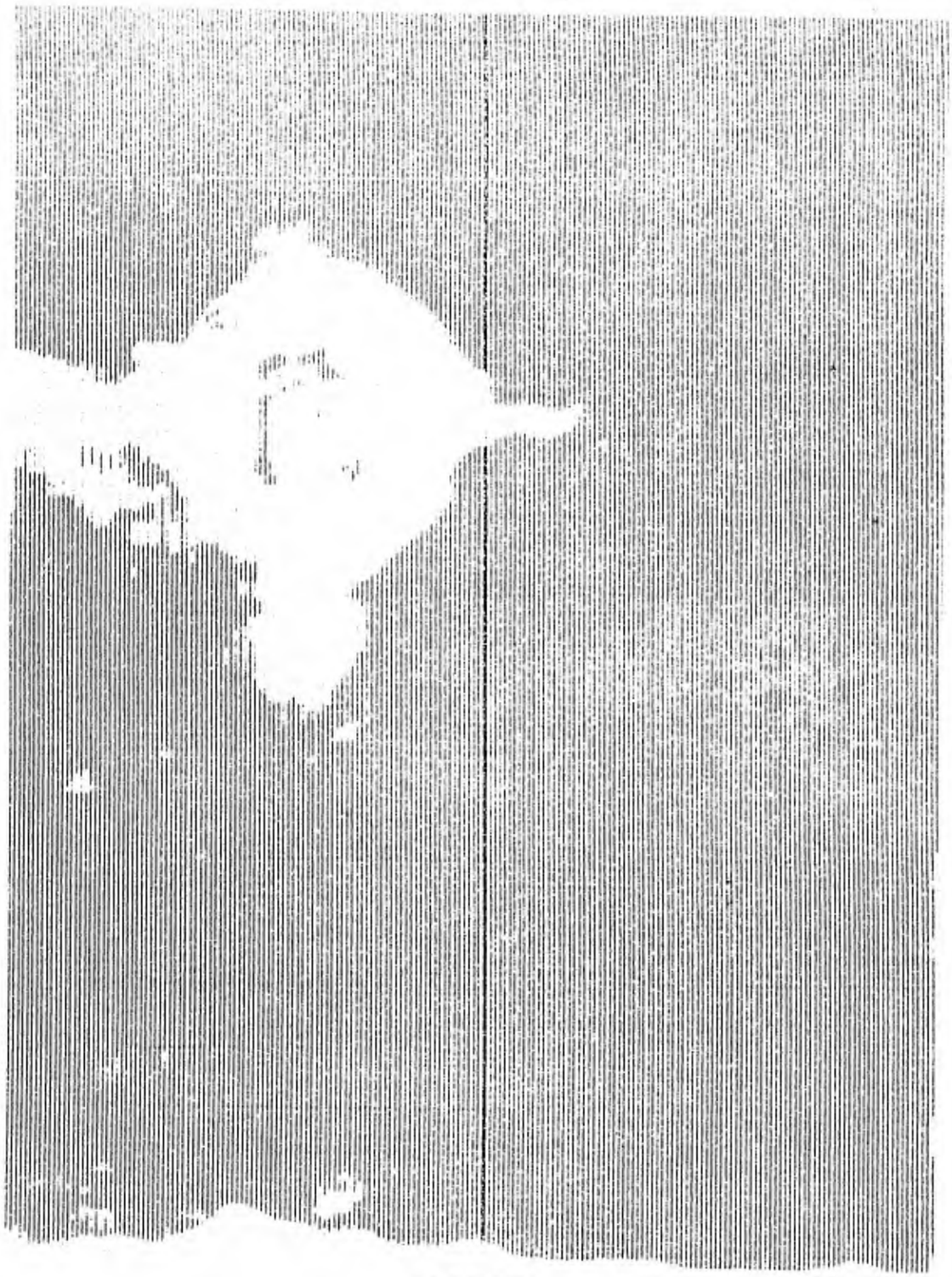

GD-LS-70-3B
(88 kA)

FIGURE 38 - Ultrasonic "C" Scan of Boron Epoxy Panel After Simulated Lightning Test

GD-LS-70-4B
(168 kA)

FIGURE 39 - Ultrasonic "C" Scan of Boron Epoxy Panel After Simulated Lightning Test

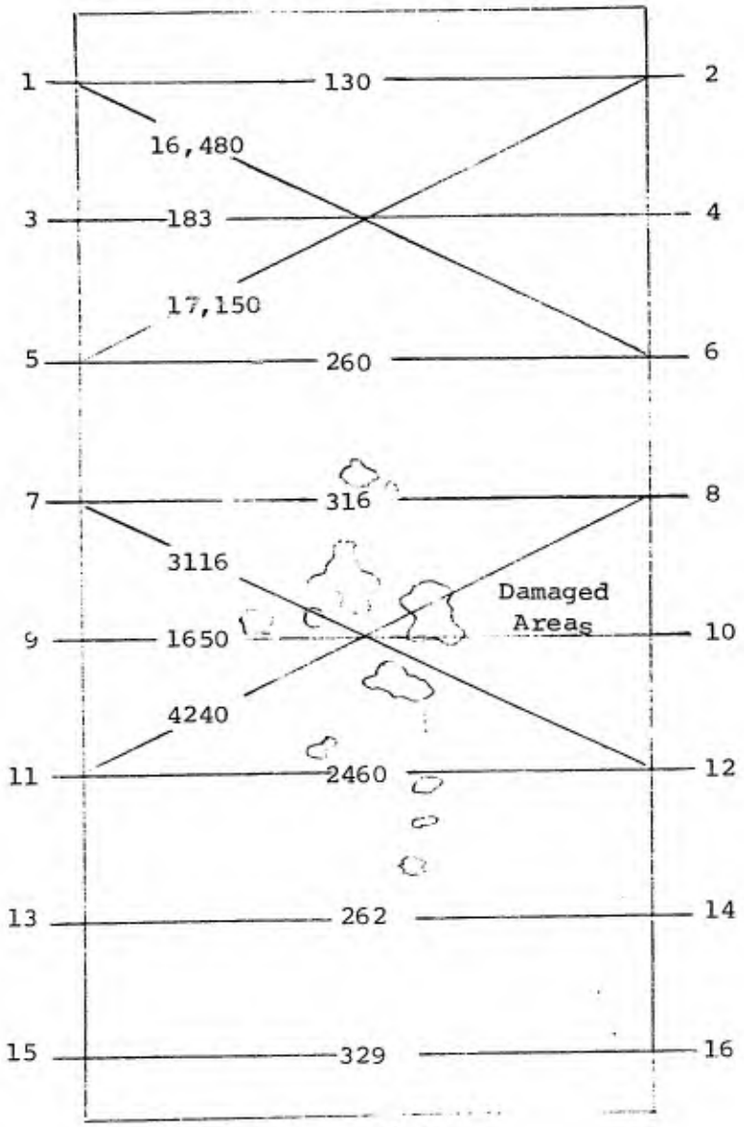

GD-LS-70-1B
(56 kA)

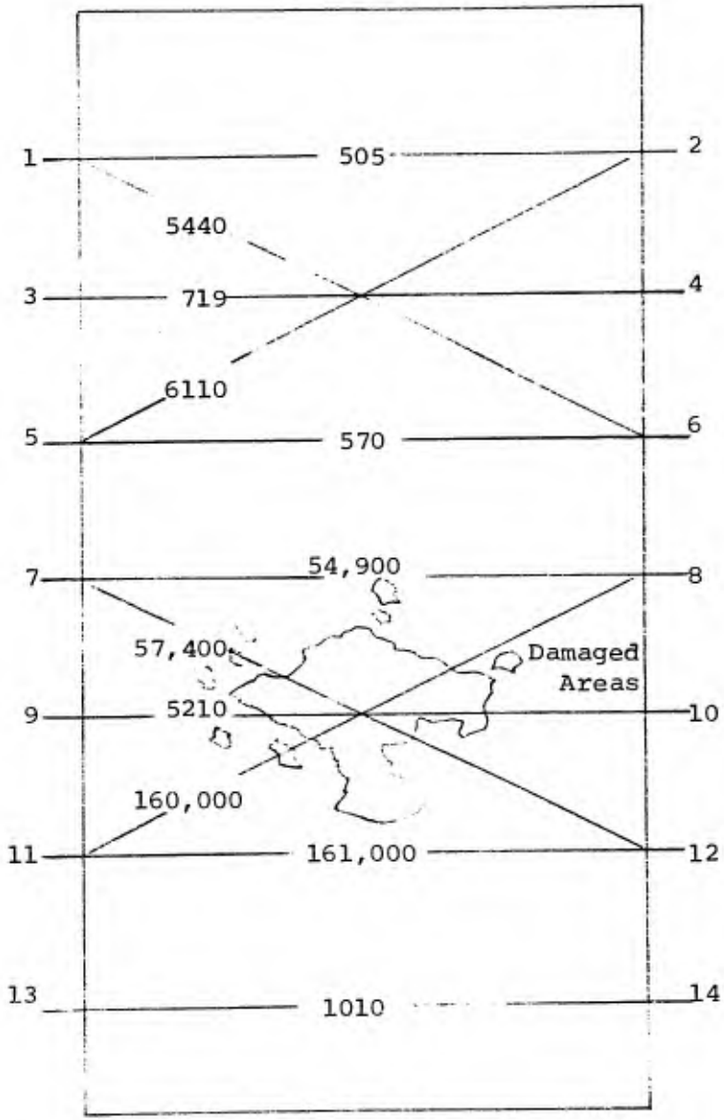

GD-LS-70-2B
(73 kA)

FIGURE 40 - Resistance Measurements on Boron Epoxy Panels After Simulated Lightning Current Exposure.
(Resistance Values Are in Ohms)

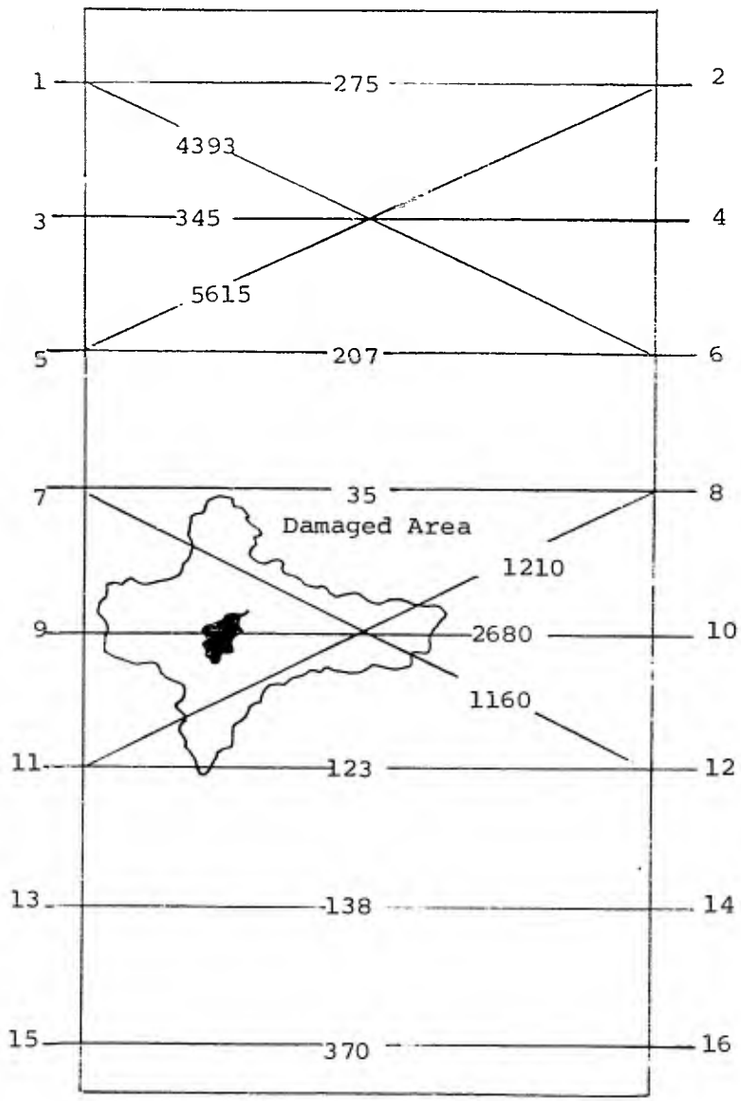

GD-LS-70-3B
(88 kA)

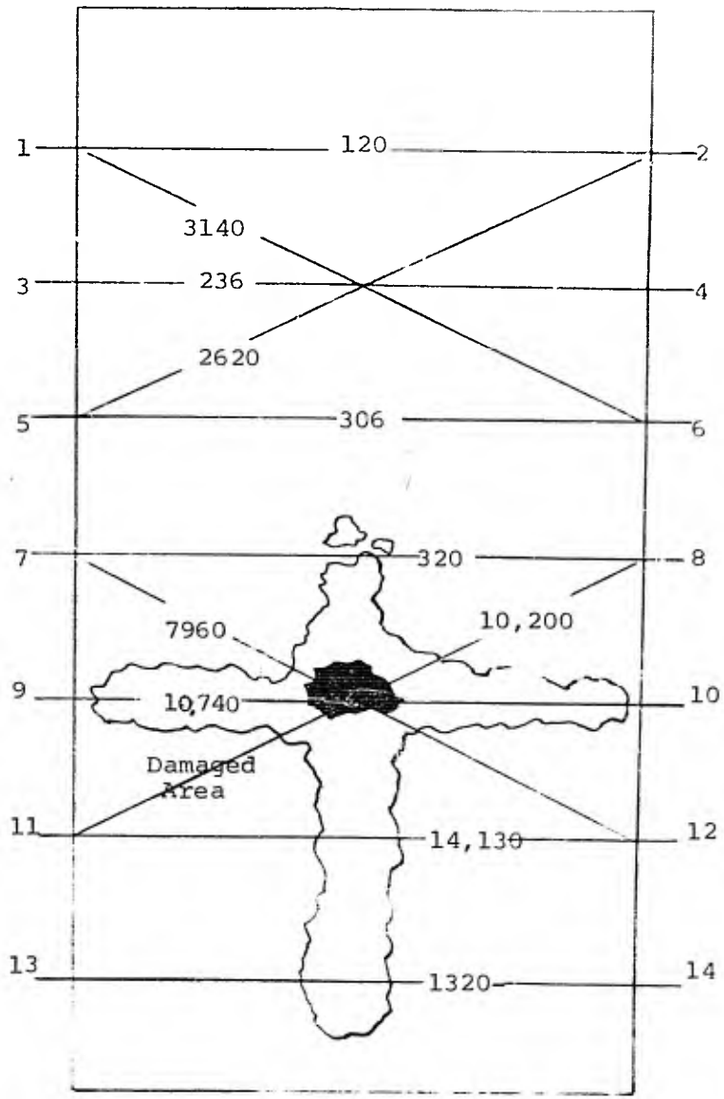

GD-LS-70-4B
(168 kA)

FIGURE 41 - Resistance Measurements on Boron Epoxy Panels After Simulated Lightning Current Exposure. (Resistance Values Are in Ohms)

values for tabs 1-6/5-2 are higher than across the 7-12/8-11 diagonals. Panels 2B and 4B show the reverse trend, indicating that if opposite tabs are evaluated, a somewhat different conclusion may be reached. Tab pairs 1-2, 3-4, and 5-6 should also have similar resistance values if the stroke attachment point is not too close. The data on the figures show this to be true, with values ranging from a minimum of 130 to 1320 ohms. The tab pairs through the damaged area at the point of stroke attachment show large changes in magnitude, always in a direction that would be predicted, based on the damage mechanism cited earlier. Panel 2B shows an interesting variation in resistance in that tabs 7-8 and 11-12 show more extensive damage as measured by resistance change than the 9-10 pair. No explanation of this effect could be deduced from X-ray extractions or "C"-scan data.

In all cases, the diagonal resistance measurements in the undamaged area, tabs 1 through 6, are much higher than the corresponding measurements directly across the panel. Presumably for current to flow from tab 1 to tab 6, it must flow through the boron fibers that run transverse to the panel, and then cross over to the fibers that run axially along the panel. These boron fibers are much larger in diameter and do not have nearly the number of intercepted points that the graphite fibers do. Photomicrographs of the boron materials later to be presented will show this more clearly. In addition, it has been found in previous reports that the lowest resistance portion of a boron fiber is in the W_4B_5 substrate. The boron itself that is deposited on the substrate is a very high resistance material.

All in all, it would appear that resistance measurements have much more chance of showing damage in boron materials than in graphite materials. There appears a good chance that they would reveal hidden damage if it were to occur, although all of the data so far presented would indicate that in the vicinity of a lightning stroke attachment point there would be no damage that was not visually evident at the surface.

2.2.4.4 Short Beam Shear Tests

Short beam shear test specimens were cut from the boron panels in the same general pattern as previously discussed for the graphite panels. Now that the data on the boron and graphite panels have both been presented, it is appropriate to discuss some more of the expected test results of these short beam shear tests. To begin with, little current should flow in the vicinity of tabs 1 to 4; thus these tabs should show little, if any, degradation. The set of tabs 1 through 4 from all tested panels, should, in fact, be representative of the

intrinsic properties of the test panels.

Tab 14 lies in the most direct line of flow from the stricken point. Current should flow axially along adjacent filaments to this tab. Tab 13 should have the same amount of current flowing through it, but the current could be expected to flow along the boron filaments that are transverse to the tab. The beam shear test, as shown on Figure 42, evaluates mostly the strength of the filaments along the axis of the tab. Filaments transverse to the tab could only transmit a force to the restraint through the resin binder acting in shear. Since the shear strength of the resin is negligible, damage to the transverse filaments should not reveal itself on a beam test. Consequently, tab 13 should always be stronger than tab 14.

Likewise, tab 16 should be weaker than tab 15, particularly since tab 15 comes from a portion of the test panel between the grounded end clamps.

Tabs 10 and 12 should show more damage than tabs 9 and 11.

In the region of tabs 5 through 8 current flow should be at an angle, with a component directed along the axis of each of the tabs. It would be reasonable to expect roughly similar amounts of damage to each of these tabs. One might also assume that tabs 10 and 12, being more nearly in line with the direct flow of current, would experience more damage than tabs 6 and 8. This discussion assumes the panel conductivity is homogeneous. The resistance measurements just presented, show that the boron panels are in fact not homogeneous, although electrically the graphite panels are much more homogeneous than the boron panels.

In addition, one might expect that the boron panels would experience more damage than the graphite panels, based on graphite's greater conductivity.

Most of these speculations are proven correct when the results of the short beam shear tests presented in Tables VIII and IX and summarized in Table X are analyzed. Apparently there is statistically significant damage on the graphite panels at the 142 kA level, but it is not as much as observed on the boron panels. The beam shear strengths are uniform, at least on panels 1G and 2G. On panel 3G, damage to the tabs near the bottom of the panel skews the frequency distribution strengths toward the lower values. This is shown more clearly on Figure 43 and Figure 44 where the percentage distributions are plotted.

On the boron samples, the pattern of damage was more clearly evident. Figure 44 shows the cumulative frequency distributions. The skew-in toward lower values simply showed that some of the tabs were damaged. One anomaly shows up in Sample GD-LS-70-3B, tested at 88 kA. This sample had higher beam strengths than did Sample GD-LS-70-2B, tested at 72.7 kA. It is not much

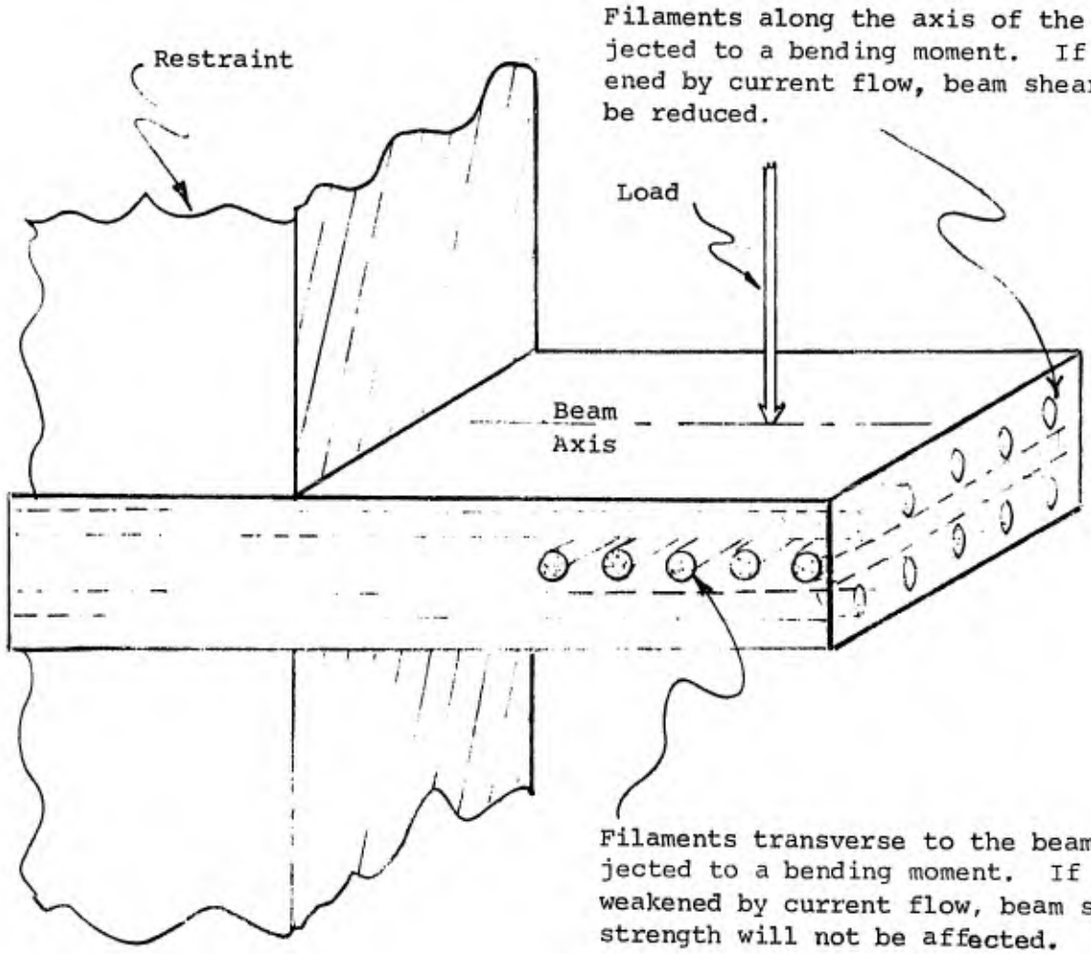

FIGURE 42

Beam Shear Test

TABLE VIII

GRAPHITE/EPOXY COMPOSITES
SHORT BEAM INTERLAMINAR SHEAR TEST

Tab Number	GD-LS-70-1G, σ PSI	GD-LS-70-2G, σ PSI	GD-LS-70-3G, σ LSI
1	11,752	13,043	12,609
2	12,061	12,519	12,560
3	11,965	12,636	12,960
4	11,333	11,986	12,058
5	13,925	13,051	12,082
6	11,373	12,118	12,579
7	12,459	13,399	11,638
8	12,092	11,938	11,111
9	12,531	12,143	12,773
10	12,342	13,396	12,383
11	11,623	12,062	12,308
12	11,343	12,177	12,328
13	10,234	13,000	9,919
14	11,458	12,495	10,300
15	13,003	15,296	11,189
16	12,806	12,264	9,781

TABLE IX

BORON/EPOXY COMPOSITES
SHORT BEAM INTERLAMINAR SHEAR TEST

Tab Number	GD-LS-70-1B, σ PSI	GD-LS-70-2B, σ PSI	GD-LS-70-3B, σ PSI	GD-LS-70-4B, σ PSI
1	6,787	7,617	7,739	8,000
2	6,036	6,726	6,491	4,573
3	8,429	6,392	7,456	6,432
4	5,682	5,833	5,939	5,877
5	6,000	6,441	5,796	2,362
6	7,719	4,669	5,594	3,915
7	6,400	6,903	2,478	2,888
8	7,273	5,304	5,152	4,709
9	6,789	7,812	8,026	4,014
10	6,343	4,934	6,785	2,681
11	7,353	7,455	7,927	3,805
12	6,344	5,110	7,170	3,059
13	6,903	7,325	6,711	4,484
14	6,696	2,600	2,403	1,723
15	6,928	6,036	5,772	5,746
16	6,795	2,333	5,022	2,368

TABLE X

SUMMARY OF SHORT BEAM SHEAR RESULTS

Panel Number	Material	Test Current Level-KA	Mean Shear Strength PSI	Adjusted Standard Deviation
Tabs 1 - 4 of Panels 1G,2G,3G		*	12290	511
GD-LS-70-1G	Graphite	64	12019	851
2G	Graphite	98	12720	846
3G	Graphite	142	11786	1029
Tabs 1 - 4 of Panels 1B,2B, 3B,4B		*	6626	1010
GD-LS-70-1B	Boron	56	6780	688
2B	Boron	72.7	5843	1639
3B	Boron	88	6029	1692
4B	Boron	168	4165	1704

* - The assumption is made that these tabs are undamaged.

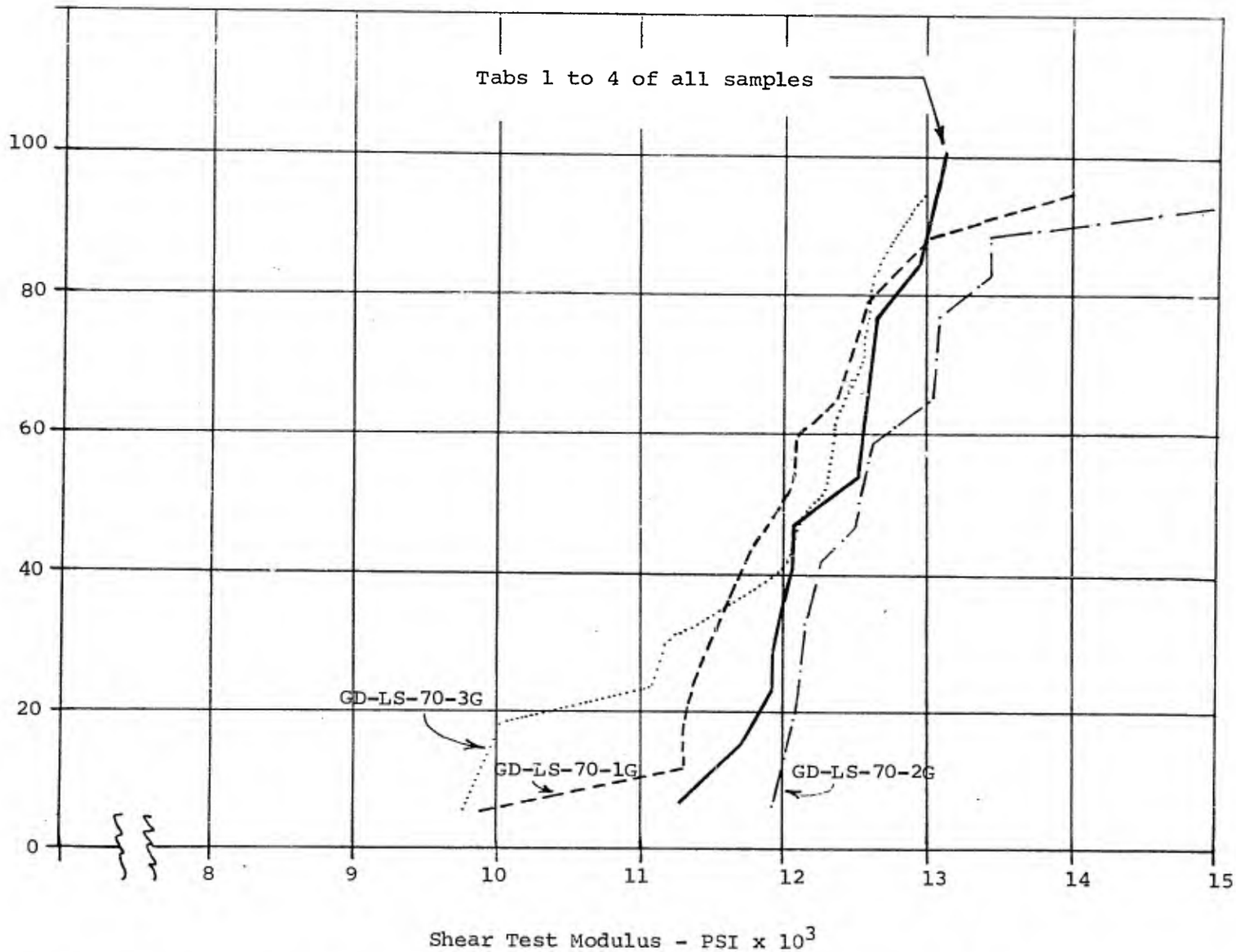

FIGURE 43 - Short Beam Interlaminar Shear Test Modulus of Graphite Test Specimens

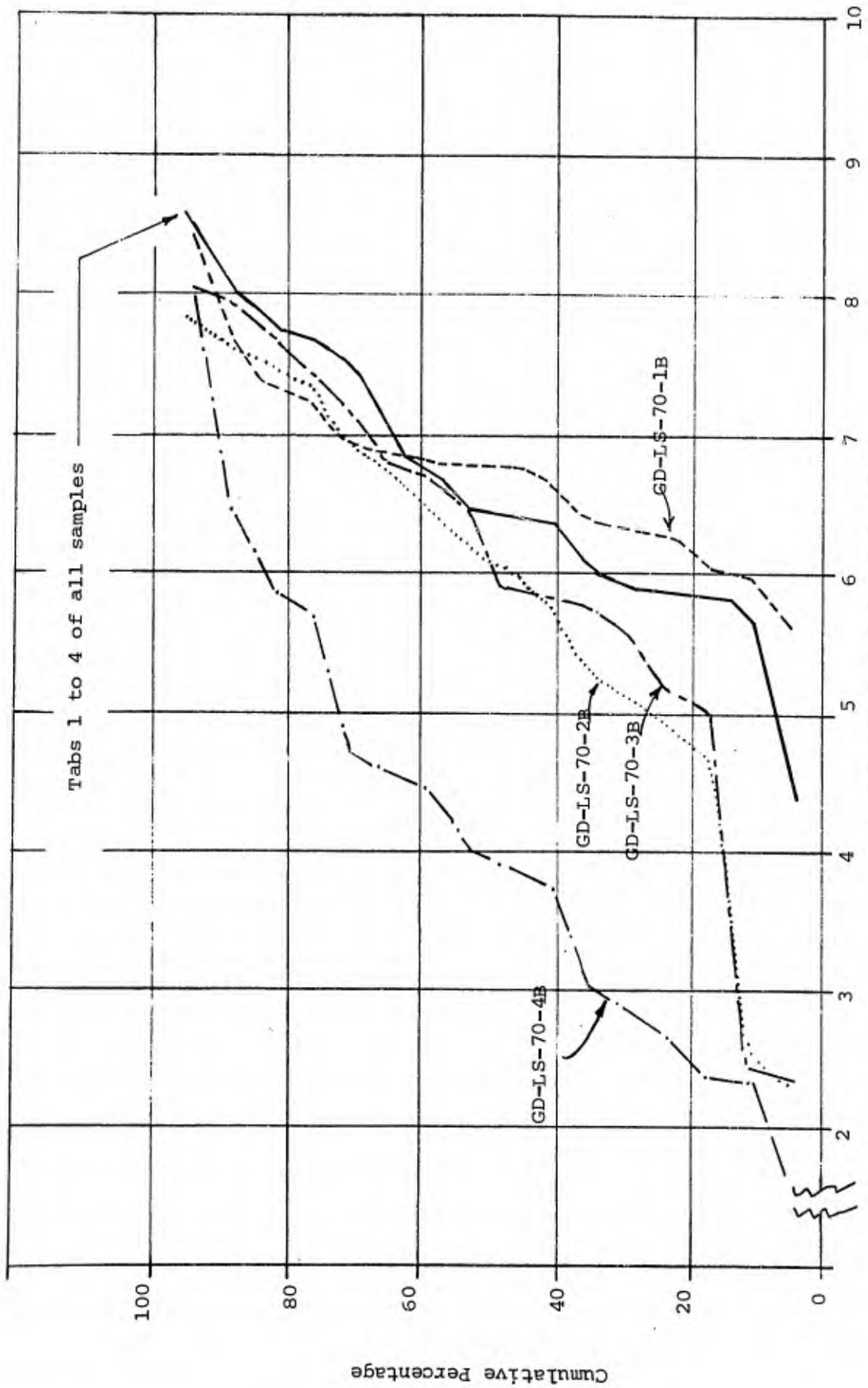

FIGURE 44 - Short Beam Interlaminar Shear Test Modulus of Graphite Test Specimens

stronger, but the trend seems real. The physical damage evident on panel 3B is also less than on panel 2B, and the same pattern showed on the resistance measurements. How much of this anomaly can be ascribed to intrinsic panel properties, and how much to the interaction of the stroke with the panel is hard to say. In any case, the boron panel was damaged significantly by a stroke that did not cause damage to a similar graphite panel.

Considerably more damage was caused by the 168 kA stroke to panel GD-LS-70-4B. Statistically significant damage was done to all tabs except tab 4. Tabs 1 to 4 were at the top of the panel. The patterns of damage revealed by studying the strength of the individual test tabs is interesting, and generally support conjectures raised earlier about how the expected current flow should relate to the expected damage. Tab 14 was damaged the most while tab 13, at right angles, was damaged much less. The same observation holds for tabs 15 and 16. Tabs 9 and 11 are stronger than tabs 10 and 12, since the current flow could be transverse to tabs 9 and 11, but axial on tabs 10 and 12. Tabs 5, 6, 7, and 8 all have roughly the same strength since the current flow should be at an angle at those tabs.

2.2.4.5 Photomicrographic Analysis

Photomicrographs of the boron samples are shown on Figures 45 through 48 and show some extremely interesting patterns. On these photomicrographs the front face of the panel again appears at the bottom of the figure. On sample GD-LS-70-1B only the bottom (on the photomicrograph), or surface rows of fiber are damaged. Cracks on other filaments are polishing cracks. The typical starshape cracking on the bottom filaments has been observed in other programs and occurs at a current density of about 10^5 amperes per square centimeter. This photograph thus provides some evidence that the current was confined, partially at least, to the plies next to the stricken face. The photomicrographs of panels GD-LS-70-2B and -3B show damage on all of the vertical plies. The damage is less intense on panel -3B than on -2B, which agrees with the visual observations of the panel surface, the short beam shear test, and the resistance measurements. Panel GD-LS-70-4B shows severe damage on all plies. This series of photographs is an excellent example of the progressive increase in the degree of damage as the arc current is increased. Figure 48, which shows the vertical destruction of almost every filament, is typical of the melting of the W_2B_5 core by excessive current.

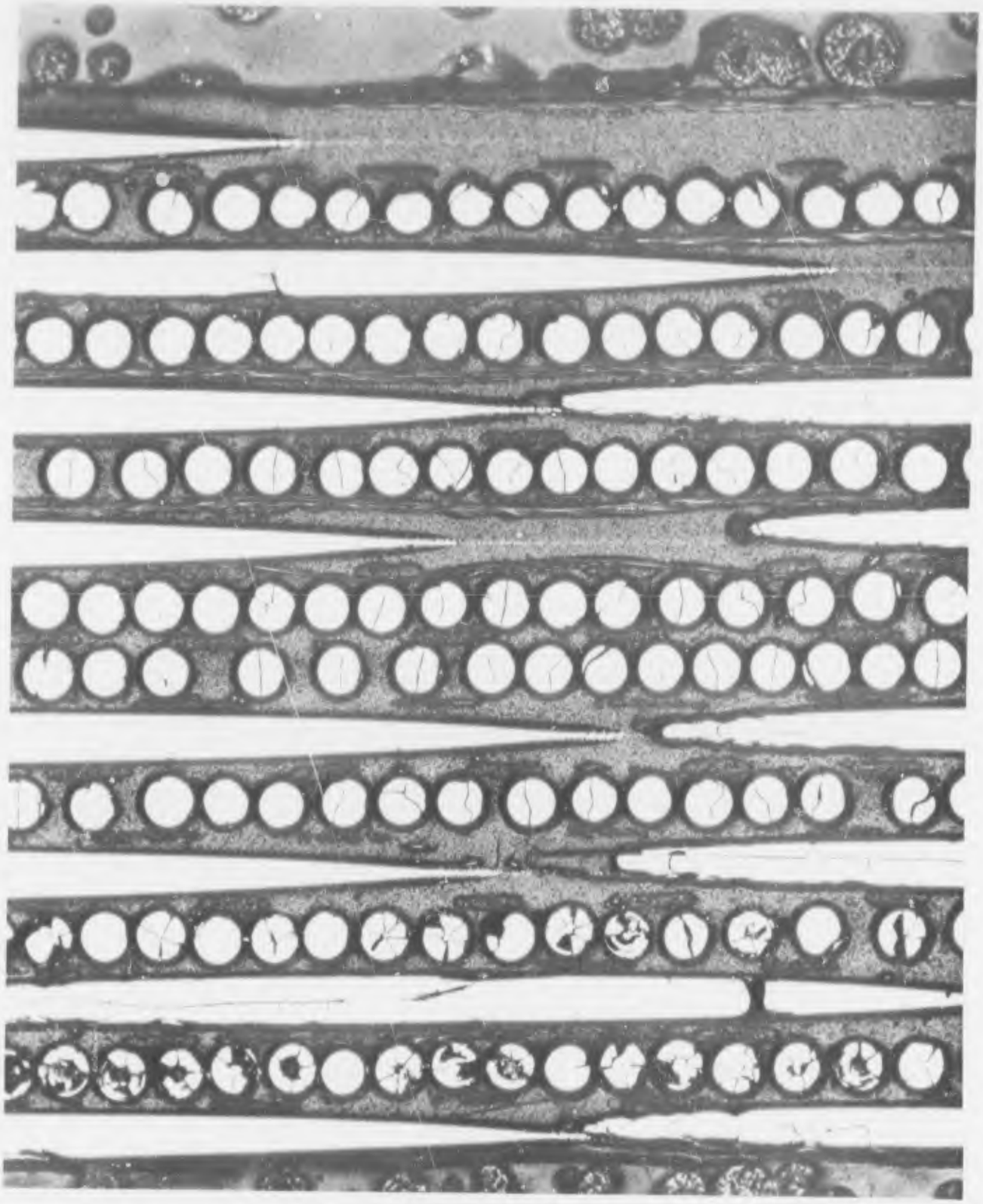

GD-LS-70-1B
(56 kA)

FIGURE 45 - 80X Photomicrograph of Tested Panel Showing Typical Star-Shaped Fractures of Boron Filaments at Bottom of Photo, First Two Rows Horizontal Fibers Undamaged. Panel Front at Bottom.

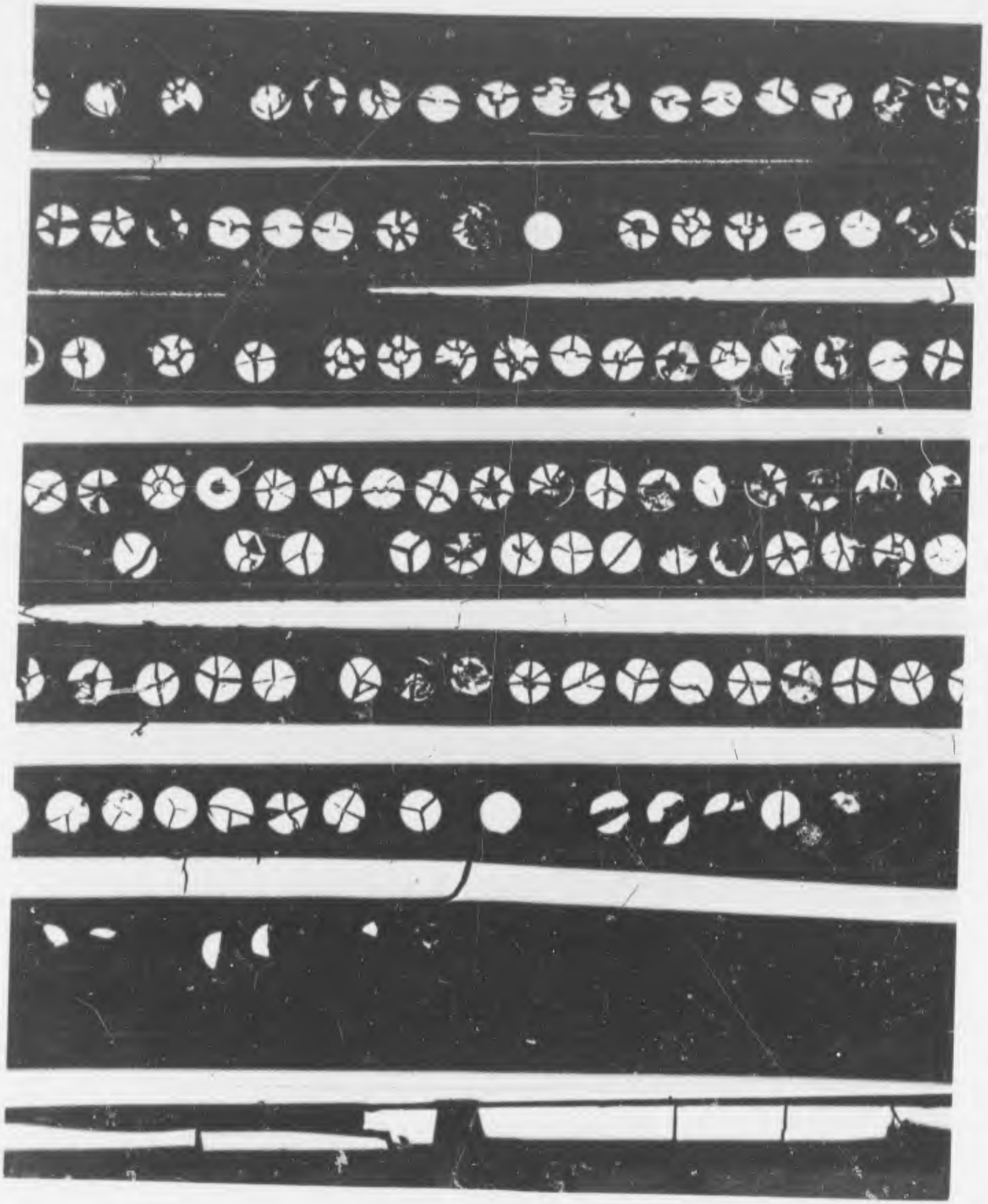

GD-LS-70-2B
(73 kA)

FIGURE 46 - 80X Photomicrograph of Tested Panel Showing Star-Shaped Damaged Filaments Dispersed. Note Beginning of Delamination at Bottom of Photograph. Panel Front at Bottom.

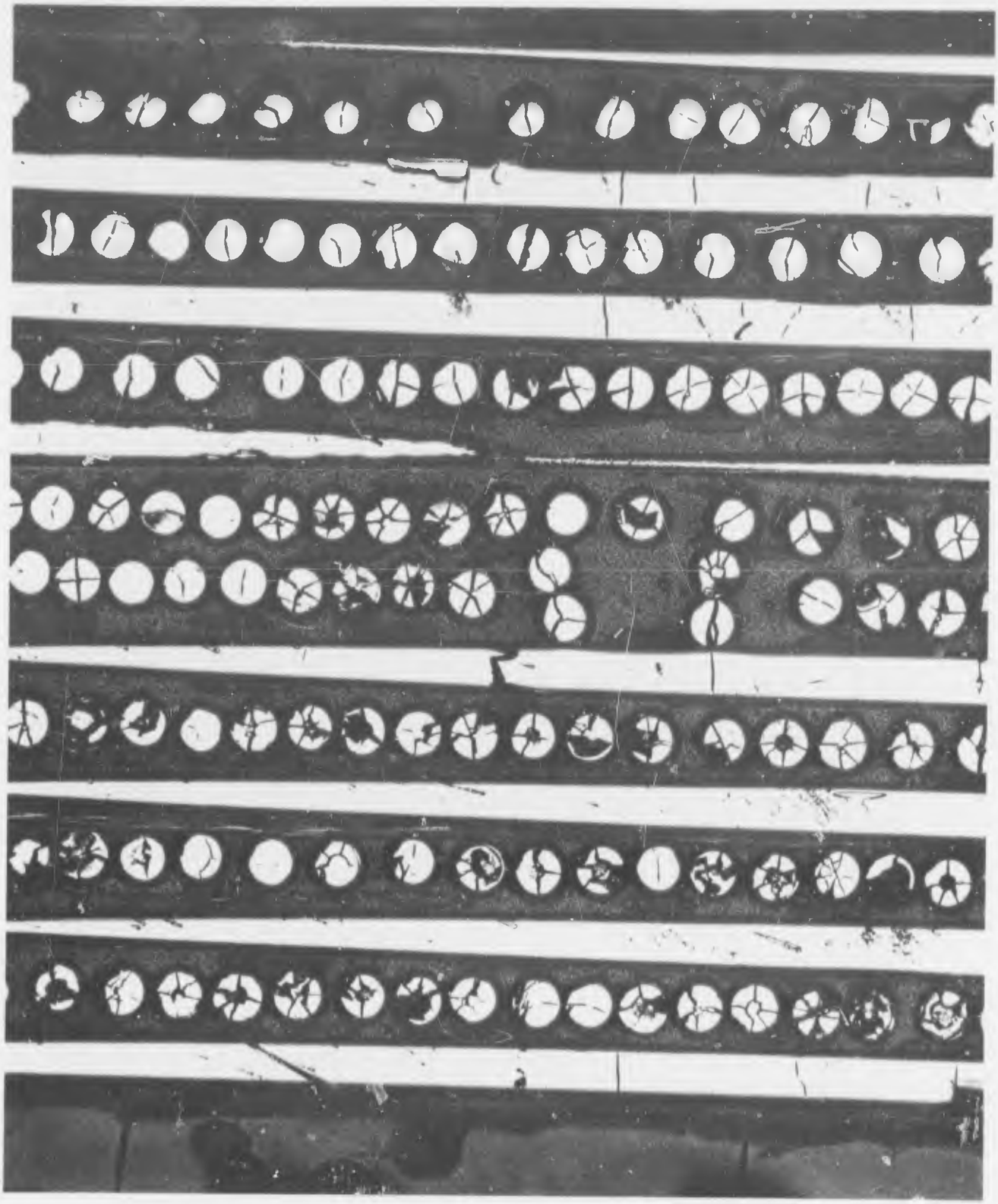

GD-LS-70-3B
(88 kA)

FIGURE 47- 80X Photomicrograph of Tested Panel. Damage Appears Less Severe than Preceding Sample. Star-Shaped Fractures Shown Slightly Past Center

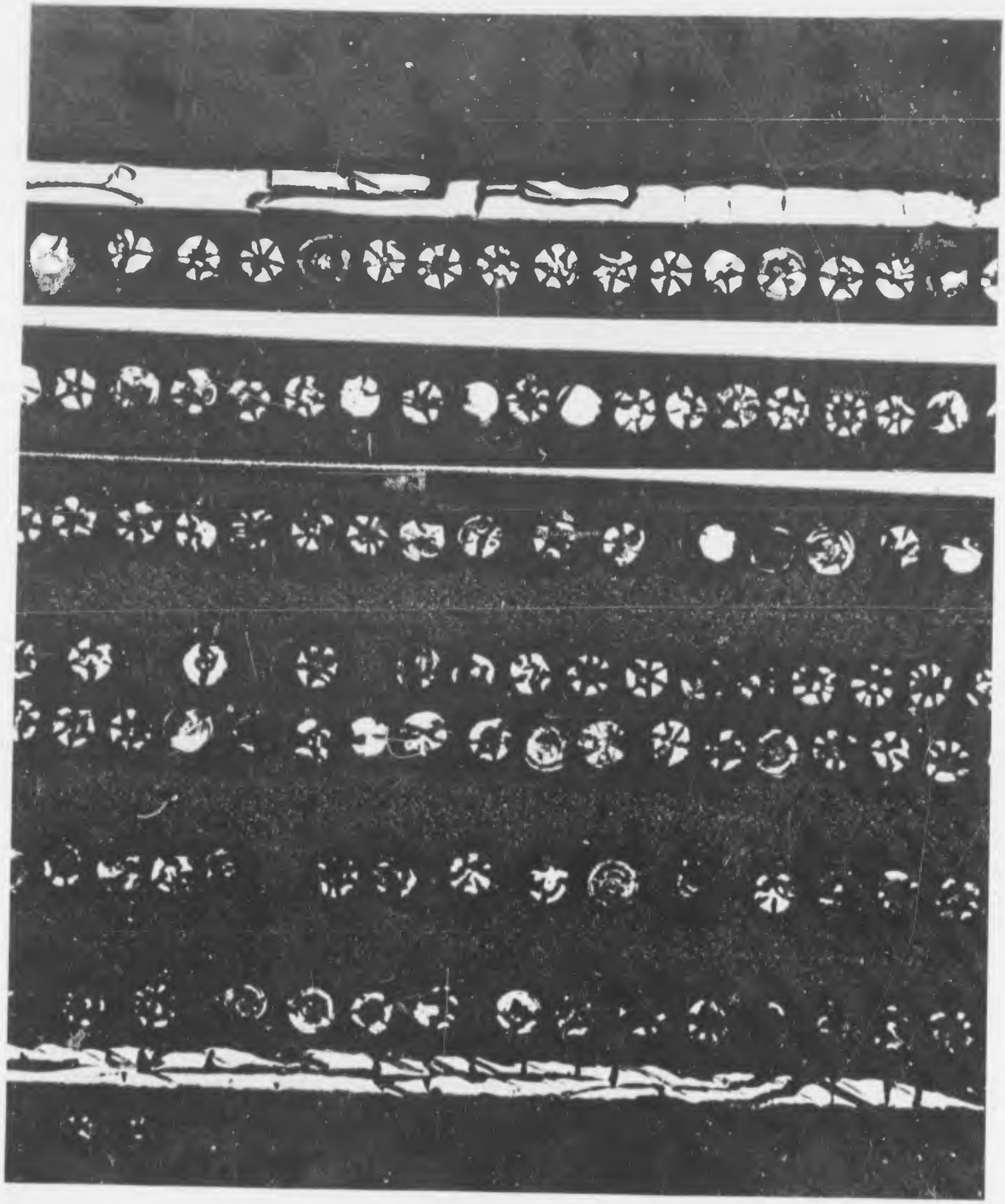

GD-LS-70-4B
(168 kA)

FIGURE 48 - 80X Photomicrograph of Tested Panel. Note Severe Damage on Nearly All Vertical Filaments and the Two Outside Horizontal Filaments Showing Decomposition. Panel Front at Bottom.

2.3 Parametric Study of Graphite Epoxy Panels

This series consisted of eighteen graphite/epoxy test panels each 13" x 13" in size. The test series was laid out to provide a parametric study of the effect of current amplitude, panel thickness, panel fiber layup and panel coatings. Table XI shows the matrix of tests made on the various panels. The general intent was to perform tests at three different lightning current levels, 50 kA, 100 kA, and 200 kA. On Table XI these are referred to as the nominal test current levels. The test current magnitudes actually attained are shown following the individual panel numbers. The panels fall into three general groups:

Group 1

These were uncoated laminates of 0° and 90° layup of two nominal thicknesses, 0.04 inch to 0.05 inch and 0.120 inch to 0.140 inch. The panels of 0.040 inch nominal thickness had four plies, arranged in a 0°, 90°, 90° and 0° pattern. Those of 0.120 inch nominal thickness were a balanced layup of sixteen plies arranged in a sequence 0°,90°,0°,90°,0°,90°,0°,90°,90°,0°, 90°,0°,90°,0°,90°,0°.

Group 2

These were uncoated panels of 0°, 45° and 90° layup, all of the same nominal laminate thickness of 0.120 inch to 0.140 inch. There were sixteen plies arranged in a pseudoisotropic pattern, 0°, 45°, 90°, 135°, 180°, 225° and so on.

Group 3

These were coated laminates using a silver epoxy coating of about 3 mils thickness. Again, two laminate thicknesses were used, 0.040 inch to 0.050 inch and 0.120 inch to 0.140 inch. Panel layups were 0° and 90°.

All panels were a graphite epoxy material. The reinforcement was Union Carbide Thornel-50 graphite yarn (PVA finish). The resin matrix was Union Carbide Bakelite ERLA 2256 epoxy/ZZL. The hardening agent was 0820 and the hardener ratio was 27 phr.

The resin system was first diluted 1:1 with an analytic grade 2-Butanone (MEK) to facilitate impregnation of the yarn with resin. The resin-impregnated continuous yarn was fed and spaced onto a 24" diameter drum winder to form a prepreg sheet. The fibers were positioned if necessary to correct for winding gaps and all excess resin was scraped from the sheet. This sheet was allowed

TABLE XI

Matrix of Tests on 13-inch Square and Circular Test Panels

Test Series	Nominal Thickness	Nominal Test Current Level			
		50 kA	100 kA	200 kA	Spare
GROUP 1 Uncoated 0°-90°	0.040"	GD-LS-70-3 (57 kA)	GD-LS-70-1 (85 kA)	GD-LS-70-4 (184 kA)	GD-LS-70-2 (61 kA)
	0.120"	GD-LS-70-10 (69 kA)	GD-LS-70-T50-18 Rectangular tab No high current tests made	GD-LS-70-17 No high current tests made	GD-LS-70-T50-16 Rectangular tab (58 kA)
GROUP 2 Uncoated 0°-45°-90°	0.120"	GD-LS-70-11 (69 kA)	GD-LS-70-12 (101 kA)		GD-LS-70-T50-19 Rectangular tab No high current tests made
GROUP 3 Coated 0°-90°	0.040"	GD-LS-70-5 (61 kA)	GD-LS-70-6 (103 kA)	GD-LS-70-7 (185 kA)	GD-LS-70-8 (105 kA)
	0.120"	GD-LS-70-9 (69 kA)	GD-LS-70-13 (101 kA)	GD-LS-70-14 (203 kA)	

to "B" stage overnight until a "tack - free to touch" condition was reached. The sheet was then cut off the winding mandrel to mold size, bagged, and stored in a freezer until enough prepreg was accumulated to produce a composite. The prepreg was placed in a proper size mold at freezer conditions to facilitate removal of the backing release material left on the tape of the winding drum. Once the appropriate number of plies in the respective orientations had been laid up, the mold was placed in a pre-heated press (180° Fahrenheit for this particular resin system). The mold was then allowed to reach platen temperature before maximum pressure was applied. The preheat time under very low pressure was usually no more than 10 minutes for this particular steel mold. The pressing and cure cycle consisted of 2 hours at 180° Fahrenheit with 100 PSI pressure and 4 hours at 300°F with 100 PSI pressure. The mold was then cooled to room temperature by running water through the press platens. A pressure of 100 PSI was kept on the mold during the cooling process to keep composite warpage to a minimum.

Some of the panels had a silver paint protective coating. The coating used was XC-4001 silver paint made by the Hanna Paint Manufacturing Company, Columbus, Ohio. The paint thickness was about 3 mils thick. The exact thickness varied between 2.8 and 3.6 mils. The corresponding weight of the coating was between 29 and 40 grams for these 13" x 13" square panels. Since the weight of the uncoated 16-ply panels was about 130 to 140 grams, the coating accounts for about 20% of the total panel weight. Some specific details of the silver-painted panels are given in Tables XII and XIII.

Three of the sixteen-ply panels had tabs brought out from the various plies so that the current flowing in each individual ply could be measured during a test. A complete description of those particular panels will be given later in the report.

Before the simulated lightning tests, most of the panels were cut into discs of 12-7/8" diameter. The purpose of a circular test panel configuration was to allow the lightning current that was injected into the panel at its center to flow to the outside perimeter along patterns controlled by the characteristics of the test specimen and not by the characteristics of the test jig. The rectangular panels described in previous sections had all been tested with a grounded structure at one end of the panel and this forced the current to follow one particular path. On the circular panels the grounded portion of the test jig was a circular clamping plate of 12" inside diameter clamped over

TABLE XII

INFORMATION ON GRAPHITE FIBER/EPOXY
LAMINATES COATED WITH SILVER PAINT

Panels LS-70-5 through LS-70-8

Property	Panel No.			
	LS-70-5	LS-70-6	LS-70-7	LS-70-8
Uncoated Panel Wt., grams	143.6	127.4	136.7	136.4
Coated Panel Wt., grams	173.1	156.6	175.2	179.6
Total Wt. Coating, grams	29.5	29.2	38.5	43.2
Coating Thickness, Mils	2.8	2.9	3.4	3.7

Heat cured for one (1) hr. at 250° F after 18 hr. air dry.

TABLE XIII

INFORMATION ON GRAPHITE FIBER-EPOXY[1] PANELS

Panels LS-70-T50-9 through LS-70-T50-14

Panel Number	Panel Thickness, inch	Number of Plies	Layup[2]	Silver Paint[3]	
				Thickness, Mils	Weight, Grams
LS-70-T50-9	0.131	16	0°, 90°	3.6	39.9
LS-70-T50-10	0.117	16	0°, 90°	---	----
LS-70-T50-11	0.117	16	0°, ±45°, 90°	---	----
LS-70-T50-12	0.125	16	0°, ±45°, 90°	---	----
LS-70-T50-13	0.142	16	0°, 90°	3.3	38.6
LS-70-T50-14	0.134	16	0°, 90°	3.3	38.5

(1) Thornel-50 graphite fiber yarn w/PVA size, Bakelite 2256 epoxy with 0820 hardener. Panels 13½" x 13½"; fabrication procedures similar to those for previously submitted four-ply panels.

(2) Specific layup for 0°, ±45°, 90°; 0°, +45°, -45°, 90°, 0°, +45°, -45°, 90°; 90°, -45°, +45°, 0°, 90°, -45°, +45°, 0°.

(3) Hanna XC-4001 silver paint.

the panel all around its outer perimeter. Assuming an isotropic specimen (which these are not) the current flow along the panel should be purely radial from the stroke attachment point at the center to the outer grounded ring. The current density at any point in the ring would then be easily determined from the geometry of the ring and the total applied current. Thus the circular configuration is more amenable to mathematical analysis than the rectangular test specimens described in earlier sections.

A photograph of a typical silver-painted specimen before it was cut to circular form is shown on Figure 49. A photograph of the uncoated back surface is shown on Figure 50. In general, the "Before" photograph of test panels did not show anything of significance, hence no other "Before" photos of this test specimen series are included in this report.

Figure 51 shows a cross-section of the silver coating of one of the silver-coated samples. There was some tendency for the silver paint to peel on the corners unless extreme care was used in handling the samples.

2.3.1 Pretest Analyses

These specimens, like the previous ones, were given pretest analyses of an ultrasonic "C"-scan and extraction radiographs were taken. In addition, these particular panels were given a sonic vibration test in order to determine the natural modes of vibration of the panel. It was felt that this latter test might be a useful technique for detecting the extent of damage to the panels. As it turned out, the damage caused by the simulated lightning currents was sufficiently massive as to make the sonic vibration tests useless.

The circular panels were X-rayed with the BALTAU unit (tungsten anode = 1.5 mm^2 focal spot) using Kodak single-coated type R X-ray film. The resultant X-ray radiographs were extracted using 3 - 4 density separations of 0.02 differences to enhance the details present of each test panel. Photo reductions of each of these extractions are included in Figures 52 through 55. The small pinpoint anomalies visible on the prints are ascribed to dust particles which have a tendency to collect on Thornel-50/epoxy composites due to a static charge buildup from handling.

Figure 52 is typical of a 0° and 90° layup of high modulus graphite. The fibers appear uniformly spaced and straight on LS-70-1.

Figure 53 of Panel LS-70-2 contains a number of dark lines generally parallel, and waviness of the plies in one direction is easily observed. Panel LS-70-3 appears reasonably uniform. Specimen LS-70-4 shows strong irregularities

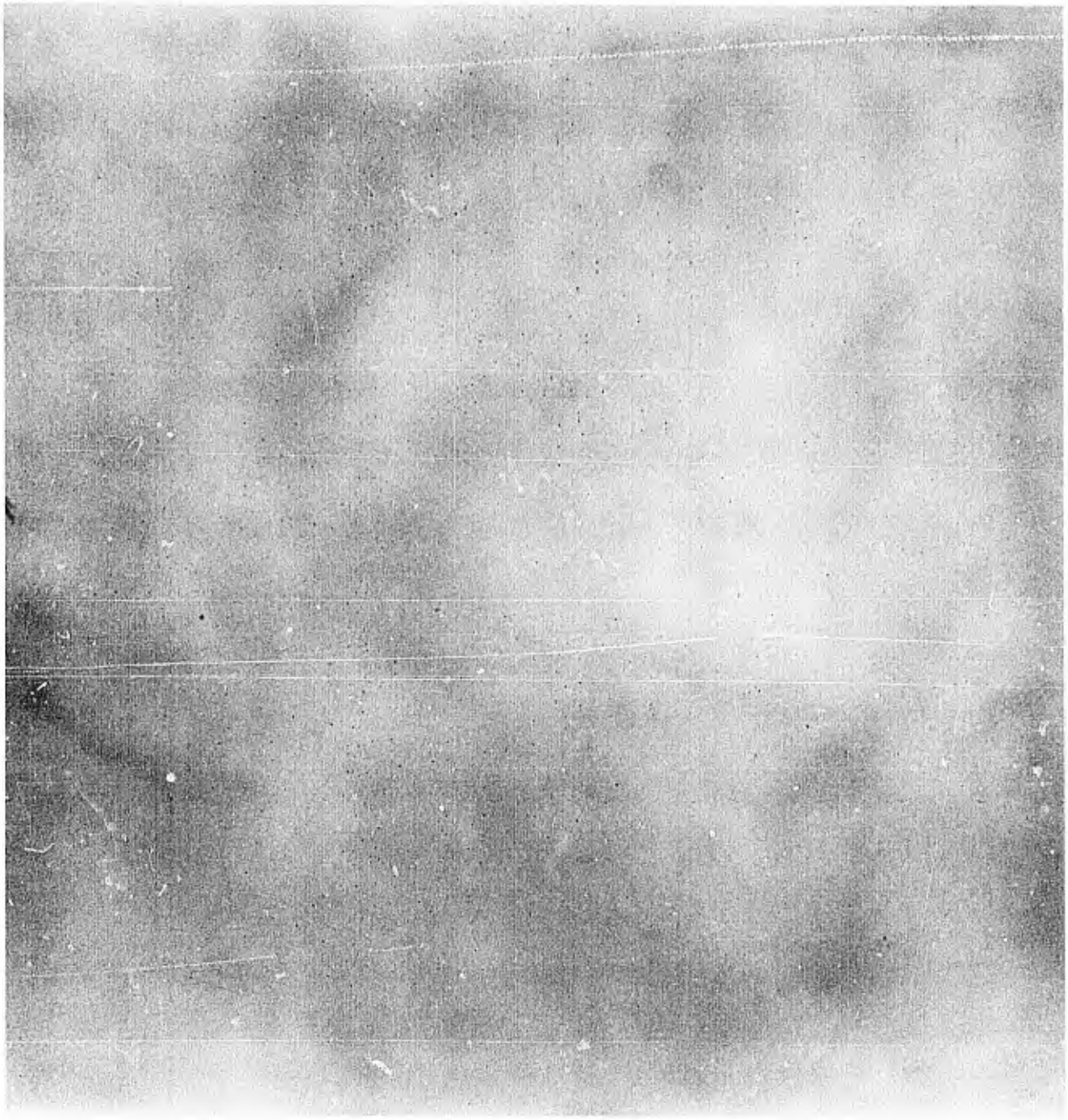

GD-LS-70-5

FIGURE 49 - Graphite Fiber/Epoxy Panel Showing Silver-Coated Side Before Simulated Lightning Tests

GD-LS-70-5

FIGURE 50 - Back Surface of Graphite Fiber/Epoxy Panel Before Simulated Lightning Tests

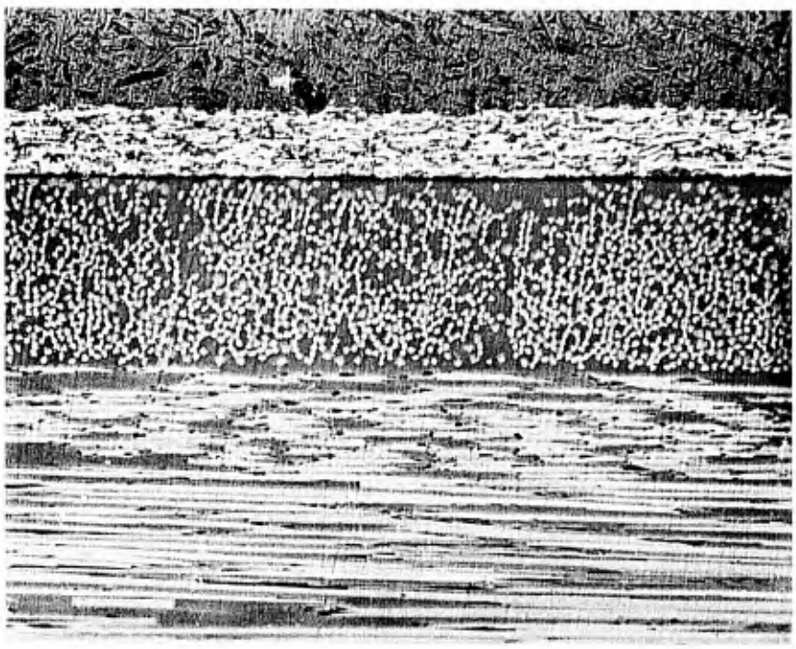

GD-LS-70-6

FIGURE 51 - 200X Photomicrograph of Graphite Fiber/Epoxy Panel, Cross-Section of Silver Paint Coating

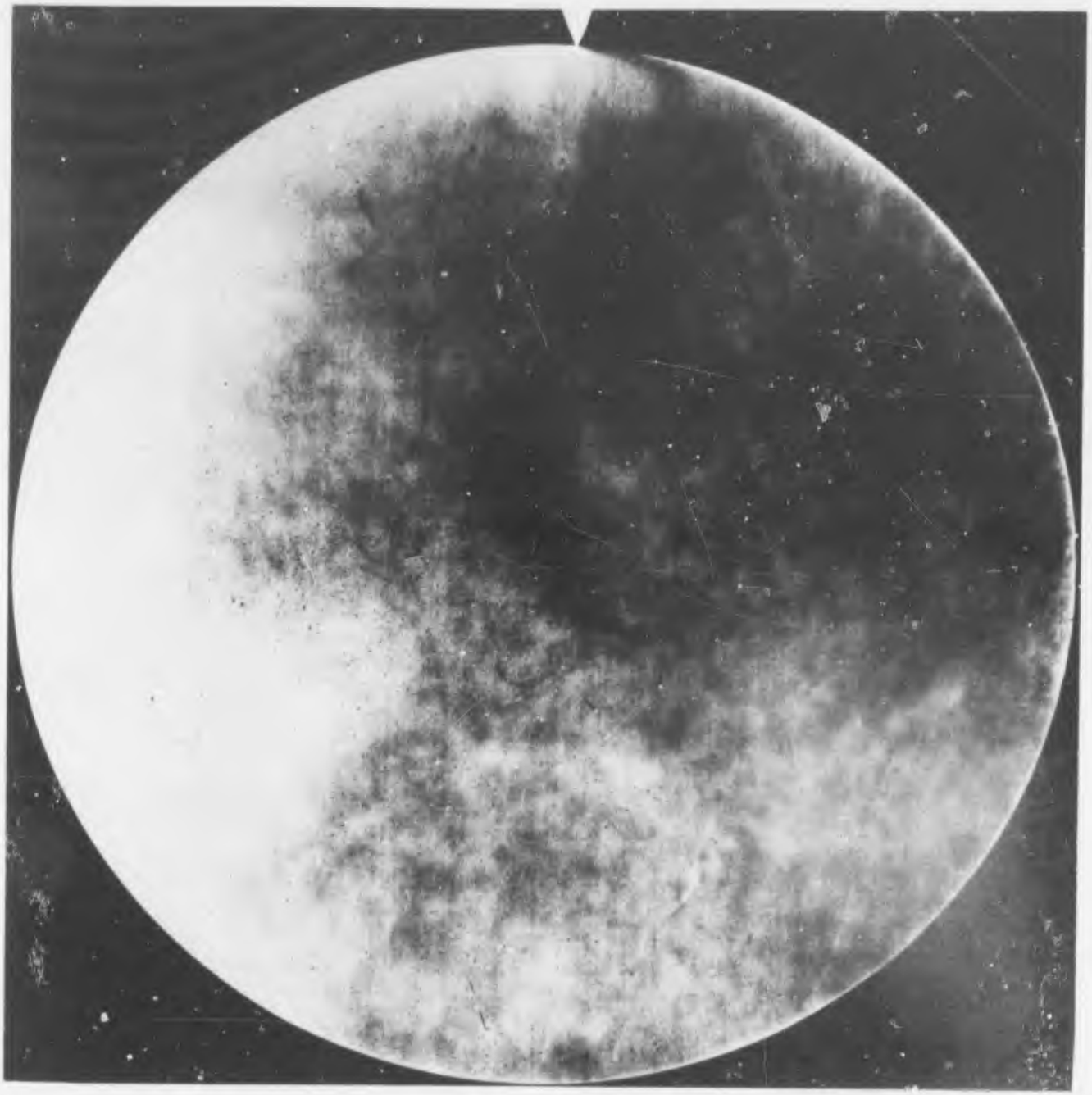

FIGURE 52 - Extracted X-Ray Radiograph of Thornel-50/Epoxy Panel LS-70-1 Before Simulated Lightning Test

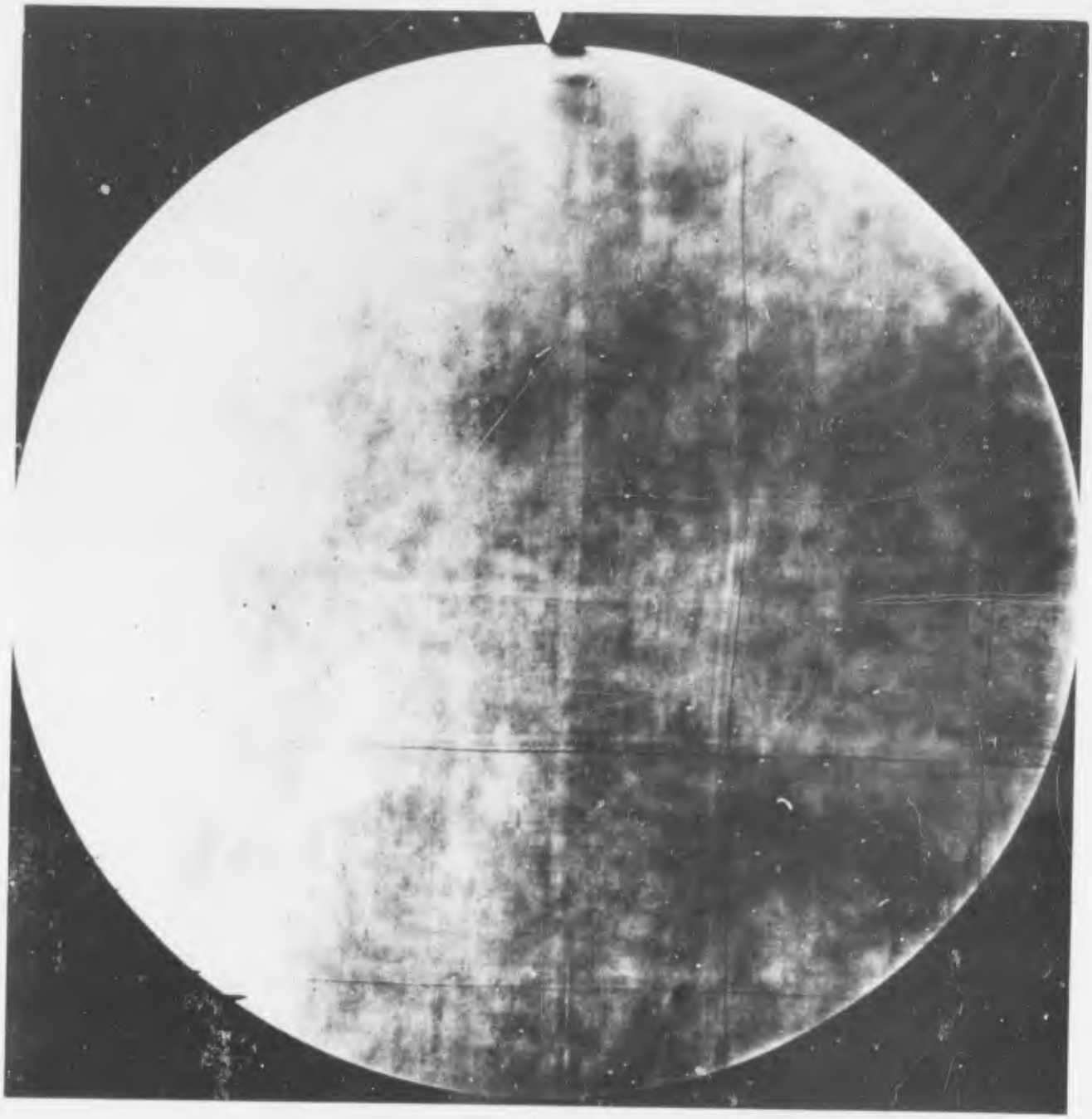

FIGURE 53 - Extracted X-Ray Radiograph of Thornel-50/Epoxy Panel LS-70-2 Before Simulated Lightning Test

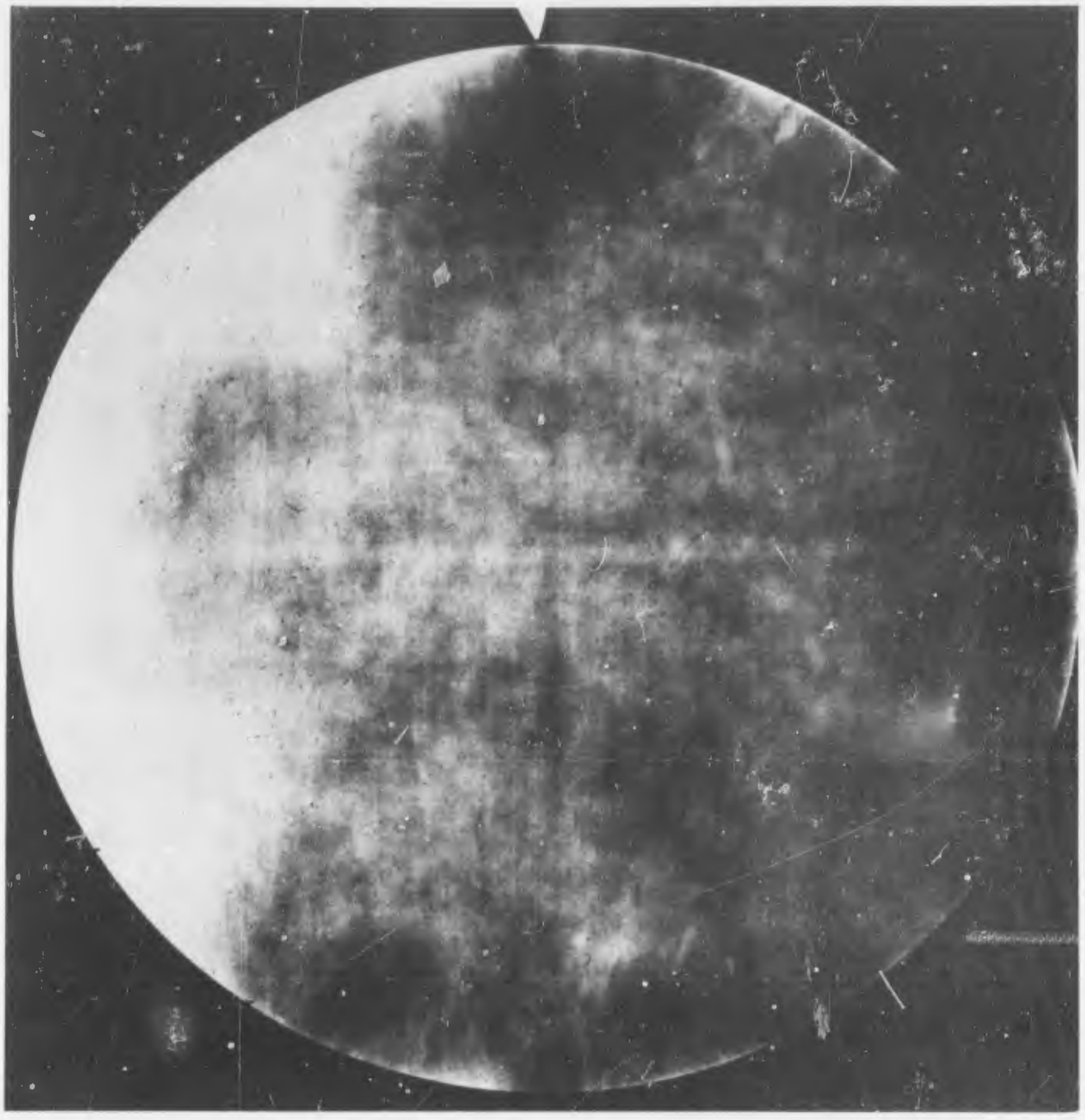

FIGURE 54 - Extracted X-Ray Radiograph of Thornel-50/Epoxy Panel LS-70-3 Before Simulated Lightning Test

FIGURE 55 - Extracted X-Ray Radiograph of Thornel-50/Epoxy Panel LS-70-4 Before Simulated Lightning Test

with two quite pronounced black bands in both the 0° and 90° orientation. These are shown on Figures 54 and 55, respectively.

In order to determine the origin of the dark bands, microscopic studies were performed. Samples for microscopic examination were cut from 3 of the 4 remnants of epoxy-filled graphite yarn plates as follows:

LS-70-1

No samples were taken since the density showed even throughout the plate.

LS-70-2

This sample was cut 90° from the peripheral reference mark, and includes two dark or lower density lines and one light or more dense line, all of them fairly wide.

LS-70-3

This sample was cut 270° from the peripheral reference mark, and contains one lighter zone of higher density.

LS-70-4

This sample was cut 180° from the peripheral reference mark, and contains two black lines of less dense material.

The remnant borders were oriented as closely as possible to reference points, on each border and on the radiograph print, and then samples were cut from the borders at those locations where there was the greatest deviation from uniform density. The samples were mounted in Lucite in order to microscopically examine those points of greatest interest.

Overall appearances of the chosen areas had no drastic or obvious physical differences in material appearance under plain and polarized reflected light. Sample LS-70-2 and LS-70-4 contained less dense (black) lines. Examination of these lines showed that the dark (lower density) lines of both samples are caused by the presence of bundles of fibers with individual fiber diameters measuring 8 to 10 microns, or twice that of the surrounding matrix graphite. The various photomicrographs are shown on Figures 56 through 58. It can be noted in the photomicrographs of LS-70-2 and LS-70-4 at 200X that packing densities for the bundles of larger diameter fibers are strikingly less than the adjacent bundles made of smaller diameter filaments. One bundle photographed at 100X shows a cross-section diameter of 0.7 millimeter. Measurements of the same line on the X-ray print shows that line to be somewhat less than 1 millimeter (estimated to be 0.75 millimeter using a millimeter scale). Two such areas in

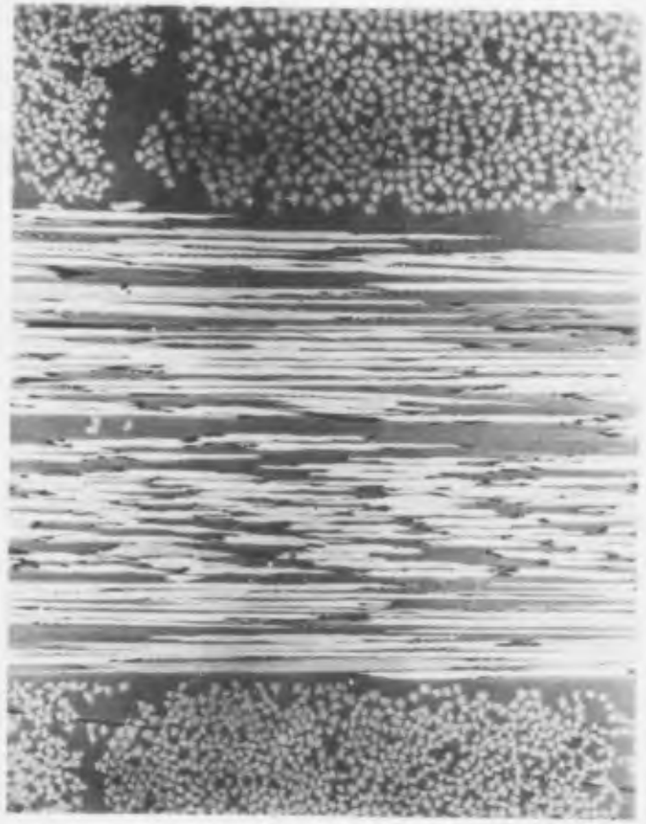

LS-70-2 200 X Low Density

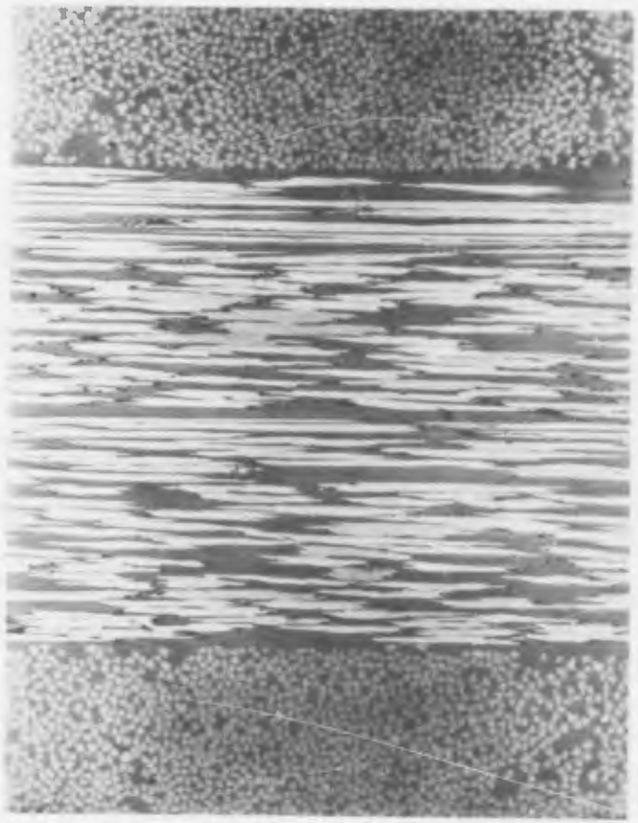

LS-70-2 200 X High Density

FIGURE 56 - Photomicrographs Showing the Differences Between Low Density and High Density Areas of Sample Panel

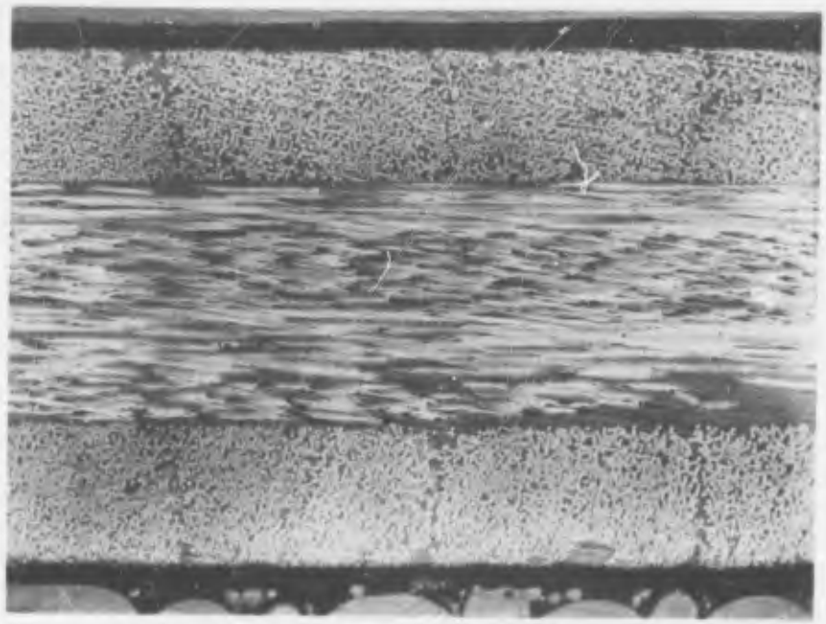

LS-70-2 100X Denser Line

Dense Line

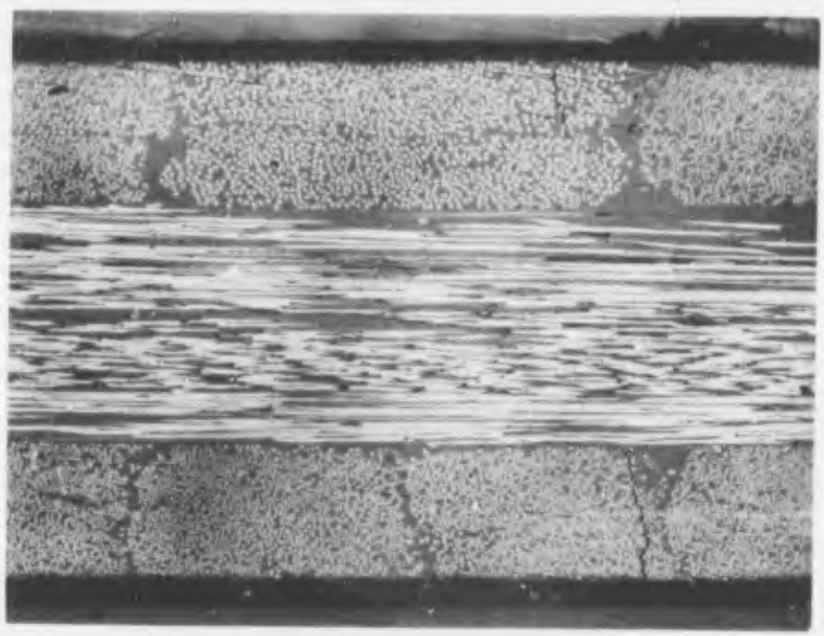

LS-70-2 100X Black Line

FIGURE 57 - Photomicrographs Showing the Differences Between a Dense Area and the Dark Line of Panel LS-70-2

8 to 10 μ 0.7 mm.

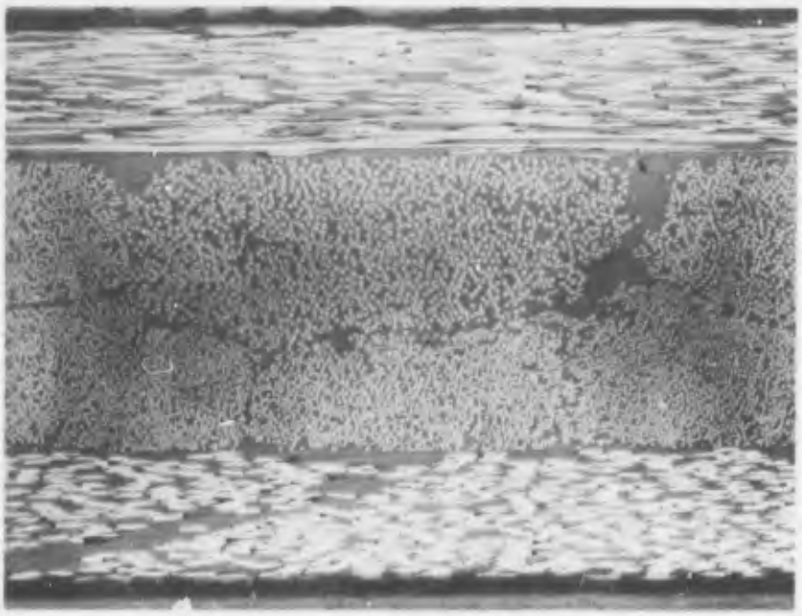

LS-70-4 100X 1 of 2 Dark Lines

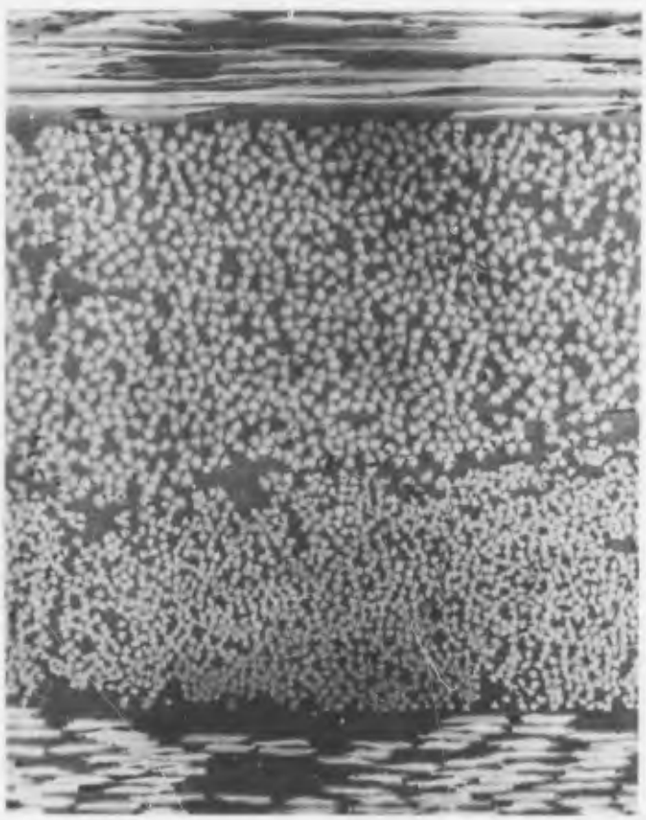

8 μ
to
10 μ

3 μ
to
5 μ

LS-70-4 200 X Dark Line (Low Density)

FIGURE 58 - Photomicrographs Showing Dark Line Areas of Panel LS-70-4

the LS-70-4 sample correspond to lines marked on the sample surface; one bundle occurs in Sample LS-70-2 closely adjacent to a mark made on the surface prior to examination.

The wider (more dense) areas of each radiograph print show no particularly discernible differences from the standard density areas examined. A fiber count would not be very conclusive unless it were done over a fairly large area of the samples. Results would then be questionable because of the thickness variation and fiber alignments in each of the plates. It seems that the wider (denser) strips on the radiographic separation prints are caused by a slightly higher number of fibers per unit area. Several photomicrographs taken at 100X seem to indicate that the average density consists of about three fiber bundles per length of each picture, whereas the more dense photos are judged to have about 3½ sheets on each side of the prints.

During the lightning withstand tests we did not notice any unusual effects that could be ascribed to the presence of these isolated bundles of fibers.

Reference X-ray radiographs were also made of the silver-paint coated panels. The very large difference in atomic numbers between silver and the graphite-epoxy makes it impossible to determine structural details of the graphite either on the original radiograph or on the separation negative. The variation of the paint film was clearly shown on each sample. Figure 59 is a typical print made from a separation negative to enhance the contrast of the original radiograph. The lighter bands represent increased thickness. Apparently the panels were spray-painted with two coats, with the gun travel at 90° on successive coats. The white specks correspond to "pimples" on the painted surface.

The above radiographs were made by a slightly different technique than that employed on the panels LS-70-1 through LS-70-4. All samples and films were placed under a laminograph and rotated seven revolutions during the exposure. This method improved the uniformity of the X-ray. Samples LS-70-5 through LS-70-8 were then machined to 12-7/8" diameter circles.

Holographic studies of these panels for detection of microflaws were considered as a good investigative method for damage analysis. The G.C. Optronics Company, Ann Arbor, Michigan, was consulted on the problem. The cost proved to be prohibitive for the program.

Some of the panels were subjected to sonic-vibration tests with equipment and procedures which are discussed below. The object was to determine a Bessel function for drum-head vibration of the circular membranes. The premise here

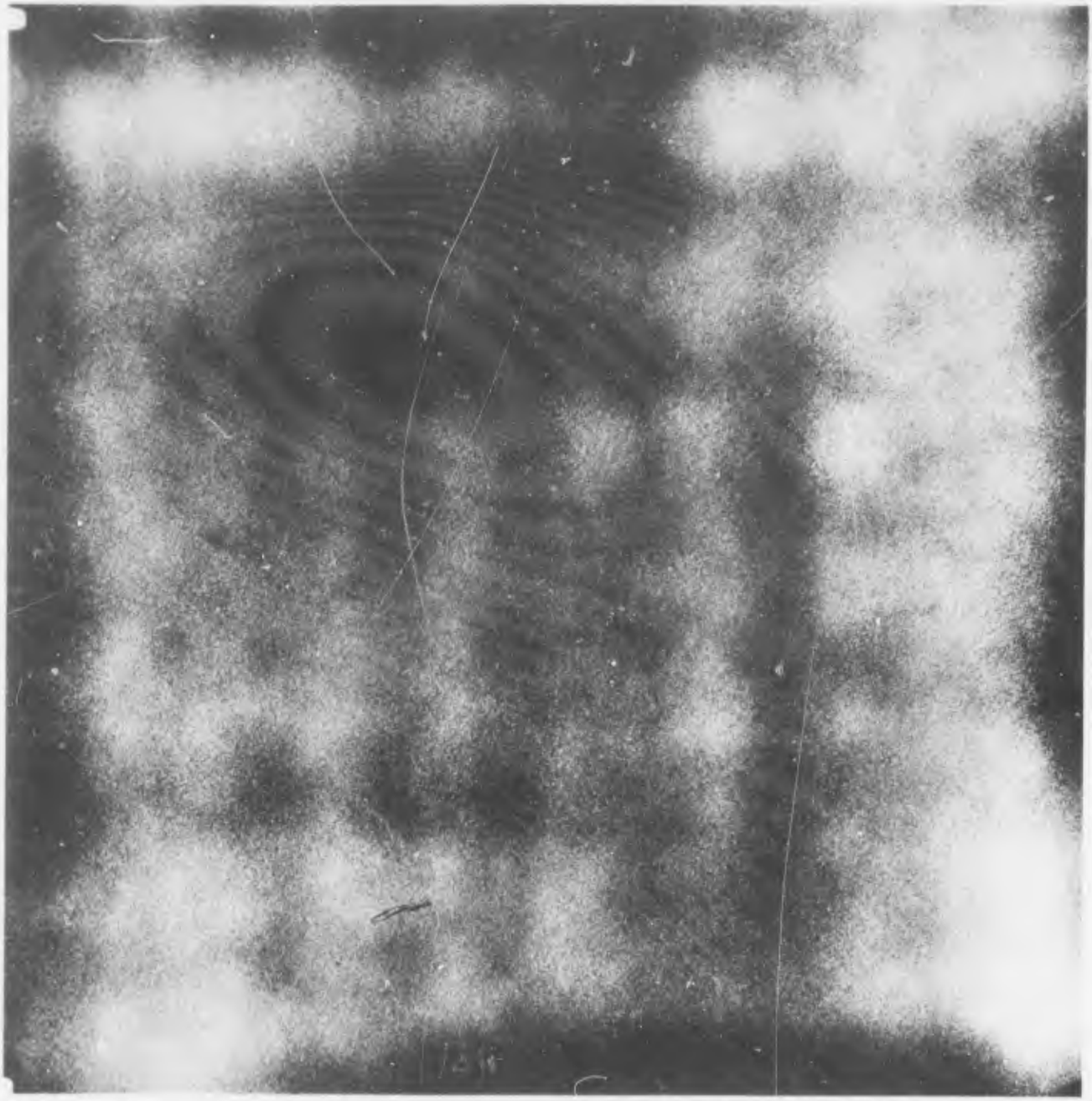

FIGURE 59 - Photo Extraction Showing Variations of Silver-Paint Coating Thickness - Typical for Panels LS-70-5 through LS-70-8

was that fiber breakdown as a result of the lightning-flash tests would lessen the modulus (which in turn would cause a decrease in the material sound velocity, producing a change of the sound pattern obtained prior to the lightning test. Another of the premises upon which the tests were made is that any defects in the test panel might show up as an uncharacteristic vibration pattern before the lightning test was made.

As it turned out, the damage at the stroke-attachment point was generally so severe as to completely destroy the original sonic-vibration patterns. While a vibration test might in theory show some evidence of broken fibers beyond the immediate, obviously damaged portion of the panel, the visual damage at the stroke-attachment point turned out to far override the lesser kinds of damage that the vibration patterns might have shown. Accordingly it was concluded that the sonic-vibration test was not a useful method of evaluating the test panels after the lightning tests. Possibly it has some usefulness as a test to evaluate panels prior to a lightning test, although even this is doubtful. Accordingly, only an abbreviated report on the sonic-vibration test method and the test results will be presented here.

A woofer-type speaker with range from 40 to 3,000 Hz. was attached to a controlled-frequency oscillator amplifier system. Panels were fastened in place over a 12" speaker by means of a circular ply-wood clamp fastened down by hand with wingnuts. The samples were sandwiched between heavy rubber gaskets to dampen any vibrations which might occur from resonant frequencies of the speaker enclosure. Preliminary scans were made of each panel to determine the frequency at which typical patterns were formed. Initially, the uniform dispersion of 120-grit silicon carbide was accomplished by setting the oscillator on 75 Hz. until the particles were evenly distributed. The oscillator was tuned to the predetermined frequency and the amplitude adjusted to produce the characteristic frequency pattern in a time span of approximately one minute, to lessen possibility of burning out the speaker with a prolonged signal.

Examination of the pattern and photomicrographs of panels LS-70-1 through LS-70-4 eliminates the possibility of equating the pattern with Bessel's function, which is appropriate only if the membrane material is isotropic and homogeneous. All photomicrographs examined displayed non-uniform dimensions for the fiber plies. The sound-vibration patterns verify this by containing two distinct axes in each pattern, lying at right angles, one axis parallel to the outside plies of the fibers, and the other parallel to the inner plies. As a consequence

data accumulated from these tests are qualitative in nature.

None of the patterns examined show any pronounced asymmetry indicative of serious panel defects. This is not surprising since careful visual examination, X-ray radiographs, and ultrasonic "C"-scan examination of the panels likewise indicated that none had any particular defects. Figures 60, 61 and 62 show the vibration patterns obtained with silver-painted panels at various frequencies. Panel LS-70-6, Figure 61 showed perhaps the greatest amount of pattern asymmetry, but this could not be correlated with any other panel properties or defects. The pattern for panel LS-70-7 (not included with this report) showed a place where the silver coating was debonded at one edge of the panel. The silver-paint coating was chipped along this edge and the chipping could be seen visually.

All in all, sonic-vibration testing did not prove to be very useful. It might have merit for pre-test analyses to determine the effects in protective coatings although this could not be readily evaluated without making tests on panels with deliberately defective coatings. This line of approach was not pursued much further during the course of this contract.

2.3.2 Test Methods

As mentioned earlier, these panels were tested with a grounded structure clamp completely around the periphery of the test panel. Primarily this was done to allow the lightning-current flow within the panel to be determined by the characteristics of the panel, rather than to force an unnatural current flow from the arc-attachment point to only one side or end of the panel. In an actual aircraft structure it is most probable that a composite panel will be bonded to a metal structural framework at a number of points around its periphery.

Figure 63 is a sketch of the test arrangement. The grounded clamping structure provided a ground current return path on both the front and the back sides of the test panel. The ground structure itself was made to the top of a cylindrical steel tank of 29 inches diameter and 38 inches height. The tank was formed from 0.5 inch thick steel. The tank itself, along with the aluminum cover plate, formed a structure that provided extremely good electromagnetic shielding. The object of using this tank was to simultaneously make measurements of the lightning resistance of the panel and of the panels' ability to provide shielding against the electromagnetic field produced by lightning. These electromagnetic-field penetration tests of the composite panels will be

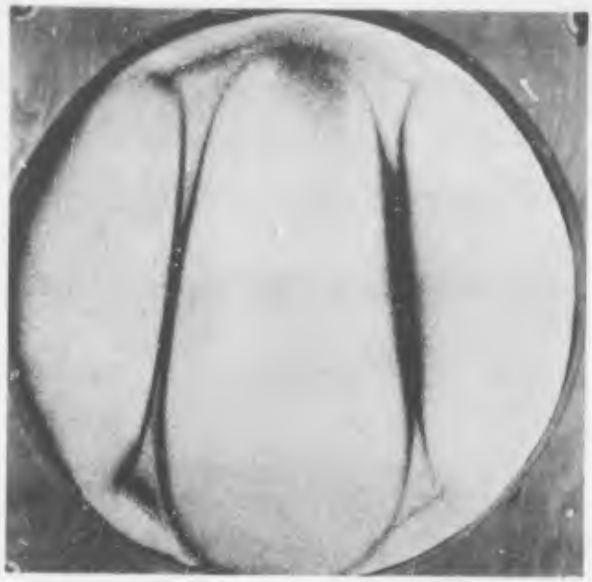

234 Cycles/Sec.

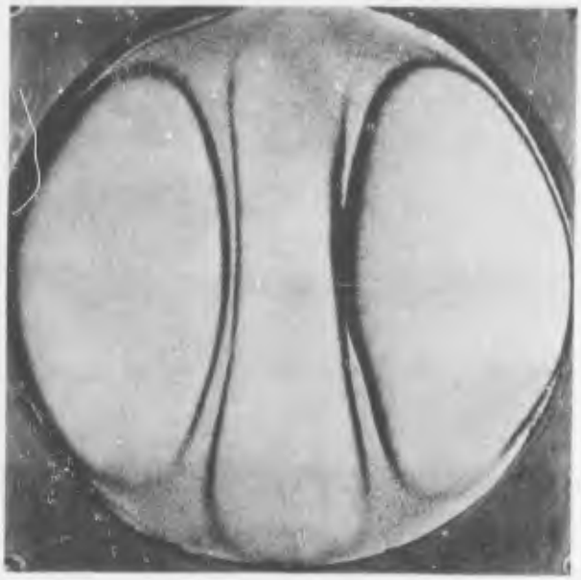

268 Cycles/Sec.

LS-70-5

337 Cycles/Sec.

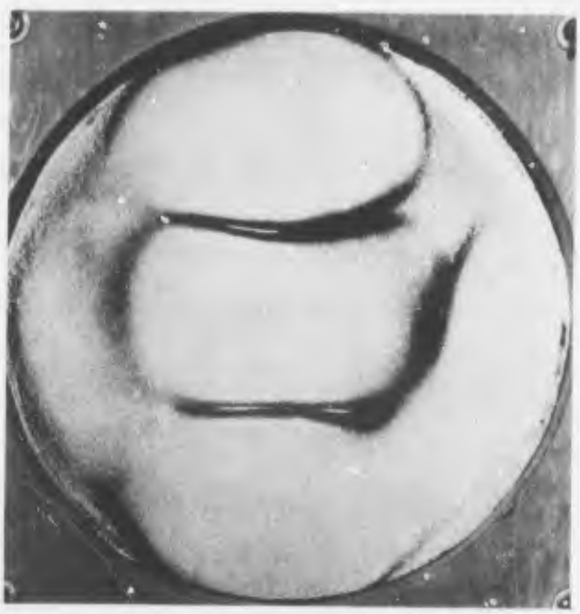

469 Cycles/Sec.

LS-70-5

FIGURE 60 - Characteristic Vibration Patterns of a 0.040" Silver-Paint Coated Panel

667 Cycles/Sec.

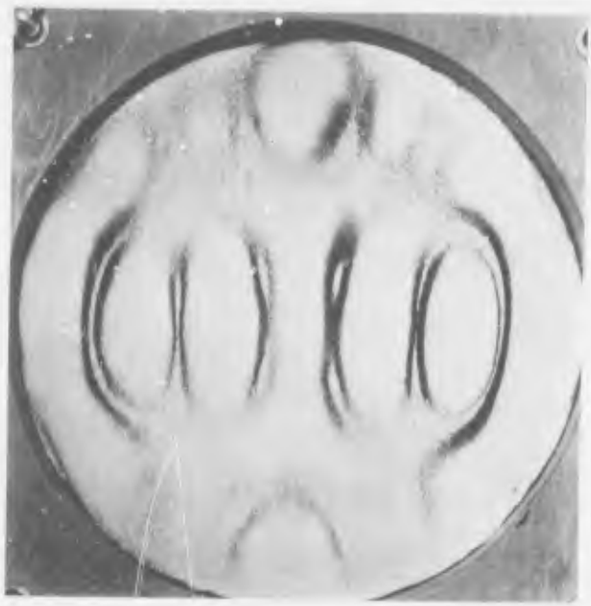

1060 Cycles/Sec.

LS-70-5

179 Cycles/Sec.

199 Cycles/Sec.

LS-70-6

FIGURE 61 - Characteristic Vibration Patterns of 0.040" Silver-Paint Coated Panel

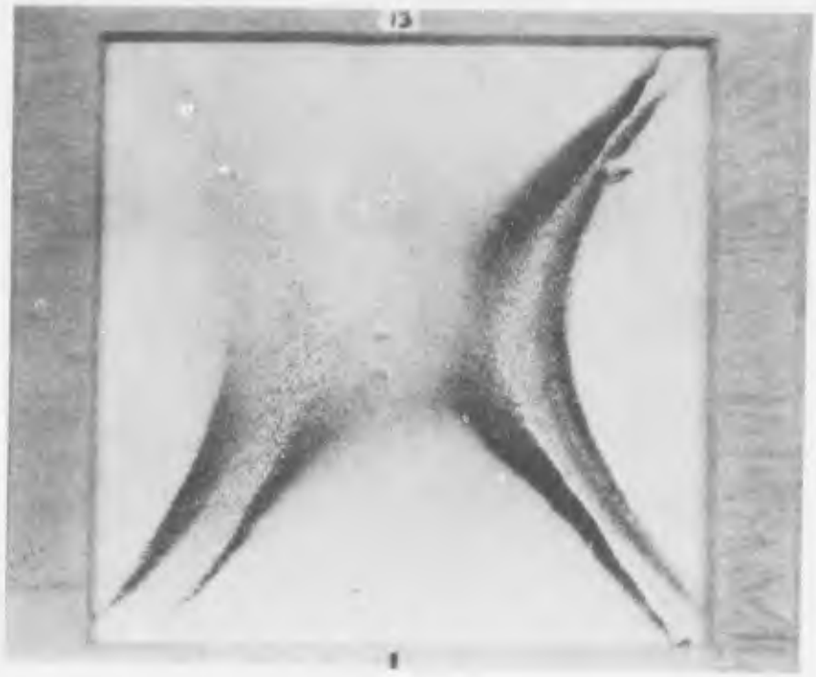

211 Cycles/Sec.

295 Cycles/Sec.
LS-70-T50-13

FIGURE 62 - Characteristic Vibration Patterns of a 0.120" Silver-Paint Coated Panel

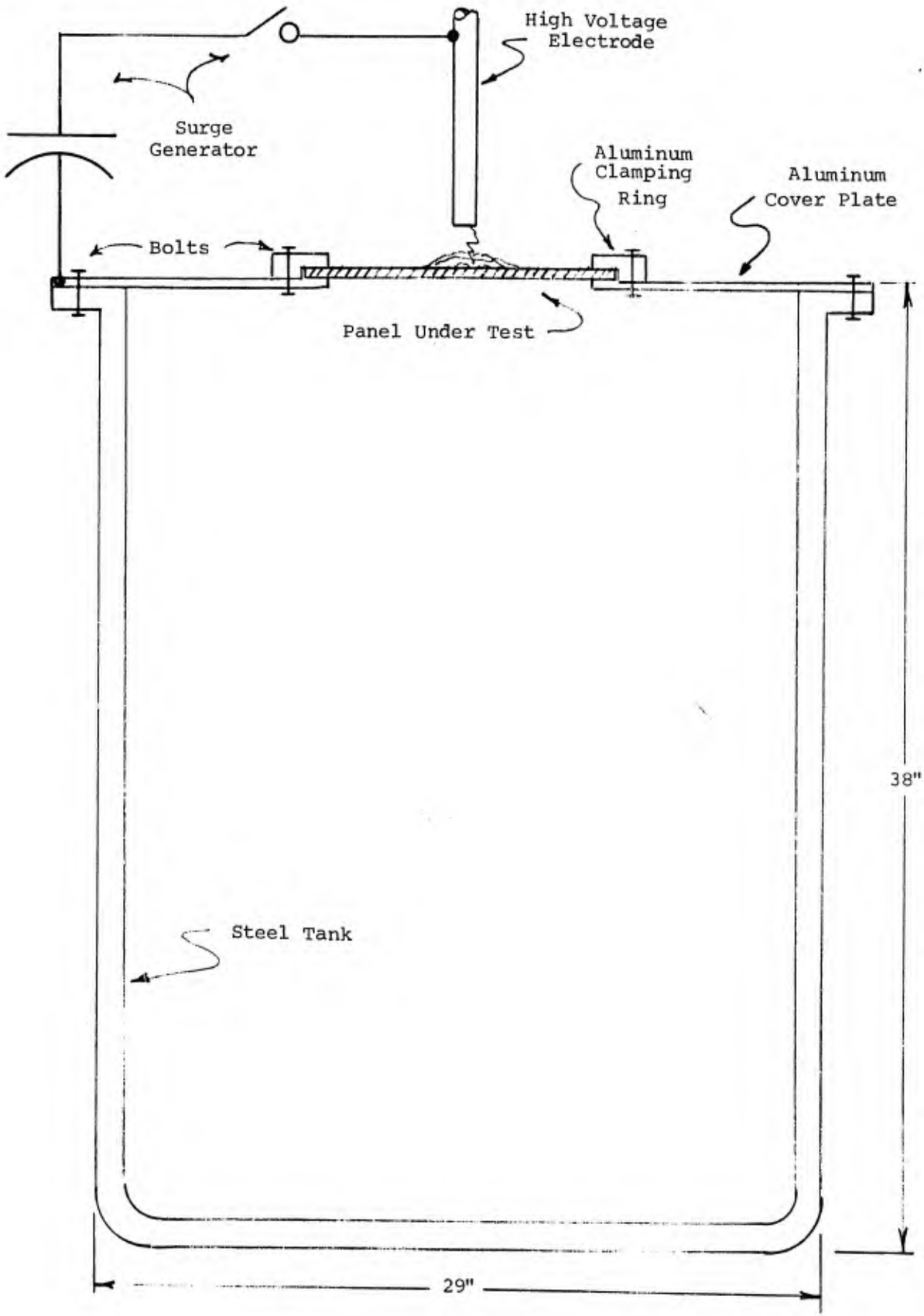

FIGURE 63 - Test Arrangement for Simultaneous Tests of Lightning Withstand and Electromagnetic Field Penetration

described in a later section of the report.

Figure 64 shows two photographs of the test chamber. In the top part of the figure there is shown a panel being tested for lightning resistance, and in the bottom photo is shown a panel being tested during one of the electromagnetic-field penetration tests.

Surge currents were then applied to the sample from the high current surge generator. The high-voltage electrodes were one inch above the center of the panel and the oscillatory discharges described during the test on the 6" x 12" panels were used also for the circular panels.

Section 2.3.3 Test Results

Photographs of the damage caused by the simulated lightning discharge to the four uncoated panels (LS-70-1 through LS-70-4) of 0.040" thickness is shown on Figure 65 through Figure 68 respectively.

Panel LS-70-3 (57 kA) and Panel LS-70-2 (61 kA)

The panels displayed nearly identical damage to the coatings. Both front surfaces were discolored to nearly identical shape and size. On panel LS-70-3 the top plies were blown off over a region of dimensions 1/8" x 2-1/2". Around the perimeter of the panel there was disruption of the laminate due to the contact of the panel at this point with the aluminum top of the test tank and the aluminum retaining ring, where the lightning current followed a path to ground. Similar discoloration had been noted on the 6" x 12" panels at the grounded end. Both of these panels were punctured through to the back of the surface. About the same amount of material was blown off of the back surface of each of these panels.

Panel LS-70-1 (85 kA)

The top layer of plies in this panel were blown off in an area 4-1/2" x 1-1/2" at the center of the lightning-stroke attachment point, with disruption of the fiber laminate in an oval area 6" x 4-1/2". At the point of contact of the high-current arc there was destruction of all four plies in the composite material, an approximate diameter of 3/4".

The panel was punctured with a small portion (3/8" x 2") of the back ply being broken by the high-current arc.

This panel has no other panel which can be used as a basis of comparison uncoated vs. coated. All of the tests, though, indicate that the damage sustained is closely associated with the current value of the simulated lightning stroke. Measurements of surge degradation and "C"-scan delamination dimensions fall between the dimensions for panels tested at 61 kA

A. Configuration for Simulated Lightning Test

B. Configuration for Electromagnetic Field Penetration Test

FIGURE 64 - Two Views of Test Chamber Used with Circular Test Panels

LS-70-1 (Front)
(85 kA)

FIGURE 65 - Damage to Uncoated Graphite Fiber/Epoxy Panel by Simulated Lightning Discharge

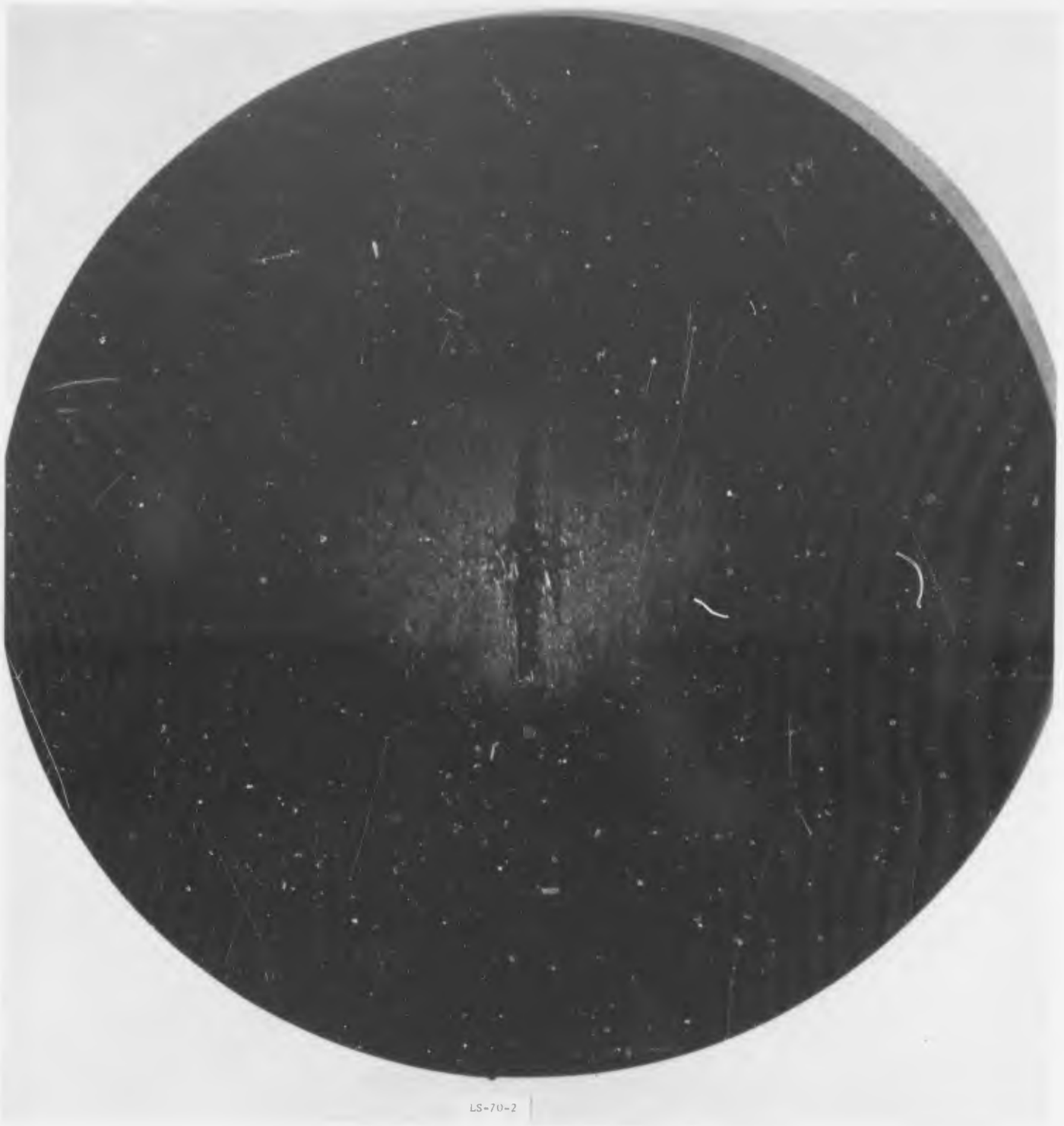

LS-70-2 (Front)
(61 kA)

FIGURE 66 - Damage to Uncoated Graphite Fiber/Epoxy Panel by Simulated Lightning Discharge

LS-70-3 (Front)
(57 kA)

FIGURE 67 - Damage to Uncoated Graphite Fiber/Epoxy Panel by Simulated Lightning Discharge

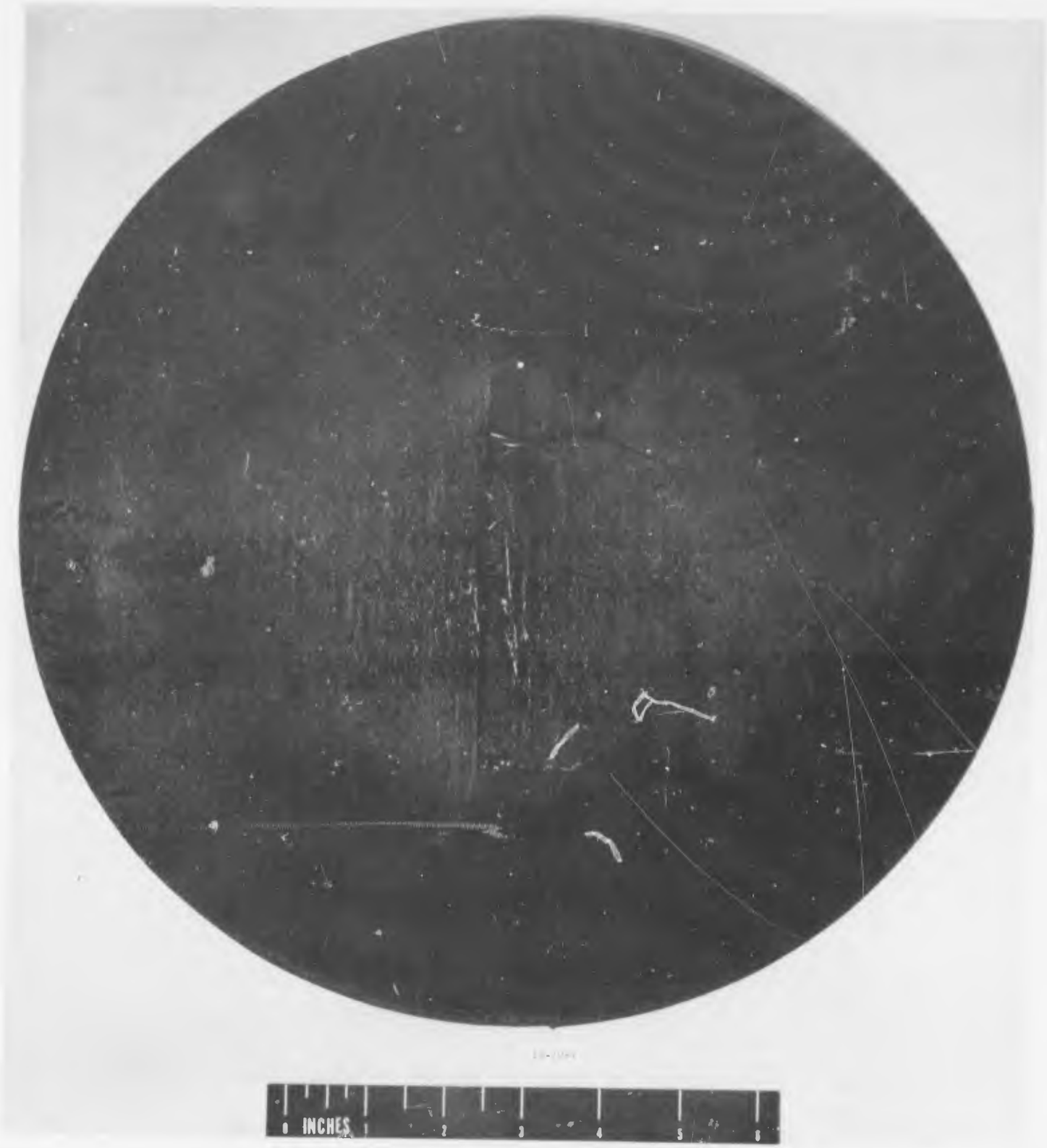

LS-70-4 (Front)
(184 kA)

FIGURE 68 - Damage to Uncoated Graphite Fiber/Epoxy Panel by Simulated Lightning Discharge

(panels LS-70-2 and LS-70-3) and 184 kA (panel LS-70-4).

Panel LS-70-4 (184 kA)

This panel sustained the same type of damage as panels LS-70-1 through LS-70-3, but on a more extensive scale. The disruption of the top ply extended approximately the diameter of the panel in a direction perpendicular to the direction of the top ply. A majority of the current flowed in this perpendicular direction, as verified by the disruption of fibers at the points where the panel is clamped to the retaining ring. The front surface damage on this panel flared outward laterally 5" with ply blow-off measuring 5-1/4" x 1/2", shredded badly at the center. The delamination extended nearly 5" along the top ply and about 1" to each side of the stroke-attachment area. Fibers in the delaminated ply were loosened but still in place. It should be noted that the actual damage to this panel appeared less extensive than that sustained by the Panel LS-70-7 which had a silver-paint coating.

Photos of the resultant damage to the panels coated with silver paint are shown on Figures 69 through 74.

Panel LS-70-5 (61 kA)

Silver paint coatings, intended as partial protection, did not seem very effective in preventing destruction of the composite material by a high-current simulated lightning strike. The current applied to panel LS-70-5, 61.3 kA, was similar to the amount of current, 61.0 kA, applied to the uncoated panels LS-70-2 and LS-70-3. Accordingly, the damage to the panels was similar. The pattern of disruption to the top ply was somewhat different on a coated vs. uncoated sample. This can be seen by comparing Figures 66 and 67 with Figure 71.

On the uncoated samples the area of the resin suffering pyrolysis was elliptical or diamond-shaped and apparently caused by resistive heating of the resin by the current flow in the various plies. On the coated sample the area of pyrolysis is circular in shape and shows much less of a ply effect. The area suffering pyrolysis shows a speckled effect around the perimeter of the pyrolyzed area. These speckles are similar to what was observed at the ground-attachment point where the current flowed back out of the graphite material into the ground electrode structure. Possibly what happened was that the current at the stroke-attachment point flowed into the graphite material as the silver-paint coating was blown away, but flowed back out of the panel and into the silver-paint coating as

LS-70-5 (Front)
(61 kA)

FIGURE 69 - Damage to Graphite Fiber/Epoxy Panel Coated with Silver Paint, After Exposure to Simulated Lightning Discharge

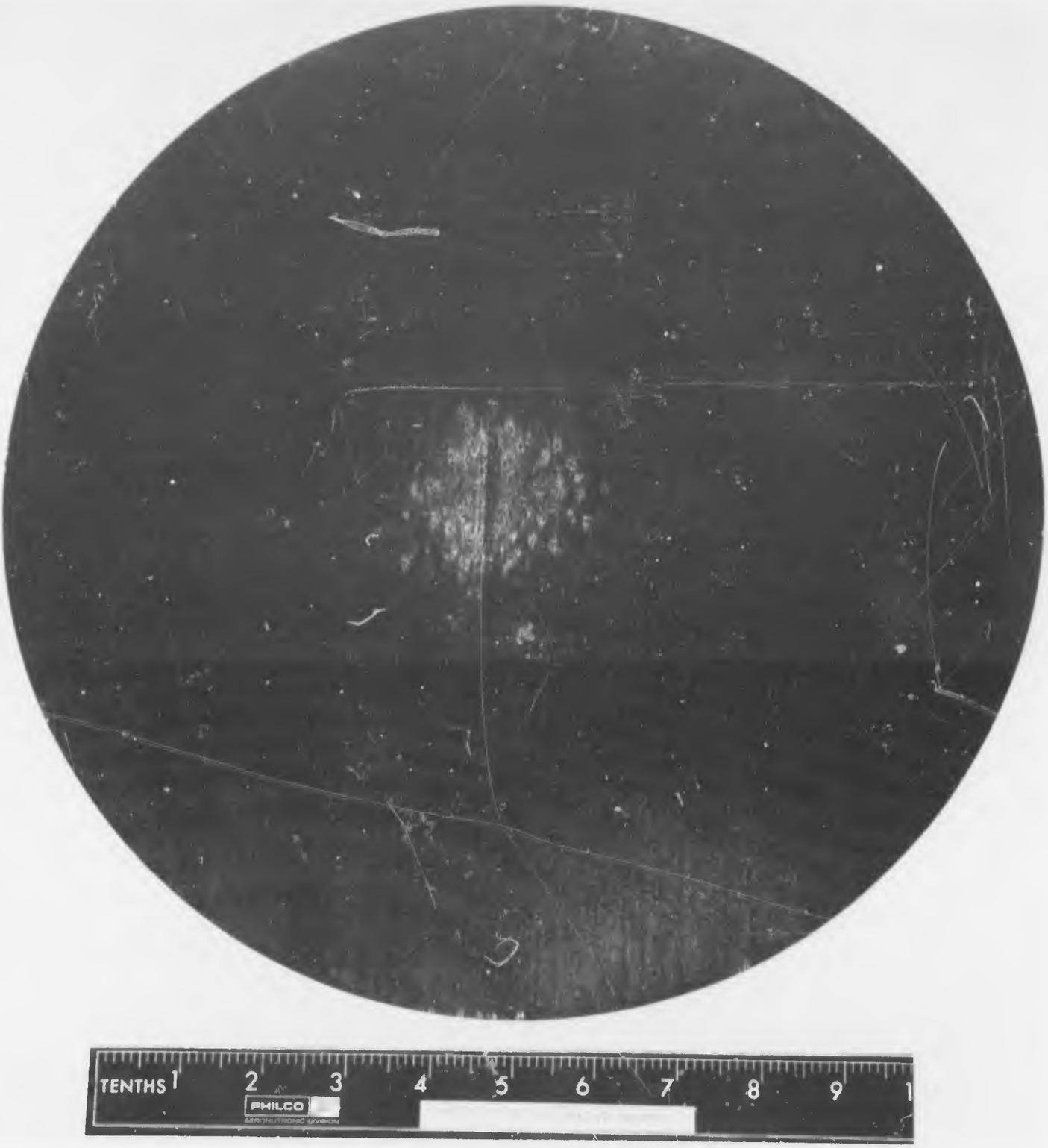

LS-70-5 (Front)
(61 kA)

FIGURE 70 - Appearance of Graphite Fiber/Epoxy Panel with Silver Paint Removed, After Exposure to Simulated Lightning Discharge

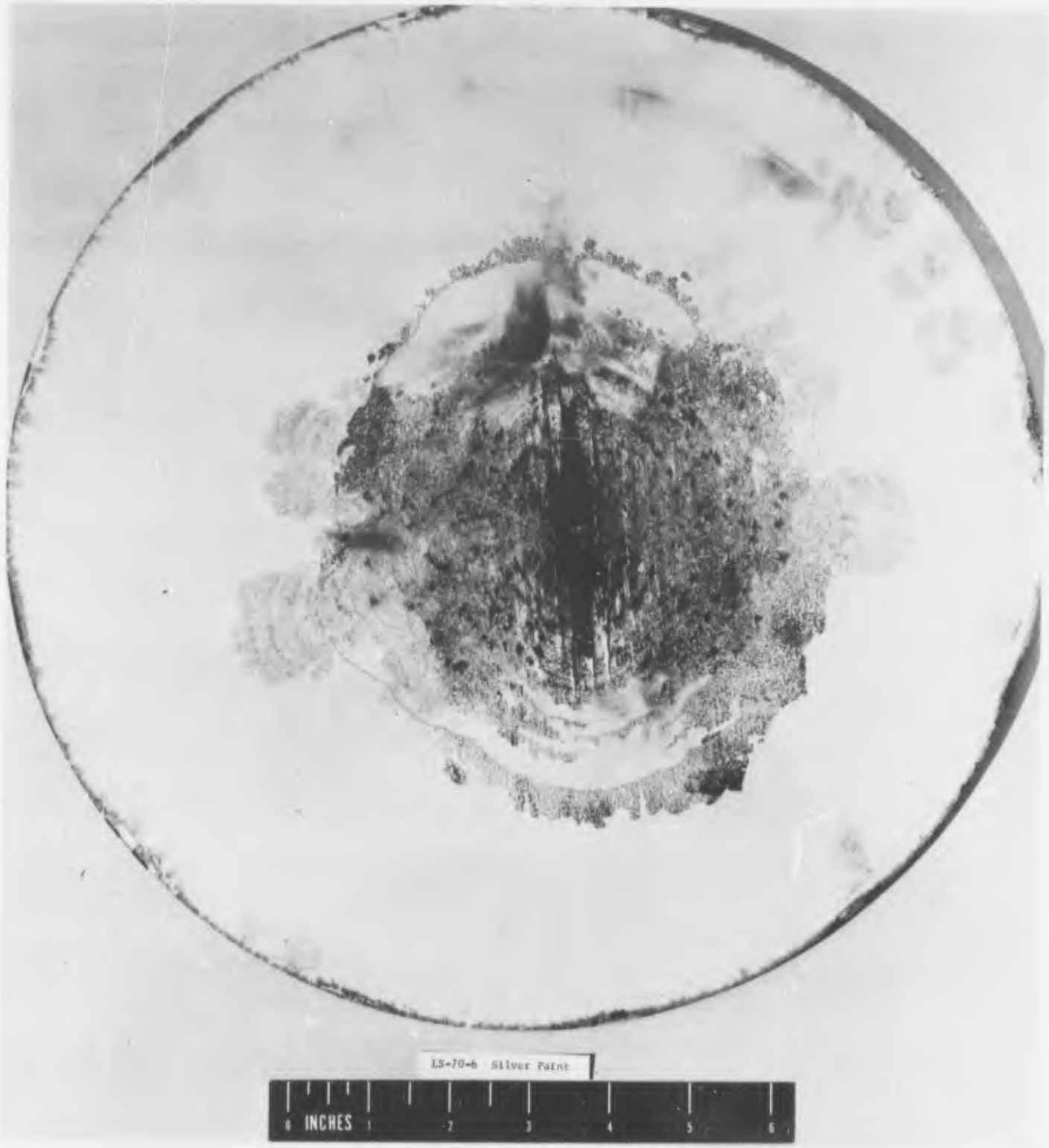

LS-70-6 (Front)
(103 kA)

FIGURE 71 - Damage to Graphite Fiber/Epoxy Panel Surface Coated with Silver Paint After Exposure to Simulated Lightning Discharge

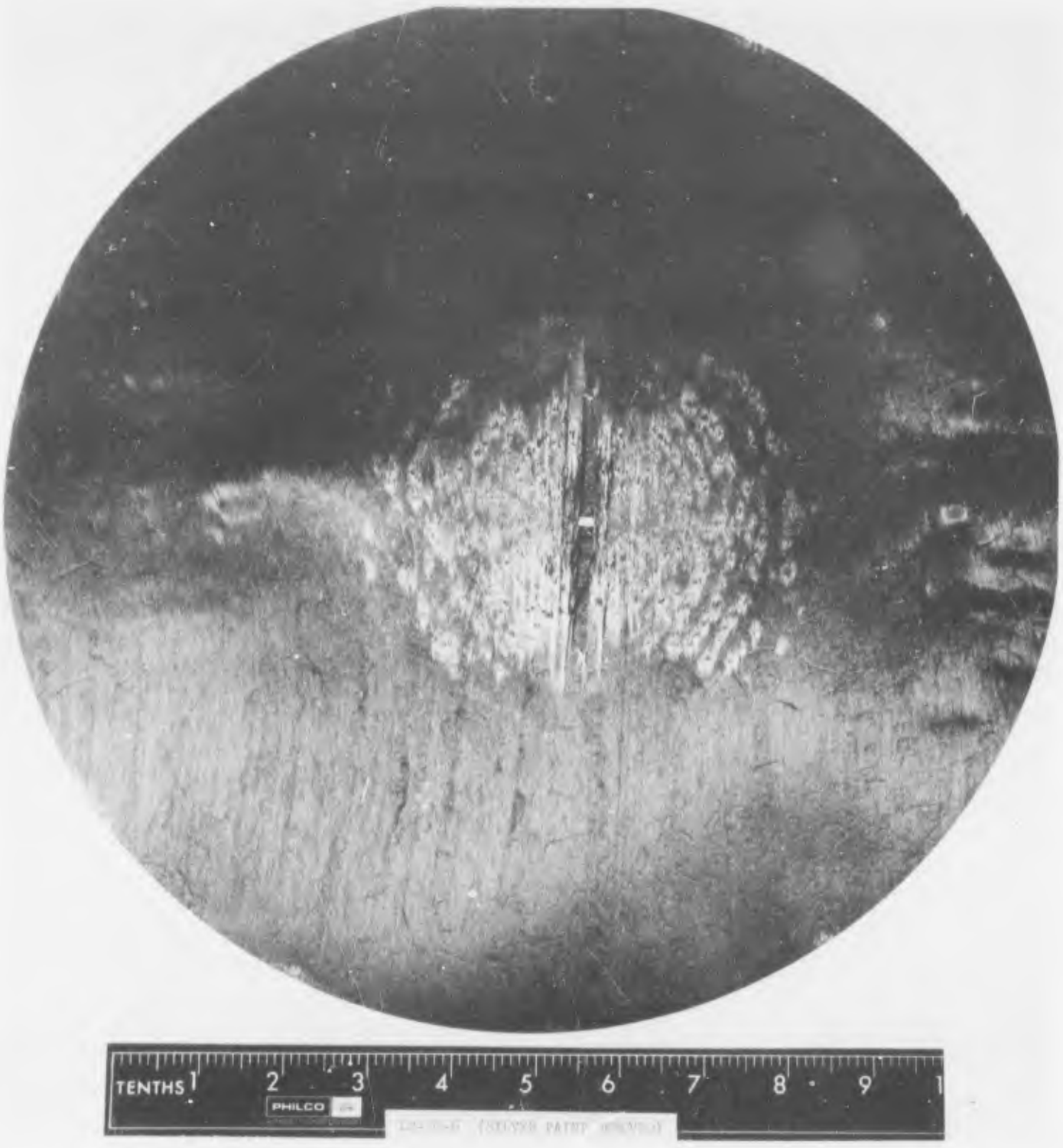

LS-70-6 (Front)
(103 kA)

FIGURE 72 - Appearance of Graphite Fiber/Epoxy Panel with Silver Paint Removed, After Exposure to Simulated Lightning Discharge

LS-70-7 (Front)
(185 kA)

FIGURE 73 - Damage to Graphite Fiber/Epoxy Panel Surface Coated with Silver Paint, After Exposure to Simulated Lightning Discharge

LS-70-8 (Front)
(105 kA)

FIGURE 74 - Damage to Graphite Fiber/Epoxy Panel Surface Coated with Silver Paint, After Exposure to Simulated Lightning Discharge

soon as the voltage gradient in the graphite material became high enough to allow the epoxy-resin binder to be punctured. Burned spots on the silver-paint coating are found in places that correspond to these speckled areas on the graphite.

The region in which plies were blown free of the panel was a bit less on the silver-paint coated sample, but not significantly so. The sample itself was punctured through to the back surface. The damage on the back surface was about the same as that observed on the uncoated sample.

Panels LS-70-6 (103 kA) and LS-70-8 (105 kA)

These panels are most nearly comparable to the uncoated panel LS-70-1 which was tested at 85 kA. Visually, the front surfaces of panels LS-70-6 (103 kA) and LS-70-8 (104.5 kA) appeared nearly alike. Damage to LS-70-6 measured 4-1/2" in diameter with front ply blow-off 3/16" x 3-1/8". The damage to the front of panel LS-70-8 was 4-1/2" x 4" with a 3/8" x 2-1/2" strip of the ply blown off. In both of these cases the back surfaces were damaged to nearly the same extent in size and shape - 3/8" tapering to 1" on both ends. The back surfaces of each show strain ripples when light is reflected from the surfaces at critical angles. Strained areas were 3-1/2" x 3" on panel LS-70-6 and 3" x 1-1/2" on panel LS-70-8. Again, the area of damage on the sample with silver-paint coating was circular in area, contrasted to the elliptical area on the uncoated panel LS-70-1. The speckled pattern was again noted around the outer periphery of the damaged area. If at these points current flows back out of the graphite material into the silver-paint coating, one would expect the current density around the outer periphery of this panel to be less than on the uncoated panel. This seems to be the case if one compares Figures 68 and 72. On the uncoated panel there were found the typical pyrolyzed points near the ground end at which current was flowing out of the panel into the ground structure. These were much less evident on the silver-paint coated panel.

The pattern of damage seen in Figures 71 and 74 to the silver coating of panels LS-70-6 and LS-70-8 was considerably different, although they were tested at almost the same current level. This occurred as a result of the method of grounding used on panel LS-70-8. This panel was tested with the uncoated side of the composite panel isolated from ground and the current path to ground attached only to the coated side, in contrast to all other panels in which grounded structure was clamped on both sides of the panel. The back side of the panel was isolated electrically

by placing an insulating board around the back perimeter of the panel. This method of test was tried in order to force the current to flow off the top plies. The result was that the coating separated from the panel and could be taken off in large flakes. On panel LS-70-6 in which the sample was grounded on both the front and back sides, the silver-paint coating remained adhering to the panel except near where the coating was vaporized by the arc.

Regardless of the effect on the coating, the effects on the panel itself were about the same.

Panel LS-70-7 (185 kA)

Damage to panel LS-70-7 was circular in shape, Figure 73. A 4-1/2" x 1/2" strip of front ply was removed. A large segment of the front ply was separated and deformed. The back of the panel showed vertical breaks across the fibers at the grounding-collar point. Warpage was bad with concentric deformation, and strain lines were noted across the fibers which extended to 2-1/2" above and below the stricken area. The back side of panel LS-70-7 was discolored over an area 4-1/2" in diameter, while the back side of the unprotected sample LS-70-4 was checked.

The silver-paint coating was almost completely vaporized and blown clear of the panel by this arc.

The thickness of these panels, 0.04", is such that they are too thin for short beam shear tests. Consequently the degree of mechanical degradation was determined by taking tensile specimens from each panel. Figure 75 shows a template, cut from vinyl sheeting, overlaying one of the circular discs and indicating the dimensions and locations of the fourteen tensile-test specimens which were cut from each panel. On those panels using a silver-paint coating the paint was stripped from the sample to insure good bonding of the tensile section surfaces to the plastic tabs which held the specimen in the tensile-test fixture. The template was designed with eight of the specimens aligned parallel to the two outer plies of the panels (tensile specimens 7 through 14), and six parallel to the inner ply (tensile specimens 1 through 6). Peripheral sections were placed in or close to the grounding-collar area and slack spacing was allowed in order that the template could be centered within reason over the lightning-strike area, if it was not in the exact center of each panel. The specimens were cut by a crystal-wafering, diamond-blade saw to produce accurate dimensions and minimize fiber damage on each cut. The tensile strengths are

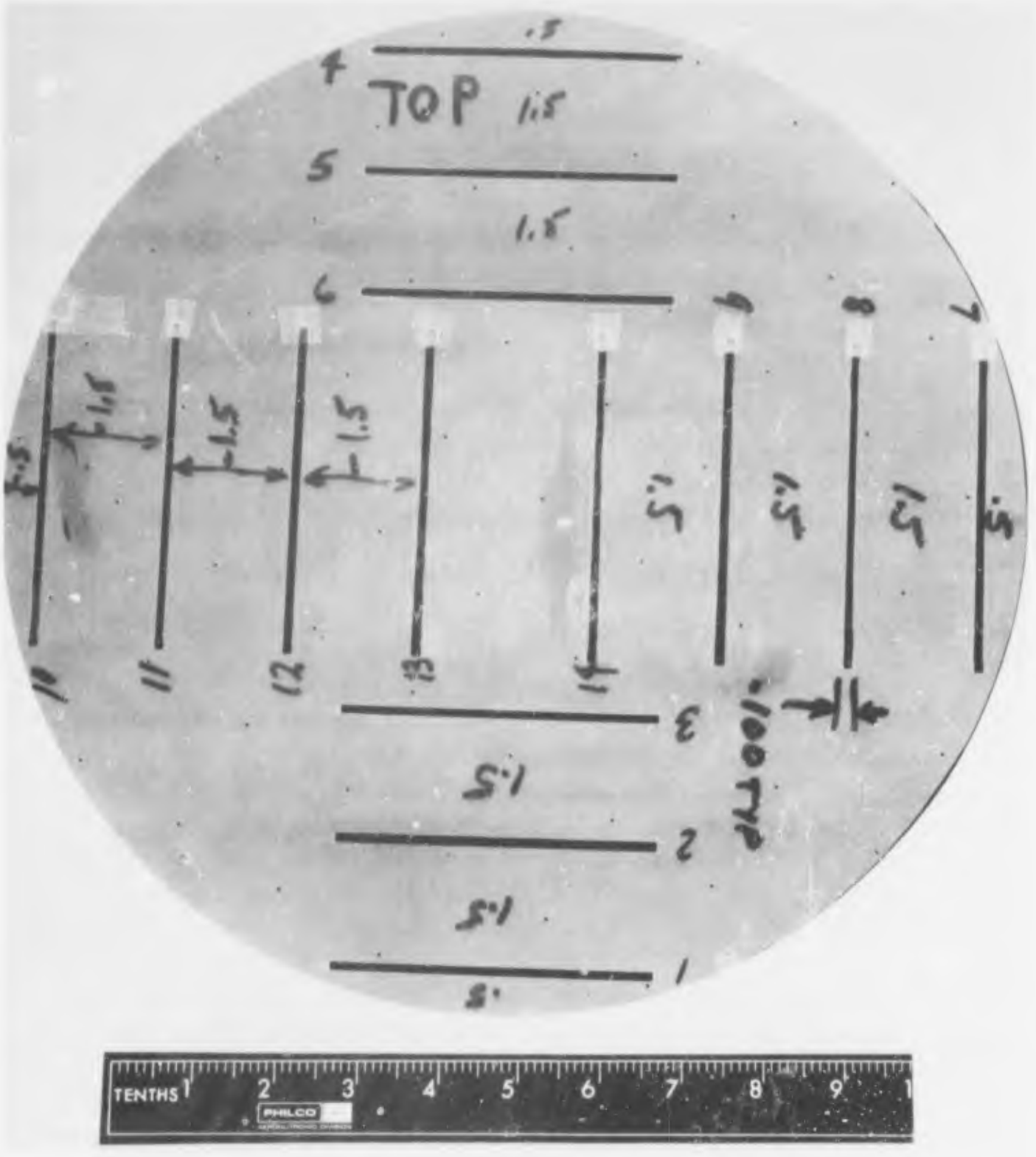

FIGURE 75 - Template of Vinyl Sheeting Used for Cutting Tensile Test Specimens

shown on Table XIV and plotted on Figures 76 through 78. On Figure 76 (for either coated or silver painted panels) the tensile strengths of all the specimens, near to and removed from the arc attachment point are grouped. There is a large spread between maximum and minimum tensile strengths since specimens near the arc at attachment point were more severely damaged than those farther away from the arc attachment point.

The samples for tensile strength measurements were cut in a pattern that allows one to compare the strength of the panel at different distances from the striken point. Figures 77 and 78 show the tensile strength at various contours around the striken point. A summary of the more obvious results of the test is as follows:

Panel 70-1

Tensile strengths were uniform except on specimens 13 and 14. Specimens 13 and 14 straddled the stroke-attachment area and fell with the area shown by the "C"-scan as being delaminated.

Panel 70-2

All tensile strengths were uniform. Specimens 13 and 14 did not reflect the delamination shown by the "C"-scan.

Panel 70-3

Specimens 3, 7, 8, 9, 12, and 14 showed lower tensile values. Specimen 13 tensile strength was high even though it straddled the area shown delaminated by the "C"-scan. Specimens 3 and 8 showed low tensile strength, but the "C"-scan did not indicate any damage at that point.

Panel 70-4

The low value obtained on specimen 6 is believed to be the result of damage in specimen preparation. Specimens 12, 13, and 14 showed low values as expected from "C"-scan data. Specimen 3 showed a very high tensile strength in spite of the "C"-scan delamination indication.

Panel 70-5

Based on "C"-scan data, specimens 3, 6, 9, 12, 13, and 14 would be expected to have shown low tensile values. Of this group only no. 3 was low.

Panel 70-6

Specimens 3, 7, and 14 showed low tensile strength. "C"-scan data would suggest that specimens 2, 3, 6, 9, 12, 13, and 14 should have been low.

Panel 70-7

Specimens 2 and 3 showed abnormally low values believed to be caused by damage in sample preparation. Specimens 1 and 10 were low, suggesting damage at the grounding-collar contact region. Specimens 13 and 14 showed low values as would be predictable from "C"-scan data.

TABLE XIV

TENSILE STRENGTH OF 13" CIRCULAR PANELS, $\sigma \times 10^3$ PSI

Calculated from $\sigma \times 10^3$ psi = $\frac{\text{ultimate}}{\text{cross section area}}$

Specimen Number	84.2 kA 70-1	61 kA 70-2	57.5 kA 70-3	184 kA 70-4	61.3 kA 70-5	103 kA 70-6	185 kA 70-7	104.5 kA 70-8
1	47.0	52.9	59.7	48.2	50.5	46.3	15.9	38.0
2	48.0	46.9	45.6	44.4	38.5	32.0	6.3*	21.1
3	65.5	40.5	29.7	60.8	28.6	19.2	5.0*	6.4*
4	51.6	56.0	44.7	55.4	52.2	39.3	51.5	40.0
5	53.6	51.3	43.4	33.5	50.8	45.4	53.1	44.1
6	53.1	48.1	46.7	8.3*	52.3	52.6	27.7	17.5
7	52.5	49.8	30.1	53.6	35.7	29.3	31.3	25.3
8	43.3	50.9	30.6	39.2	50.0	32.7	34.4	47.8
9	44.9	56.0	36.4	41.4	46.9	39.9	32.8	41.1
10	49.3	54.9	44.4	37.6	53.3	31.3	28.8	36.5
11	43.8	58.1	40.1	52.9	49.6	42.5	47.1	35.0
12	45.7	58.5	36.6	23.6	47.5	31.4	44.7	37.9
13	24.1	48.0	54.7	31.8	54.2	40.1	21.0	26.2
14	24.2	49.0	39.7	27.0	55.1	24.7	23.3	26.9

* - Low value perhaps due to damage during preparation of the specimen

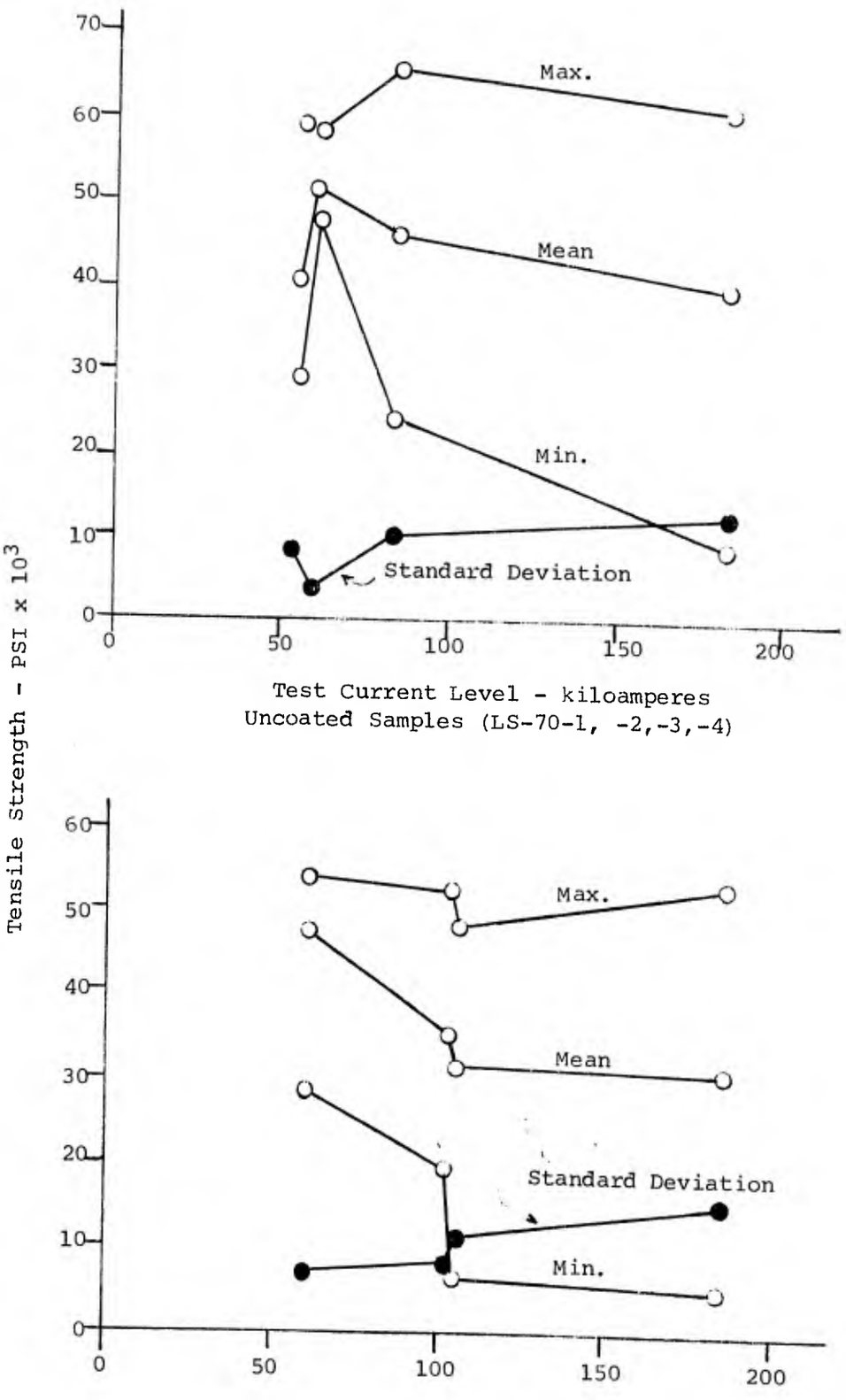

FIGURE 76 - Tensile Strengths of All Specimens Cut From 0.040" Thick Graphite Fiber/Epoxy Panels

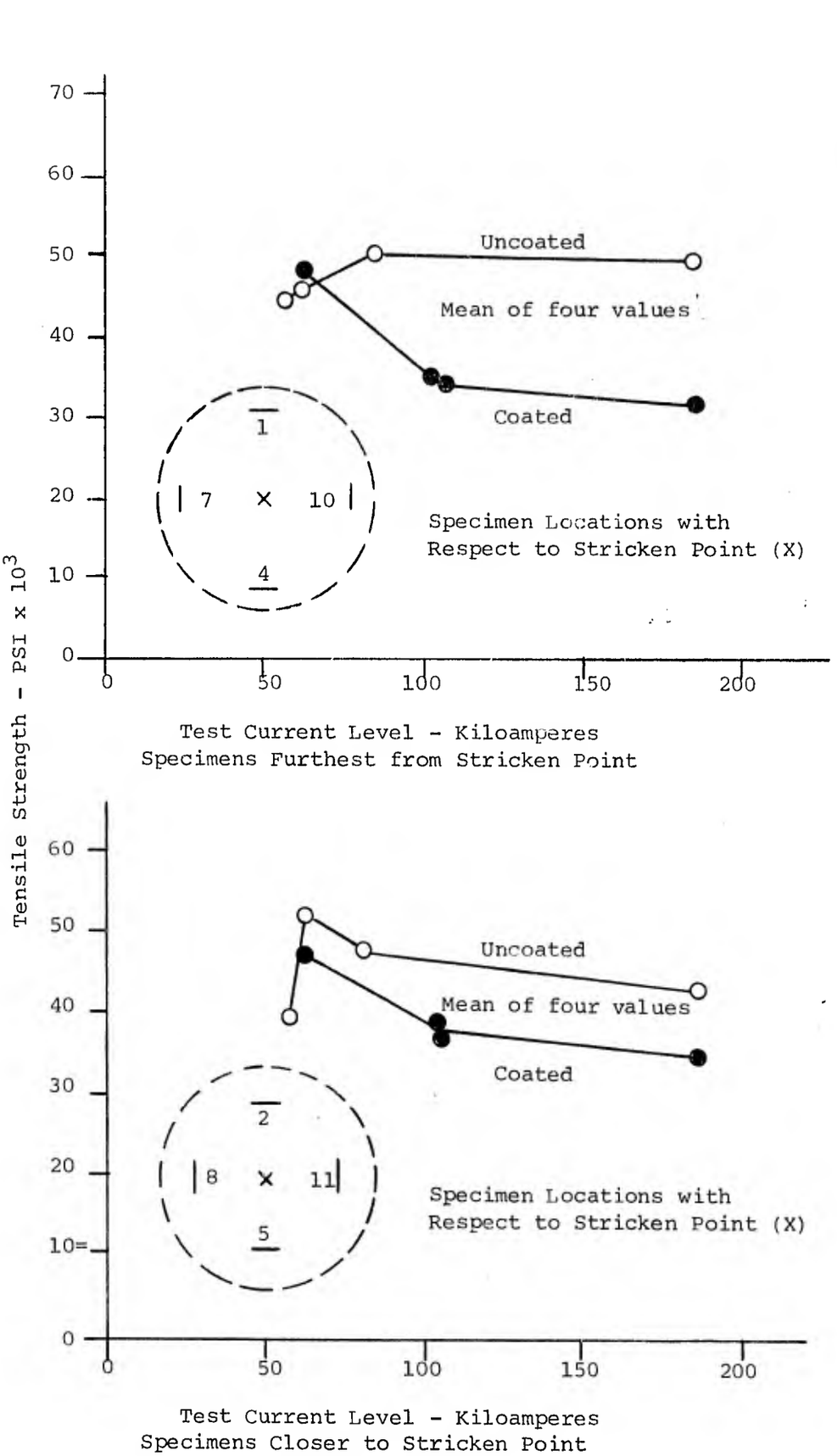

FIGURE 77 - Tensile Strengths of 0.040" Thick Graphite Fiber/Epoxy Panels at Different Distances from the Stricken Point

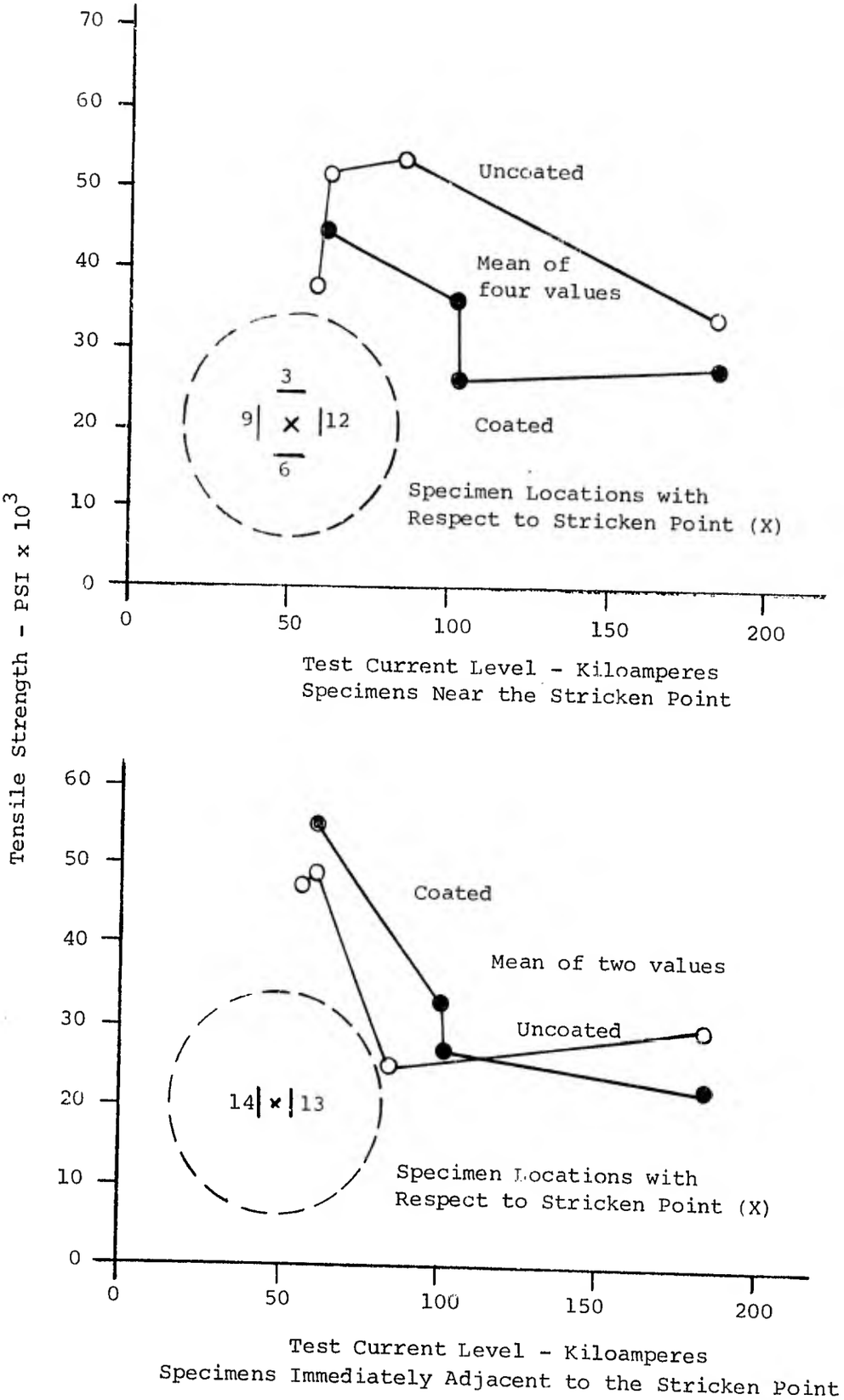

FIGURE 78 - Tensile Strengths of 0.040" Thick Graphite Fiber/Epoxy Panels at Different Distances from the Stricken Point

Panel 70-8

Specimens 2, 3, 6, 7, 13, and 14 showed low tensile values. Specimens 2 and 7 were beyond the "C"-scan damaged area.

Two other items about the data in Table XIV seem to be apparent. The first is that the critical damage threshold seems to be about 75 kA. A critical threshold is hard to define, but around 75 kA the mean tensile strength of all specimens for several inches around the striking point seemed significantly lower than for the sample tested at the nominal 50 kA level. Of more significance is that the silver-paint coating did not seem to provide any protection. If anything, the data indicates that the damage was greater on those panels that were coated with silver paint than on uncoated ones.

The samples for tensile strength measurements were cut in a pattern that allows one to compare the strength of the panel at different distances from the stricken point. Figures 77 and 78 show the tensile strength at various contours around the stricken point. No significant difference in mean values was noted at the different locations, at least as regards test current levels around 50 - 75 kA. At the highest test current levels (or immediately adjacent to the stricken point) the mean tensile strengths were low, but visual observation of the surface of the panel at those points would indicate that the strength should be low. The fact that the specimens from the panels "protected" with silver paint were lower than those from the unprotected panels should not be overlooked.

In summary, perhaps one can say that significant degradation in the structural strength of a panel might be expected to a distance away from the stricken point of twice the dimensions of the area in which the fibers were lifted or blown away by the stroke. This rule of thumb should be applied cautiously.

Resin content was determined on all tensile specimens of panels 70-1 and 70-4 to determine the probable spread of values over the panel. Only specimens 1, 2, 3, 8, 9, and 14 were analyzed for resin content on the remaining 6 panels. The resin content analytical results are compiled in Table XV. No significant trends are evident except the fact that all panels show an abnormally high resin content compared to the preferred range of 35% to 40% resin.

Specimens were selected for microscopic examination from areas adjacent to the mid-section of each tensile specimen. Twelve photomicrographs at 100X were

TABLE XV

WEIGHT PER CENT RESIN CONTENT FROM TENSILE SPECIMENS OF GD-LS-70-1 THROUGH -8

Tensile Number	84.2 kA GD-LS 70-1	61 kA GD-LS 70-2	57.5 kA GD-LS 70-3	184 kA GD-LS 70-4	61.3 kA GD-LS 70-5	103 kA GD-LS 70-6	185 kA GD-LS 70-7	104.5 kA GD-LS 70-8
1	55.2	50.2	49.7	44.4	51.4	50.4	39.4	42.2
2	54.2	52.0	51.4	47.8	53.4	52.0	40.3	43.5
3	61.8	52.2	50.3	45.8	53.8	50.6	44.4	44.2
4	54.2			44.1				
5	54.8			45.1				
6	56.6			47.7				
7	53.3			42.2				
8	56.0	50.8	50.7	43.8	51.6	48.6	40.6	40.2
9	50.0	51.7	47.7	51.9	52.3	54.8	41.7	39.7
10	57.8			45.8				
11	56.2			47.0				
12	58.4			46.5				
13	55.5			46.1				
14	58.0	52.1	51.2	44.4	51.6	52.5	37.0	41.9

prepared for each panel. Since no significant differences were observed, only one complete set is included in this report to illustrate the micro-morphology of the damaged area. These are shown on Figures 79 through 90. Figures 79 through 84 refer to panel GD-LS-70-3, which was tested at 57 kA and Figures 85 through 2.90 refer to panel GD-LS-70-4, which was tested at 184 kA. Both of these panels were 0.040" uncoated panels.

All photomicrograph designations correspond to the tensile specimen numbers listed in Table XIV. Thus, Figure 79 represents the appearance of the fibers perpendicular to and parallel to the outer plies in the immediate vicinity of tensile specimen no. 1.

Most of the damage observable on these photomicrographs appeared to be mechanical in nature, and not due to thermal degradation of the fibers. Particularly as regards panel LS-70-3, the characteristic damage observed consisted of a series of cracks running parallel to the individual fibers. Some cracks were noted on the photomicrographs taken before the lightning withstand tests; see Figure 58 for example. None of those cracks were as large as these however. The panels would split easily in a direction parallel to the fiber reinforcements because the only strength of the panel lies in the resin binder. These cracks do not seem to have degraded the tensile strength particularly. Tensile specimens 1 and 2 of panel LS-70-3 both showed average tensile strength,while specimen 3 showed a significantly lowered tensile strength. Specimen 3 had the largest cracks of any of these three, which one might expect, since it was closest to the arc-attachment point. Tensile specimen 8 again showed a lowered strength, but the photomicrographs of it did not reveal cracking any worse than that observed on specimens 1 and 2. Specimens 9 and 14, even closer to the stroke-attachment point, showed reasonably high tensile strengths, even though specimen 14 on the photomicrographs began to show a good amount of physical tearing and lifting of the fibers on the top ply.

On panel LS-70-4, tested at 184 kA, it is interesting that the tensile strengths of specimens 1 and 2 are normal while specimen 3 is significantly stronger in spite of the massive damage to the top ply shown on Figure 87. Specimen 3 was, of course, immediately below the stroke-attachment point. Again, the fibers and resin on the two inner plies of this specimen do not look any different than do the fibers and resin on specimens further from the stroke-attachment point or on panel LS-70-3 which was tested at a 57.5 kA level. On photomicrograph 3a of Figure 87 one can see a considerable amount of blacken-

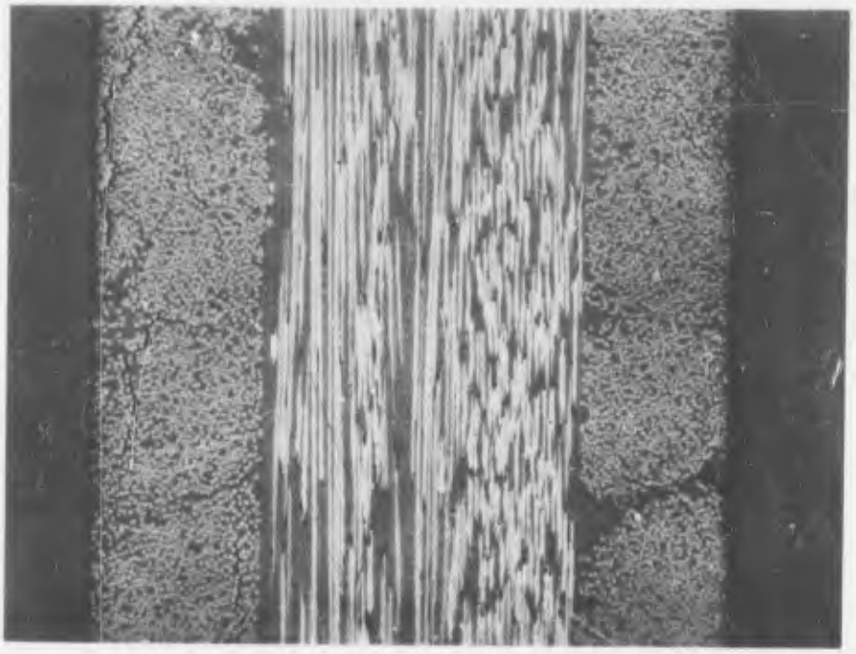

Tensile Specimen 1A

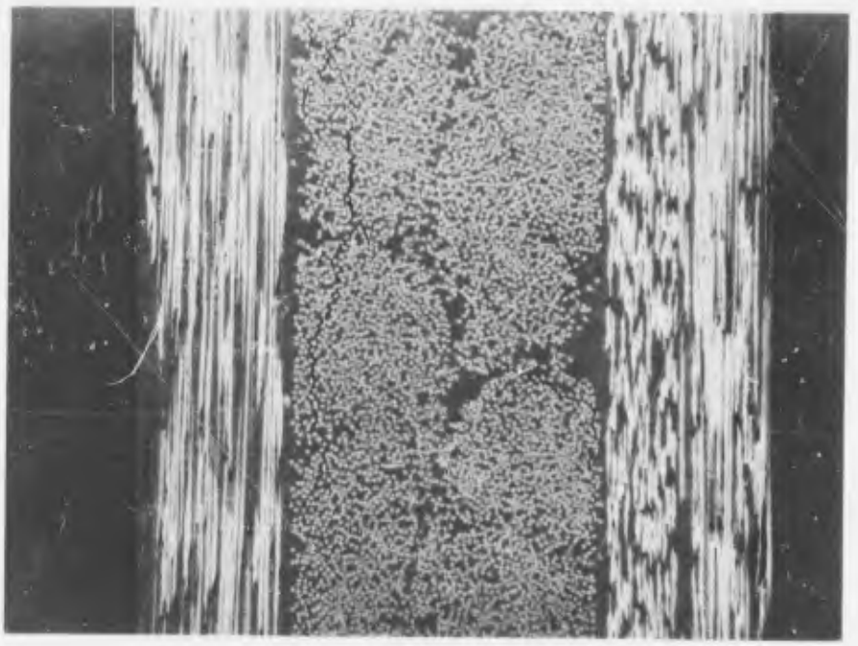

Tensile Specimen 1B
GD-LS-70-3
(57.5 kA)

FIGURE 79 - 100X Photomicrograph of a Damaged Area of Graphite Fiber/ Epoxy Panel After Exposure to Simulated Lightning Discharge

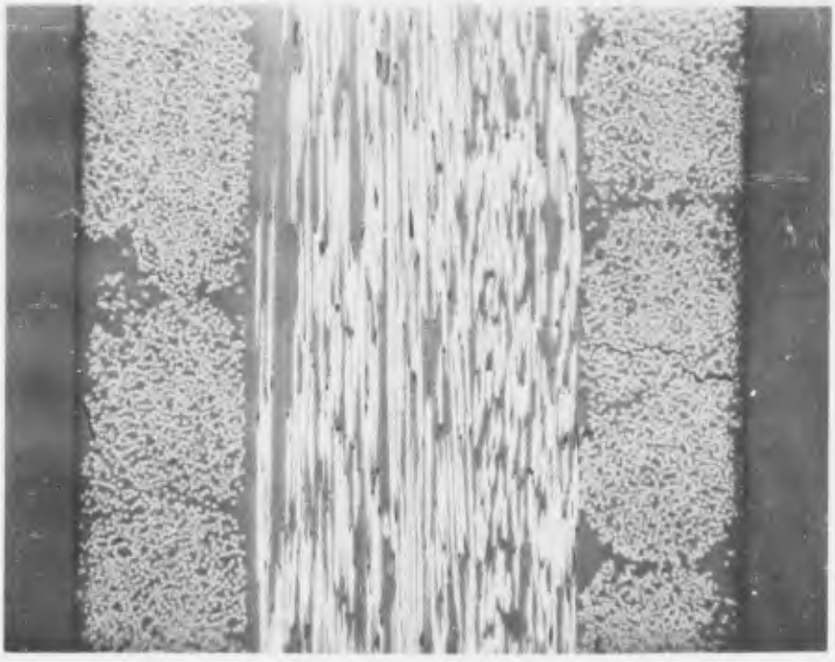

Tensile Specimen 2A

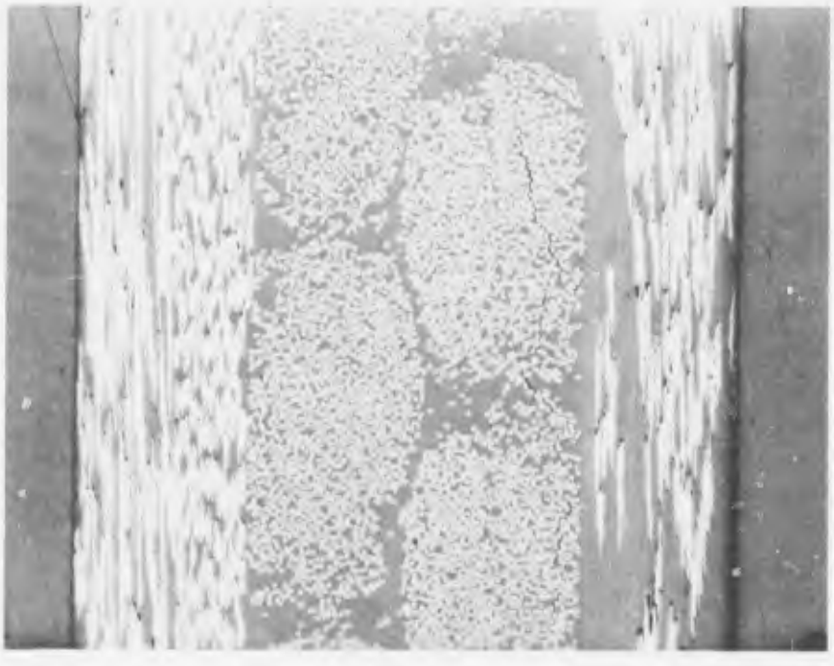

Tensile Specimen 2B
GD-LS-70-3
(57.5 kA)

FIGURE 80 - 100X Photomicrograph of a Damaged Area of Graphite Fi
Epoxy Panel After Exposure to Simulated Lightning Dis

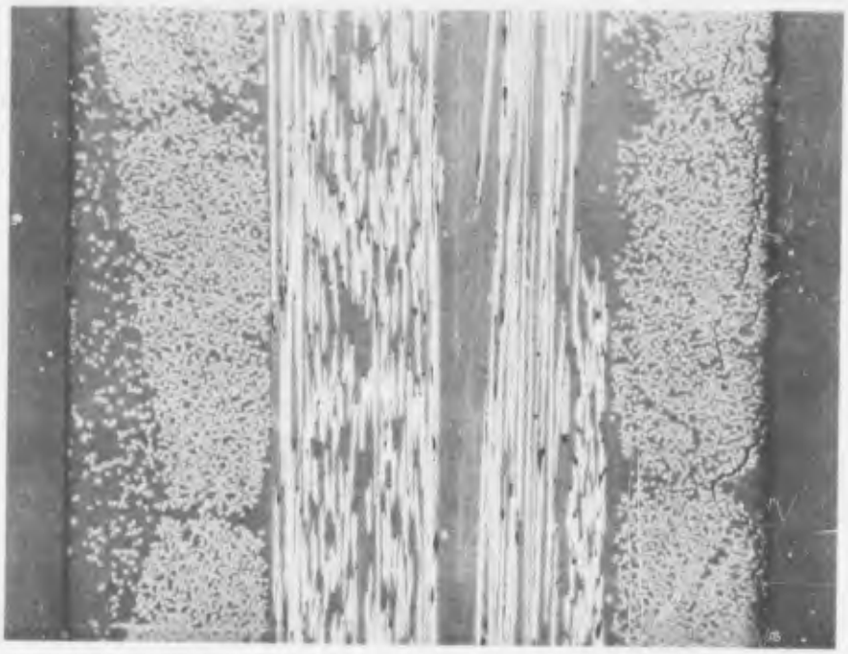

Tensile Specimen 3A

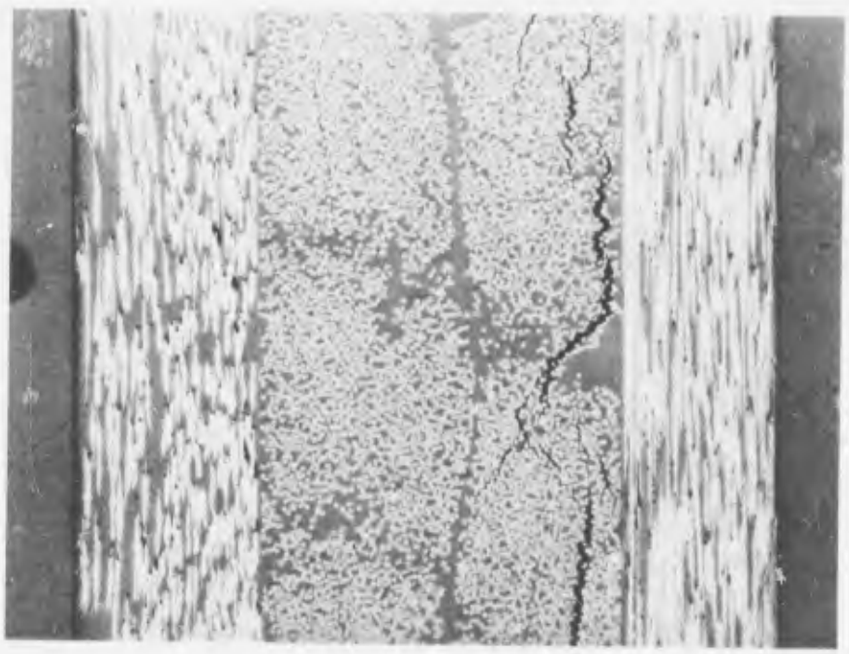

Tensile Specimen 3B
GD-LS-70-3
(57.5 kA)

FIGURE 81 - 100X Photomicrograph of a Damaged Area of Graphite Fiber/ Epoxy Panel After Exposure to Simulated Lightning Discharge

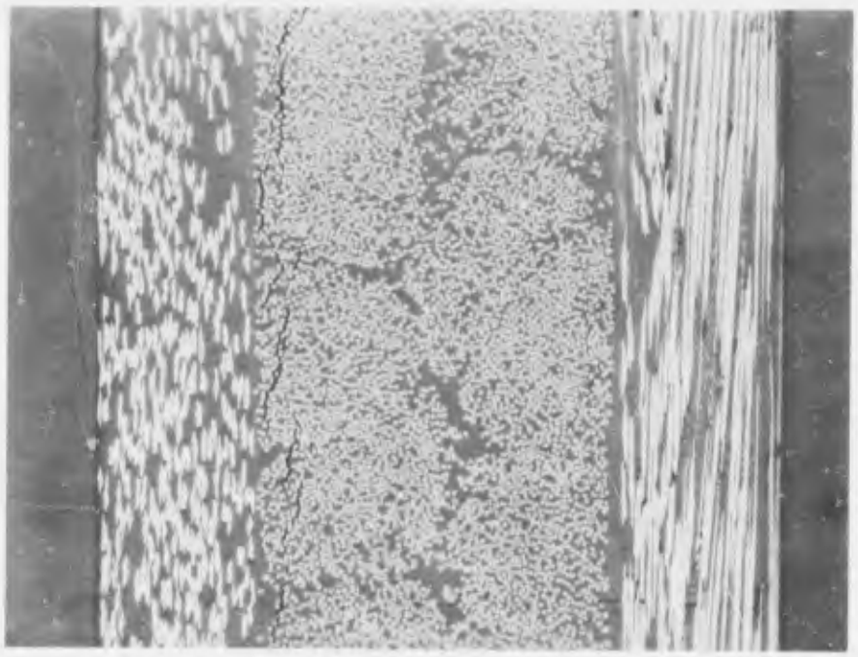

Tensile Specimen 8A

Tensile Specimen 8B
GD-LS-70-3
(57.5 kA)

FIGURE 82 - 100X Photomicrograph of a Damaged Area of Graphite Fiber/Epoxy Panel After Exposure to Simulated Lightning Discharge

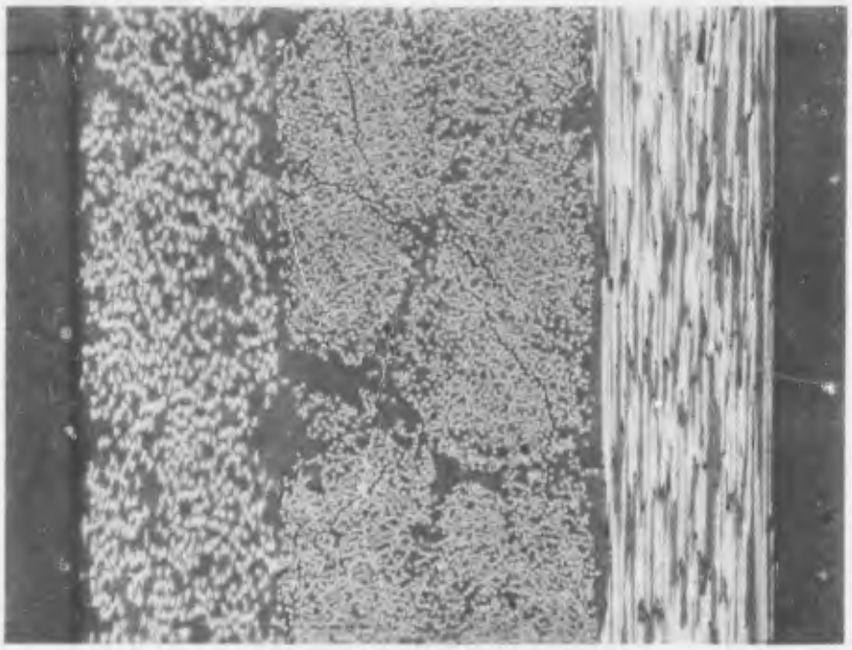

Tensile Specimen 9A

Tensile Specimen 9B
GD-LS-70-3
(57.5 kA)

FIGURE 83 - 100X Photomicrograph of a Damaged Area of Graphite Fiber/Epoxy Panel After Exposure to Simulated Lightning Discharge

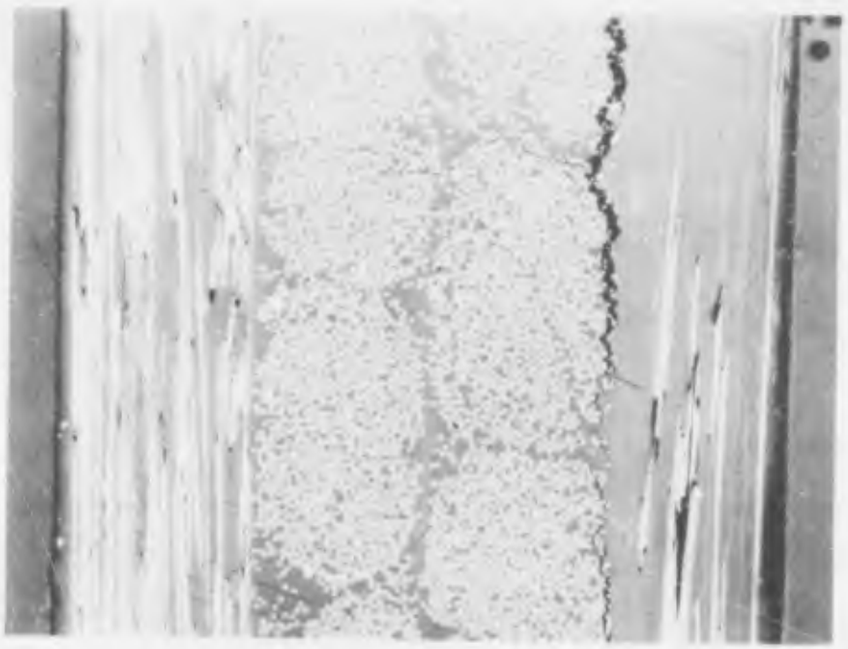

Tensile Specimen 14A

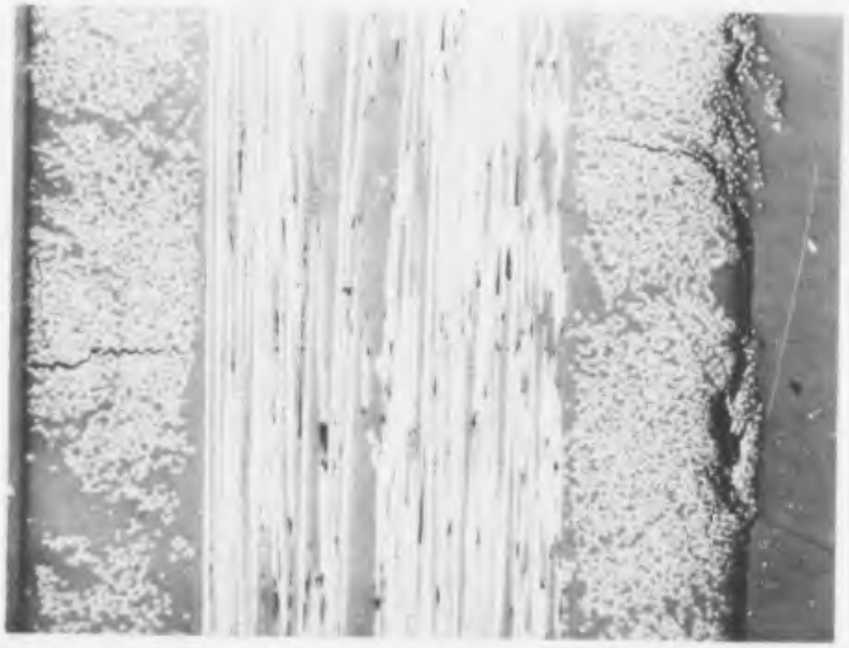

Tensile Specimen 14B
GD-LS-70-3
(57.5 kA)

FIGURE 84 - 100X Photomicrograph of a Damaged Area of Graphite Fiber/ Epoxy Panel After Exposure to Simulated Lightning Discharge

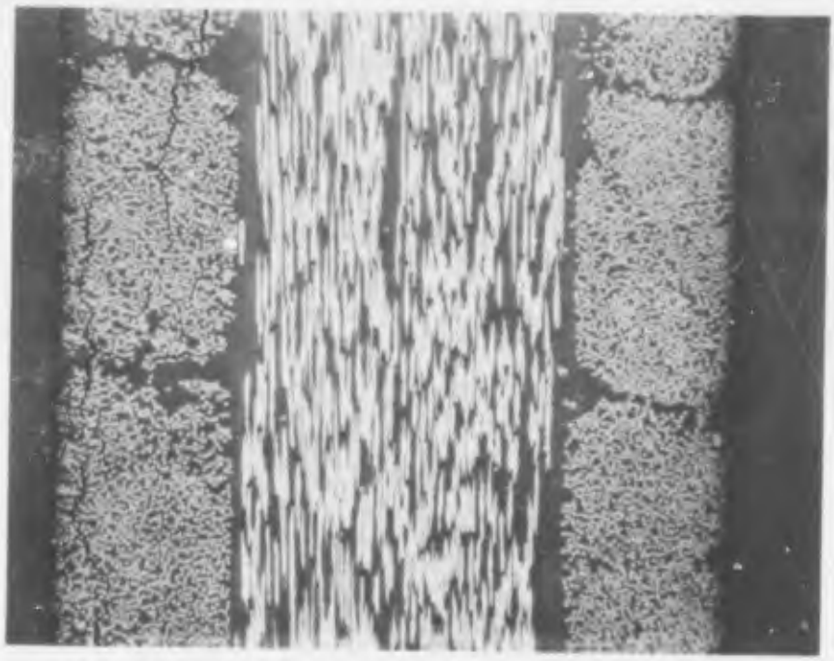

Tensile Specimen 1A

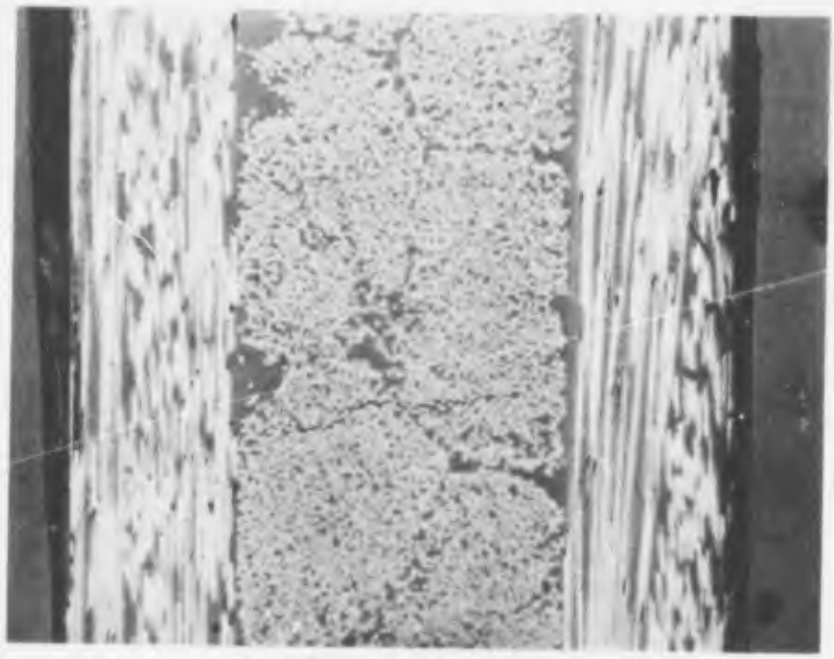

Tensile Specimen 1B
GD-LS-70-4
(184 kA)

FIGURE 85 - 100X Photomicrograph of a Damaged Area of Graphite Fiber/Epoxy Panel After Exposure to Simulated Lightning Discharge

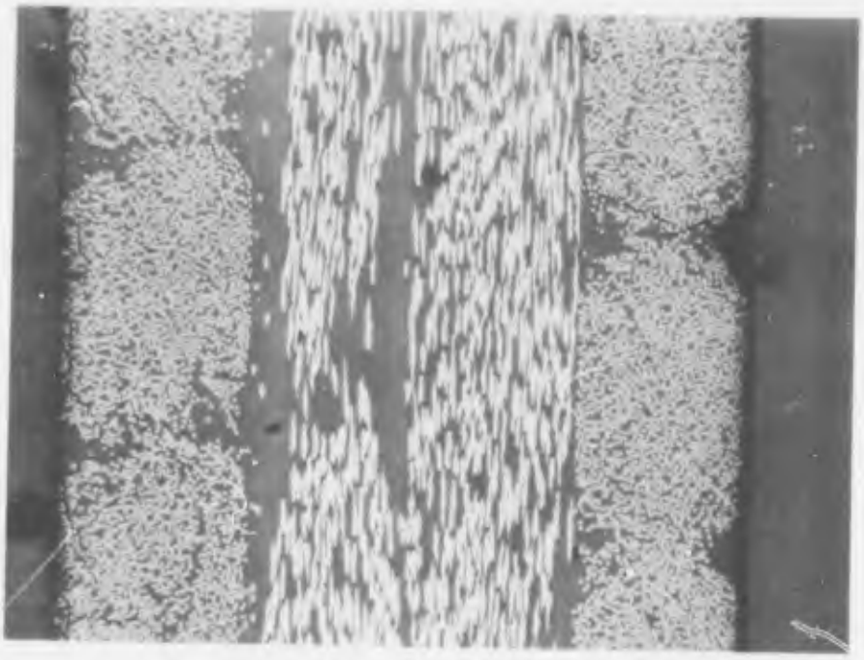

Tensile Specimen 2A

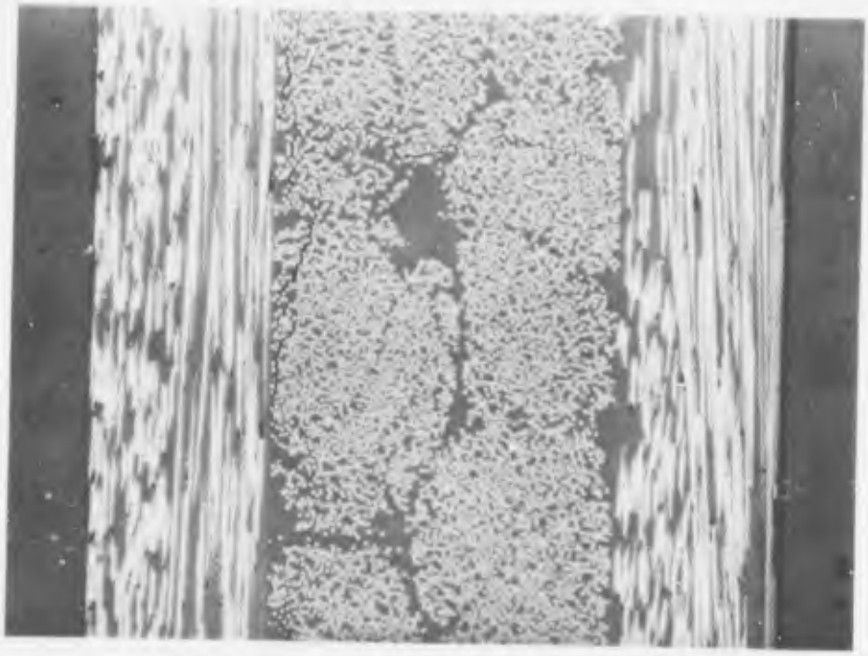

Tensile Specimen 2B
GD-LS-70-4
(184 kA)

FIGURE 86 - 100X Photomicrograph of a Damaged Area of Graphite Fiber/ Epoxy Panel After Exposure to Simulated Lightning Discharge

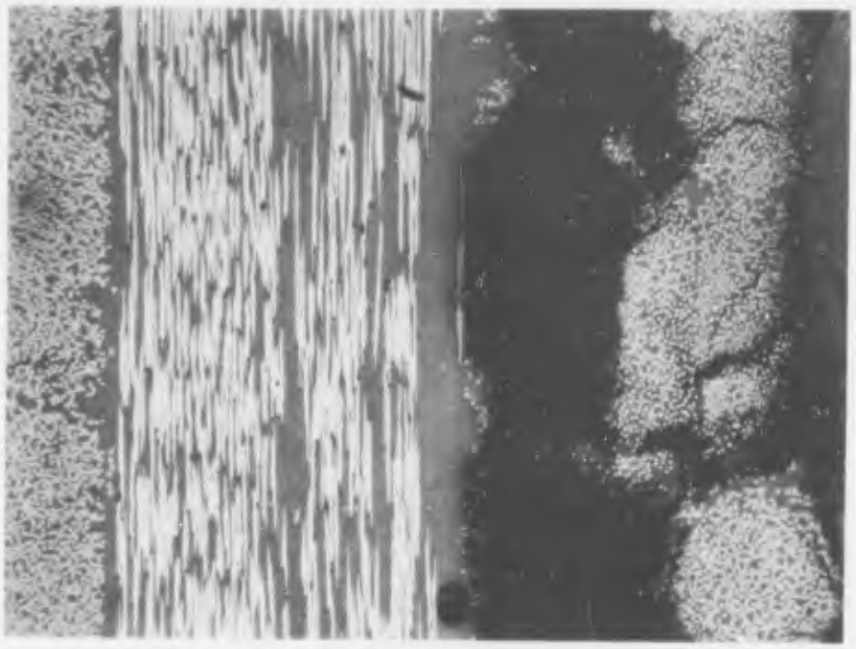

Tensile Specimen 3A

Tensile Specimen 3B
GD-LS-70-4
(184 kA)

FIGURE 87 - 100X Photomicrograph of a Damaged Area of Graphite Fiber/ Epoxy Panel After Exposure to Simulated Lightning Discharge

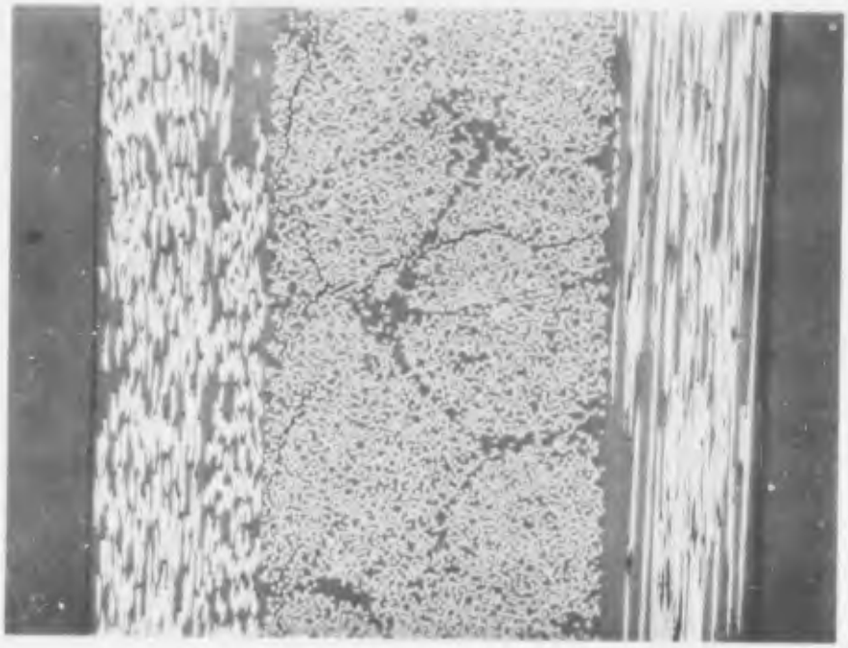

Tensile Specimen 8A

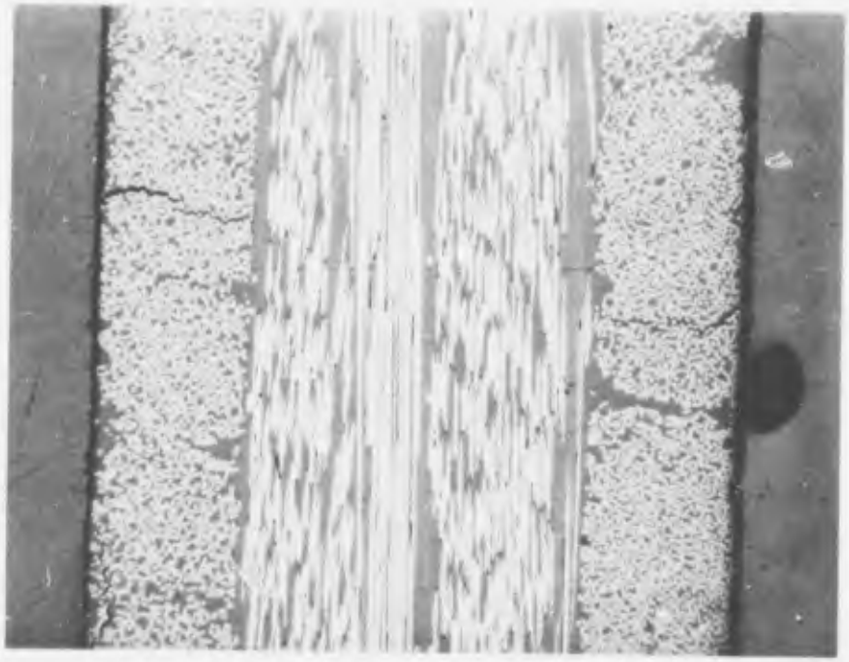

Tensile Specimen 8B
GD-LS-70-4
(184 kA)

FIGURE 88 - 100X Photomicrograph of a Damaged Area of Graphite Fiber/ Epoxy Panel After Exposure to Simulated Lightning Discharge

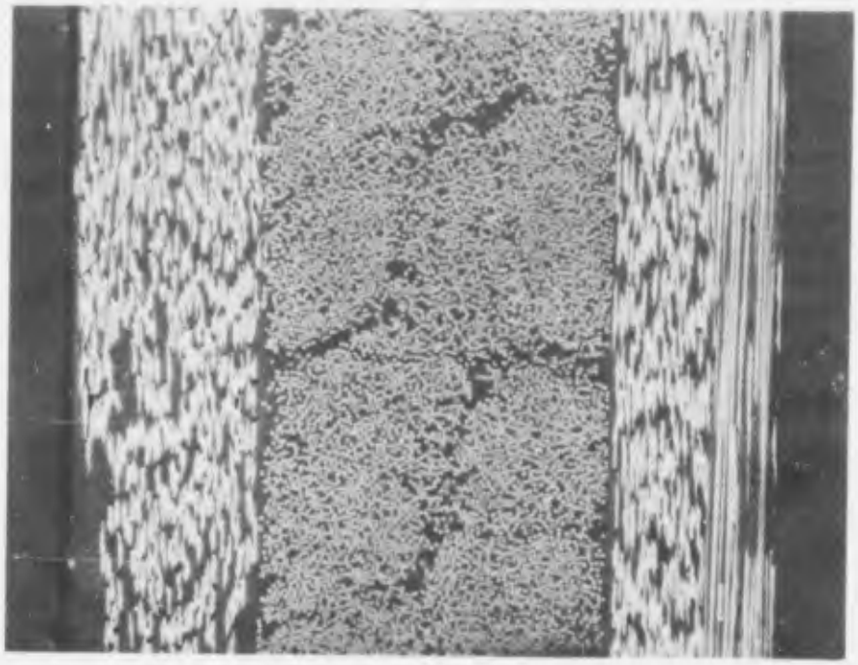

Tensile Specimen 9A

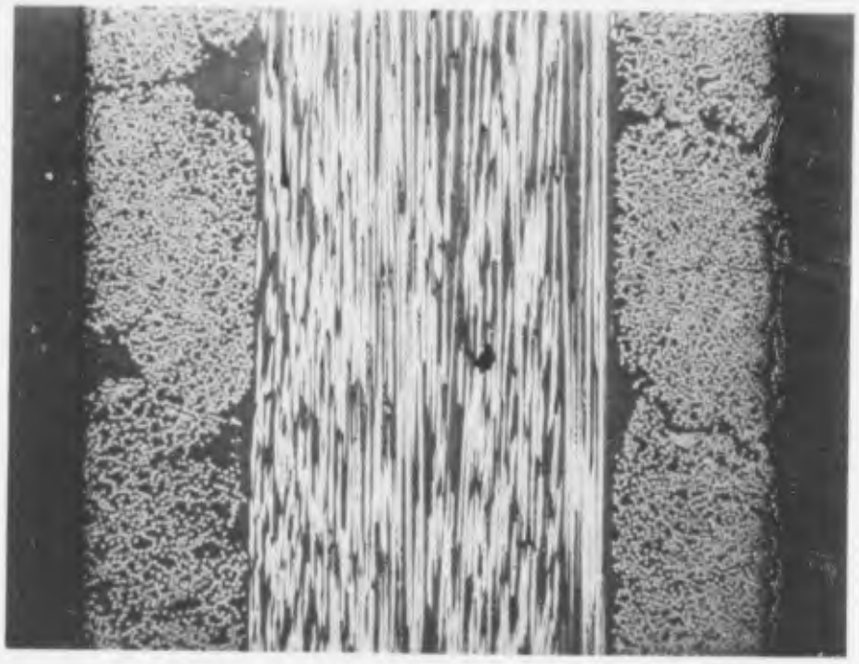

Tensile Specimen 9B
GD-LS-70-4
(184 kA)

FIGURE 89 - 100X Photomicrograph of a Damaged Area of Graphite Fiber/ Epoxy Panel After Exposure to Simulated Lightning Discharge

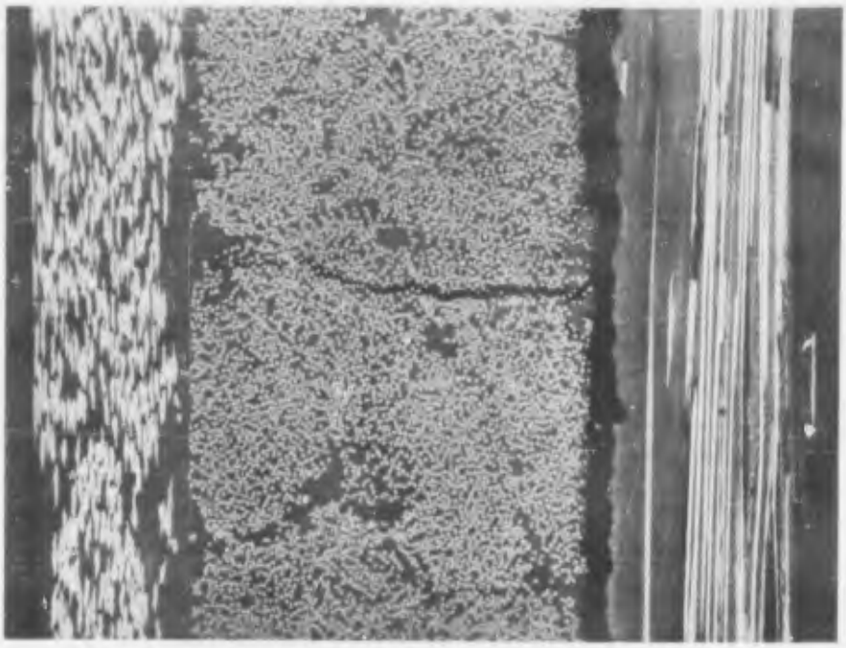

Tensile Specimen 14A

Tensile Specimen 14B
GD-LS-70-4
(184 kA)

FIGURE 90 - 100X Photomicrograph of a Damaged Area of Graphite Fiber/ Epoxy Panel After Exposure to Simulated Lightning Discharge

ing of the resin around the fibers in the top ply. Presumably this would represent pyrolyzed resin surrounding these fibers that should carry the most current and should get the hottest. A little of this same blackening of the resin is noted on the inner ply at the left of the picture, but only around the isolated fibers and around the one small crack shown. Specimen 2 also shows a few isolated fibers having this blackening of the resin around the fibers. The pyrolysis of the resin, if indeed that is what it is, appears on both the outer and inner plies. Specimen 8 does not show any of this. Specimen 9 shows a few isolated fibers having what are believed to be burned spots around them. Specimen 14 shows the top ply split away from the remaining plies and shows the lifting and physical tearing of the fibers that was also observed visually.

In summary, the photomicrographs would indicate that most of the damage to the graphite panels is due to mechanical shock caused by vaporization of the resin leading to breaking of plies and splitting of bundles. This is in considerable contrast to the patterns observed on the 6" x 12" boron panels in which the photomicrographs clearly showed thermal degradation of the individual boron fibers.

Since much of the physical damage seemed to be due to cracking parallel to the fiber orientation or cracking transverse to the panel thickness, one could speculate that if the graphite fibers were woven like cloth, there would be more resistance to the cracking observed on these photomicrographs. Certainly the points where the fibers would cross would allow a more even distribution of current within the panels. If a three-dimensional weave, somewhat like carpet tufting could be fabricated, the resistance to lightning damage of the graphite panels should be improved even more. However, even if the graphite fibers could be woven, the packing density of the individual fibers would be decreased and the net mechanical strength of the panel might be reduced over what is now.

The test made on the thicker graphite panels of nominal thickness 0.120" will not be described. Photographs of the damage to panels LS-70-9 through LS-70-14 are shown on Figures 91 and 92. Also shown on these figures are data pertaining to an acoustic impedance test. The significance of this latter will be described later.

Panel LS-70-10 (69 kA)

This was an uncoated, 0-90° layup panel of 0.120" thickness. It was tested at a current level intermediate between the 0.040" panels LS-70-2 (61 kA), LS-70-3 (57 kA), and panel LS-70-1 (85 kA). The area of disruption of the panel surface, or the discolored area, was about the same on

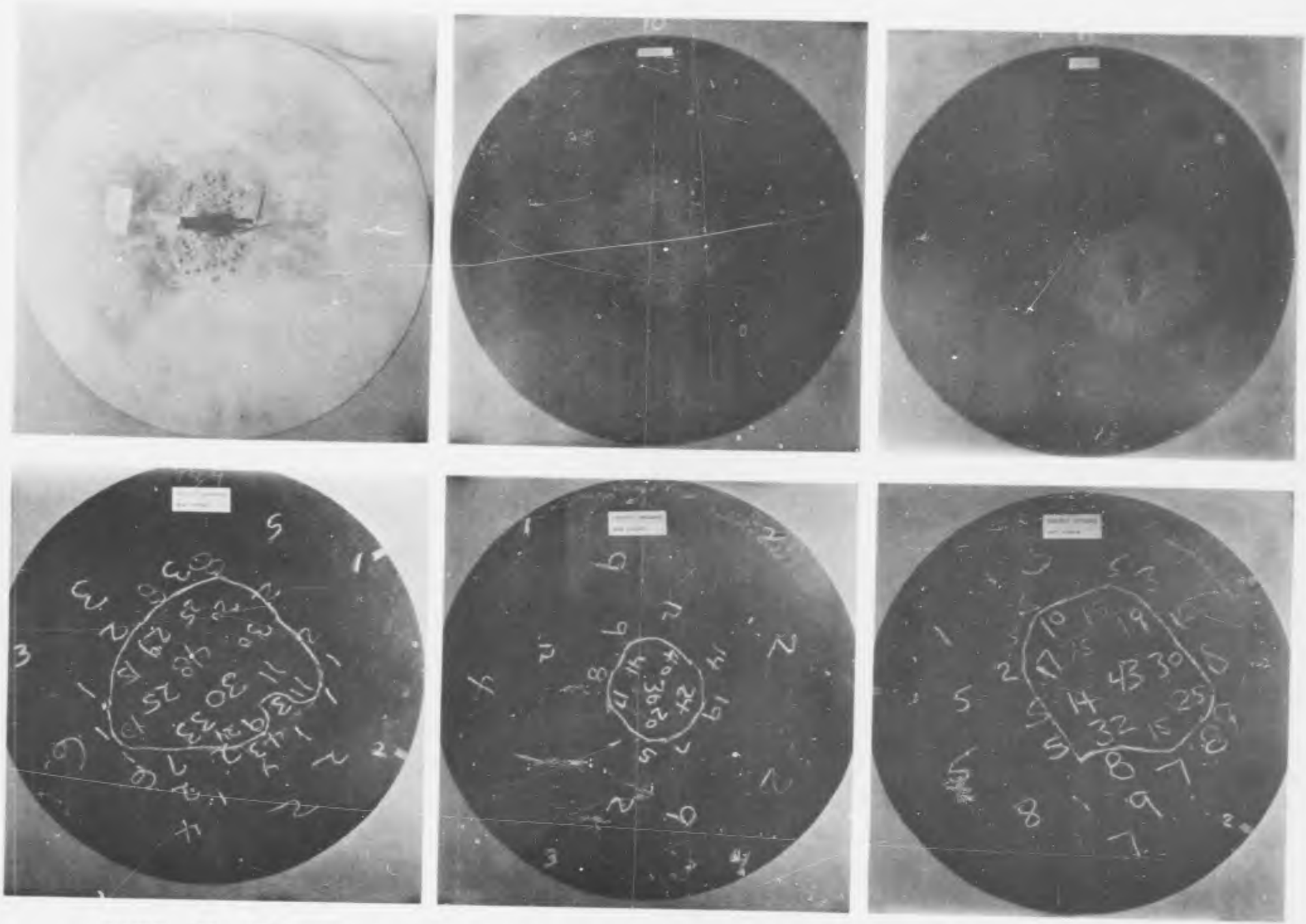

FIGURE 91 - Photographic Reductions of Panels LS-70-9, LS-70-10 and LS-70-11 Showing Both Sides After Strikes of Simulated Lightning

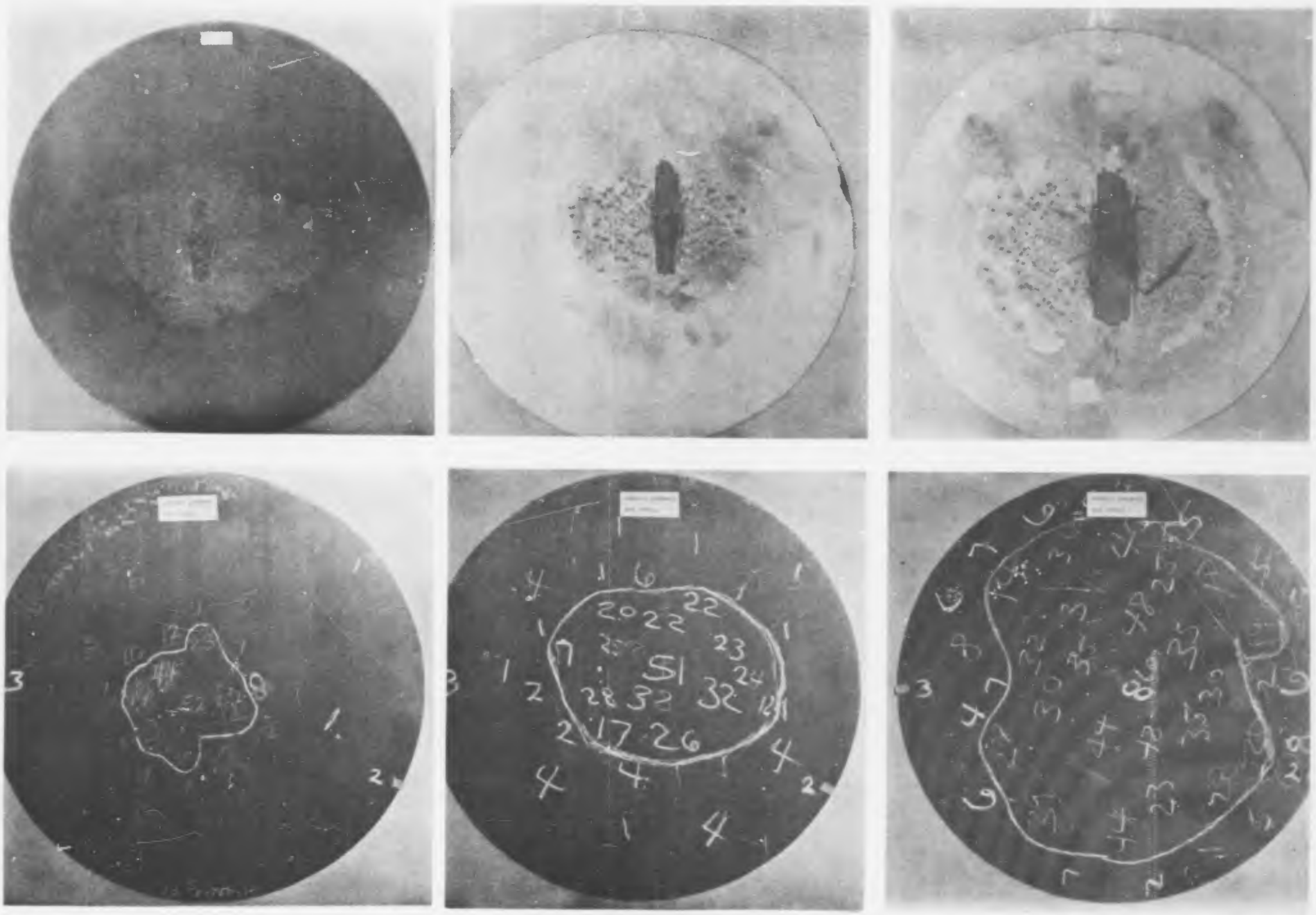

FIGURE 92 - Photographic Reductions of Panels LS-70-12, LS-70-13, and LS-70-14 Showing Both Sides After Strikes of Simulated Lightning

this thick panel as on the thinner 0.040" panels, but the physical lifting or destruction of the first layer of fibers was less on this thick panel. The arc did not blow a hole through this panel as it did on the thinner panels. The back surface was undamaged, at least visually; however, tapping the back surface with a coin showed a dead area in the center. At the outer edges the panel rang clearly as though the fibers were undamaged.

Panel LS-70-11 (69 kA)

This was an uncoated panel of 0.120" thickness with a 0-45°-90° layup. It can be compared to panel LS-70-10 to see the effects of ply layup. Basically there does not seem to be any difference between the amount of damage to these two panels, or any other obvious ply effects. Neither panel was burned through to the back side.

Panel LS-70-12 (101 kA)

This was an uncoated panel of 0.120" thickness with a 0-45°-90° layup. There was no uncoated panel that had been tested in a directly comparable manner. The closest was panel LS-70-1, a 0.040" panel that was tested at 85 kA. Again, there were no obvious defects that could be attributed to the effects of ply layup. This panel at 101 kA did not burn through to the back surface as did the thinner panel 70-1 (85 kA).

Panel LS-70-9 (69 kA)

This was a silver-paint coated panel of 0.120" thickness with a 0-90° layup. It can be compared to uncoated panels LS-70-10 and LS-70-11, both of which were 0.120" thickness and tested at the same current level. The damage looked about the same on the coated and uncoated panels, both with respect to the damaged area and the amount of fibers lifted or blown away.

Panel LS-70-13 (101 kA)

This was a silver-paint coated panel of 0.120" thickness with a 0-90° layup. It can be compared to the uncoated panel LS-70-12 of 0-45°-90° layup. Again, the physical damage looked about the same coated and uncoated. The damaged area was, of course, greater than was observed at the lower current level on panel LS-70-9.

Panel LS-70-14 (203 kA)

This was also a silver-paint coated panel of 0.120" thickness with a 0-90° layup. It can be compared to panels LS-70-4 (184 kA), uncoated,

0.040" and LS-70-7 (185 kA), coated, 0.040". There was an increase of damage to the first layer of panel LS-70-14 compared to panels LS-70-4 and LS-70-7. However, the extent of vaporization of silver paint on panel LS-70-7 was more extensive than on panel LS-70-14. The only variable between these two panels was the thickness of composite material. It seems that this thicker composite material carried more of the current instead of the current being diverted onto the silver paint coating. The silver-paint coating of the thinner (0.040") panel 70-7 carried more of the impulse current, thereby destroying more of the silver-paint coating.

Following the simulated lightning current testing, the panels were given the usual nondestructive tests to determine the extent of damage. The most significant finding is the fact that the Thornel-50/epoxy composites coated with silver paint were more severely degraded than the uncoated panels. While visual comparisons of the front surfaces (coated sides) of panels LS-70-9, LS-70-13, and LS-70-14 suggest that the damage of both groups are about equal, the ultrasonic "C"-scan data measurements show the damaged regions to be much larger on the coated panels. As examples, panel LS-70-9 (coated), and panels LS-70-10 and LS-70-11 (uncoated) all were subjected to the same current. The ultrasonic C-scan data revealed two to four times larger areas of damage on the coated panels compared to the uncoated panels.

During the evaluation of these test panels, measurements were made of acoustical impedance, a type of measurement not used during previous test analyses, but one which turned out to show considerable promise as a nondestructive tool for the evaluation of damaged areas. Basically, the instrument detects changes in an acoustical standing wave, resulting from acoustic impedance variations in the structure of the composites. Acoustic impedance is defined as:

$$\text{impedance} = \text{density} \times \text{velocity} \qquad \text{Eqn. 2-1}$$

$$Z = p \times v \qquad \text{Eqn. 2-2}$$

this product consists of both a resistive and a reactive component, depending on whether or not a reflective wave (or standing wave) condition is present in the material. A fairly detailed treatment of acoustic impedance is given in the two references cited below.[1,2]

---

1. R. Botsco, "Nondestructive Testing of Composite Structure with the Sonic Resonator", Materials Evaluation, November, 1966.
2. P. Hueter and R. Bolt, "Sonics", John Wiley and Sons, New York, 1955

Acoustical impedance is strongly affected by structural damage such as unbonded areas. Therefore, this type of test measurement is especially well suited for detecting damage caused by lightning strokes on these reinforced composite materials.

A small diameter piezoelectric probe is used to both generate and detect the standing wave in the material being tested. Changes in the acoustic impedance in the material under test, in turn, affect the electrical impedance of the piezoelectric probe. These electrical changes, although quite small, are then suitably amplified,processed and displayed for visual readout. The probe frequency, shape and size are important factors related to the success of measurement.

The instrument is calibrated by adjusting its readout to some arbitrary value on a reference sample (or area of a material) having a known structural condition. Measurements on other nominally similar materials (or areas), should show the same instrument meter reading, unless internal damage is present. Thus, after calibration, the material can be scanned with the probe, while an operator watches for (and notes) any changes in meter readout.

Acoustic impedance measurements were made in many locations of each panel. These are shown on Figures 91 and 92, along with the visual appearance of the panels after a test. For these two figures the photographs of each front surface were reversed so that areas of arc impingement would correspond to acoustic impedance values mapped on back sides of each panel. On the figures high numbers correspond to damaged areas while low numbers correspond to structurally-sound areas. The scales are relative, but the larger the number, the greater the damage. The relative acoustical impedance was written on the panels with chalk. In a few cases, the photographs of the panel have been retouched with white ink to make numbers reproduce better for this report. Those areas where the tests show significant damage are outlined in chalk. Again, as a rough rule of thumb, it appears that the diameter of the damaged area, as determined acoustically, is about twice the diameter of the area on the panel in which fibers were physically lifted or blown away by the resulting arc.

It seems evident that the damage to the panels "protected" with silver paint seems to be greater than the damage to the uncoated panels.

All of these uncoated panels, and all of the uncoated panels described earlier, show a crazing of the epoxy resin around the arc-attachment point.

Exactly what this is caused by is not certain, but it at least does not seem to be indicative of fiber damage. Panel GD-LS-70-T50-11 was tested with a piece of masking tap adhesive to the front surface near the arc-attachment point. Examination of this at 100X magnification showed no crazing or cracks on the surface of the panel. Adjacent areas all showed the typical crazing. This observation could infer any of three damage mechanisms: (1) mechanical shock due to blow-off of material at the arc-attachment point, (2) sonic blast effects from the arc-pressure wave, or (3) radiation/thermal effects from the stroke itself. At present it is believed that mechanisms (1) and/or (2) are more reasonable than (3). Further work is needed to fully clarify this effect.

2.4 Current Division Tests

One of the questions that consistently arises during lightning-resistance tests on these laminated composite materials is the degree to which lightning current penetrates the material. At the stroke-attachment point the current is initially confined only to the outer ply, at least until such time as the arc burns the outer ply or plies away and makes physical contact with the inner plies. What is not obvious is how the current then divides within the panel while flowing to grounded structures around the periphery of the panel. To help resolve this question, three of the 13" x 13" panels were made up with the ends of the individual graphite plies exposed to allow the current flowing on the individual plies to be measured.

2.4.1 Description of Test Panels

The panels manufactured with these tabs for current measurements were designated LS-70-T50-16, -18, and -19. All of these were uncoated panels of 0.120" nominal thickness. Panels 16 and 18 were of a 16-ply layup with alternating 0° and 90° orientations of the inner plies, the panel being symmetrical about the mid-plane, the two plies at the center (plies 8 and 9) both being 90° plies. The two outer plies were designated 0° plies. Panel 19 was a 0°-45°-90° panel.

Counting from the top of the panel, current measurement tabs were brought out of plies 1, 2, 8 and 9 (both plies joined together on one tab), and 16 as shown on Figure 93. On each ply to which taps were made the graphite fibers were grouped into five bundles running the full width of the panel and extending out beyond on the edge of the panel for about 1.5". The protruding fibers in each bundle were then electrically interconnected with silver epoxy. Figure 94 shows the orientation of these current-measuring tabs and the terminal

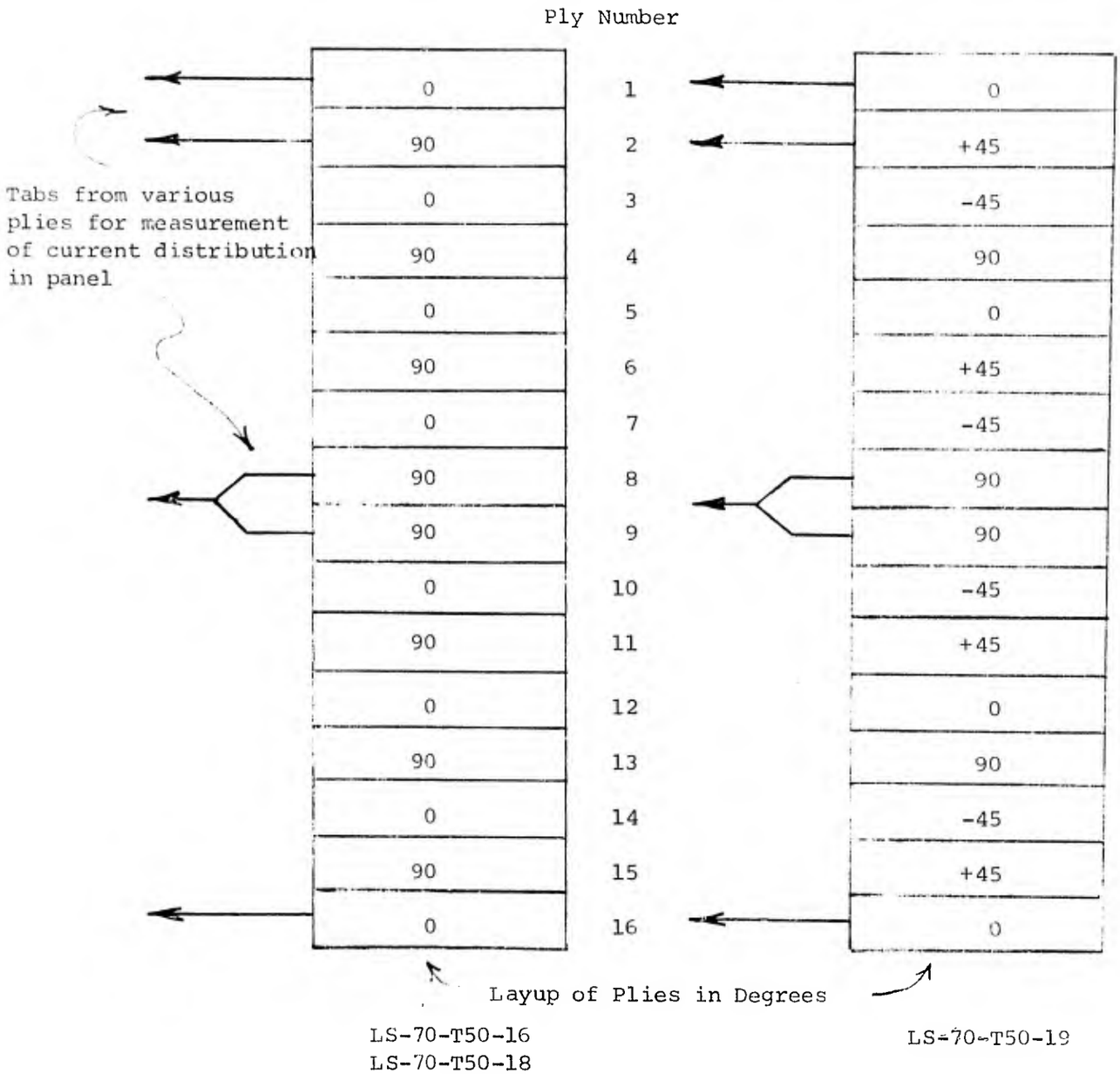

FIGURE 93 - Uncoated 0.120" Graphite Fiber/Epoxy Panels. Plies from Which Current Measurement Tabs were Brought

* Note: Tab Designation - First number denotes ply, second number denotes tab
(Example: 1-2 is first ply, second tab)

** X Denotes point of contact of applied current lead.

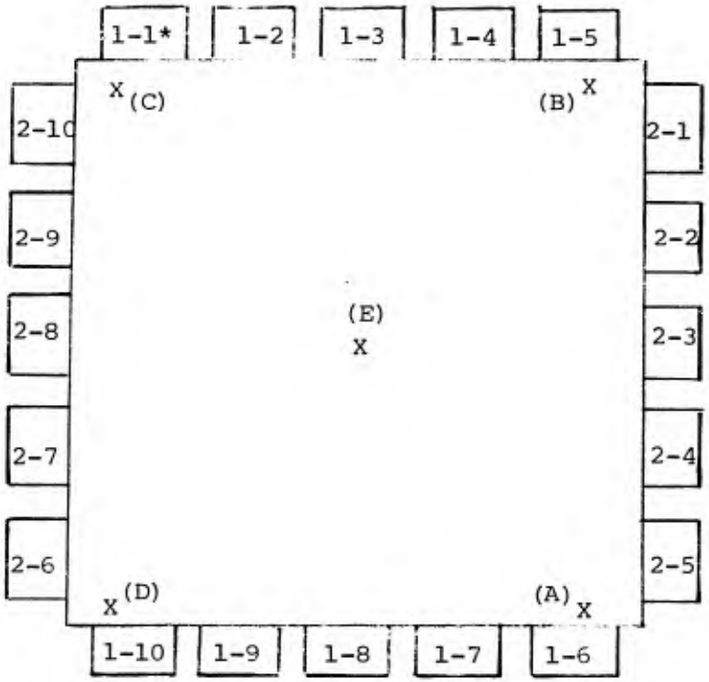

A. Top Two Plies

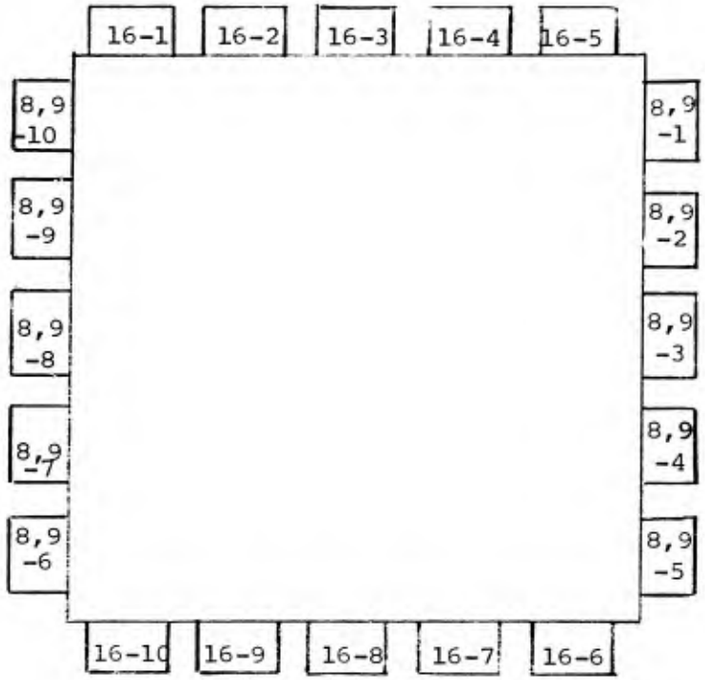

B. Lower Two Plies

FIGURE 94 - Top View of Graphite Fiber/Epoxy Panel LS-70-T50-18 Showing Tabs Brought Out From Various Plies for Current Measurements and Impulse Points on Panel Face

designations given to them. Sketch A shows the orientation of the top two plies; sketch B shows the orientation of the two plies underneath. Figure 94 is representative of panels LS-70-T50-16 and -18. It is also representative of panel LS-70-T50-19 with the exception that Tabs 2-1 through 2-10 come out at a 45° angle.

2.4.2 Test Methods

Ideally, one would like to apply a lightning-surge current to the panel and simultaneously measure the current coming from each of the measurement tabs, measurements being made of both current amplitude and current waveshape. Since each panel has 40 tabs such a measurement would involve 40 channels of instrumentation. No such number of measurement channels was available for the tests and consequently the problem of current division was approached in a series of small tests, rather than one all-or-nothing test. Furthermore, the initial tests were made with a relatively low-amplitude surge generator rather than the high-current surge generator used for the tests described so far. The low amplitude generator operated at a charging level of about 15 - 20 kV, and produced a surge current of the order of 100 amperes. This amount of current was essentially non-destructive to the panels, but still came from a high enough voltage source to cause breakdown of the insulating-epoxy films in the panel. With a low-current source it was possible to inject current into the panel at a number of points and measure the current division successively on the different tabs.

Another prime reason for starting the test series at a relatively low voltage and current level was that the high-voltage, high-amplitude surge generator would occasionally misfire and discharge before it was expected to. One ran the risk of trying to set up an elaborate instrumentation scheme to measure the current division only to have the test panel destroyed due to a malfunction of the impulse generator and not have any measurements to show for the test.

The test generator used for the test series is shown on Figure 95. Also shown is one of the test panels undergoing tests. The circuit diagram and method of making tests is shown on Figure 96. Briefly, the impulse generator was connected with a wire directly to one point on the test panels. When the generator was discharged, the current was injected into the panel. This could be measured by a pulse current transformer over the current-injection lead, while the current flowing from the panel on any of the individual measurement tabs could be measured with a similar current transformer.

The first meaningful series of measurements were made with current injected into the center of the panel and the 20 tabs from plies 1 and 2 grounded

FIGURE 95 - Impulse Generator Used to Produce Impulse Current Injected Into Composite Panel LS-70-T50-16, and Close-Up of Panel In Test Cell

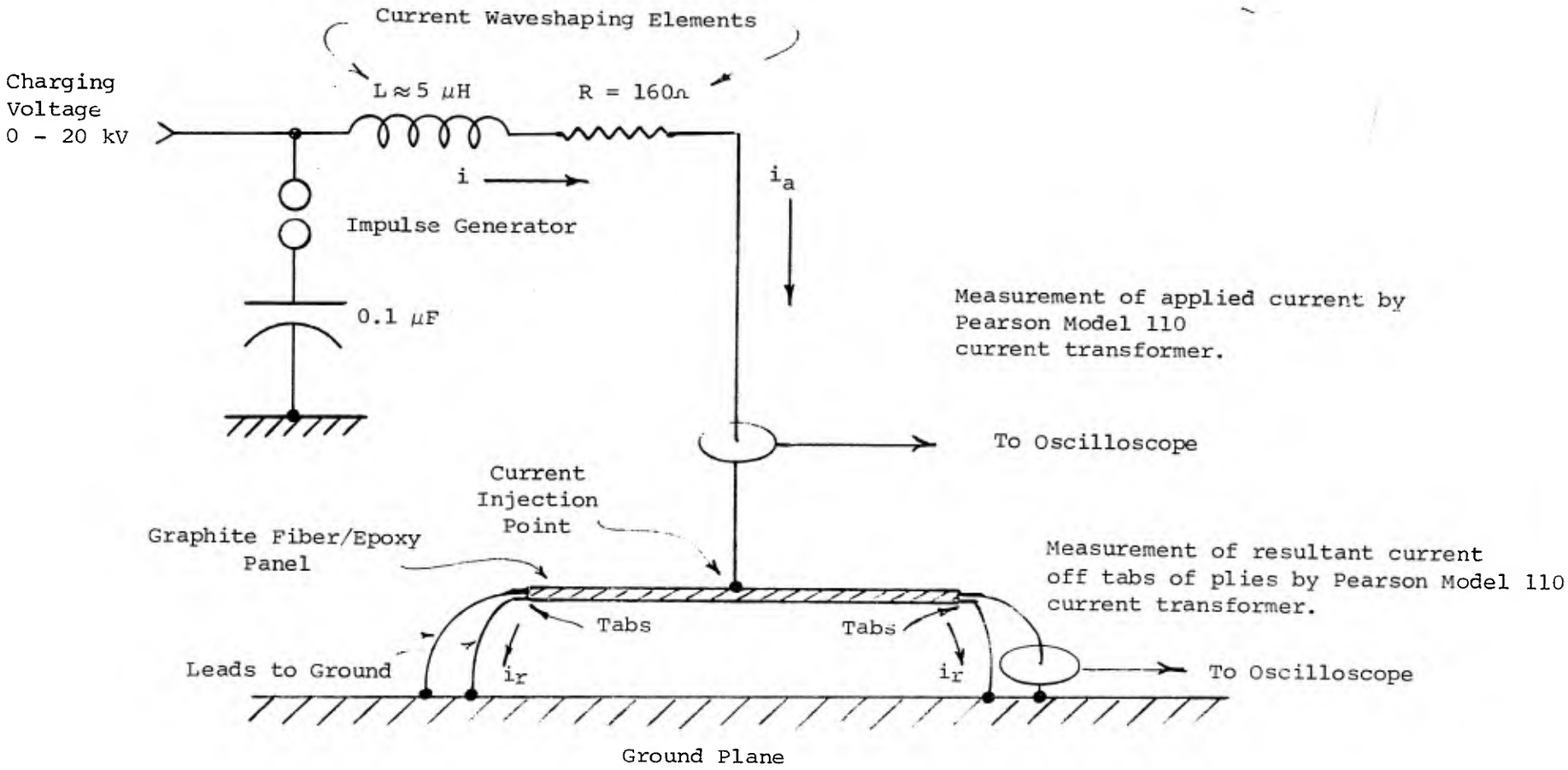

FIGURE 96 - Test Setup of Current Impulse Generator and Connection of Current Injection Lead to Panel, Showing Tab Leads to Ground and Position of Current Transformers for Measurement of Applied and Resultant Currents

while the remaining tabs from plies 8, 9, and 16 were left insulated from ground. The results of the measurements are shown in graphical form on Figure 97. The format of this chart is explained on Figure 98. Basically, Figure 97 shows the 20 current measurement tabs along the four edges of the rectangular panel rolled out into a straight line. The peak magnitude of the current coming off the various tabs is then shown on the vertical axis. If one were to make a cutout of this figure, cutting along the tops of the individual vertical bars that correspond to current on individual plies, and then fold the cutout into a closed box form, one would obtain a three-dimensional representation of the division of current among the various plies.

The first thing that is immediately obvious is that there is a concentration of current at one corner of the panel. While at first it was thought this was a ply effect in the panel, it turned out that the high current at this one corner was caused only by the configuration of the external leads bringing the surge current into the test panel from the current surge generator. This supply lead was draped toward the particular corner that had high currents. The general configuration of this lead is shown on Figure 98. As a result, the magnetic fields around this supply lead tended to force the current from the tabs to be concentrated near the supply lead, producing the current distribution that resulted in a minimum-energy configuration for the total magnetic field in the circuit. The significant point then is how much the external current-carrying members can influence the current distribution within the various parts of the composite test panel.

When plies 2 and 16 were grounded and plies 1, 8 and 9 left ungrounded, the distribution of surge currents is as shown on Figure 99. Again, there is a concentration of current around the corner closest to the lead carrying the current that was injected into the test panel.

Having once recognized the need to keep the configuration of the supply lead symmetrical with respect to the test panel, we arranged for the supply lead to be brought directly down into the center of the test panel. Under these conditions the current division among the various tabs was quite uniform. When all of the 40 tabs were grounded, the distribution of currents became as shown on Figure 100. The peak current in almost all plies was between 2 and 3 amperes. Since the current injected into the center was 97 amperes and there were 40 tabs, the average current should be 2.4 amperes per tab.

The waveshapes of three of the representative currents from the various tabs are shown on Figure 101. They show that the current divides among the

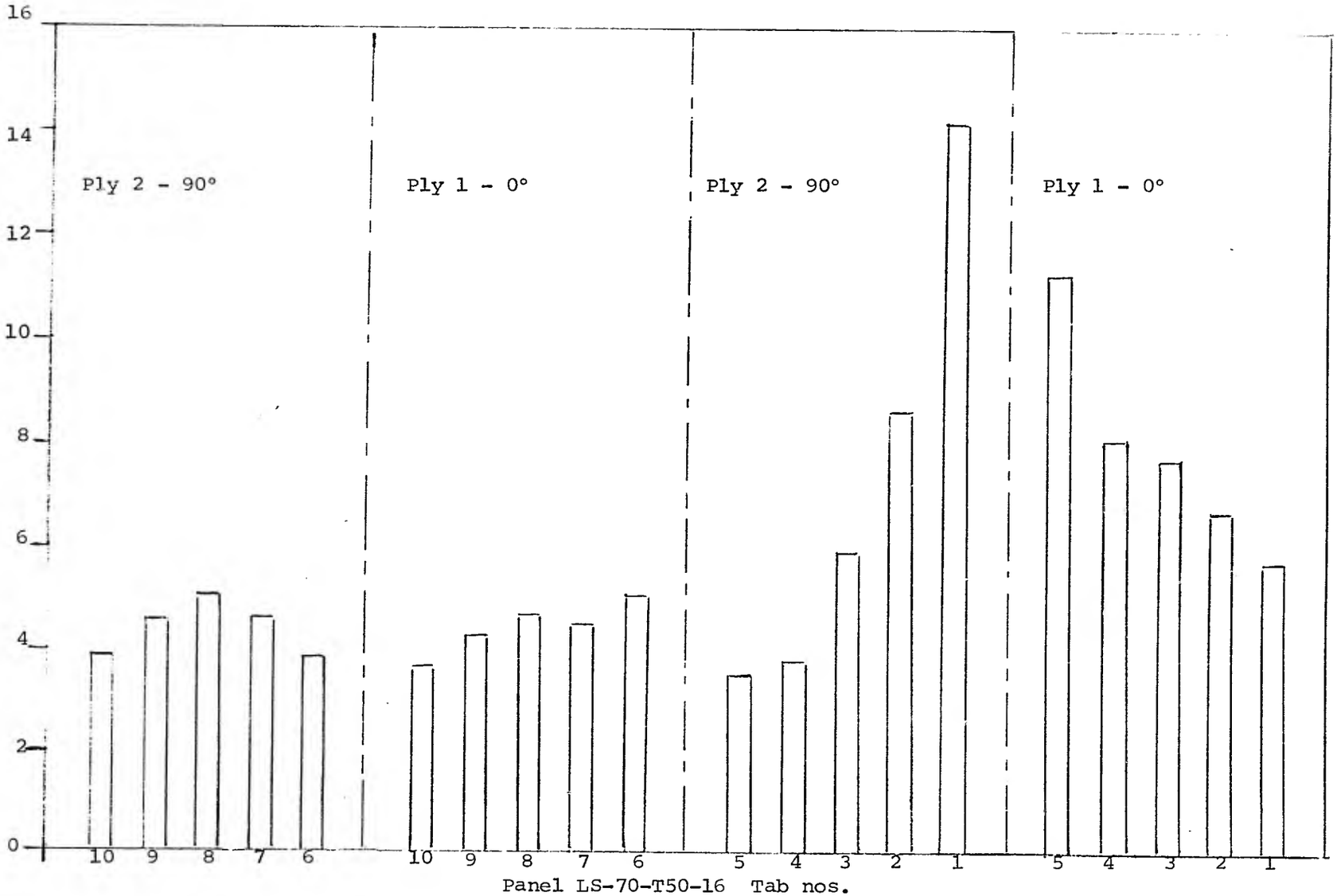

FIGURE 97 - Impulse Current Division When Plies 1 and 2 are Grounded, Plies 8, 9 and 10 Not Grounded
Current Injected at Center = 102 Amperes

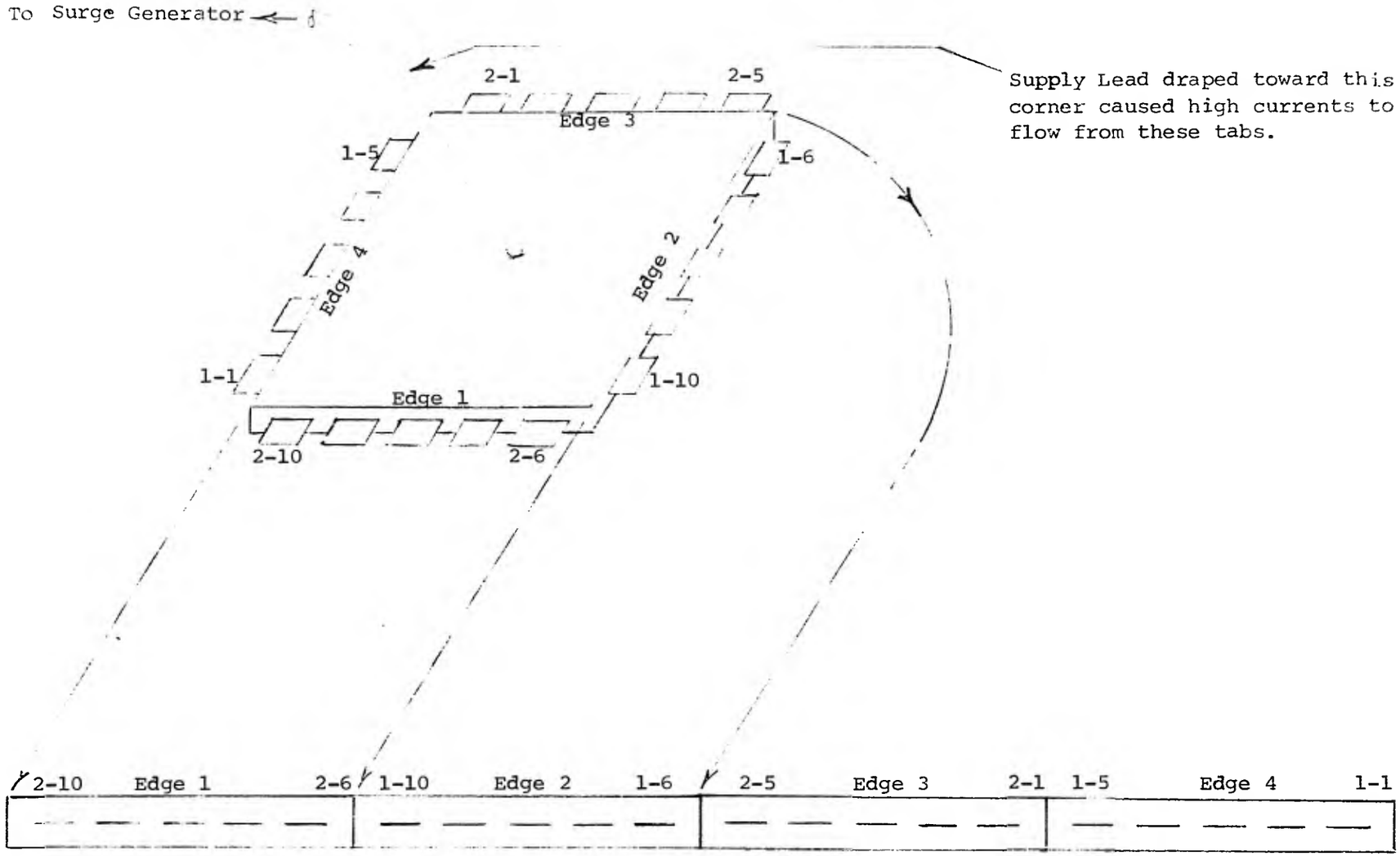

FIGURE 98 - Development of Tabs for Data Presentation

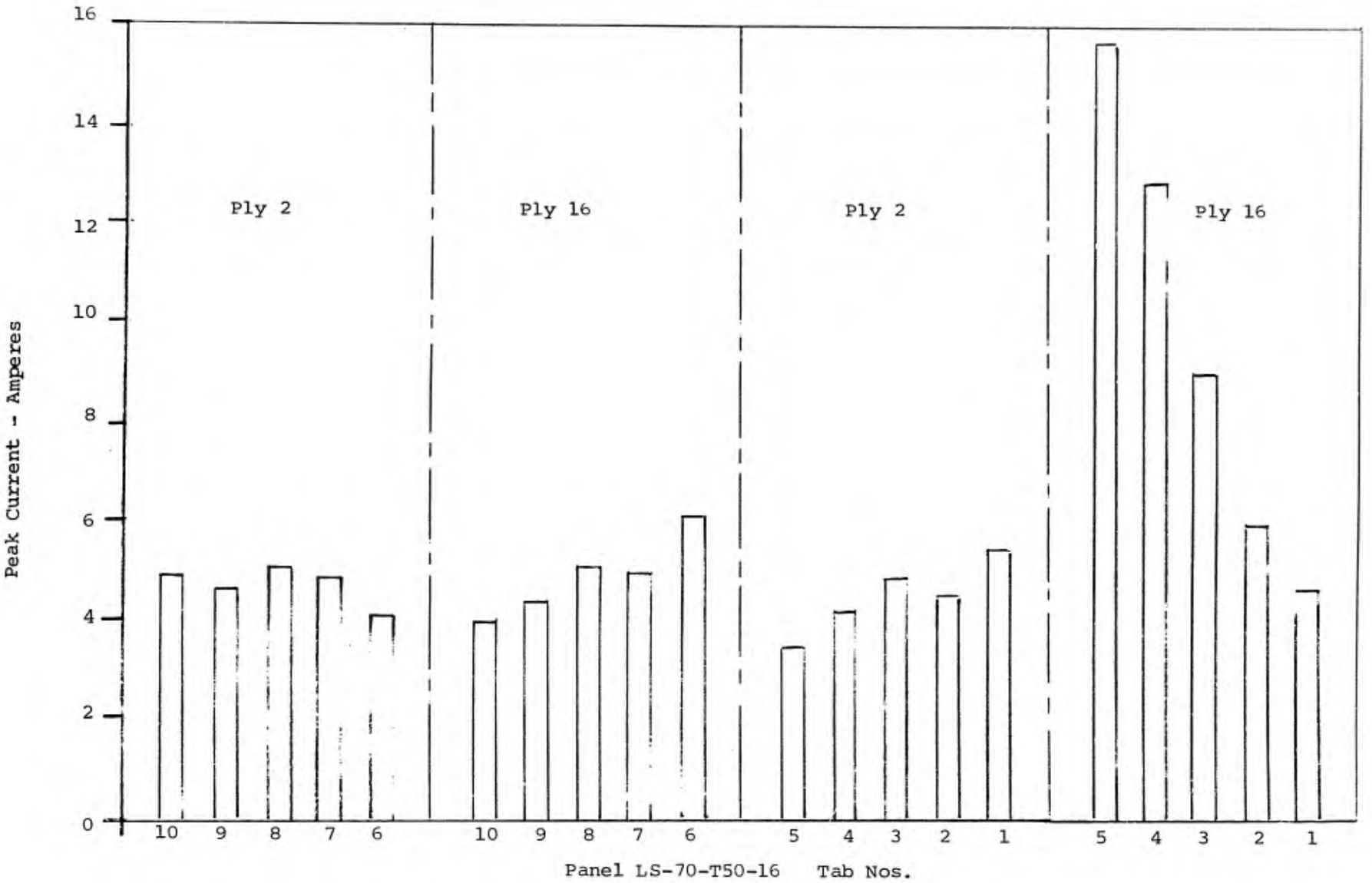

FIGURE 99 - Impulse Current Division When Plies 2 and 16 are Grounded, Plies 1 and 8 and 9 Not Grounded
Current Injected at Center = 98 Amperes

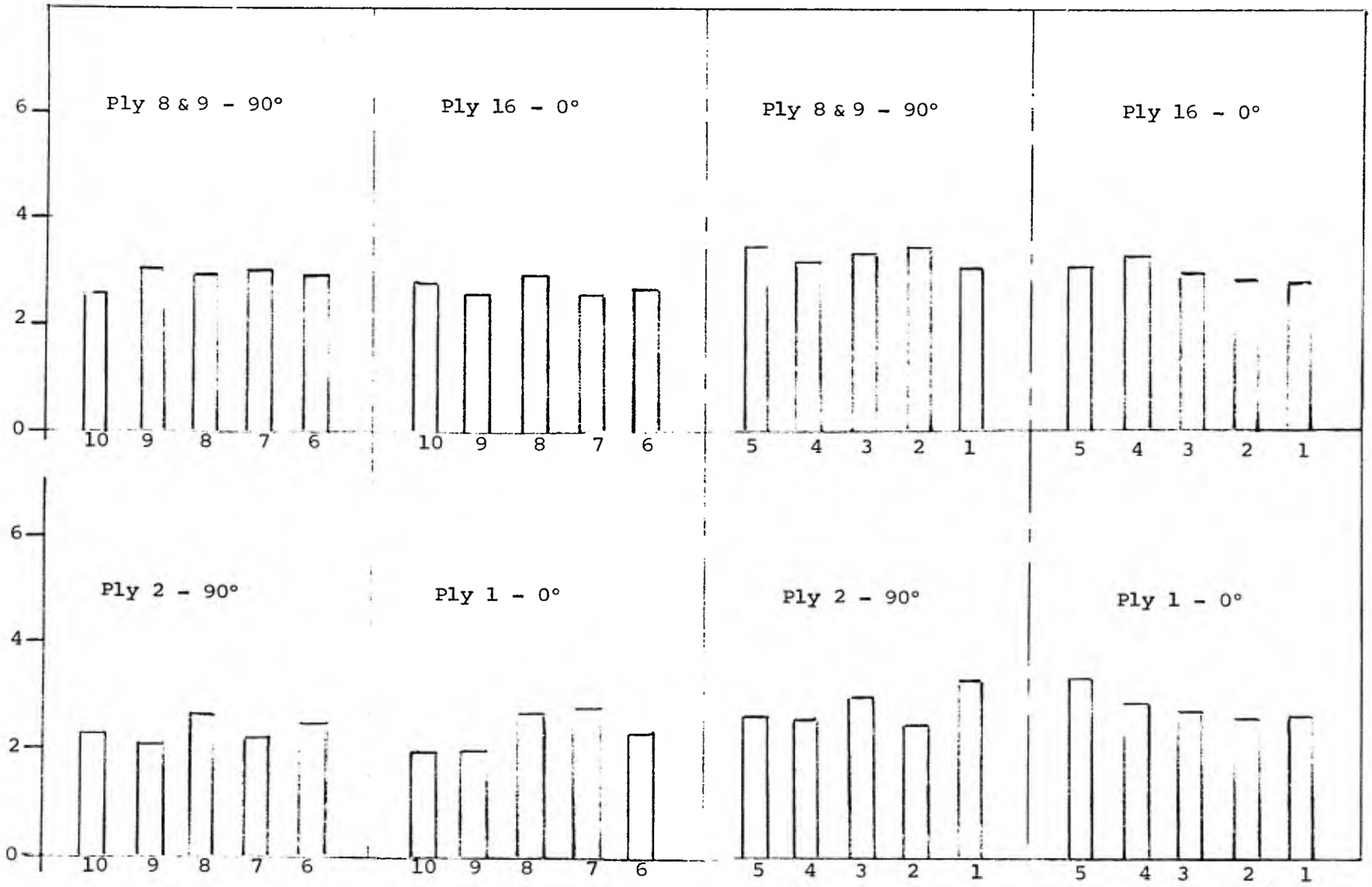

FIGURE 100 - Impulse Current Division When All Plies are Grounded. Current Injected at Center = 97 Amperes

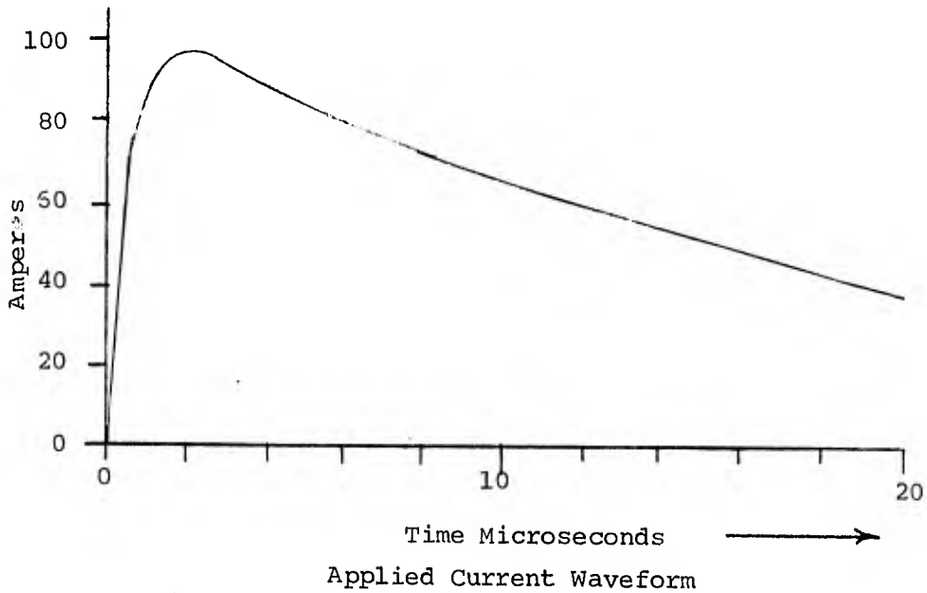

Applied Current Waveform

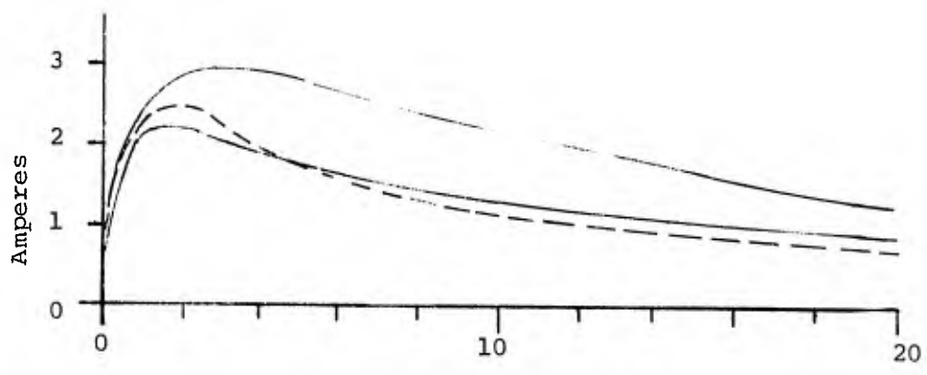

Waveforms of Current From Individual Tabs

FIGURE 101 - Impulse Current Division on Panel LS-70-T50-16

various tabs in the panel almost, but not quite, according to the resistance of the various current tabs. If the flow of current were controlled only by resistance, the waveshape of the current flowing from each tab would be the same as the applied current waveshape, even if the maximum current amplitude were not the same. It is evident that the waveforms are slightly different among the various tabs. This is an indication that the flow of current is controlled at least partially by the inductance of the various current paths. The effects of resistance, however, predominate since these three currents were chosen as extreme examples of the deviation from a resistance-controlled distribution.

If the conductivity of the panel were very good, (comparable to a metal like aluminum) one would expect the current to diffuse from the center into the various inner plies much more slowly than it would if the conductivity were very low.

The current division on the other two panels with tabs was also measured in a similar manner, with results as shown on Figure 102 and 103. On panel LS-70-T50-18 the current division was not quite as uniform as on panel LS-70-T50-16, but in no case were there really pronounced differences in the peak current among the various tabs. Ply effects did not seem to make a difference since there is no clearly discernable difference between the results measured on panel LS-70-T50-19 (the one with ply 2 at a 45° angle) and the data from panels LS-70-T50-16 or LS-70-T50-18.

A point of considerable significance is that none of the oscillograms of current in the various plies showed any discontinuities or sudden changes in current that would be indicative of a breakdown of the dielectric-resin layers between the various plies. The panels seemed to behave more or less as an isotropic panel. Evidently the pressure applied to the panels during the layup procedure presses the individual graphite fibers into contact with each other at enough points that the current can divide among them without the necessity of puncturing a film of epoxy resin to get from one fiber to another. What percentage of the fibers made contact with each other or what percentage is truly necessary to ensure good current division is difficult to say. The photomicrographs of the 6" x 12" graphite panels do not show very many fibers making a contact with each other, particularly between the plies, but perhaps not very many contacts are truly necessary.

If the current division among the plies is fairly uniform at this relatively low-current and low-voltage level, one would expect the separation between plies

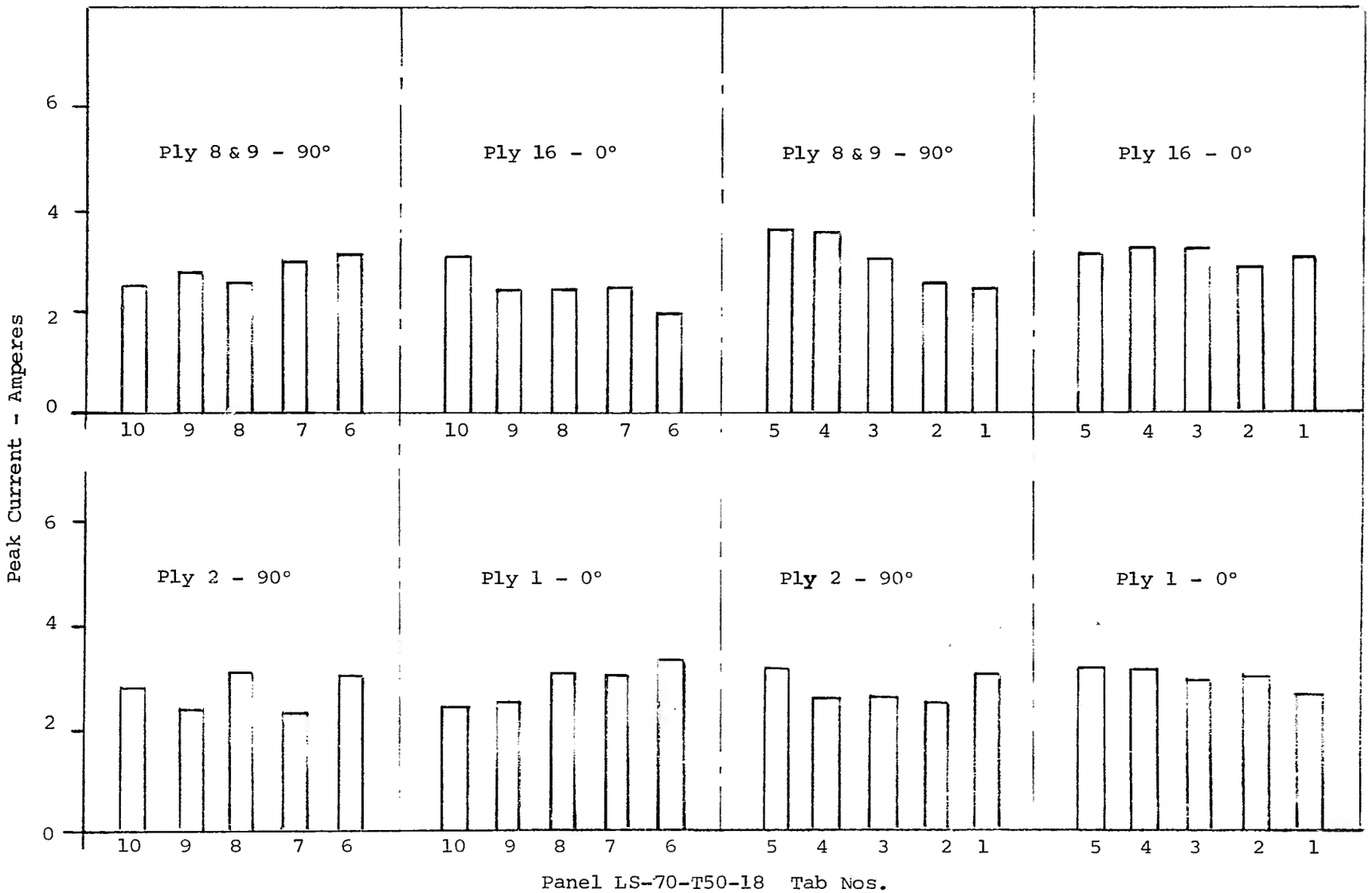

FIGURE 102 - Impulse Current Division When All Plies are Grounded. Current Injected at Center = 98 Amps

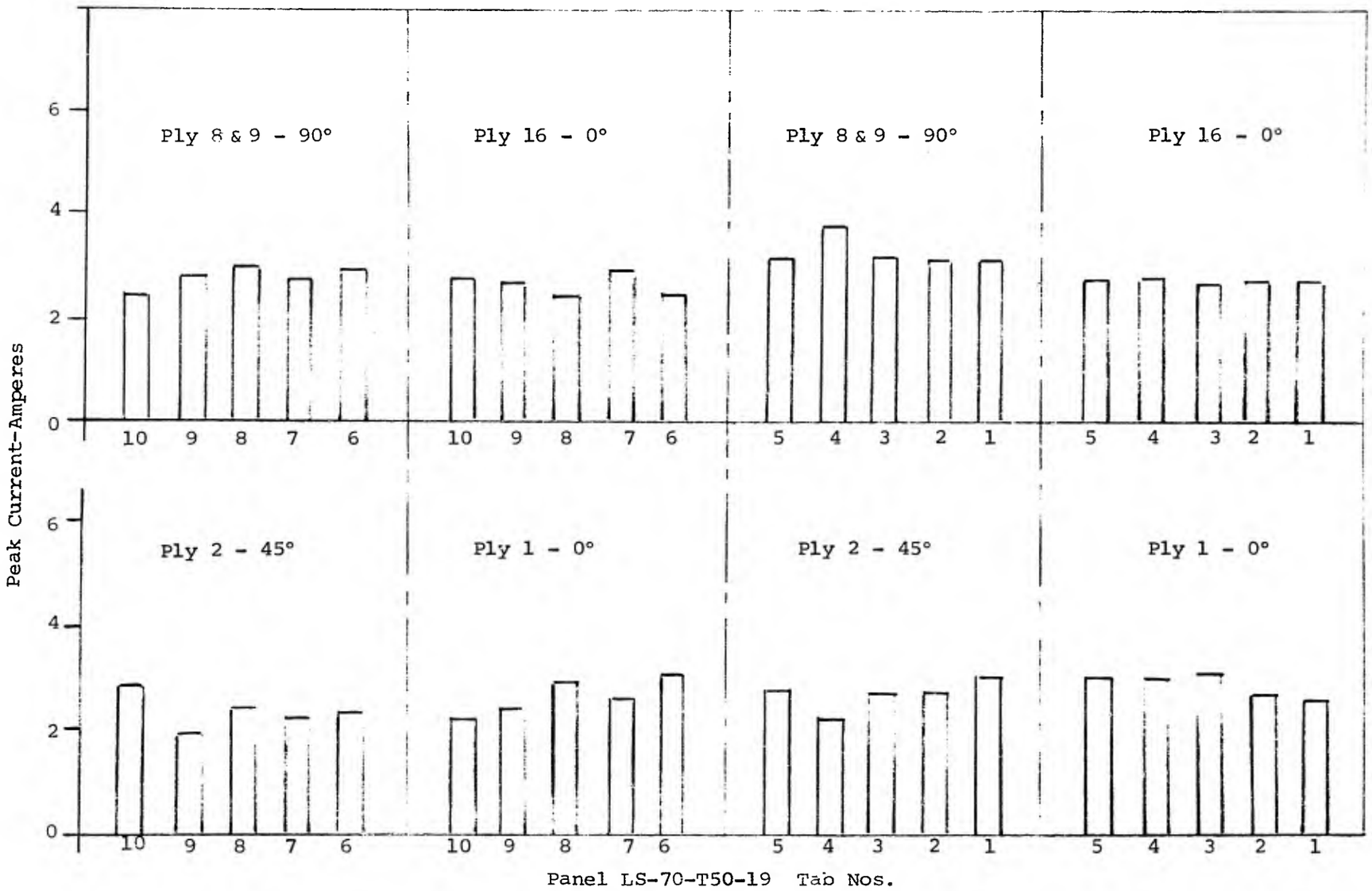

FIGURE 103 - Impulse Current Division When All Plies are Grounded. Current Injected at Center = 96 Amperes

by the resin matrix to have even less effect at the high-current and high-electric field levels associated with an actual lightning contact. In all probability it would appear that the current division among the various plies of the panels would depend more upon the external current paths (or upon the external magnetic fields produced by such current paths) or upon the mechanical contact at the edge of the panels than it would upon the internal construction of the panels. Assuming a homogeneous body, the division of current in a structure like this sheet is controlled by the resistance and inductance of the path through which the current must flow. For transients of short duration (or high frequencies) the current divides up according to the inductance of the various paths. At lower frequencies, or with longer-duration pulses, the current divides up according to the resistance of the various paths. In order to get a "ballpark" analytical handle on which effect predominates, we made a series of resistance measurements between the various tabs of panel LS-70-T50-18. The results are displayed on Table XVI. They show that the resistance between practically any two tabs on the panel is from 0.1 to 0.15 ohms. The inductance between any of the tabs was not measured, but would be of the order of 0.1 μh. Thus the characteristic time constant of the panel (T = L/R) would be of the order of 1 μs. Current pulses of duration shorter than 1 μs. would divide predominantly according to the inductance of the various current paths on the panel. These would be controlled primarily by the mechanical shape of the panel. Current pulses of duration longer than 1 μs. would be controlled primarily by the resistance of the panel.

The diagonal resistance of the panel was approximately 0.135 ohms. This resistance was compared to the diagonal resistance of a square of 0.13 mil thick aluminum foil of approximately the same dimensions as the graphite test panel. The conductivity of the aluminum foil was calculated at about 2 micro-ohm centimeters. Allowing for thickness of the panel (0.123") the equivalent resistivity of the graphite test panel material would then be about 2000 micro-ohm centimeters.

Knowing the resistivity of the bulk graphite material and assuming it to be homogeneous, one can calculate the equivalent skin depth of the material as a function of frequency. Skin depth is that depth at which the current density falls off to $1/\epsilon$ of its value at the surface of the panel. The calculated skin depths were as given in Table XVII.

TABLE XVI

DC Resistance Between Selected Tabs on Panel LS-70-T50-18

Points between which Measurements were Taken			Resistance	
Tab 1-1	to	Tab 1-10	0.117Ω	
1-2		1-9	0.132	
1-3		1-8	0.115	
1-4		1-7	0.123	
1-5		1-6	0.165	
1-1		1-6	0.132	
1-5		1-10	0.136	
2-1		2-10	0.123	
2-2		2-9	0.102	
2-3		2-8	0.097	
2-4		2-7	0.120	
2-5		2-6	0.114	
1-1		2-10	0.108	
1-3		2-8	0.114	
1-5		2-6	0.151	
1-1		2-5	0.120	
1-1		16-6	0.134	
1-5		16-10	0.130	
1-1		8,9-10	0.098	
1-1		16-1	0.250	(half of Tab 16-1 broken off)
1-5		16-5	0.118	

TABLE XVII

Skin Depth of Panel LS-70-T50-18

Frequency	Skin Depth
1 kHz	2.80"
10 kHz	0.89"
100 kHz	0.28"

If the waveshape of a typical lightning surge current is subjected to a Fourier analysis, one finds that the dominant frequency components lie in the range 1 to 100 kHz, with a peak in the neighborhood of 10 kHz. This data in Table XVI then would indicate that at the frequencies of interest the current density should not be greatly different over the thickness of the test panel. These calculated skin depths would then again indicate that the division of current among the various tabs of these panels should be controlled primarily by the dc resistance of the paths, an observation in agreement with all of the other attempts to measure the actual distribution of current.

While all of the testing at the low current level indicated that there should be no particular ply effects, it was still felt desirable to attempt a measurement of the current distribution at a high-current level typical of lightning currents. Since at high currents only one shot can be applied to the panel, it was necessary to devise a method of measuring the current in the individual plies that would allow 40 measurements to be made simultaneously. The method finally chosen for the test employs magnetic links. A magnetic link is a small bundle of permanently-magnetizable metal strips which, when placed in a magnetic field, become magnetized to a degree depending upon the peak magnetic field intensity in the neighborhood. This magnetic field intensity can then be related to the peak current flowing in the conductor that produced the magnetic field.

The dimensions of the magnetic link, the method of mounting the link and attachment to the tab to be measured, and the method of measuring the magnetic state of the link are shown on Figure 104. The magnetic link itself is tubular in form and about 9 millimeters diameter by 37 millimeters long. In order to use the links, short strips of copper ribbon were attached to each of the tabs on the test panel. This copper ribbon was wrapped around the magnetic link in a manner as to force the resultant magnetic field along the axis of the link. A copper strap then conducted the current from the different measurement tabs to ground and produced a magnetic field within the copper strap proportional to the current flowing through the strap.

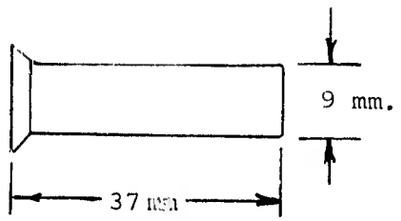

Magnetic Link Outline

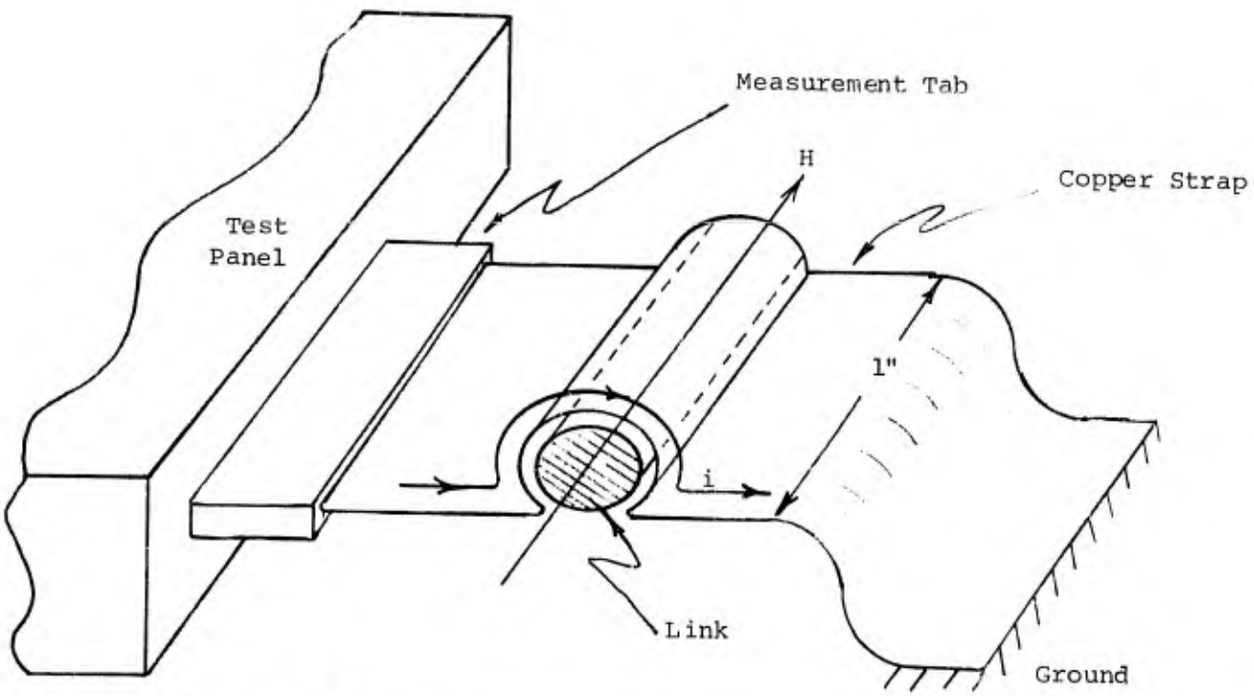

Method of Mounting Magnetic Link

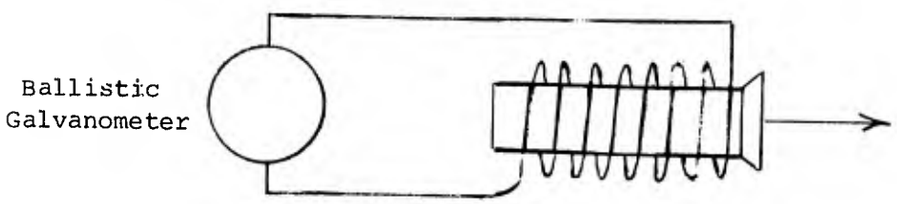

Method of Measurement of State of Magnetization

FIGURE 104 - Magnetic Link Used to Measure Impulse Current Division

In order to measure the degree of magnetization of the link, and hence the peak current, the link was inserted into a coil of wire to which was attached a ballistic galvanometer. If the link is suddenly removed from the coil, the changing magnetic field associated with the motion of the link induces a voltage in the coil which in turn produces a deflection of the galvanometer. The deflection of the galvanometer can be calibrated against the state of magnetization by injecting known currents through the copper strap and determining the deflection produced as the link is magnetized by the resultant magnetic field.

Panel LS-70-T50-16 was the first panel tested in this way. A photograph of the panel arranged for test and an oscillogram of the current wave used for the test are shown on Figures 105 and 106. The recorded current division is shown on Figure 107. The results of the measurements were not too encouraging. As can be seen on Figure 107, the indicated peak currents are greatly different for the different tabs and do not sum up to anywhere near the total peak current injected into the center of the panel. It is felt that quite possibly the links were arranged so that the magnetic field induced in one link had an undue influence on the adjacent links.

2.5 Tests on Honeycomb Sandwich Panels

As part of the test effort on this contract, simulated lightning tests were performed on six panels fabricated by Grumman Aerospace Corporation under Air Force Contract F33-615-69-C-1498, "Repair Technology for Boron/Epoxy Composites". Five of the panels were sandwich elements containing boron/epoxy skins over an aluminum honeycomb core. The skins were finished with a silver-filled epoxy coating that was 0.003 - 0.004" thick. The panels were all 9" wide, but of varying thicknesses and lengths. The panels, prior to coating, had been completely non-destructively tested and found free of defects.

A sixth panel, fabricated by Grumman, was similar to the other five panels in that it had a boron/epoxy skin and an aluminum honeycomb core. Instead of a silver-bearing coating, however, the Boeing Company had applied a lightning protection system to this panel in the form of a coating consisting of an aluminum wire fabric impregnated with an epoxy-polyimide resin. The wire fabric was a 200 x 200 mesh, 0.0021" wire-twilled weave. This was approximately equivalent to a 2 or 1.4 mil aluminum foil. This coating was developed under Air Force Contract F33(615)-69-C-1612, "Coatings for the Lightning Protection of Reinforced Plastics". Each sample had two finished sides so that more than one lightning test could be made on each panel.

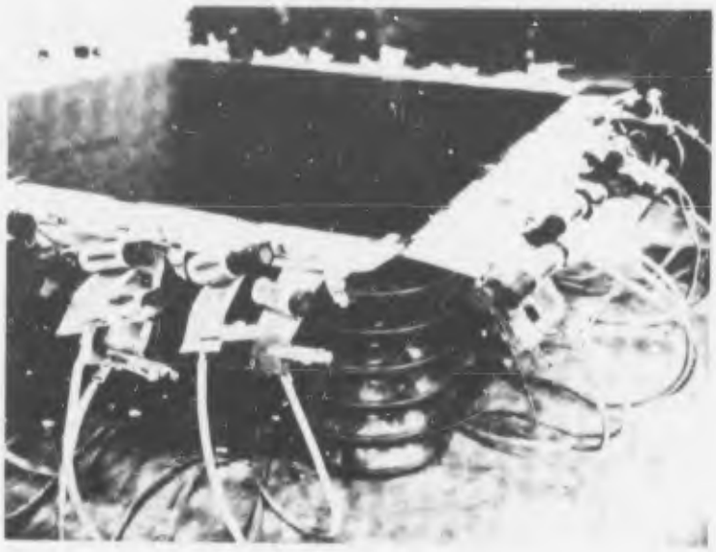

FIGURE 105 - Graphite Epoxy Tab Panel LS-70-T50-16 in Test Position Showing Magnetic Links Sheathed in Copper Foil

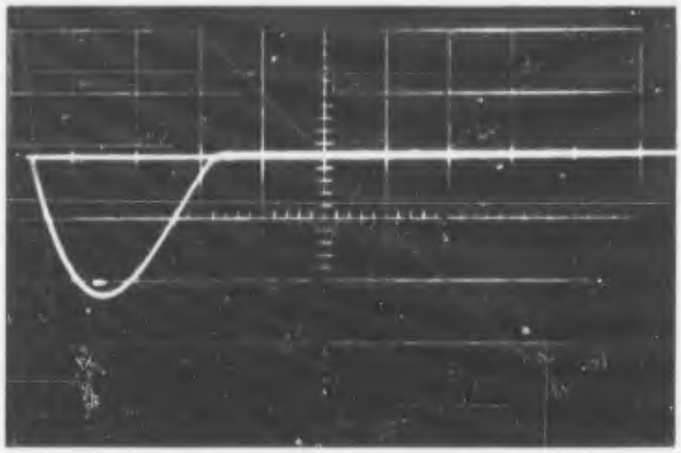

Peak Current = 57.5 kA
5 μs/div. 25.7 kA/div.

FIGURE 106 - Applied Current Waveshape Used In Simulated Lightning Tab Panel Tests on Graphite/Epoxy LS-70-T50-16

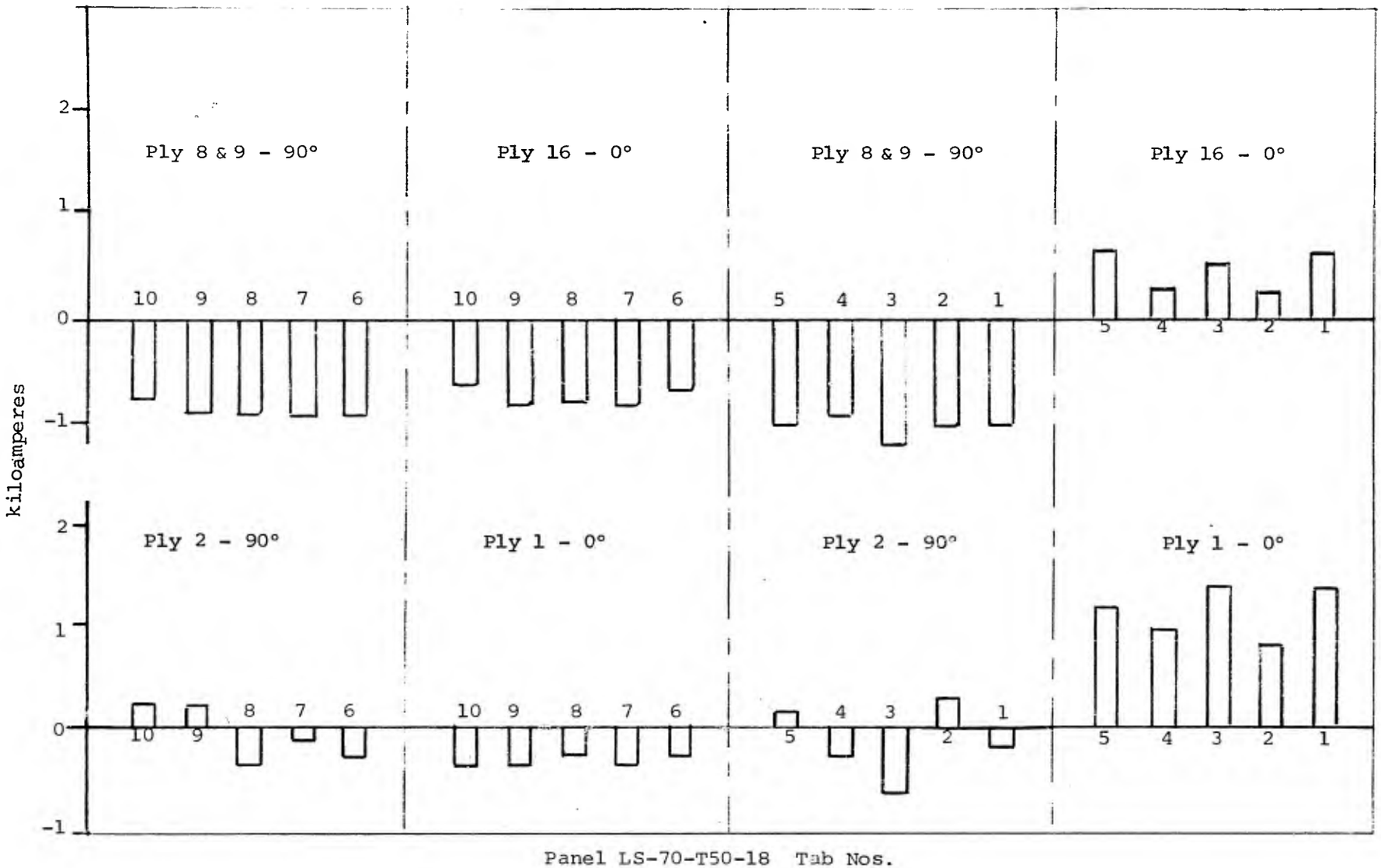

FIGURE 107 - Impulse Current Division when all Plies Are Grounded.
Current Injected at Center = 57.5 kA

The objectives of the test were to determine the amount of damage caused by the simulated lightning strokes and to determine if any of the panels could withstand a 200 kA simulated lightning stroke. Originally, the damaged panel and coating was to be re-worked and repaired with the intention of exposing the panel to simulated lightning strokes again, in order to assess the worth of the repair structure. As it turned out, the panels were never retested.

2.5.1 Test Methods

These panels were tested using the method shown in Figure 108. One end of the panel was clamped in a ground return structure consisting of two pieces of aluminum angle held onto the test panel with clamps. The high current arc was struck to the selected point on the panel through a 1" air gap. In general, two discharges were struck to each side of each test panel. The objective was to divide the 9" dimension of each panel into four 2-1/4" wide specimens for mechanical tests by Grumman after the lightning exposure. The two outside segments were to be control specimens and receive no direct lightning discharges while the two interior specimens were to receive discharges, each specimen being tested at a different current level.

The current discharges for all of these tests were oscillatory like those used for the tests on the other panels.

2.5.2 Test Results

Specimen No. BR-109-3

This was a rectangular honeycomb panel that received four test shots on one side and one on the other. Photos taken before and after the tests are shown on Figure 108. The first shot was at a current level of 4.85 kA peak. This shot did little more than discolor the coating over a 3.5" diameter circle around the contact point. No other visual damage to the honeycomb material was noted. The test did, however, increase the resistance of the silver coating. Before the test, resistance had been measured diagonally across the panel, and between the two sets of edges. The measurements of resistance before and after are given in Table XVIII.

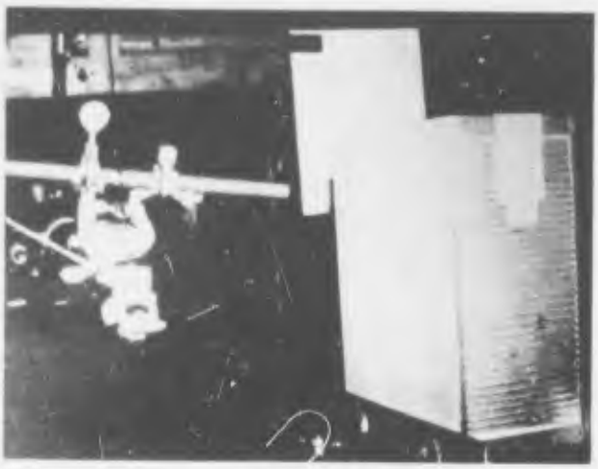

A.

Before Test

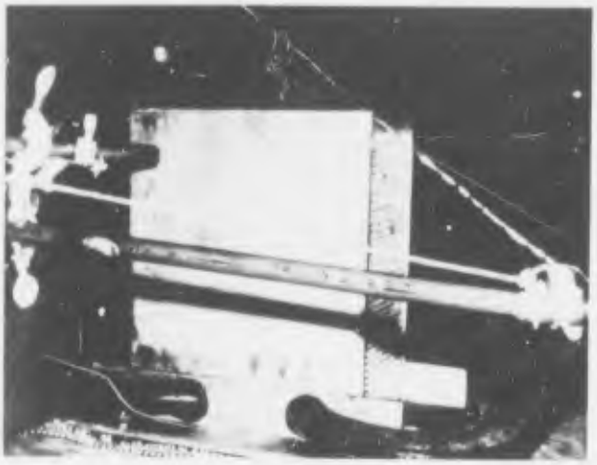

B.

Side 2, After
72.7 kA Discharge

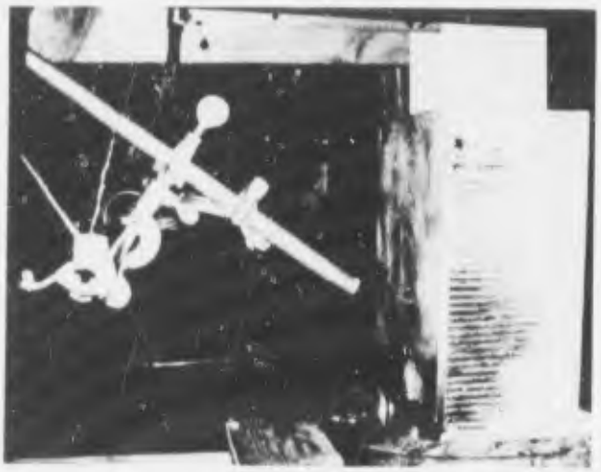

C

Side 2, After
111 kA
Discharge

D.

Side 1, After
168 kA Discharge

FIGURE 108 - Before and After Photographs - Panel BR-109-3

TABLE XVIII

Resistance Measurements Before/After Lightning Test

Tab Measured	Resistance Before Test	Resistance After Test
Diagonal	0.34 ohms	520 ohms
Short Side	0.510 ohms	475 ohms
Long Side	0.28 ohms	410 ohms

No particular effort was made to analyze the reason for increase in coating resistance. Possibly the shock wave destroyed the continuity of the silver particles of the coating, or possibly it broke them loose from the boron fibers in the panel.

The second shot was to a different point on the panel, but on the same side. At a current level of 72.7 kA, there again was only discoloration of the surface coating, with no damage to the panel itself (Figure 108B).

The third shot, at 111 kA, again resulted in a discoloration over about a 3.5" diameter circle, and produced pitting of the coating at the point of stoke contact. It did not, however, result in any apparent damage to the panel itself (Figure 108C).

The fourth shot was at the level of 168 kA. This shot again gave pitting of the surface at the point of contact. By tapping the panel around the stroke-impingement point, there was found a 0.5" wide dead area. This shot also gave burning of the honeycomb material between the two panel faces (Figure 108D). At the time of test, no attempt was made to determine how deep into the honeycomb the damage extended.

The last test on this panel was made on the other side at a current level of 149 kA. The damage to the coating covered an area of about 2.5" x 2.0". There were approximately 15 pits in the surface of the panel, the largest pit being 0.75" x 0.375". Tapping of the panel with a coin did not reveal any dead areas like those found at the 168 kA level on the other face of the panel. The test did cause considerable blackening of the honeycomb material. None of the tests, however, seemed to cause any major structural damage to the panels.

Specimen No. BR-109-1

This was another rectangular sample with a skin thickness of .250", but it had a thinner section of aluminum honeycomb material. The first test on side 1 was at 88 kA. This test caused some pitting of the coating and some damage to the aluminum coating on the side of the test panel.

The next test was again on side 1, at a current level of 134 kA.

The surface was pitted over a distance of .125" x 0.25". There were a few smaller holes around the stroke-impingement point and some more of the honeycomb was blown out near the corners.

The second side also received two shots. The first, at a current level of 84 kA, caused pitting of the surface about 0.25" diameter. There were a number of smaller pits also, these pits forming a cluster about 3" in diameter.

The last shot on the panel was on side two at 111 kA. Again, this caused numerous small pits over a region approximately 2" in diameter. It also caused three pits of dimensions approximately .25" x .25".

Figure 109-A shows the damage on the second side of this panel.

While all the tests caused extensive discoloration of the protective coating, they did not seem to cause any pronounced structural damage to the panels.

Sample No. BR-103-3

This panel had a thickness of 0.045" and a thinner honeycomb section than either of the two previous panels. The sample received two shots, both on the same side. The first, at a level of 107 kA, blew a hole approximately 0.5" x 0.5" into the panel.

The second shot was at a level of 72.7 kA. It blew a 1" x 0.5" hole in the panel and blew a piece of honeycomb (1" square) loose from the edge of the panel at the point nearest to the arc. A photograph of the resultant damage is shown on Figure 109-B.

Sample No. BR-108-1

This panel had a skin thickness of 0.045". This sample received two shots. The first was at 107 kA on side 2. The arc blew a hole into the panel of 0.5" x 0.125" dimension, gave pitting of the surface over an area of about 1.5" x 0.5" and caused delamination of the skin from the honeycomb over an area of about 2" diameter.

The second shot was at 87 kA on side one and caused approximately the same damage as observed on the other side of the 107 kA level. See Figure 109-C.

Sample BR-108-3

All of the previous panels had been tested with one end of the honeycomb panel clamped in a ground support structure. A question arose as to what would happen if a panel were not mechanically and electrically connected to the ground structure of the generator and the arc were allowed

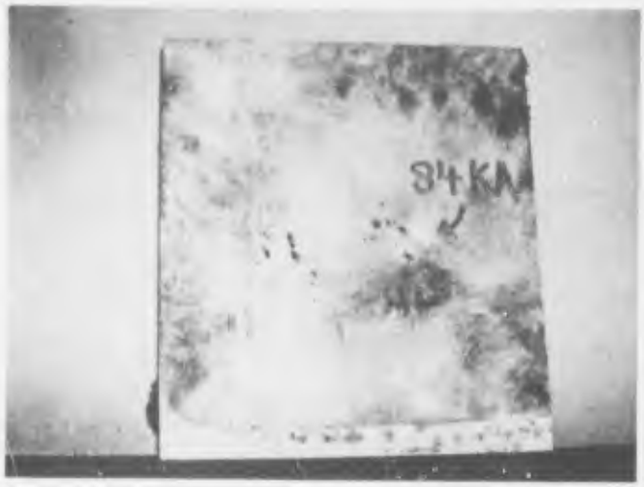

A. Sample BR-109-1 Side 2 After 84 kA and 111 kA Discharges

B. Sample BR-103-3 Side 2 After 73 kA and 107 kA Discharges

C. Sample BR-108-1 Side 1 After 87 kA Discharge

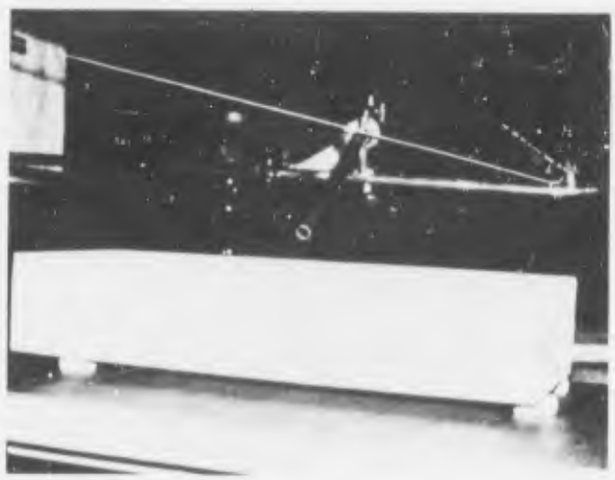

D. Sample BR-103-3 Before Test

FIGURE 109 - Simulated Lightning Tests on Honeycomb Panels

to strike the panel on one side and then flash from the panel to the ground structure on the other side. Accordingly, this panel was spaced about 0.75" from a grounded metal plate by the use of 4 small porcelain insulators. The high-voltage electrode was positioned 1" above the center of the panel. A photograph of the panel before undergoing test is shown on Figure 109D.

In this configuration, there was one test on the panel at a current level of 71.5 kA. At the arc-impingement side, the arc blew one small hole in the center of the panel. On the other side, the arc exited from one corner of the panel. At both points the damage was about the same as was caused by similar current levels with the sample clamped in the ground structure.

After this test with the panel isolated from the ground structure, it was then tested with one edge solidly grounded, like the previous panels that had been tested. The test was made at a level of 71.5 kA on the other face. The shot again caused some puncturing of the panel and discoloration over the surface of the panel. Figure 110-A shows the damaged panel after the above tests.

Specimen BR-103-1 (Boeing Panel)

This panel received two tests, the first at 154 kA and the second at 203 kA. At the 154 kA level, there was apparently no damage to the panel except a slight discoloration of the surface. The amount of this discoloration was far less than was observed on the silver-paint coated samples at a much lower current level. At the second level of 203 kA, there was some pitting of the surface accompanied by a mechanical separation of the laminated surface from the honeycomb filler. Presumably the mechanical shock associated with the arc cracked the adhesive joining the panel to the honeycomb. Pictures of the resulting damage are shown on Figures 110-B and 110-C.

A. Sample BR-108-3
After Tests at
72 kA

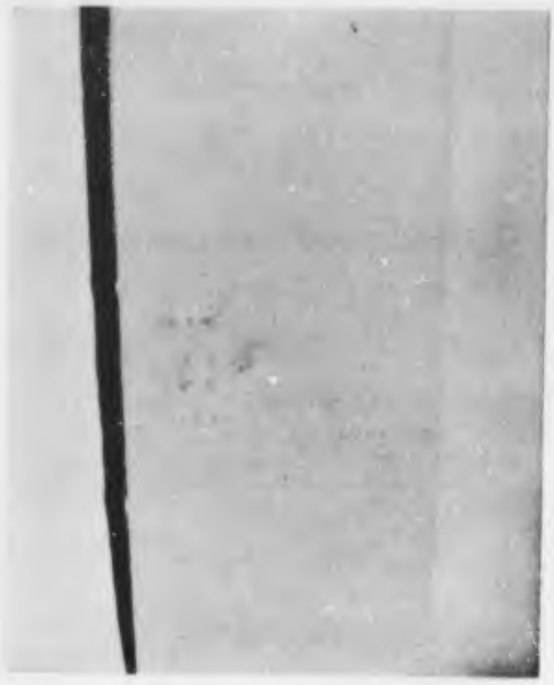

B. Sample BR-103-1
(Boeing Panel)
After 154 kA and
203 kA Discharges

C. Sample BR-103-1 (Boeing Panel)
Showing Delamination caused by
203 kA Test Current

FIGURE 110 - Simulated Lightning Tests on Honeycomb Panels

SECTION

3.0 Electromagnetic Shielding Properties of Composite Materials

Lightning protection of aircraft involves not only protection against the direct burning and blasting effects of lightning, but against the electromagnetic interference associated with lightning as well.

Electromagnetic interference is perhaps too mild a term to use in connection with lightning. Electromagnetic damage potential is perhaps a more valid term.

Control of the electromagnetic damage potential associated with lightning is a many sided problem. Some key questions are:

1. What electromagnetic threat level is presented to an airplane by a lightning stroke?
2. What shielding is provided against the electromagnetic fields?
3. What kind of surge voltages and currents are produced on aircraft electrical systems?
4. What is the vulnerability of avionic equipment to the fields, voltages and currents associated with a lightning strike?

This section deals with the second question above. The first question above is dealt with in Section 5. The third and fourth questions above were not covered in the original scope of this program. During the conduct of this program, however, simultaneous work was being done (and funded by NASA) to relate the surge currents flowing through an aircraft to the surge voltages produced on avionic equipment. By an amendment to the contract covering the present work, similar test work was also done on an F-4 aircraft. This work on the F-4 aircraft is still continuing however, and is not covered in this report. The objectives of the test effort are covered in more detail in Section 7 of this report.

3.1 Pulse Measurements of Shielding Factors

The original goal during this program was to measure electromagnetic fields at points on the back side of the composite sheets during the high current tests on the panels and to relate these measurements to the intrinsic shielding effectiveness of the panels. The intent of making simultaneous measurements of resistance to lightning effects and electromagnetic field measurements was two-fold: to obtain field strengths under conditions representative of actual lightning strokes and to obtain the maximum amount of data at minimum cost, both in time and in number of test panels.

This original objective was not fulfilled too well for two reasons: delays and partial shipment of test panels interfered with the continuity of testing and the idea proved not to be as attractive as it originally seemed. Measurements of shielding factors obtained with continuous wave (CW) test techniques yielded more useful data. Nevertheless, some interesting data was obtained under high current pulse conditions.

3.1.1 Test Equipment

The principle of measurement involved two field sensors mounted inside the steel tank described in Section 3.2. One of the sensors was a three axis H-field sensor and one was a parallel-plate electric field sensor. The H-field sensor is shown on Figure 111.

It consisted of three orthogonally-mounted loop antennas (Figure 111a), each of two inch diamter and wound with 10 turns (Figure 111b). A changing magnetic field inside the tank would induce in these loops signals proportional to the time rate-of-change of the field, the output from each coil being proportional to the vector component of the field. The outputs of the coils were coupled to three identical integrating amplifiers, the output of which was thus proportional to the H-field inside the test enclosure. A circuit diagram of the integrator is shown on Figure 111c. Most of the circuitry shown is that of a 1 Hertz filter to prevent the amplifier drifting into saturation. The loop antennas and integrator were tested in a Helmholtz coil calibrating system (not shown) and their sensitivity was found to be 0.0196 volts output per ampere/meter of H-field.

The loop antennas were placed 28 inches from the rear surface of the panel under test. Dimensions were as shown on Figure 112.

An attempt was made to measure electric fields within the box, through the use of a parallel-plate electric field sensor. These measurements were unsuccessful, since the output from the transducer was masked by spurious noise pickup.

3.1.2 Measurements

The first measurement made was an attempt to establish a reference field inside the enclosure. To do this, two conductors at right angles and joined at the center were placed over the opening as shown on Figure 113. The high current surge generator was connected to the center of these conductors and then discharged. Presumably the current divided uniformly among the four

A. Mounting of Sensors

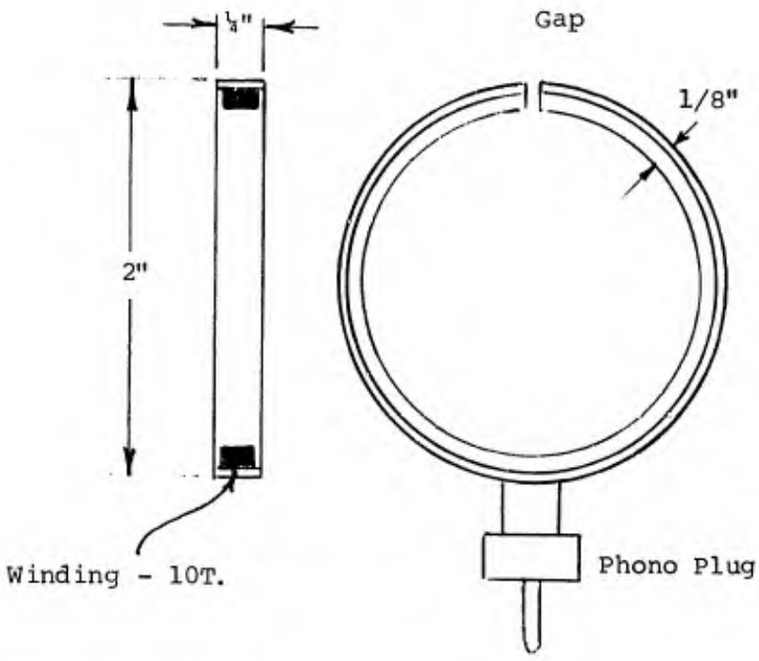

B. Details of Pickup Coil

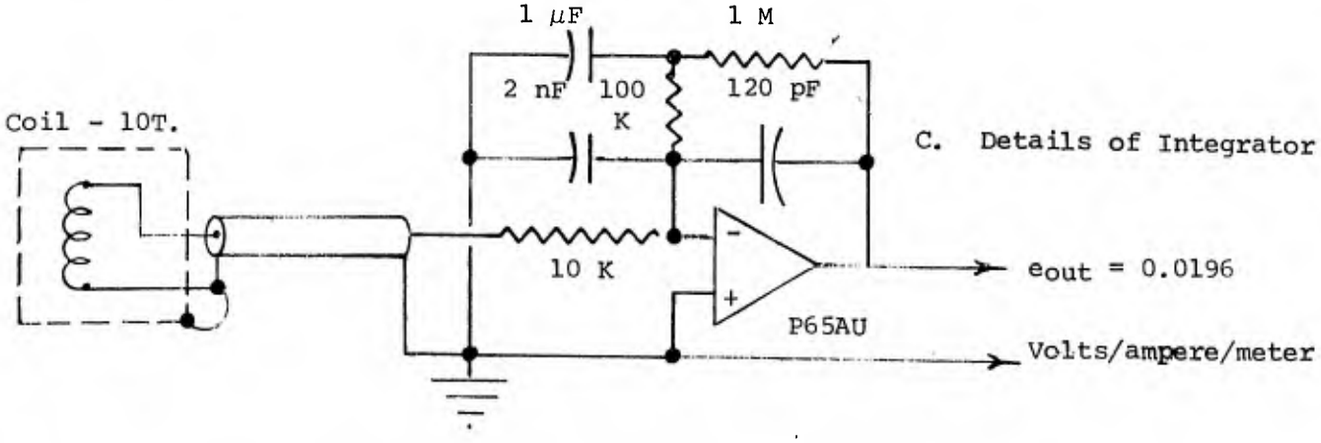

C. Details of Integrator

FIGURE 111 - Three Axis H-Field Measurement System

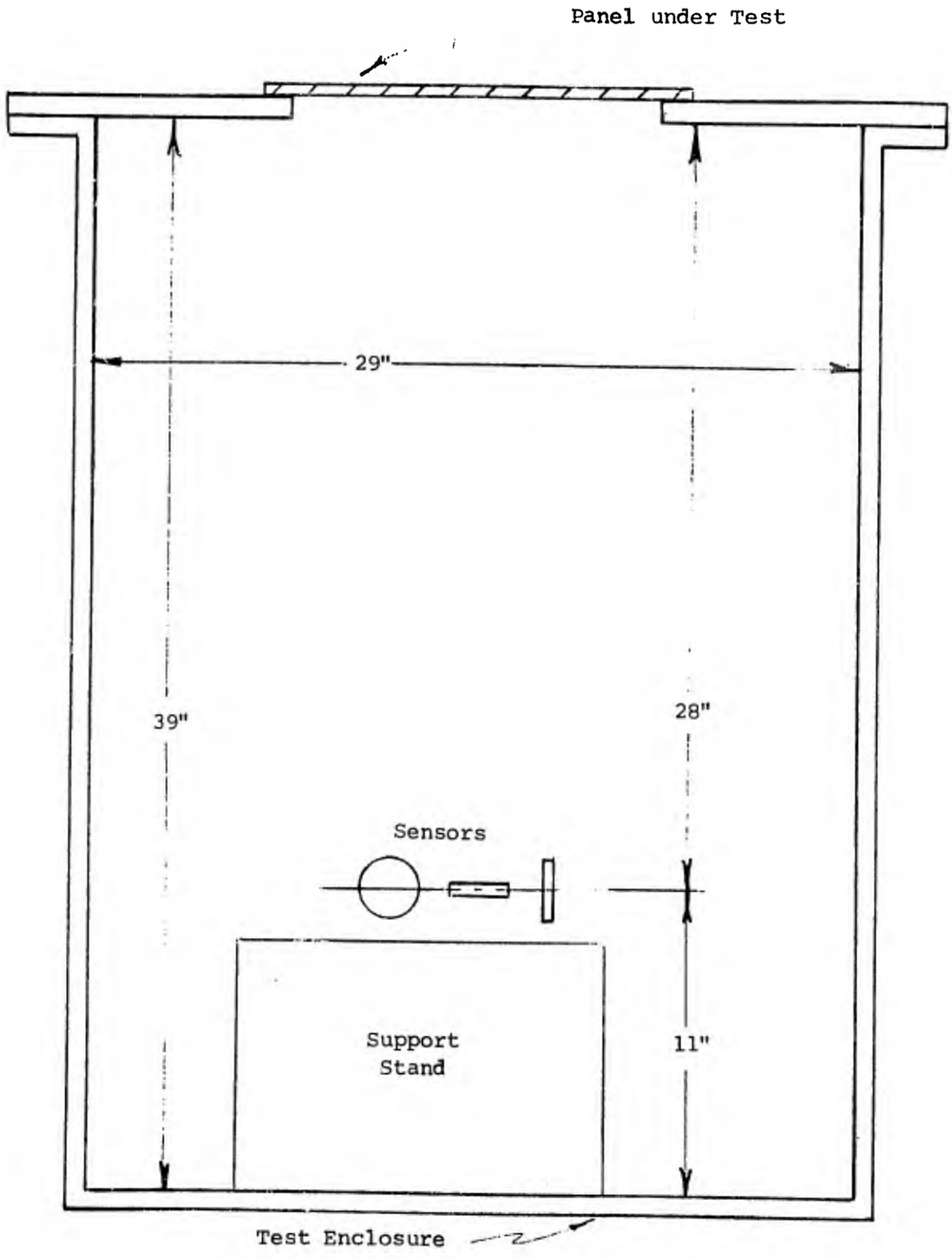

FIGURE 112 - Location of H-Field Sensors In Test Enclosure

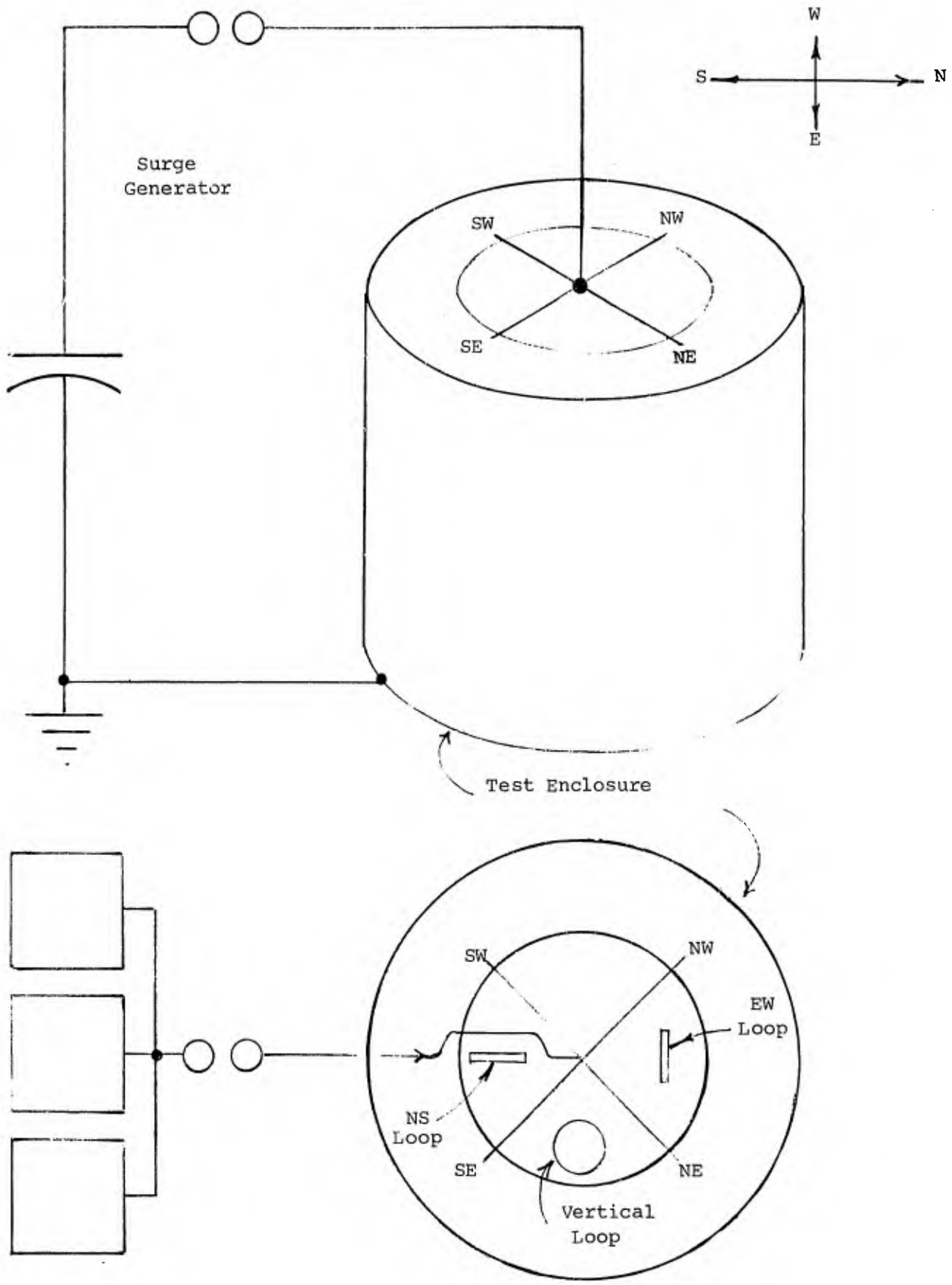

FIGURE 113 - Orientation of Conductors and Loop-Antennas for Ambient Field Measurements

conductors. At test current levels of 61.3 kA and 76.6 kA, the field intensities (at the probe locations) inside the enclosure were 140 A/M and 168 A/M, respectively, with the field directed mostly towards the generator. Test panel LS-70-3 (.040" thick, uncoated) was then placed over the opening in the test enclosure. A discharge of 57.5 kA was then directed to the center of the test panel. The field intensity inside the enclosure then reached a value of 346 A/M. The direction of the field was also changed. Apparently the current flow in the panel was not completely radial and the non-symmetrical current flow contributed to the increase in field with the panel.

Only this one test was made of field intensity during high current tests on the panel since it was felt that the fields would be controlled only by the pattern of current flow and not by the characteristics of the panel. The absolute magnitude of the field is of some interest, but is hardly representative of the field inside an aircraft.

With a 1/8" thick aluminum plate covering the opening, the fields inside the enclosure were reduced to levels too low to be recorded.

Oscillograms of the current and the resulting fields are shown on Figure 114.

Somewhat more meaningful measurements were made using high level fields not connected with discharges to the panel. The H-field 3-dimensional sensing loop arrangement was located centrally in the test tank one foot below the composite panel mounting hole. The tank was grounded, but the generator output current was not passed through the panel/tank combination. Instead, the current was passed through a two foot diameter loop radiator made of ½ inch diameter copper tubing and located one foot above the panel mounting hole. This was done because, in order to obtain consistent H-field measurements, the current path must remain the same for both an ambient field measurement (no panel in place) and a measurement of shielding effectiveness (with panel in place).

Test data is shown on Table XIX.

The damped-oscillatory current wave used had a period of 27.5 μsec., which corresponds to a frequency of 36.4 kHz.

A check was also made on the effect of the panel fiber orientations with respect to the field-radiating loop. To do this, Panel LS-70-10 (uncoated, 0°-90° orientation) was used and mounted at three relative angular positions: 0°, 45°, and 90°. The loop was left in the same position for all three cases and the current magnitude was the same (102 kA). No significant differences in either

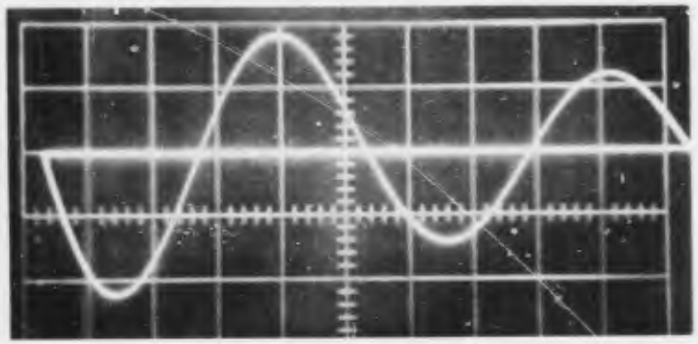

Applied Current

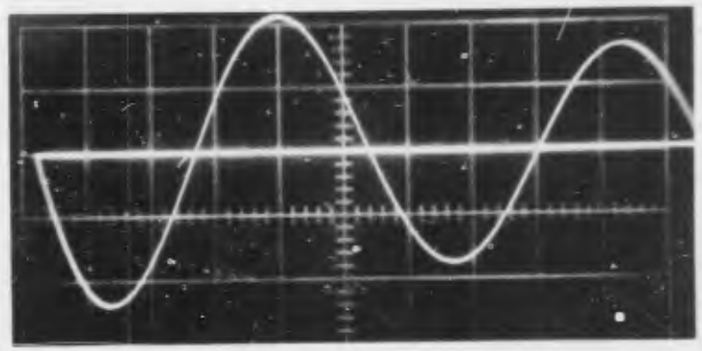

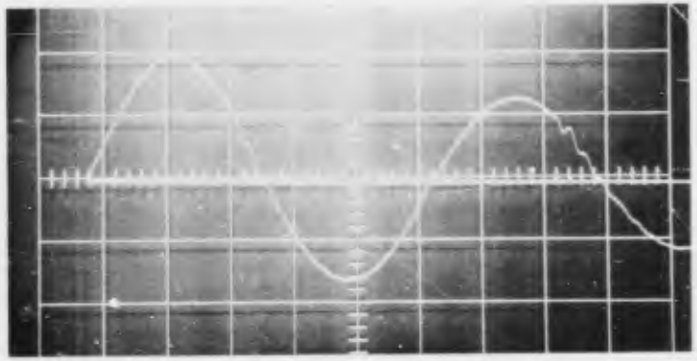

E-W Loop

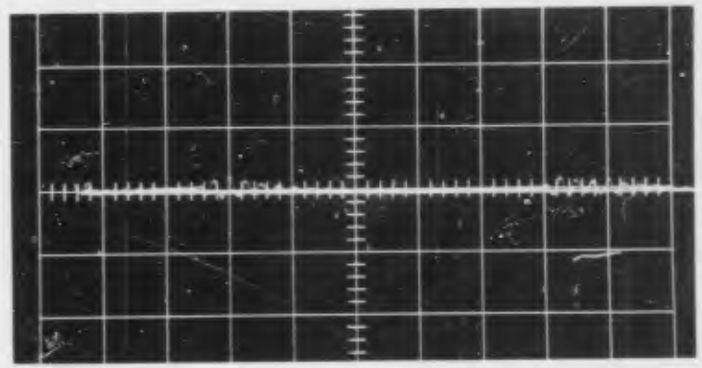

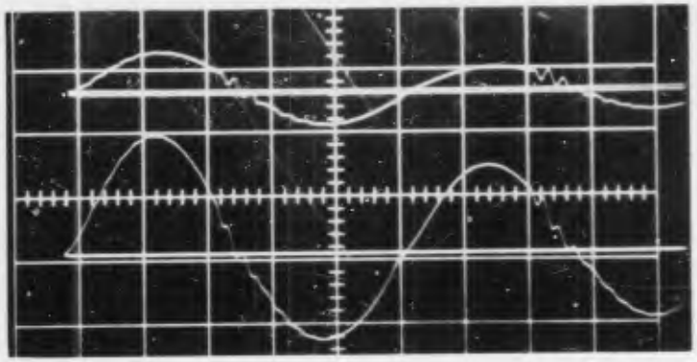

Vertical Loop

NS Loop

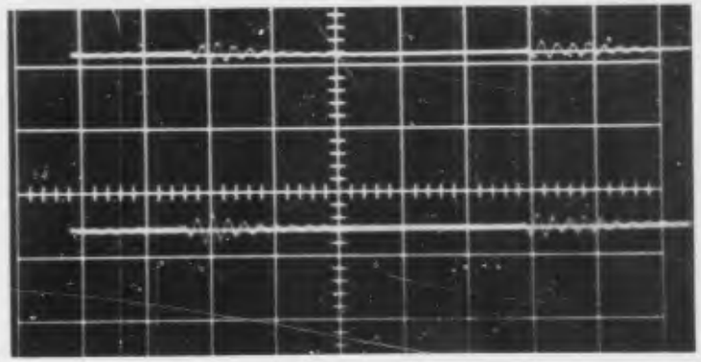

Panel LS-70-3(57.5 kA)

1/8" Aluminum Panel(61.3 kA)

FIGURE 114 - Pulse H-Field Measurements

All Horizontal Time Scales = 5 μs/div.
All H-Field Measurements = 102 AT/m/div.

TABLE XIX

H-Field Shielding Factor Measurements Using a Damped-Oscillatory Field of 36.4 kHz.

Panel	Thickness	Coating	Current Level	Ambient Field*	Absolute Field	Shielding
			kA	A·T/M	A·T/M	dB
LS-70-4	.040	none	43.4	130	120	0.7
LS-70-4	.040	none	84.4	241	227	0.5
LS-70-4	.040	none	130	360	348	0.3
LS-70-5	.040	Silver paint	84.4	241	227	0.5
LS-70-6	.040	" "	84.4	241	226	0.5
LS-70-7	.040	" "	84.4	241	221	0.5
LS-70-8	.040	" "	84.4	241	227	0.5
LS-70-8	.040	" "	130	360	336	0.6
LS-70-9	.120	Silver paint	102	440	384	1.2
LS-70-10	.120	none	102	440	373	1.4
LS-70-11	.120	none	102	440	388	1.1
LS-70-12	.120	none	107	418	385	0.7
LS-70-13	.120	Silver paint	107	418	378	0.9
LS-70-14	.120	Silver paint	107	418	378	1.1
1.6 mil aluminum foil			130	360	16.5	26.8
1.6 mil aluminum foil			107	418	32	22.8

Measurements were made at several different times. Slight physical changes in the location of the loop through which current was circulated resulted in different values of ambient field for the same current in the loop. With any given loop setup, field strength was proportional to loop currents.

the three field components or in the total field magnitude were seen.

3.2 Continuous Wave Measurements of Shielding Factors

The best data on shielding effectiveness of the composite materials was obtained with CW measurements. The measurement technique employed was one described by Eckersley[1].

3.2.1 Measurement Equipment

The principle of measurement is shown on Figure 115. A constant current is maintained in a transmitting loop and a receiving loop connected to a detector. The relative readings of the detector with and without a test specimen between the loops is related to the shielding effectiveness of the specimen. For most metallic materials a ground on each coil is sufficient to prevent electrostatic pickup and erroneous measurements. With these non-metallic materials we found that a single ground on each coil was not sufficient, and that each coil had to be completely screened to prevent errors due to electric-field coupling through the material. This alone is a measure of the poor shielding effectiveness of these materials, since even the thinnest sheet of metal provides almost complete shielding against a high impedance electric field if it is well grounded.

Figure 116 shows photographs of the test equipment. The transmitting and receiving coils were identical, each consisting of 25 turns wound on a 0.75 inch diameter coil form.

The transmitting coil was excited with an oscillator and wideband amplifier, creating a magnetic field (H-Field) between the transmitting and receiving coils, thereby producing a voltage across the receiving coil.

The receiving coil was connected by coaxial cable to a Tektronix 1A1 plug-in mounted in a Tektronix Type 547 oscilloscope, which served as a detector.

The procedure was to establish an ambient voltage level as read on the oscilloscope, with the coils coaxial and the test panel absent at a specific frequency. It was important that the distance between the coils with and without the composite sample in place be the same, since the energy coupled between two coils at close spacings varies inversely as the cube of the distance between

---

1. "H-Field Shielding Effectiveness of Flame-Sprayed and Thin Solid Aluminum and Copper Sheets", A. Eckersley, IEEE Transactions on Electromagnetic Compatibility, March 1968.

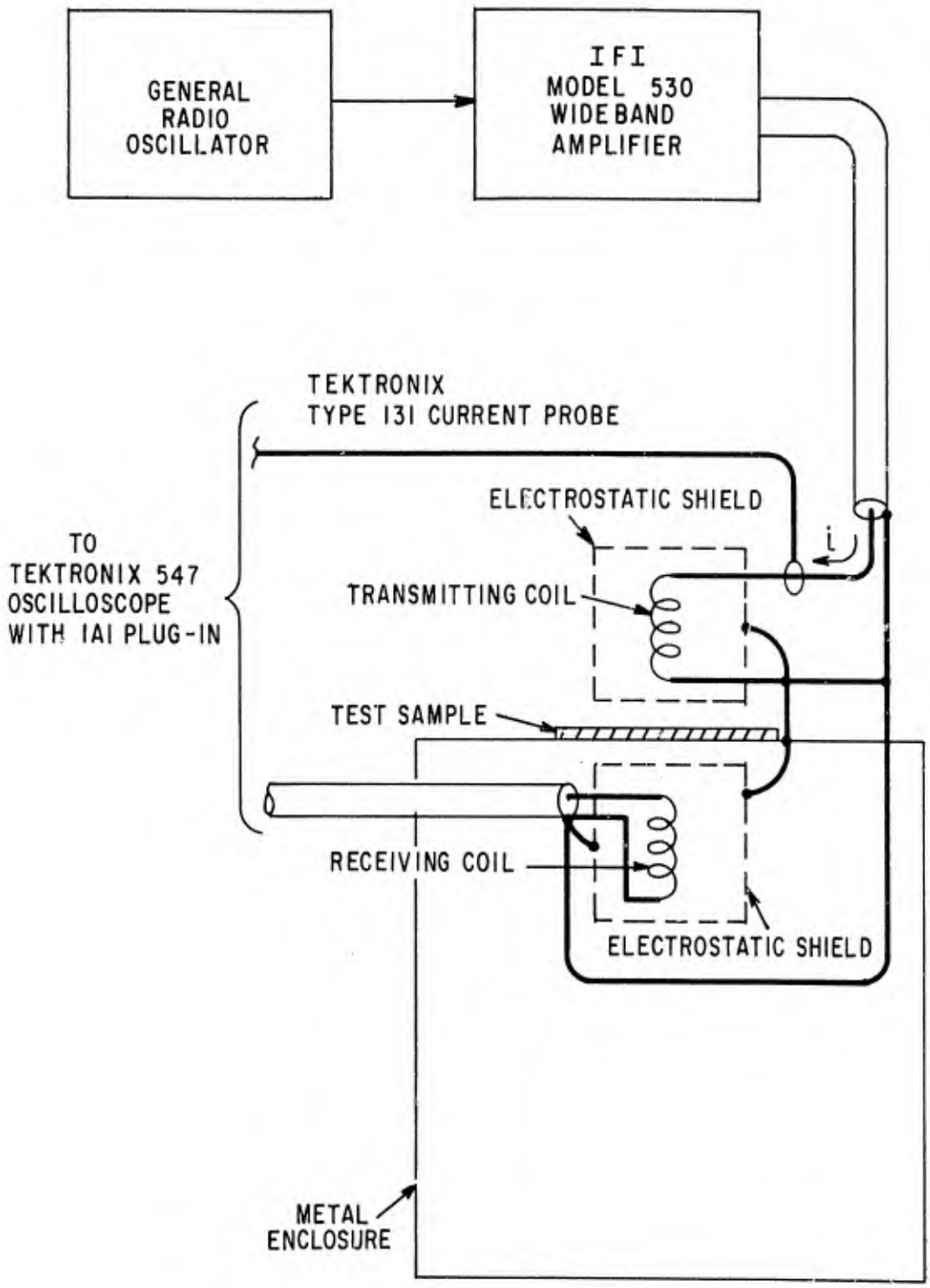

FIGURE 115 - TEST SET UP FOR SHIELDING EFFECTIVENESS TESTS

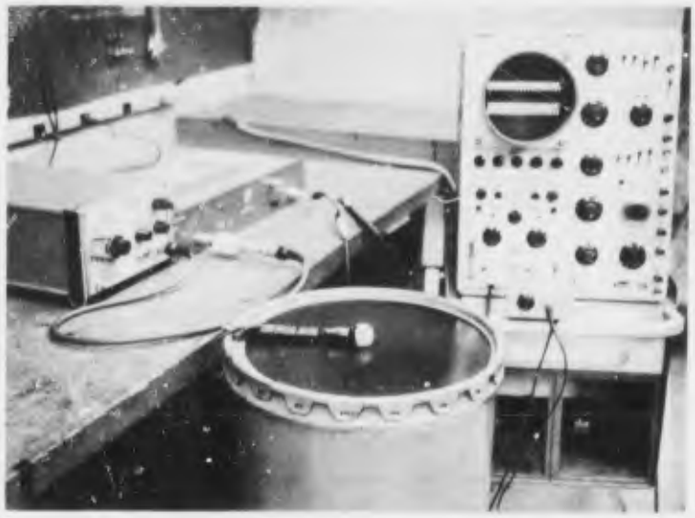

Test Set-Up and Equipment

Electrostatically Shielded
"Transmitting" and "Receiving" Coils

FIGURE 116

Photographs of Shielding Effectiveness Test Set-Up Showing Equipment Used, With Close-Up View of "Transmitting" and "Receiving" Coils

them.

The current in the transmitting coil was kept constant during the tests, and was monitored using a Tektronix Type 131 current probe. A change in current in the transmitting coil could be caused by reflection of part of the created H-field back to the transmitting coil when the test panel is placed between the two coils. This change in current, I, would change the ambient voltage level and an error would result in the measurement and subsequent attenuation calculation.

The amount of H-field attenuation afforded by the shielding properties of the composite material was calculated by:

$$\text{Attenuation} = 20 \log \frac{V_1}{V_2} \qquad \text{Eqn. } 3.1$$

where V_1 is the ambient voltage reading and V_2 is the voltage read on the oscilloscope with the composite material placed between the coils. The energy transfer between two closely spaced loops was primarily a condition of magnetic coupling, and thus the attenuation values measured in this fashion are applicable chiefly when the shield material is to be used against low impedance or predominately magnetic fields.

To avoid fringing effects the receiving coil was placed in a metal enclosure and during tests the composite test panel was placed over an opening in the top of the metal enclosure, as shown in Figure 116.

3.2.2. Measurements

An initial series of measurements was made on four materials:

1) 0.125" thick aluminum plate
2) 0.0016" thick aluminum foil
3) .0625" mesh bronze screen
4) a borch-epoxy laminate

Results are shown on Figure 117.

As might be expected, the laminated material produced little electromagnetic shielding. The measurements on the other materials show some anomalies, the shielding effectiveness not increasing uniformly with frequency.

It was these anomalies that led to the conclusion that the transmitting and receiving coils had to be well-shielded. While the absolute accuracy of the data of Figure 117 is questionable, it does indicate the relative shielding effectiveness that may be expected from some representative materials.

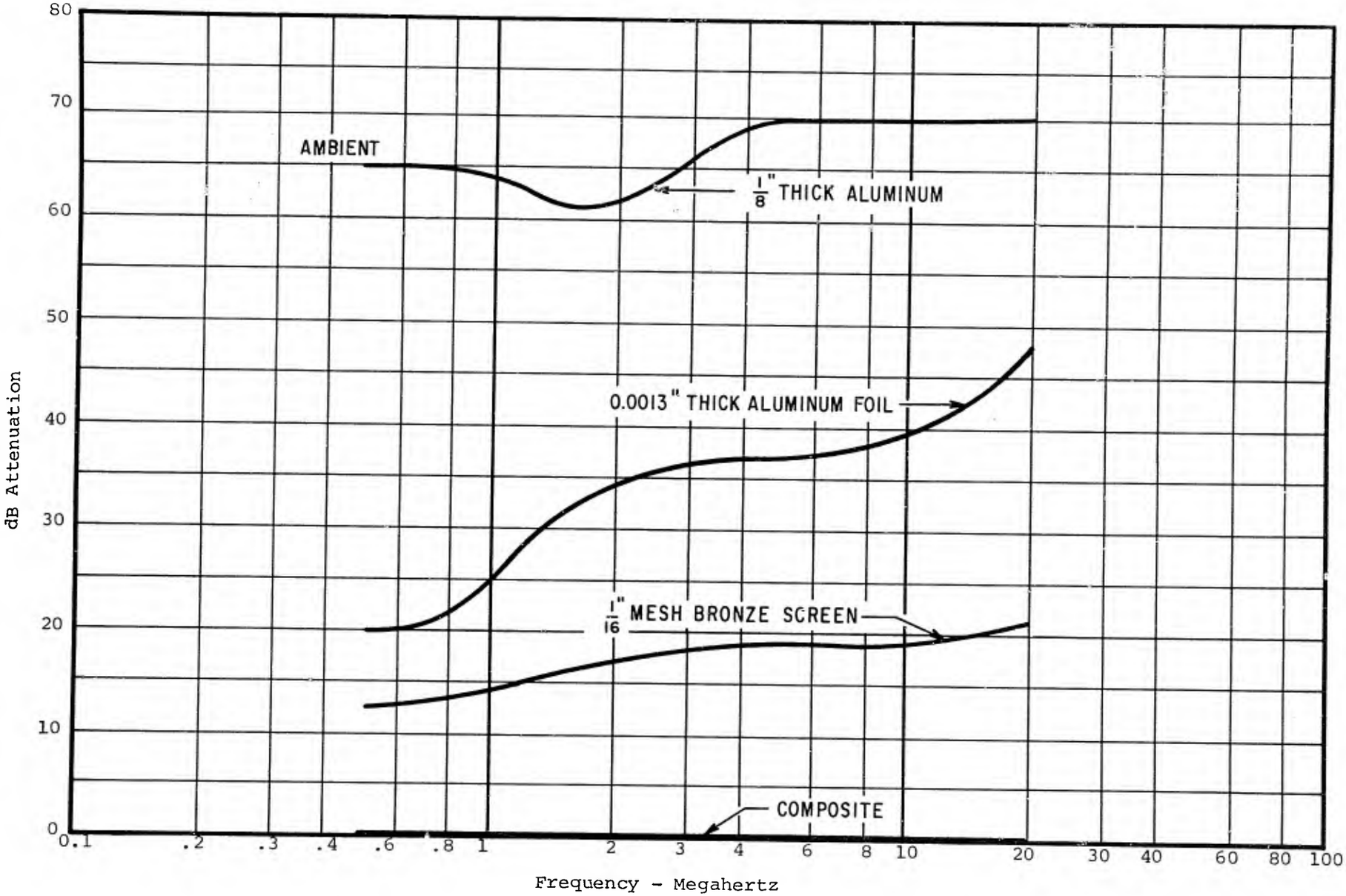

FIGURE 117 - H-Field Shielding Effectiveness of Representative Materials

Once the measurement technique was debugged, measurements were made on the following types of composite materials:

1) 13" diameter graphite panels with no protective coating - 0.040" and 0.120" thickness.

2) 13" diameter graphite panels with silver-paint coating - 0.40" and 0.120" thickness.

3) 6" x 12" rectangular graphite panels with black carbon coating - one thickness - 0.083".

4) 6" x 12" rectangular graphite panels with black carbon coating.

5) 6" x 12" rectangular boron panels with black carbon coating.

6) 6" x 12" rectangular graphite panels with silver-paint coating.

7) 6" x 12" rectangular boron panels with silver-paint coating.

8) 6" x 12" rectangular graphite panels with flame-sprayed aluminum coating.

9) 6" x 12" rectangular boron panels with flame-sprayed aluminum coating.

The results of the measurements are given in Tables XX through XXIV. The data is summarized in graphical form on Figures 118 and 119. Strictly speaking, the data is valid only for the coil spacing used in these tests since the coil spacing affects the impedance of the magnetic field and the shielding is determined in part by the impedance mismatch between the field and the shielding material. However, implications of the data are quite clear:

1) The shielding effectiveness of both graphite-epoxy and boron-epoxy materials is much less than an equivalent thickness of aluminum.

2) A thin piece of aluminum foil has much greater shielding effectiveness than even a 0.120" panel of graphite-epoxy.

3) Graphite-epoxy, by virtue of its higher conductivity, provides more effective shielding than does boron-epoxy.

4) The conductive coatings likely to be needed for control of the direct burning and blasting effects of lightning will probably have more effectiveness as electromagnetic shields than do the composite materials they protect.

5) Measurements made at high field conditions at a frequency of 35 kHz are in agreement with the CW measurements made at low levels.

TABLE XX

H-Field Shielding Effectiveness of Thirteen-Inch Diameter Uncoated Graphite Panels. 0.120" Nominal Thickness, 0-90° Layup

Frequency Megahertz	Attenuation in dB				Average
	LS-70-1	LS-70-2	LS-70-3	LS-70-4	
5	5.9	7.2	7.65	7.91	7.2
10	8.84	11.7	11.7	10.85	10.8
12.5	10.12	12.42	13.7	13.85	12.5
15	13.0	15.1	15.0	14.00	14.3
18	13.4	16.9	16.9	17.5	16.2
20	13.6	18.75	17.95	18.22	17.1
22.5	15.32	18.87	20.0	20.7	18.7
25	14.0	18.6	17.5	21.42	17.9
27.5	16.7	17.0	18.12	*	17.3
30	15.6	19.2	20.4	24.0	19.8

* No readings taken at this frequency.

TABLE XXI

H-Field Shielding Effectiveness of Thirteen-Inch Diameter Uncoated Graphite Panels. 0.120" Nominal Thickness

Frequency Megahertz	Attenuation in dB			Average
	LS-70-T50-10	LS-70-T50-11	LS-70-T50-12	
0.5	6.03	4.77	5.26	5.35
1.0	8.88	7.5	7.66	8.00
5.0	21.0	17.6	18.2	18.9

Panel 10 - 0-90° layup

Panels 11 and 12 - 0-45°-90° layup

TABLE XXII

H-Field Shielding Effectiveness of Thirteen-Inch Diameter Graphite Panels with Silver Paint Coating 0.040" Nominal Thickness, 0-90° Layup

Frequency Megahertz	Attenuation in dB				Average
	LS-70-5	LS-70-6	LS-70-7	LS-70-8	
0.5	2.42	2.15	3.47	2.61	2.66
1	3.41	3.23	4.92	3.65	3.80
5	10.8	9.55	*	11.3	10.6
10	16.4	14.0	21.2	17.6	17.3
12.5	18.75	16.35	22.3	18.1	18.9
15	19.6	19.1	28.3	21.1	22.0
18	21.6	1.4**	28.7	23.6	24.6
20	23.7	22.3	30.0	26.1	25.5
22.5	25.4	24.9	*	27.3	25.9
25	26.5	25.0	32.0	28.6	28.0
27.5	27.3	24.5	*	30.3	27.4
30	26.6	25.2	33.0	30.7	28.9
Coating Thickness	2.8 mils	2.9 mils	3.4 mils	3.7 mils	

* No readings taken at this frequency.

** Questionable reading - ignored in average.

TABLE XXIII

H-Field Shielding Effectiveness of Thirteen-Inch Diameter Graphite Panels with Silver Paint Coating 0.120" Nominal Thickness, 0-90° Layup

Frequency Megahertz	Attenuation in dB			Average
	LS-70-T50-9	LS-70-T50-13	LS-70-T50-14	
0.5	6.11	5.94	5.98	6.00
1.0	8.66	8.77	8.54	8.66
5.0	20.3	20.1	19.4	19.9

TABLE XXIV

H-Field Shielding Effectiveness of 6" x 12" Graphite Panels with Black Carbon Coating 0.083" Nominal Thickness

Frequency Megahertz	Attenuation in dB			Average
	GD-LS70-1G-BC	GD-LS70-2G-BC	GD-LS70-3G-BC	
0.5	4.88	5.02	5.85	5.25
1.0	7.38	7.97	8.54	7.96
2.0	12.06	12.06	13.4	12.5
5.0	18.4	18.1	20.6	19.0
10.0	27.3	27.1	30.4	28.3
14.0	26.1	33.1	35.6	31.6
20.0	26.1	34.9	36.6	32.6
25.0	32.1	36.3	36.7	35.0
30.0	23.0	20.8	14.7	19.5

TABLE XXV

H-Field Shielding Effectiveness of 6" x 12" Graphite Panels with Black Carbon Coating 0.083" Nominal Thickness

Frequency Megahertz	Attenuation in dB			Average
	GD-LS70-1B-BC	GD-LS70-2B-BC	GD-LS70-3B-BC	
0.5	0.38	1.19	1.9	1.16
1.0	1.14	1.67	3.12	1.98
2.0	2.61	3.94	6.35	4.30
5.0	4.67	7.2	9.93	7.3
10.0	9.38	12.06	15.6	12.3
14.0	13.1	14.0	20.0	15.7
20.0	12.06	15.6	20.0	15.9
25.0	13.8	16.3	22.5	17.5
30.0	29.0	28.4	19.8	25.7

TABLE XXVI

H-Field Shielding Effectiveness of 6" x 12" x 0.083" Nominal Thickness, Graphite Panels with Aluminum Foil Coating

Frequency Megahertz	Attenuation in dB			Average
	GD-LS70-1G-A1F	GD-LS70-2G-A1F	GD-LS70-3G-A1F	
0.35	24.2	23.7	25.0	24.3
0.5	27.3	28.8	29.2	28.4
0.75	31.2	32.8	33.0	32.3
1.0	32.1	40.0	40.0	37.4

TABLE XXVII

H-Field Shielding Effectiveness of 6" x 12" x 0.083" Nominal Thickness, Boron Panels with Aluminum Foil Coating

Frequency Megahertz	Attenuation in dB			Average
	GD-LS70-1B-A1F	GD-LS70-2B-A1F	GD-LS70-3B-A1F	
0.35	26.3	26.5	26.6	26.5
0.5	29.6	29.2	29.6	29.5
0.75	33.0	33.1	33.2	33.1
1.0	46.0	46.0	46.0	46.0

TABLE XXVII

H-Field Shielding Effectiveness of 6" x 12" x 0.083" Nominal Thickness, Graphite Panels with F.S.Al. Coating

Frequency Megahertz	Attenuation in dB			Average
	G-1	G-2	G-3	
0.5	17.7	16.8	15.7	16.7
0.75	19.65	18.45	17.7	18.6
1.0	22.4	21.3	19.9	21.2
5.0	37.5	37.0	35.4	36.6

TABLE XXIX

H-Field Shielding Effectiveness of 6" x 12" x 0.083" Nominal Thickness, Boron Panels with F.S.Al. Coating

Frequency Megahertz	Attenuation in dB			Average
	B-1	B-2	B-3	
0.5	16.75	11.6	19.1	15.8
0.75	19.1	13.9	22.0	18.3
1.0	20.1	16.8	24.45	20.4
5.0	32.6	27.5	37.3	32.4

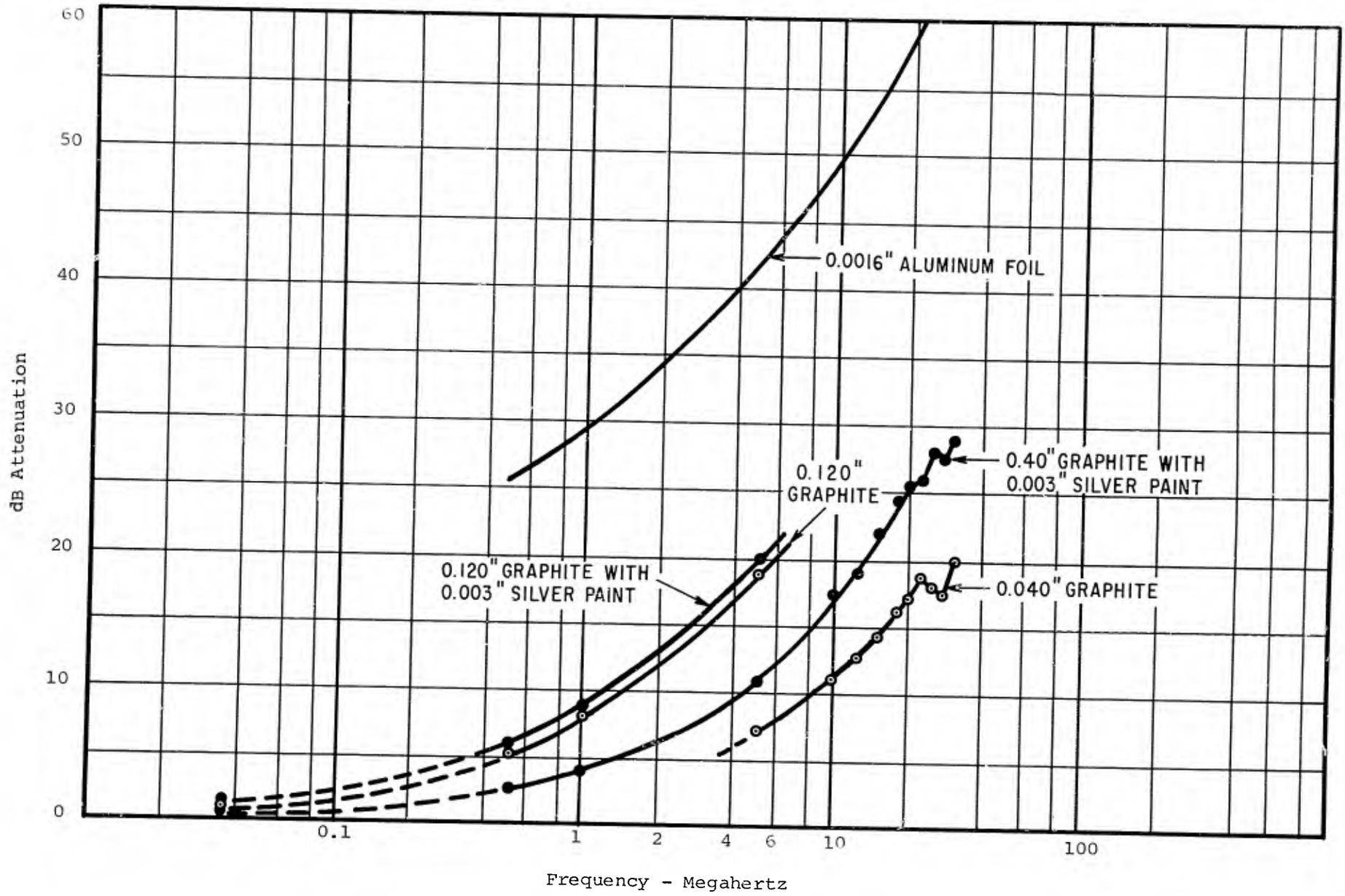

FIGURE 118 - Shielding Factor Measurements on 13-Inch Diameter Graphite Panels

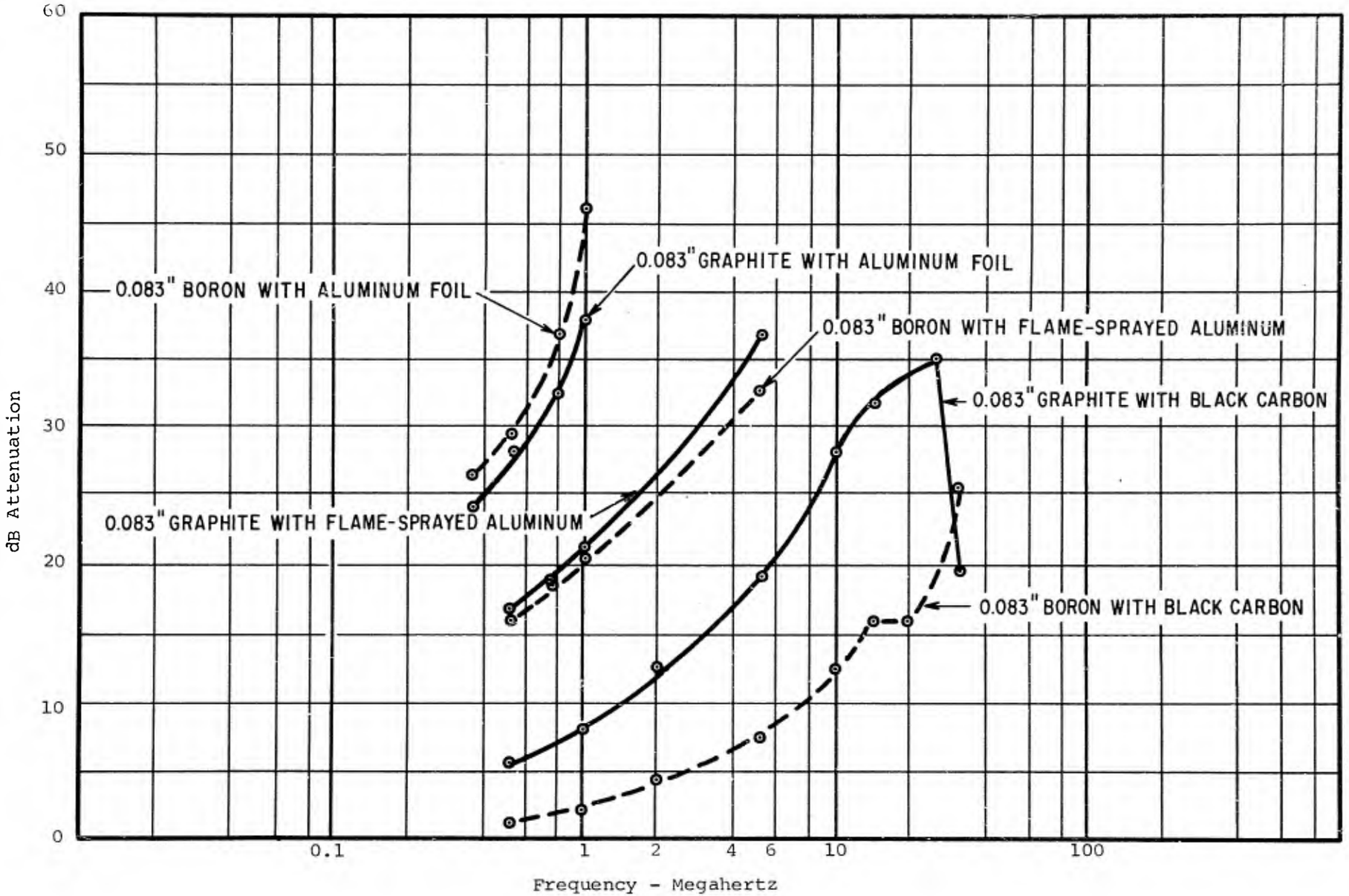

FIGURE 119 - Shielding Factor Measurements on 6" x 12" Graphite and Boron Panels

Some other observations on test results that are not readily apparent from the above data are:

1) In no case did panel orientation or ply lay-up seem to affect the test data.

2) During the high field tests made with the surge generator, there did not appear to be any non-linearities due to differences in field level. The measured attenuations were quite small however, and any non-linearities would have been hard to detect.

Apparently there is sufficient contact between the fibers in the different plies that effective contact is made between plies, in spite of the fact that the individual fibers are held together by a non-conductive epoxy binder. These results would then agree with the measurements of current division made and reported in Section 2. In these cases also, we did not observe any pronounced ply effects or any evidence that the individual plies were separated electrically from each other.

3.3 Comparison of Theoretical and Measured Values of Attenuation

The theoretical value of shielding effectiveness can be calculated for shield material. To check the validity of the test method used to determine the shielding effectiveness of composite materials, the shielding effectiveness of a sheet of 1.6 mil aluminum foil was determined using the above test method. The amount of attenuation provided by the aluminum foil was found to be 40.4 decibels at 5.0 megahertz.

Using the theoretical approach to calculating attenuation, the total reduction (S) in energy of an electromagnetic field in passing through a conducting shield can be divided into two main losses: the attenuation loss (A) which the wave experiences in traveling through the body of the shield material, and the total reflection loss (R) occurring at each surface. There is another term (B) used as a correction term for successive re-reflections when A is small. Therefore, the total shielding effectiveness, S, in decibels, is given as:

$$S = A + R + B \qquad \text{Eqn. 3.2}$$

$$A = 131\ell\sqrt{\mu_R \sigma_R f} \qquad \text{Eqn. 3.3}$$

$$R = 20 \log_{10} \frac{|1 + k|^2}{4|k|} \qquad \text{Eqn. 3.4}$$

$$B = 20 \log_{10} \left| 1 - \left(\frac{k-1}{k+1}\right)^2 10^{-0.10\lambda}\ \epsilon^{-j0.23\lambda} \right| \qquad \text{Eqn. 3.5}$$

where:

f = frequency in hertz (5 megahertz for this calculation)

ℓ = shield thickness in meters (4.065×10^{-5} meters for 1.6 mil foil)

ℓ_r = coil-to-coil distance in meters (0.952×10^{-2} meters for this test)

μ_R = permeability of shield material relative to vacuum ($\mu_R = 1$)

σ_R = conductivity of shield material relative to copper ($\sigma_R = 0.6$)

λ = wavelength in meters (5 MHz $\approx$ 60 meters)

$$k = \left| (1 + j) \left| Z_w \right| 1.915 \times 10^6 \sqrt{\frac{\sigma_R}{f \mu_R}} \right| \qquad \text{Eqn. 3.6}$$

where:

$|Z_w|$ = wave impedance, ohms

$$|Z_w| = (7.9 \times 10^{-6} r)\ (jf) \qquad \text{Eqn. 3.7}$$

The theoretical total shielding effectiveness for the 1.6 mil aluminum foil was calculated to be as follows:

$$S = A + R + B \qquad \text{Eqn. 3.8}$$

$A = 9.2$ dB

$R = 33$ dB

$B = 0$ negligible

$S = 42.2$ dB

The theoretical value of attenuation compared favorably with the measured value of attenuation, 40.4 dB, for 1.6 mil aluminum foil.

3.4 Comparison with Other Investigations

Similar measurements of shielding effectiveness of boron and graphite composite materials have also been made by Shulz.[2] While he has reservations about the absolute accuracy of the data, due to difficulties in determing the time absorption and reflection components of shielding effectiveness, his data is in general agreement with the data obtained during this contract. An excerpt of his data is presented in Figure His data covers the range 10 - 500 MHz and thus complements the previous data, extending it to higher frequencies. The agreement is quite good. He observed shielding factors in the range of 1 dB for .0375" thick graphite and 30 MHz whereas we observed 17 dB at 20 MHz on 0.040" graphite. He observed about 3 dB on 0.105" thick boron at 30 MHz whereas we observed about 16 dB on 0.083" boron with a black carbon coating

2. Preliminary Evaluation of RF Shielding and Electrical Properties of Boron and Carbon Fiber Reinforced Composites, R.B. Schulz, Southwest Research Institute. Presented during panel discussion at 1970 Lightning and Static Electricity Conference - San Diego, California.

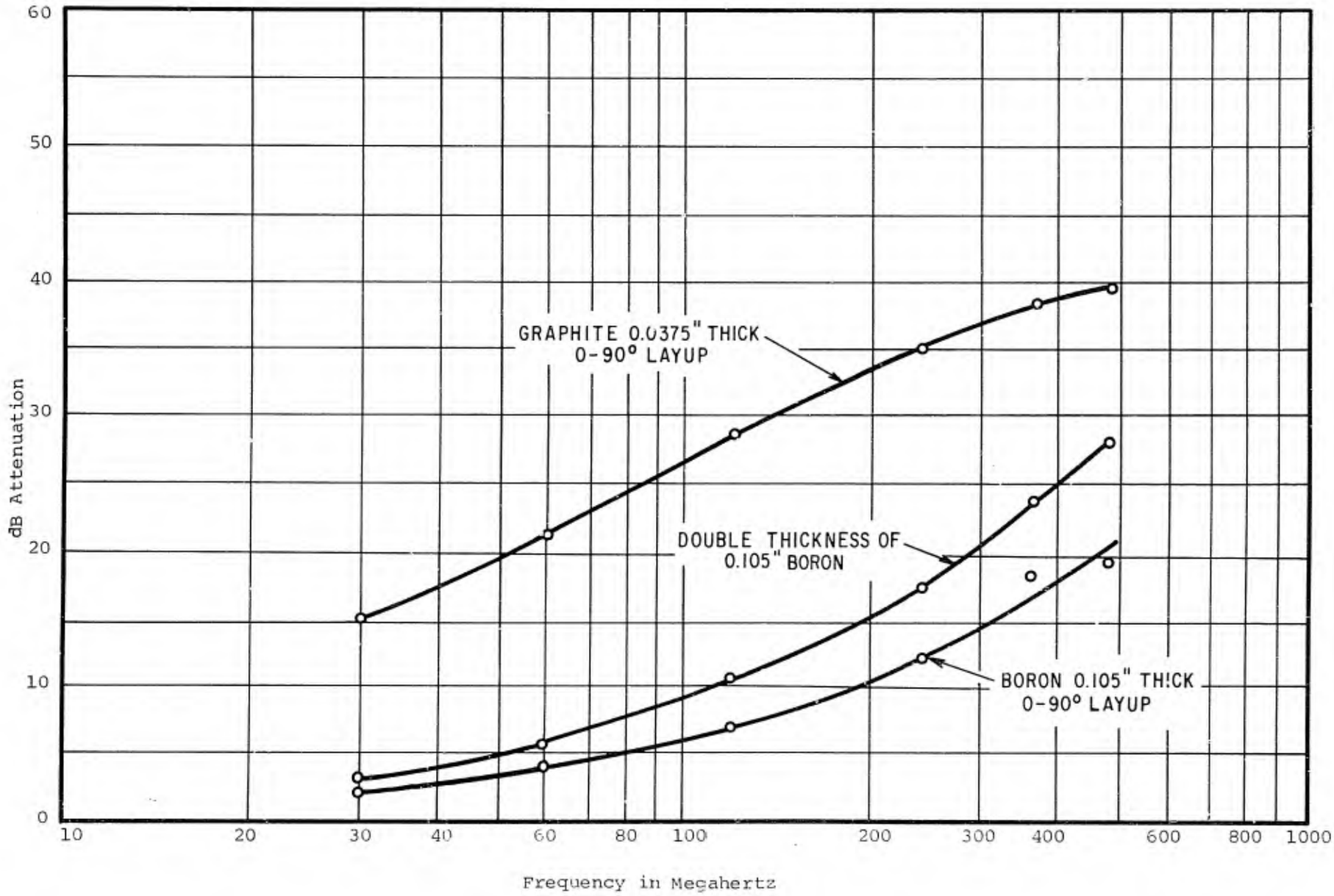

FIGURE 120 - Shielding Effectiveness of Composite Materials

at 20 MHz. He also observed that panels with alternating ply lay-ups gave significantly better shielding performance than a panel with all fibers arranged in parallel. This again is an indication that there is generally good contact between the plies in the different layers.

The measurements of shielding effectivness of panels covered with flame-sprayed aluminum indicated that most of the shielding came from the aluminum. Values of 16 dB and 20 dB were measured at 0.5 MHz and 1.0 MHz for .083" boron with a coating of flame-sprayed aluminum. The thickness of the aluminum on the particular panel under test was not known, but on two other panels the aluminum was between 0.010 and 0.020" thick. Eckersley measured shielding factors of 30, 37 and 42 dB at 0.5 MHz for a 5, 10 and 20 mil thickness of aluminum. Apparently, the electrical contact between the particles of aluminum was not as good as that used by Eckersley.

In previous High Voltage Laboratory work, many investigations of shielding effectiveness of enclosures have been made. One in particular is of interest to this program[3]. One excerpt from this report is shown on Figure 137. Several conductive coatings were evaluated for their shielding effectiveness.

The test samples consisted of 4' x 4' x 4' Masonite and wood boxes covered with the shielding material to be tested. Since access to the inside was required for the placement of measuring equipment, a covered opening was provided on each sample. The coatings tested were:

1. A single layer of 0.001" thick aluminum foil.
2. An approximate 0.007" coating of flame-sprayed aluminum.
3. Two coats of conducting paint (300 - 600 Ω/sq.).

The construction techniques used for these samples enter into the results obtained. For this reason, those areas which are of most interest are described herein.

1. Aluminum Foil Boxes

The foil was in 18" wide strips. Each peripheral strip was continuous

---

3. Investigations of H-Field Shielding Effectiveness of Thin Conductive Coatings and Reduction of Induced Current on Penetrations, E.R. Uhlig, 1 May 1969, HVL Report 69U06. Work done for Corps of Engineers, Department of the Army - Contract Number DA-49-129-ENG-543.

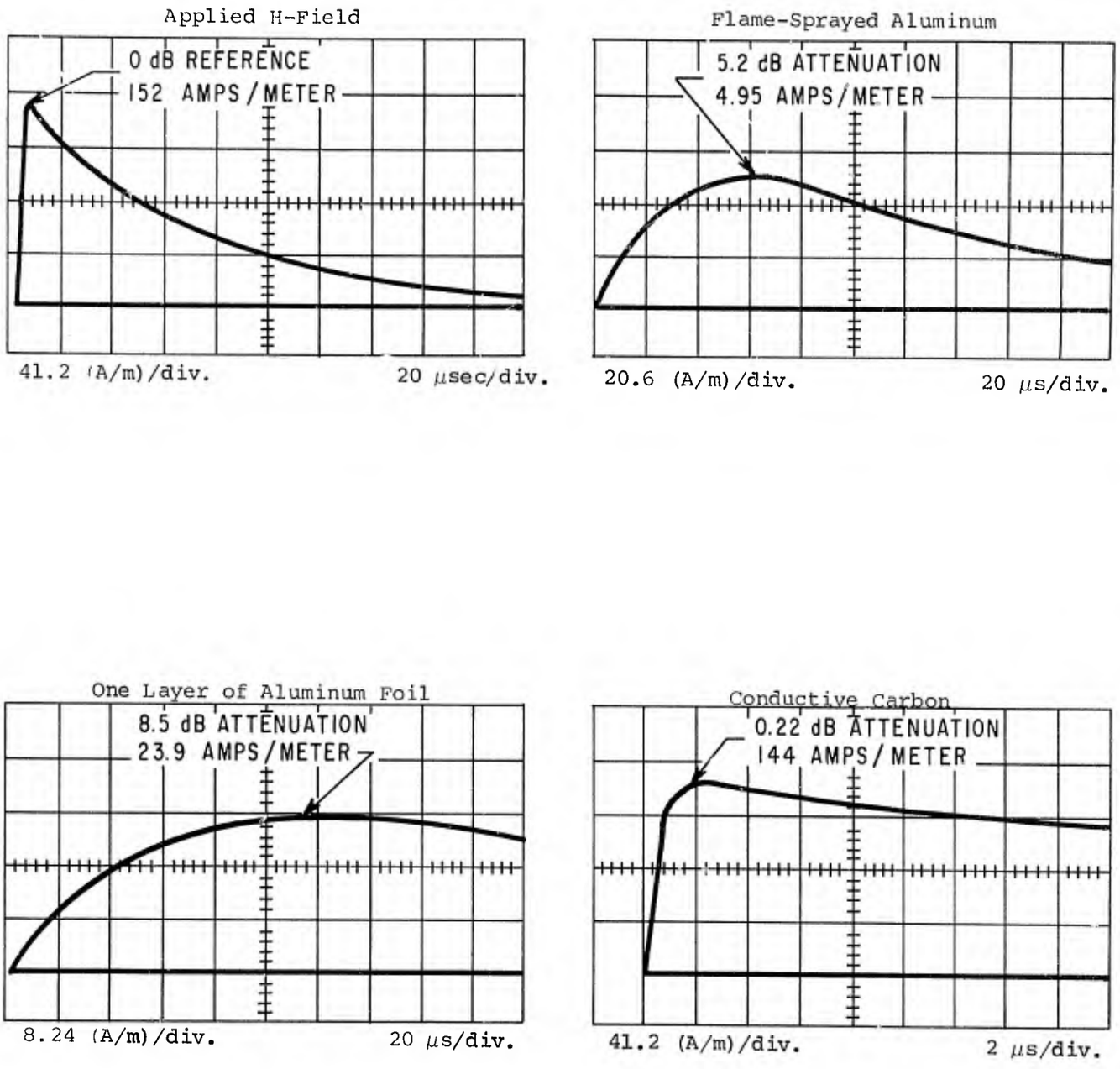

FIGURE 121

H-Field Shielding Effectiveness of Various Conductive Coatings

and adjoining strips were overlapped six inches and taped. The direction of the wrapping was such that the induced current path along the continuous strips occurred when the H-field entered and was normal to the sample face with the access panel.

2. Sprayed Aluminum Box

This box was assembled from six individually sprayed panels. Continuity between panels was then obtained by folding 3" strips of 0.005" aluminum over the edges and stapling every 1½ inches.

3. Conductive-Paint Coated Box

The two coats of conductive paint were applied by brush.

The average surface resistivities for each of the coatings tested is shown in Table XXXIV.

TABLE XXX
Comparison of Surface Resistivities of Materials Under Test

Coating	Average Surface Resistivity (Ω/sq.)
0.001" Aluminum Foil	0.00144
Sprayed Aluminum (approximately 0.007" thick)	0.006
Conductive Paint (2 coats)	344

The testing area consisted of a loop type radiator 26 feet wide and 10 feet high.

The test area was a shielded room measuring 45 feet by 35 feet by 20 feet high. The H-field generator employed consisted of a rectangular loop 26 feet wide and 10 feet high, having as its sides a capacitor discharge pulse generator and a ba.. f four 12-foot lengths of two-inch aluminum conduit spaced about two feet apart; as its bottom, the aluminum floor of the test area; and as its top, four parallel copper conductors spaced about two feet apart.

Figure 121 shows the ambient H-field wave form produced by this radiating system. It is seen to have a rise time of 1.0 microsecond with a half value tail time of 55 microseconds. This test wave is very representative of the current in the return stroke phase of a lightning flash. In the testing area the H-field peak value varied from a minimum of 148 A/m, 10" above the floor to a maximum of 165 A/m, 45" above the floor.

Figure 121 also shows the H-field measured at the center of the various enclosures. A 7 mil thickness of flame-sprayed aluminum gave a H-field attenuation of 5.2 dB as contrasted to 23.9 dB produced by a 1 mil thickness of aluminum foil. Conductive paint gave practically no attenuation.

DISTRIBUTION LIST

Number of Copies	Addressee
27	AFAL (AAA/Mr. H.M. Bartman) Wright-Patterson AFB OH 45433
1	AFAL (TEM) Wright-Patterson AFB OH 45433
1	AFAL (XP/Mr. R.G. Stimmel) Wright-Patterson AFB OH 45433
1	AFAPL (PO) Wright-Patterson AFB OH 45433
1	AFAPL (TB) Wright-Patterson AFB OH 45433
1	AFAPL (TFE/Mr. D.A. Starbuck) Wright-Patterson AFB OH 45433
1	AFFDL (FBC/P.A. Parmley) Wright-Patterson AFB OH 45433
1	AFFDL (FBC/Mr. C.D. Wallace) Wright-Patterson AFB OH 45433
1	AFFDL (FBT/Mr. F. Hughes) Wright-Patterson AFB OH 45433
1	AFFDL (FGL/Capt D.R. Rossbach) Wright-Patterson AFB OH 45433
1	AFFDL (FYS/Mr. M. Shirk) Wright-Patterson AFB OH 45433
1	AFML (CA/Dr. Tsai) Wright-Patterson AFB OH 45433
1	AFML (LA/W.P. Conrardy) Wright-Patterson AFB OH 45433
1	AFML (LAA/Mr. W. Iller) Wright-Patterson AFB OH 45433
1	AFML (LAE/Mr. T. Reinhart) Wright-Patterson AFB OH 45433
1	AFML (LAM/Mr. D. Watson) Wright-Patterson AFB OH 45433

Number of Copies	Addressee
1	AFML (LC) Wright-Patterson AFB OH 45433
1	AFML (LC/Capt T. Woodrum) Wright-Patterson AFB OH 45433
1	AFML (LL) Wright-Patterson AFB OH 45433
1	AFML (LLN/Mr. H. Stevens) Wright-Patterson AFB OH 45433
22	AFML (LN/Mr. H.S. Schwartz) Wright-Patterson AFB OH 45433
1	AFML (LN) Wright-Patterson AFB OH 45433
1	AFML (LNC/J.D. Ray) Wright-Patterson AFB OH 45433
1	AFML (LNE) Wright-Patterson AFB OH 45433
1	AFML (LNF/J. Ross) Wright-Patterson AFB OH 45433
1	AFML (LP) Wright-Patterson AFB OH 45433
1	AFML (LP/W.G.D. Frederick) Wright-Patterson AFB OH 45433
1	AFML (LT) Wright-Patterson AFB OH 45433
1	AFML (LTF/F. Harsacky) Wright-Patterson AFB OH 45433
1	AFML (LTF/S. Litvak) Wright-Patterson AFB OH 45433
1	AFML (LTF/Mr. L. Marler) Wright-Patterson AFB OH 45433
1	AFML (LTP/Mr. T. Cornsweet) Wright-Patterson AFB OH 45433
1	AFML (SU) Wright-Patterson AFB OH 45433

Number of Copies	Addressee
1	AFML (SU/Capt J.G. Breland, Jr.) Wright-Patterson AFB OH 45433
1	AFML (XR) Wright-Patterson AFB OH 45433
1	AFML/Mr. James H. Weaver Wright-Patterson AFB OH 45433
1	AFSC (EIUM/Mr. F.S. Lamaster) Richards-Gebaur AFB MO 64030
1	AFSC (SCTSM/Dr. S. Strauss) Andrews AFB Wash DC 20332
1	AFSC (SDEC) Andrews AFB Wash DC 20332
1	AFSC (SDME/Capt M.A. Creamer) Andrews AFB Wash DC 20331
1	AFWL (SES/Maj W. Bicher) Kirtland AFB NM 87117
1	AMRRC (AMXMR-OR/Mr. M. Kornitzky) Watertown MA 02172
1	ASD (ENFS/Mr. G. Purkey) Wright-Patterson AFB OH 45433
1	ASD (ENFSS/Capt G. Smith) Wright-Patterson AFB OH 45433
1	ASD (ENJIF/D. Wright) Wright-Patterson AFB OH 45433
1	ASD (ENVCC) Wright-Patterson AFB OH 45433
1	ASD (ENVCC/Mr. D.F. Baseley) Wright-Patterson AFB OH 45433
1	ASD (ENVCC/Lt D.G. Lockie) Wright-Patterson AFB OH 45433
1	ASD (ENVCC/Mr. C.E. Seth) Wright-Patterson AFB OH 45433

Number of Copies	Addressee
1	ASD (ENVCD/Mr. P.W. Kelly) Wright-Patterson AFB OH 45433
1	ASD (ENZDE) Wright-Patterson AFB OH 45433
1	ASD (FTZDE) Wright-Patterson AFB OH 45433
1	ASD (OIP) Wright-Patterson AFB OH 45433
1	ASD (SDK) Wright-Patterson AFB OH 45433
1	ASD (SDK/Mr. R.S. Whitlock) Wright-Patterson AFB OH 45433
1	ASD (SD4E/Mr. C.E. Tyzzer) Wright-Patterson AFB OH 45433
1	ASD (SR-WE 6WW/Mr. R.E. Dean) Wright-Patterson AFB OH 45433
1	ASD (YAEJ/Mr. R.C. Rotterman) Wright-Patterson AFB OH 45433
1	ASD (YAT/Maj R.A. Brown) Wright-Patterson AFB OH 45433
1	ASD (YHL/B-1 SPO/Mr. V. Sokoloski) Wright-Patterson AFB OH 45433
1	AUL (Air Univ. Library) Maxwell AFB AL 36112
2	DDC Cameron Station Alexandria VA 22314
1	OCAMA (AFLC/MMES/Mr. D. Cantrell) Tinker AFB OK 73145
1	OSD (DDR&E) Materials Division Office of Assistant Director (Chemical Technology) Wash DC 20301

Number of Copies	Addressee
1	HQ SAC (OAI) Offutt AFB NE 69193
1	SAMSO (SMTAE/Lt J.J. Smith) Air Force Unit Post Office Los Angeles CA 90045
1	HQ USAF (AFRSTC/Col R.V. Hemm) Wash DC 20330
1	HQ USAF (RDPS/Mr. C. Porter Wash DC 20330
1	HQ USAF (SAMID) Wash DC 20330
1	HQ USAF (SA) Wash DC 20330
1	USAF ETAC/ID Bldg 159 Navy Yard Annex Wash DC 20333
1	WRAMA (MMEEI/Mr. W. Robinson) Robins AFB GA 31093
1	Det 21 SMAMA (MMREE/Mr. V. Wiegand) Wright-Patterson AFB OH 45433
1	HQ 1002 Insp Gen Gp Lt Col Bruce M. Elvin Norton AFB CA 92409
1	HQ 1002 Insp Gen Gp HQ USAF Directorate of Aerospace Safety AF-IGDSFR/Robert B. Shanks Norton AFB CA 92409
1	2750th ABWg (SSL) Wright-Patterson AFB OH 45433
1	HQ 3246 Test Wing TGYL/Mr. R.V. Gressang Eglin AFB FL 32542
1	HQ 3246 Test Wing TGYL/Mr. Hugh A. Lindsey Eglin AFB FL 32542

Number of Copies	Addressee
1	4950/TZHM/Mr. P.T. Marth Wright-Patterson AFB OH 45433
1	6570th AMRL (HEF/Lt E.J. Jumper) Wright-Patterson AFB OH 45433
1	AF Cambridge Research Labs AFCRL/CRHC/Mr. D.R. Fitzgerald L.G. Hanscom Field Bedford MA 01730
1	AF Flight Dynamics Lab Attn: Mr. Andre J. Holten Wright-Patterson AFB OH 45433
1	Aerospace Research Laboratories Metallurgy & Ceramics Rsch Lab Attn: Mr. Norman M. Tallan Wright-Patterson AFB OH 45433
1	Picatinny Arsenal Attn: Mr. Daniel Waxler Dover NJ 07801
1	Commanding General Watertown Arsenal Attn: Mr. E.N. Hegge Watertown MA 02172
1	Commanding General Picatinny Arsenal ATTN: SMUPZ-VP-6/Mr. R.T. Wegman Dover NJ 07801
1	Picatinny Arsenal Plastic Support Gp PO Box 19006 Wash DC 20037
1	Picatinny Arsenal Plastics Technical Evaluation Ctr SMUPA-VP-3/Mr. H.E. Pebly, Jr. Dover NJ 07801
1	US Army Electronics Command Attn: Dr. Rudolf G. Buser Ft Monmouth NJ 07703

Number of Copies	Addressee
1	US Army Electronic Command Attn: Hans E. Inslerman Ft Monmouth NJ 07703
1	US Army Aviation Systems Command Attn: Mr. Clemence P. Mudd PO Box 209 12th & Spruce Streets St Louis MO 63166
1	US Army Aviation Material Lab Attn: Dr. E. Paxson Ft Eustis VA 23604
1	US Army Aviation Material Lab Attn: Mr. R.L. Echols Ft Eustis VA 23604
1	US Army Missile Command Redstone Scientific Information Ctr Document Section Redstone Arsenal AL 35809
1	US Army ARDC BRL-TBL Solid Mechanics Attn: Capt Roger A. Heimbuch Aberdeen Proving Grounds MD 21005
1	Naval Air Systems Command AIR-53356/Mr. Joseph J. Fisher Wash DC 20360
1	Office of Naval Research Attn: Mr. James Hughes Arlington VA 22217
1	Office of Naval Research CDR Robert F. Lawson 1030 East Green Street Pasadena CA 91101
1	Office of Naval Research Br Office Attn: Mr. Ben J. Cagle 1030 East Green Street Pasadena CA 91101

Number of Copies	Addressee
1	Naval Air Development Center Aero Structures Dept, Code STD-8 Attn: Mr. A. Manno Johnsville PA 18974
1	Naval Air Engineering Center Attn: Mr. R. Fonash Philadelphia PA 19101
1	Naval Air Systems Command Attn: Mr. M. Stander Wash DC 20360
1	Naval Air Systems Command Engineering Division Attn: Mr. O.M. Goodwin Wash DC 20360
1	Commanding Officer Naval Security Engineering Facility Attn: CODE 024/Mr. R. Weilminster 3801 Nebraska Ave NW Wash DC 20390
1	Naval Avionics Facility CODE 441 Indianapolis IN 46218
1	Naval Air Development Center STD-7-ASD/Mr. A. E'Zil Warminster PA 18974
1	Naval Air Development Center STD-7-ASD/Mr. Aris Pasles Warminster PA 18974
1	NASA/Lewis Research Center Attn: Mr. R. Lark, MS 49-1 21000 Brookpark Rd Cleveland OH 44135
1	Federal Aviation Administration Attn: Mr. Robert J. Auburn Wash DC 20590
1	National Bureau of Standards Div 272.70 Attn: Mr. Harold E. Taggart Boulder CO 80302

Number of Copies	Addressee
1	Federal Aviation Administration DOT/FAA/NAFEC Attn: Mr. Samuel V. Zinn, Jr. Atlantic City NJ 08405
1	Federal Aviation Administration Office of Supersonic Transport Development SS110 (Mr. E.R. Bartholomew) 800 Independence Ave SW Wash DC 20590
1	FAA, Eastern Region Library Federal Bldg J.F.K. International Airport Jamaica NY 11430
1	Aerospace Corporation Attn: Mr. James R. Coge 2350 E. El Segundo Blvd El Segundo CA 90245
1	Aerospace Corporation Attn: Mr. Ernest W. Frank, Jr. 2350 E. El Segundo Blvd El Segundo CA 90245
1	Aerospace Corporation Attn: Mr. Carl B. Pearlston 2350 El Segundo Blvd El Segundo CA 90245
1	Autonetics Attn: Mr. John W. Cox 3370 Miraloma Ave Anaheim CA 92803
1	Avco Corp Aerostructures Div Attn: Mr. R. Lantz PO Box 210 Nashville TN 37202
1	Avco Corp Space Systems Div Attn: Mr. A.J. Patrick Lowell Ind Park Lowell MA 01851

Number of Copies	Addressee
1	American Aviation Corp Attn: Mr. Dick Jarvis 318 Bishop Rd Cleveland OH 44143
1	Aerojet-General Corp Attn: Mr. I. Petker PO Box 296 Azusa CA 91703
1	The Boeing Company Attn: Mr. Rowan O. Brick Mail Stop 4C-74 Seattle WA 98124
1	The Boeing Company Attn: Mr. Alfred Eckersley GAG Box 3733 Seattle WA 98124
1	The Boeing Company Attn: Mr. Lars Jorgensen PO Box 3707 MS 17-01 Seattle WA 98124
1	The Boeing Company Attn: Mr. Stanford D. Schneider Box 3733 Seattle WA 98124
1	Boeing Center Vertol Div Attn: Mr. Richard Freeman Box 16858 Philadelphia PA 19142
1	The Boeing Company Vertol Div Attn: Mr. Bob Pinckney Morton PA 19070
1	The Boeing Company Vertol Div Attn: Mr. D. Hoffstedt Morton PA 19070
1	The Boeing Company Vertol Div Attn: Mr. J. Solak PO Box 16858 Philadelphia PA 19142

Number of Copies	Addressee
1	The Boeing Company Attn: Mr. J. R. Galli PO Box 3733 Seattle WA 98124
1	The Boeing Company Missile & Information Systems Div Attn: Mr. J. Hoggatt PO Box 3999 Seattle WA 98124
1	The Boeing Company Attn: Mr. R.M. Robbins 3801 S. Oliver Wichita KS 67210
1	Bell Helicopter Company Attn: Mr. Richard C. Henschel PO Box 482 Ft Worth TX 76101
1	Bell Helicopter Company Attn: Mr. M. Glass PO Box 482 Ft Worth TX 76101
1	Bell Aerospace Division of Textron Attn: Mr. F. Anthony PO Box 1 Buffalo NY 14240
1	Breeze Illinois Inc/J.S. Bates Walter D. McKerchar Wyoming IL 61491
1	Cornell Aeronautical Lab, Inc. Attn: Mr. John J. Earshen 4455 Genesee Street Buffalo NY 14221
1	Dynasciences Corporation Scientific Systems Division Attn: Mr. Michael C. Becher Township Line Road Blue Bell PA 19422
1	Eastern Air Lines, Inc. International Airport Attn: Mr. Dale N. Jones Miami FL 33148

Number of Copies	Addressee
1	Fairchild Electro Metrics Attn: Mr. H. Dean McKay 14547 Titus Panorama City CA 93065
1	Fairchild-Hiller Corp Republic Aviation Div Attn: Dr. R. Levy Farmingdale LI NY 11735
1	Fairchild-Hiller Corp Republic Aviation Div Attn: Mr. G. Phanner Farmingdale LI NY 11735
1	General Dynamics Div Attn: Mr. Donald D. Martin PO Box 748 Fort Worth TX 76101
1	General Dynamics Attn: Mr. B. Bates PO Box 748 Fort Worth TX 76101
1	General Dynamics Corp Attn: Mr. C. Rogers PO Box 748 Fort Worth TX 76101
1	General Dynamics Corp Attn: Mr. P.D. Shockey PO Box 748 Fort Worth TX 76101
1	General Dynamics/Convair Aerospace Attn: Mr. J.L. Moe PO Box 748 Fort Worth TX 76101
1	General Dynamics/Convair Aerospace Attn: Mr. Richard L. Evans 5001 Kearny Villa Road San Diego CA 92123
1	General Electric Company Attn: Mr. Andrew J. Davis Lakeside Ave Burlington VT 05401

Number of Copies	Addressee
1	General Electric RESD Attn: Mr. K. Hall PO Box 855 Philadelphia PA 19101
1	General Electric Co Aircraft Engineering Gp Attn: Mr. D. Wright Dept M-87 Evendale OH 45215
1	General Electric Co Research & Development Center Attn: Mr. R.W. Shade Schenectady NY 12301
1	General Electric Co Evendale Plant Attn: Mr. Floyd Grossoehme Cincinnati OH 45215
1	General Electric Co Advanced Engineering & Tech Dept Attn: S. Harrier Bldg 500, M-74 Cincinnati OH 45215
1	General Electric Co Attn: L.R. McCreight PO Box 8555 Philadelphia PA 19101
1	General Electric Co Advanced Engine & Tech Dept Attn: Mr. J.H. Young Evendale OH 45215
1	Granger Associates Attn: Mr. Robert A. Peterson 1360 Willow Road Menlo Park CA 94025
1	Granger Associates Attn: Mr. William G. Hoover 1360 Willow Rd Menlo Park CA 94025
1	Granger Associates Attn: Mr. Carl Berg 1360 Willow Road Menlo Park CA 94025

Number of Copies	Addressee
1	Grumman Aerospace Corp Advanced Composites Attn: Mr. A. August/Plant 35 Bethpage LI NY 11714
1	Grumman Aerospace Corp Advanced Manufacturing Div Attn: J.H. Borstel/Plant 12 Bethpage LI NY 11714
1	Grumman Aerospace Corp Attn: Mr. S. Dastin S Oyster Bay Rd Bethpage LI NY 11714
1	Grumman Aerospace Corp Attn: Mr. G. Lubin S Oyster Bay Rd Bethpage LI NY 11714
1	Grumman Aerospace Corp Attn: Mr. D. Hadcock/Mr. G. Tokin S Oyster Bay Rd Bethpage LI NY 11714
1	Grumman Aerospace Corp RF Engineering Plant 14 Attn: Mr. A.G. Zimbalatti Bethpage NY 11714
1	Goodyear Aerospace Corp Attn: Mr. Fred P. Wilcox Litchfield Park AZ 85340
1	Goodyear Aerospace Corp Attn: Mr. L. Toth 1210 Massilon Rd Akron OH 44314
1	Goodyear Aerospace Corp D 454 Plastic Eng Attn: Mr. G. Wintermute Litchfield Park AZ 85304
1	General Motors Corp Allison Div Attn: Mr. E.C. Stevens PO Box 894 Indianapolis IN 46208

Number of Copies	Addressee
1	Hughes Aircraft Co MS B-112 Attn: Mr. Harold R. Schultz Centinela & Teale Streets Culver City CA 90230
1	Hughes Aircraft Co Aerospace Group Attn: Mr. Jack Hoffman Culver City CA 90230
1	Harry Diamond Laboratories Attn: Mr. Daniel W. Finger Wash DC 20438
1	Harvey Aluminum Laboratories Attn: Mr. L. Davis 19200 Southwestern Ave Torrance CA 90509
1	Hercules, Inc. Attn: Mr. C. Friend PO Box 210 Cumberland MD 21501
1	Hexcel Aerospace Attn: Mr. T.W. Engelbrecht 11711 Dublin Blvd Dublin CA 94566
1	ITT Research Institute Attn: Mr. R. Cornish 10 W. 35th St Chicago IL 60616
1	Joslyn Electronic Systems Attn: Mr. Donald M. Worden PO Box 817 6868 Cortona Drive Goleta CA 93017
1	Joslyn Electronic Systems Attn: Mr. John J. Gilmour 6868 Cortona Drive PO Box 817 Goleta CA 93017
1	Joslyn Electronic Systems Attn: Mr. Donald B. Hamister PO Box 817 6868 Cortona Drive Goleta CA 93017

Number of Copies	Addressee
1	Joslyn Electronic Systems Attn: Mr. Walter Pranke, Jr. PO Box 817 6868 Cortona Drive Goleta CA 93017
1	Joslyn Electronic Systems PO Box 817 6868 Cortona Drive Attn: Mr. David W. Bodle
1	Joslyn Electronic Systems Attn: Mr. Wilhelm H. Kapp PO Box 817 6868 Cortona Drive Goleta CA 93017
1	Joslyn Electronic Systems Attn: Mr. Chester J. Kawiecki PO Box 817 6868 Cortona Drive Goleta CA 93017
1	Joslyn Electronic Systems Attn: Mr. Ron Thompson Box 817 6868 Cortona Drive Goleta CA 93017
1	Kaman Aircraft Corp Attn: Mr. F.F. Morrison E&A Bldg Old Windsor Road Bloomfield CT 06007
1	Lockheed Aircraft Corp Attn: Mr. William B. Frazier, Jr. PO Box 551 Burbank CA 91503
1	Lockheed-Georgia Company Attn: Mr. Floyd P. Holder 86 South Cobb Drive Marietta GA 30060
1	Lockheed-Georgia Co Advanced Materials & Structural Div Dept 72-26, Zone 459 Attn: Mr. W.A. Pittman Marietta GA 30060

Number of Copies	Addressee
1	Lockheed-Georgia Co Research Laboratory Attn: Mr. W. Cremans Marietta GA 30060
1	Lockheed Missile & Space Co Attn: Mr. A. Johnson PO Box 504 Sunnyvale CA 94086
1	Lockheed-Georgia Co Dept 72-36, Zone 322 Attn: Mr. D.W. Matthias Marietta GA 30062
1	Lockheed-Georgia Co Advanced Composites Information Ctr Attn: Mr. W. Juervic Marietta GA 30060
1	Lockheed-Georgia Co Dept 72-14, Zone 317 Attn: Mr. G.W. Burton Marietta GA 30060
1	Lockheed-California Bldg 170 Plant B-1 Attn: Mr. J.C. Ekvall 74-44 Burbank CA 91503
1	Lockheed-Missiles and Space Co Attn: Mr. R.W. Fenn 1111 Lockheed Way Sunnyvale CA 94088
1	Lightning & Transients Rsch Inst Attn: Mr. J.D. Robb 3011 Roshay Tower Minneapolis MN 55402
1	Lightning & Transients Rsch Inst Attn: Mr. James R. Stahmann PO Box 1529 Miami FL 33139
1	LTV Aerospace Corp Vought Aerospace Div Attn: Mr. E.E. Koltko PO Box 5907 Dallas TX 75222

Number of Copies	Addressee
1	LTV Aerospace Corp Vought Aerospace Div Attn: Mr. S. McClaren PO Box 5907 Dallas TX 75222
1	McDonnell Douglas Astronautics Attn: Mr. Sidney A. Moses 5301 Balsa Ave Huntington Beach CA 92647
1	McDonnell Douglas Attn: Mr. James W. Morris 5301 Balsa Ave Huntington Beach CA 92647
1	McDonnell Douglas Corp Attn: Mr. J. Finn PO Box 516 St Louis MO 63166
1	McDonnell Douglas Corp Attn: Mr. H. Schjelderup 3855 Lakewood Blvd Long Beach CA 90800
1	McDonnell Douglas Corp McDonnell Aircraft Co Attn: Mr. A.H. Pederson Bldg 101 M/S 414 PO Box 516 St Louis MO 63166
1	McDonnell Douglas Corp Dept 256 Bldg 62 Attn: Mr. Ed Schulte PO Box 516 St Louis MO 63166
1	McDonnell Douglas Corp Attn: Mr. Myron P. Amason 3855 Lakewood Blvd Long Beach CA 90801
1	McDonnell Douglas Corp Dept 311-B33N Attn: Mr. G. Weinstock St Louis MO 63166

Number of Copies	Addressee
1	McDonnell Douglas Corp Attn: Mr. R.C. Goran PO Box 516 Lambert, St Louis Arpt St Louis MO 63166
1	McDonnell Douglas Corp M&P Dept Bldg 33 Attn: Mr. R. Kollmansberger PO Box 516 St Louis MO 63166
1	Martin Marietta Corp Attn: Mr. Robert W. Ellison PO Box 179 Denver CO 80201
1	Martin Marietta Corp Attn: Dr. W.F. Stuhrke PO Box 5837 MP-10 5 Orlando FL 32805
1	Martin Co Attn: Mr. E. Strauss Denver CO 80201
1	Mitre Corp Attn: Mr. Alan S. Margulies Box 208 Bedford MA 01730
1	Marquardt Corp Attn: Mr. B.A. Webb 16555 Saticoy St Van Nuys CA 91406
1	North American Rockwell Attn: Mr. Harry Z. Wilson 5701 Imperial Highway Los Angeles CA 90009
1	North American Rockwell Corp Space & Information Systems Attn: Mr. M. Fields MS BB-47 12214 Lakewood Blvd Downey CA 90241

Number of Copies	Addressee
1	North American Rockwell Corp Attn: Dr. L. Kackman International Airport Los Angeles CA 90009
1	North American Rockwell Corp Attn: Mr. F. McDonald International Airport Los Angeles CA 90009
1	North American Rockwell Corp Attn: Mr. G.A. Clark 4300 E 5th St Columbus OH 43216
1	North American Rockwell Corp Attn: Mr. Benjamin F. Varney 5601 W Imperial Highway Los Angeles CA 90009
1	North American Rockwell Attn: Mr. Dudley O. Losee Los Angeles CA 90009
1	Northrop Corporation Attn: Mr. R.D. Hayes 3901 W Broadway Hawthorne CA 90250
1	Northrup-Norair Corp Attn: Mr. E.L. Harmon 3901 W Broadway Hawthorne CA 90250
1	Owens-Corning Fiberglass Corp Scientific Director Attn: Dr. A.C. Siefert PO Box 415 Granville OH 43023
1	Parker-Hannifin Corp Attn: Mr. Philip H. Jones 18321 Jamboree Blvd Irvine CA 92664
1	Piper Aircraft Corp Attn: Mr. Fred Strickland Lock Haven PA 17745

Number of Copies	Addressee
1	Philco-Ford Corp Aeronutronic Div Materials & Processes Lab Attn: Mr. A.P. Penton Newport Beach CA 92663
1	Pratt & Whitney Aircraft Corp Attn: Mr. J. Mangiapane 400 E Main St Hartford CT 06118
1	Rohr Corp Attn: Mr. Henry R. Voss H Street Chula Vista CA 92012
1	Sikorsky Aircraft Attn: Mr. J. DeSouza N Main St Stratford CT 06602
1	Sikorsky Aircraft Div of United Aircraft Corp Attn: Dr. Michael Salkind Chief, Structures & Materials Stratford CT 06602
1	Sikorsky Aircraft A.C.& S.S. Branch Engineering Dept Attn: Mr. Jerry Parkinson N Main St Stratford CT 06497
1	Stanford Research Institute Attn: Mr. Edward Vance 333 Ravenswood Ave Menlo Park CA 94025
1	Stanford Research Institute Attn: Mr. Joseph E. Nanevicz 333 Ravenswood Ave Menlo Park CA 94025
1	Stanford Research Institute Attn: Dr. Edward T. Pierce 333 Ravenswood Ave Menlo Park CA 94025

Number of Copies	Addressee
1	Southwest Research Institute Attn: Mr. Richard B. Schulz 8500 Culebra Rd San Antonio TX 78228
1	Sargent-Fletcher Co Attn: Mr. Darrell Page 9400 Flair Drive El Monte CA 91731
1	Sandia Laboratories Composites Research & Development Dept Attn: Mr. H.M. Stoller Albuquerque NM 87115
1	Teledyne Ryan Associates Attn: Mr. William F. Bodenhamer Harbour Drive San Diego CA 92111
1	Teledyne Ryan Aeronautical Co Attn: Mr. Carl P. Burman 701 Harbor Drive San Diego CA 92112
1	Texaco Inc Richmond Research Labs Attn: Dr. A. Lasday Richmond VA 23202
1	TRW Systems Div Attn: Dr. E.A. Burns 1 Space Pk Redondo Beach CA 90278
1	TRW Equipment Laboratories Attn: Mr. Winters 23555 Euclid Ave Cleveland OH 44117
1	University of Dayton Research Institute Office of the Director Attn: Mr. R. Askins Dayton OH 45409

Number of Copies	Addressee
1	University of Illinois Attn: Mr. Charles D. Hendricks 343 EEB Urbana IL 61801
1	Ohio State University Dept of Mechanical Engineering Attn: Mr. Henry R. Velkoff 206 W 18th Columbus OH 43210
1	Union Carbide Corporation Carbon Products Div Attn: Mr. J.C. Bowman PO Box 6166 Cleveland OH 44101
1	United Aircraft Corp Hamilton Standard Composite Material Div Attn: Mr. H.P. Borie Windsor Locks CT 06096
1	Whittaker Corp Narmco R&D Div Attn: Mr. B. Levenetz 3540 Aero Court San Diego CA 92123
1	Whittaker Corp Narmco Materials Div Attn: Mr. A.B.C. Dexter 600 Victoria St Costa Mesa CA 72627
1	Whittaker Corp Narmco R&D Div Attn: Mr. C. Segal 3540 Aero Court San Diego CA 92123
1	The Truax Co Attn: Mr. Robert Truax PO Box 23627 Oakland Park FL 33307

Unclassified

Security Classification

DOCUMENT CONTROL DATA - R & D

(Security classification of title, body of abstract and indexing annotation must be entered when the overall report is classified)

1. ORIGINATING ACTIVITY (Corporate author)
General Electric Company
High Voltage Laboratory
Pittsfield, Mass.

2a. REPORT SECURITY CLASSIFICATION
Unclassified

2b. GROUP

3. REPORT TITLE
Lightning Effects Relating to Aircraft.
Part I. Lightning Effects on and Electromagnetic Shielding Properties of Boron and Graphite Reinforced Composite Materials.

4. DESCRIPTIVE NOTES (Type of report and inclusive dates)
Final Report for the period 15 Nov 69 to 15 Oct 71

5. AUTHOR(S) (First name, middle initial, last name)
F.A. Fisher, W.M. Fassell

6. REPORT DATE
January 1972

7a. TOTAL NO. OF PAGES
227

7b. NO. OF REFS
3

8a. CONTRACT OR GRANT NO.
F33615-70-C-1144

9a. ORIGINATOR'S REPORT NUMBER(S)
SRD-72-054-1

8b. PROJECT NO.
AF-4357

c.

9b. OTHER REPORT NO(S) (Any other numbers that may be assigned this report)
AFAL-TR-72-5-Pt-1

d.
LI35712

10. DISTRIBUTION STATEMENT
Distribution limited to US Government agencies only for reason of test and evaluation, dated January 1972; other requests for this document must be referred to AFAL/AAA, Wright-Patterson AFB, Ohio.

11. SUPPLEMENTARY NOTES

12. SPONSORING MILITARY ACTIVITY
Air Force Avionics Laboratory
Air Force Systems Command
Wright-Patterson Air Force Base, Ohio

13. ABSTRACT

An investigation employing both destructive and nondestructive testing techniques affirms that lightning-produced currents adversely affect boron- and graphite-reinforced composites for aircraft. While such composite materials offer significant structural advantages over conventional metals, they are much more easily damaged by the high currents associated with lightning. A majority of the coatings tested to determine their ability to protect composites in a lightning environment actually aggravated composite deterioration. To mitigate lightning damage, composite coatings must be either highly conductive or highly insulating. Limitations are identified that must be overcome before coatings of either type can be deemed acceptable.

Several nondestructive testing evaluation techniques are compared. Acoustic impedance measurement holds the greatest promise, because it requires access to only one side of the material and it correlates well with physical inspections.

Studies were made of the electromagnetic shielding properties of composite materials. It is shown that they have much poorer shielding properties than conventional metal structures. The implications as regards the electrical design of future aircraft are discussed.

DD FORM 1 NOV 65 1473

Unclassified

Security Classification

402 503

14 KEY WORDS	LINK A		LINK B		LINK C	
	ROLE	WT	ROLE	WT	ROLE	WT
Lightning Effects Electromagnetic Shielding Boron-Epoxy Graphite-Epoxy Composite Materials						